# Understanding ageing through biogerodemography

# **Bruce Zhang**

Institute of Healthy Ageing,

Department of Genetics, Evolution and Environment,

University College London



Ph.D. Thesis 2022–2025

The work presented in this thesis is my own,
and where information has been derived from other sources, this has been acknowledged.

#### **Abstract**

The biological process of ageing (senescence) affects all life forms, with inescapable effects upon health and survival. However, its cause, course and consequences are far from understood, despite increasing scientific and commercial efforts in recent decades. A cornerstone of ageing research is the study of lifespan – the timing of that transition from life to death. Classical demographic studies of lifespan attempt to understand the biological ageing process through these mortality patterns. Most notably, the Gompertz model of mortality mathematically captures the exponential rise in mortality rates in diverse animal populations, including humans. The two parameters of this model have been widely used to infer biological properties of these populations; for instance, it is commonly thought that the scale parameter reflects the level of ageing-independent mortality, whereas the rate parameter reflects the rate of ageing. However, an empirical foundation for these views has not yet emerged, despite continued application of such mortality models in ageing research. In this thesis, I use the nematode Caenorhabditis elegans to develop a "biogerodemographic" approach to understanding ageing, which couples the collection and analysis of biological data to the traditional demographic analysis of lifespan. This enables explanation of population-level mortality features (e.g. Gompertz parameters) in terms of individual-level biological processes. I find in C. elegans an unexpected inversion of traditional views: the Gompertz scale parameter better reflects ageing rate than ageingindependent mortality, whereas the Gompertz rate parameter better reflects inter-individual variation in the ageing process than ageing rate itself. Remarkably, these new biological interpretations also provide a parsimonious explanation for the enigmatic, inverse Strehler-Mildvan correlation between the Gompertz parameters. Finally, I demonstrate the broader utility of the biogerodemographic approach, in making sense of the individual- and age-specific role of insulin/IGF-1 signalling in C. elegans ageing. The intention of this thesis is therefore to provide a methodological roadmap between demographic and biological ageing, whose combined study has been and will continue to be an unavoidable and important challenge on the path to understanding the biology of ageing.

# **Impact statement**

The leading cause of human morbidity and mortality is the biological ageing process. This entails complex age-related changes, some of which produce pathologies and disease that can reduce the quality and duration of life. For instance, the most common causes of death globally in recent years include cardiovascular diseases, respiratory diseases, cancers, neurodegenerative diseases and COVID-19 infection, all of which primarily affect older people. Thus, research on the biology of ageing is a fundamentally humanitarian endeavour aimed at improving health, and the quality and duration of life.

This doctoral thesis makes conceptual and methodological advances in understanding the biology of ageing within populations. As a complex phenomenon that varies between individuals, and for statistical rigour, the ageing process is best studied across multiple individuals. For example, the field of gerodemography concerns itself with understanding the biology of ageing through the study of population lifespan data. These data reveal that mortality rates increase exponentially with age in most human and animal populations, providing potential clues about the underlying biological ageing process. This exponential mortality rate increase is frequently studied using the Gompertz model, which models the trajectory of increase using two mathematical parameters. Since the proposal of this model 200 years ago (Gompertz, 1825), its parameters have become associated with specific biological aspects of mortality; in particular, that the scale parameter reflects ageing-independent mortality and the rate parameter the rate of biological ageing. However, these ideas have not been empirically tested, yet continue to be used.

This thesis thus investigates the biological basis of the Gompertz parameters, using a nematode model that, like humans, exhibits Gompertzian mortality. Strikingly, the data invert the traditional interpretations, where in fact the scale rather than rate parameter describes biological ageing rate. This highlights the distinction between biological and population ageing, and argues against the common practice of inferring biology from demographic phenomena without empirical (biological) support. The discovery offers a new biological interpretation of the Gompertz parameters, whose validation (using methods developed in this thesis) in other species and interventions may reveal fundamental, evolutionarily conserved properties of the biological ageing process. The work also highlights the great individual variability in the ageing process, and provides a means to understand it. These insights not only inform about the underlying ageing process, but are critical for navigating the management and treatment of ageing in human populations, which are comprised of individuals with diverse biological characteristics and external influences.

# Acknowledgements

This thesis and the discoveries described within have been possible through the invaluable support and contributions of many individuals: Prof. David Gems for his generous, committed supervision and insightful scientific discussions from which many of my ideas have emerged; Assoc. Profs. John Labbadia and Teresa Niccoli for their attentive supporting supervision; Prof. Dame Linda Partridge and Assoc. Prof. Michalis Barkoulas for their careful critical contributions as thesis examiners; Prof. Scott Pletcher for kindly providing the WinModest software and for constructive discussions of key concepts; Dr Yuan Zhao for incisive conceptual feedback and for providing my experimental training in the years prior; Reva Biju, Hannah Chapman, Zibo Gong, Dr Kuei Ching Hsiung, Melisa Kelaj, Chiminh Nguyen, Alice Vere-Hopegood and Dr Aihan Zhang for all of their invaluable research contributions; Xiaoya Wei for both research contributions and dedicated technical support; and the UCL Overseas Research Scholarship and the Gems Laboratory for funding that made this research possible.

# Contents

Abstract	3
Impact statement	4
Acknowledgements	5
Abbreviations	8
Glossary of key terms	9
Chapter 1 – An introduction to biogerodemography	
1.1 – The biology of ageing	1
1.2 – Ageing as a demographic phenomenon	5
1.3 – Mortality patterns in human populations	7
1.4 – Mortality patterns in Caenorhabditis elegans	9
1.5 – Between biological and demographic ageing	21
1.6 – Biological interpretation of demographic ageing	23
Chapter 2 – A conceptual study of Gompertzian mortality	
2.1 – Mathematical properties of the Gompertz parameters	25
2.2 – Biological interpretation of the Gompertz parameters	26
2.3 – A literature survey of interpretations of the Gompertz parameters	31
Chapter 3 – An empirical investigation of Gompertzian mortality in <i>C. elegans</i>	
3.1 – Introduction and experimental design	1
3.2 - Three life-extending intervention classes disproportionately extend gerospan	18
$3.3$ – Correspondence between reduced $\beta$ and increased relative gerospan	52
$3.4$ – Reduced $\beta$ reflects inter-individually variable gerospan expansion	54
$3.5$ – Reduced $\alpha$ reflects slowed biological ageing	54
$3.6 - \alpha$ and $\beta$ describe inter-individual heterogeneity in age-related infection	59
$3.7 - \beta$ reflects inter-individual heterogeneity in bacterial contact during early adulthood 8	30
<b>Chapter 4</b> – An empirical investigation of the Strehler-Mildvan correlation in <i>C. elegans</i>	
4.1 – Reinterpretation of the Gompertz parameters resolves paradoxes of the S-M correlation	Į.
8	34
4.2 – Life-extending interventions in <i>C. elegans</i> produce S-M correlations	•0

4.3 – Rectangularising S-M correlations reflect decelerated ageing and inter-individual	
homogenisation9	)4
4.4 – Testing the antagonistic pleiotropy explanation of rectangularising S-M correlations 9	8
4.5 – Triangularising S-M correlations arise from hyper-variable gerospan expansion 10	1
<b>Chapter 5</b> – A biogerodemographic study of insulin/IGF-1 signalling in <i>C. elegans</i> ageing	
5.1 – Roles of <i>daf-16</i> in Gompertzian biogerodemography	
5.2 – Effects of age-specific IIS reduction on Gompertzian biogerodemography11	4
5.3 – Age-specific effects of IIS reduction on lifespan reflect inter-individual variation in	
ageing rate	:7
$5.4-$ Effects of healthspan and gerospan on $\alpha$ and $\beta$ given age-specific IIS reduction 13	4
5.5 - Characterisation of an intermediate stage of locomotory ageing in DAF-2 AID longevity	y
	9
5.6 – Late-life elevation of IIS enhances longevity	4
Chapter 6 – Impacts and perspectives	
6.1 – A biogerodemographic approach to understanding ageing	52
6.2 – An empirical reinterpretation of the Gompertz parameters	;4
6.3 – Wider reinterpretations of Gompertzian mortality	7
6.4 – Understanding the Gompertz parameters in higher organisms	0
6.5 – A complex relationship between ageing and lifespan	3
Conclusions	8
Methods	
General methods	9
Chapter-specific methods	′3
References	7

# **Abbreviations**

AP Antagonistic pleiotropy

Carb Carbenicillin

C. elegans Caenorhabditis elegans

DAF-2 AID DAF-2 auxin-inducible degradation

daf-2(rf) daf-2(reduction of function)

DH Differential heterogeneity

DMSO Dimethyl sulfoxide

E. coli Escherichia coli

ETL Extended twilight longevity

G-span Gerospan

G-span<sup>abs</sup> Absolute gerospan G-span<sup>rel</sup> Relative gerospan

H-span Healthspan

H-span<sup>abs</sup> Absolute healthspan H-span<sup>rel</sup> Relative healthspan

IIS Insulin/IGF-1 signalling

L4 4<sup>th</sup> larval stage

NGM Nematode growth media

ns Non-significant

N2 Wild-type strain of *C. elegans* 

P "Big p"

pIC "Small p" with intestinal colonisation

pnIC "Small p" with no intestinal colonisation

RFP Red fluorescent protein

S-M Strehler-Mildvan

# Glossary of key terms

# Gerodemography (new term)

The study of the ageing of populations, by the analysis of lifespan data.

# Biogerodemography (new term)

The study of the biology of ageing of populations, by the analysis of lifespan data as well as biological information collected prior to death. This is the approach taken in this thesis.

# Demographic ageing

Any age-related increase in mortality rate of a population. This differs from biological ageing, which describes the age-related changes occurring within individual animals.

# Gompertz model

A two-parameter exponential function widely used to model age-related mortality rate increases (demographic ageing) in human and animal populations. The two parameters are  $\alpha$  (scale parameter) and  $\beta$  (rate parameter).

#### Strehler-Mildvan (S-M) correlation

An inverse relationship between the two Gompertz parameters that is often observed in comparisons between populations.

# Rectangularisation

A life-extending change in the survival curve that steepens it by increasing lifespan more in shorter-lived population members (in the survival curve shoulder). This produces an S-M correlation by decreasing  $\alpha$  and increasing  $\beta$ . De-rectangularisation entails the inverse change, in the life-shortening direction (increasing  $\alpha$  and decreasing  $\beta$ , also an S-M correlation).

#### *Triangularisation* (new term)

A life-extending change in the survival curve that flattens it (i.e. reduces its steepness) by increasing lifespan more in longer-lived population members (in the survival curve tail). This can correspond to a decrease in  $\beta$  (without change in  $\alpha$ ), or an S-M correlation with increasing  $\alpha$  and decreasing  $\beta$ . De-triangularisation entails the inverse change, in the life-shortening direction (increasing  $\beta$  only or decreasing  $\alpha$  and increasing  $\beta$ ; the latter also an S-M correlation).

# Parametric antagonism (new term)

Short for *mortality parameter antagonism* (new term), referring to the simultaneous opposing effects of mortality model parameters on lifespan. For example, in the S-M correlation, inverse changes in the Gompertz parameters result in the simultaneous increase and decrease in lifespan

which, depending on the relative magnitudes of change in each parameter, may overall increase lifespan, cancel each other out, or decrease lifespan.

Antagonistic pleiotropy (AP)

Where a gene has both beneficial and deleterious effects on fitness (and individual health). AP has been proposed as an explanation for the occurrence of S-M correlations.

Differential heterogeneity (DH)

Where a population is comprised of individuals with variation in susceptibility to death, which arises from readily quantifiable differences in biology (e.g. presence of distinct subpopulations) rather than noise. DH has been proposed as an explanation for the occurrence of S-M correlations.

Absolute healthspan, absolute gerospan (H-spanabs, G-spanabs) (new terms)

Length of time (number of days of life) spent in a state of health or senescence, respectively.

Relative healthspan, relative gerospan (H-span<sup>rel</sup>, G-span<sup>rel</sup>) (new terms)

The proportion of life spent in a state of health or senescence, respectively.

Extended twilight longevity (ETL) (new term)

Lifespan extension (in a comparison of two populations) that occurs primarily through an interindividually variable expansion of absolute gerospan, that is greater in longer-lived population members. This results in an inter-individually variable expansion of relative gerospan, that is also greater in longer-lived population members. This term references the extended relative "twilight" (i.e. gerospan) of longer-lived population members that was previously reported within a single population of *C. elegans* (Zhang et al., 2016).

# **Chapter 1** – An introduction to biogerodemography

# 1.1 – The biology of ageing

Amongst few certainties in life is the inescapable event of death, which befalls all living organisms. Here, chronological age is the greatest risk factor for death. Human society and culture are inextricably shaped by the physical, emotional, and philosophical impacts of this final stage of life, contributing to, for instance, development of mythologies and religions, motivation of war, subscription to life-course sequences (education, work, retirement), and the design of financial, political and healthcare systems.

Why is death so universal and unsparing? Causes of human death before the 18<sup>th</sup> century are poorly documented, but based on preindustrial and modern hunter-gatherer societies, are largely attributable to infectious diseases (Finch, 2009). Such communicable diseases belong to a category of so-called extrinsic hazards, describing mortality risks arising from phenomena external to the organism such as starvation, childhood infections, predation, homicide, suicide, and natural disasters (Carnes and Olshansky, 1997). These deaths typically arise from relatively short and unpredictable exposures to extreme traumatic or physiological stress, which typically result in, through different routes, hypoxia in vital organs (Nuland, 1994).

Over the last two centuries, healthcare and economic advancements have dramatically reduced the incidence of extrinsic mortalities, leading to dramatic increases in life expectancy (Riley, 2001). However, as is common and intuitive knowledge, even in the absence of extrinsic mortality, death is only postponed. This residual mortality is commonly interpreted as intrinsic mortality, or that arising from an internal, more gradual process of deteriorative change in physiological and behavioural function (Carnes and Olshansky, 1997). The aim of biogerontologists, who study the biology of ageing (also known as senescence), is to understand the biological basis of these deteriorative changes, which includes their evolutionary origins, mechanistic processes, and organismal consequences.

Numerous potential explanations of ageing have been proposed, as early as by Plato and Aristotle (Seguchi, 2007), and which over three decades ago already numbered above 300 (Medvedev, 1990). Broadly speaking, theories can be grouped into evolutionary and mechanistic theories which distinguish between, respectively, why and how ageing occurs. Amongst these are also evolutionary physiology theories, which deal with both aspects, such as the disposable soma and programmatic theories (Kirkwood, 1977, Gems, 2025). Below, I will briefly describe several influential theories and emerging ideas about the evolution and mechanisms of ageing, which no doubt represent mere tips of the full literature.

The first evolutionary theory of ageing is widely attributed to the German evolutionary biologist August Weismann (1834–1914), who proposed that ageing evolved adaptively (by natural selection) to free up resources for younger generations (Weismann, 1882). Mechanistically, he theorised that each species possesses a unique limit on the number of possible cell divisions, after which death consequently occurs (Weismann, 1892). A limit to proliferative capacity was subsequently shown experimentally in cultured cells (Hayflick and Moorhead, 1961, Hayflick, 1965), but not that this is a cause of death. However, Weismann's theory of programmed ageing is largely discounted today. In particular, the theory is circular in assuming that older individuals have lower reproductive fitness (due to ageing), few individuals survive to such ages in the wild (pre-empting selection for an adaptive death programme), and it is difficult for selection of altruistic "suicide" to occur amongst genetically-diverse individuals (Vijg and Kennedy, 2015). Indeed, Weismann himself shifted to a less adaptive view of ageing in his later studies (Kirkwood and Cremer, 1982).

In the following century, a better understanding of the evolution of ageing emerged, based on natural selection of individual rather than group fitness. It was proposed that the force of natural selection declines with increasing age (Fisher, 1930, Haldane, 1941, Medawar, 1946, Medawar, 1952), which was later mathematically formalised (Hamilton, 1966). In particular, Medawar developed this idea conceptually, arguing that this evolutionary "selection shadow" emerges and increases with age because extrinsic mortality (e.g. predation, infection, accidents) ensures that few individuals survive to older ages. Consequently, the reproductive contribution to the gene pool of older individuals is lower than that of younger individuals.

Medawar recognised that a consequence of the selection shadow is that deleterious mutations that become phenotypically penetrant at later ages would not be effectively selected against. (Similarly, beneficial mutations acting at late ages would be poorly selected for.) Therefore, these deleterious mutations can accumulate within the gene pool and cause ageing in later life. This is known as the mutation accumulation theory of ageing (Medawar, 1952).

Subsequently, George Williams extended these ideas to propose the antagonistic pleiotropy theory of ageing, which describes ageing as resulting from the adaptive selection for pleiotropic alleles that promote reproductive fitness in earlier life but cause deleterious effects on individual (and reproductive) fitness in later life (Williams, 1957). Such trade-offs can be favoured given the selection shadow in later life, which causes the fitness detriments to be outweighed by the fitness benefits acquired in earlier life when selection is stronger.

The mutation accumulation and antagonistic pleiotropy evolutionary theories of ageing have since acquired a sound mathematical foundation (Charlesworth, 1994, Charlesworth, 2001), reasonable empirical support (Hughes et al., 2002, Rodríguez et al., 2017, Austad and

Hoffman, 2018), and together form the foundation of the present understanding of the evolution of ageing. Importantly, the two theories are not mutually exclusive, but the relative contribution of these two mechanisms to the evolution of ageing remains unclear.

Many mechanistic theories of ageing have also been proposed, including those incorporating evolutionary concepts, and fall very approximately into two camps: viewing ageing either as a consequence of stochastic damage accumulation or of programmatic (genetic) mechanisms. Damage-based theories focus on the accumulation of chance molecular insults over time, from intrinsic physiological processes (e.g. metabolism) and/or external stressors (e.g. UV radiation), and is often likened to a process of gradual wear and tear, akin to that occurring in inanimate machines (Gavrilov and Gavrilova, 2001). Additionally, this view suggests that such damage can exacerbate ageing by impairing damage-repair mechanisms. Perhaps the most influential was the free radical theory, which argued that free radicals (particularly those containing oxygen) react with organic molecules such as proteins, lipids and DNA, and impair their function (Harman, 1956). A prominent offshoot was the mitochondrial free radical theory, which attributed the primary source of free radicals to reactive oxygen species production from physiological mitochondrial respiration (Harman, 1972). However, free radical theories of ageing have mostly proved unable to withstand experimental scrutiny and have since been discredited, at least in their original forms (Howes, 2006, Back et al., 2012, Gladyshev, 2014).

Another notable damage-based theory is the disposable soma theory, which posits that ageing arises from trade-offs between reproductive investment and maintenance and repair of somatic cells (Kirkwood, 1977). Here, it is argued that energy constraints (from finite resources) prevent maximisation of both somatic and reproductive (germline) investments, and that through antagonistic pleiotropy, reproductive investment is evolutionarily favoured. This theory builds mechanistically upon an earlier "error catastrophe theory", which supposed that stochastic molecular damage, particularly of protein synthesis machinery, accumulates over time and if unrepaired, causes ageing (Orgel, 1963). However, the veracity of the disposable soma theory to ageing has been experimentally contested, and it currently seems implausible (for instance, Blagosklonny, 2010, Chereji et al., 2013, Mitchell et al., 2024).

Many other damage-based theories have gained traction, focusing on different forms of biomolecular damage, such as DNA mutation and telomeric attrition (Harley et al., 1990, Schumacher et al., 2021), protein cross-linking and glycation (Bjorksten, 1968, Monnier, 1989), protein aggregation (Cuanalo-Contreras et al., 2023), and lipid peroxidation (Praticò, 2002). Although all these mechanisms may contribute to ageing to some extent, their relative importance, particularly as primary causes of ageing, remains unclear.

In contrast to damage-based theories, programmatic theories argue that ageing arises from genetically encoded processes (de Magalhães and Church, 2005, Blagosklonny, 2006, Gems, 2022). Importantly, programmatic theories do not deny a role for "damage", but rather assert that this damage is largely a consequence of non-stochastic genetic processes, than of stochastic molecular changes. This view also shifts the conceptual emphasis from molecular, cellular damage to deleterious changes at the supramolecular level (cells, tissues and organs, and their interactions).

In contrast to programmed ageing, such as that proposed by Weismann (Weismann, 1882), programmatic ageing occurs non-adaptively, particularly as by-products of adaptive genetic programmes in earlier life, whose deleterious effects in later-life are not eliminated given the selection shadow at these ages (Medawar, 1952). Therefore, programmatic theories are often grounded in the antagonistic pleiotropy theory. Indeed, Williams posed a hypothetical programmatic ageing mechanism, whereby a gene promoting bone calcium deposition would be selected for its developmental benefits, even if it contributes to pathogenic vascular calcification in later life (Williams, 1957). Many putative, real examples of antagonistic pleiotropic mechanisms of ageing are now known (Austad and Hoffman, 2018), such as chronic inflammation (which otherwise fights infection at younger ages) (Franceschi et al., 2000), the accumulation of non-proliferating senescent cells (which protect against cancer and facilitate wound-healing and development at younger ages) (Giaimo and di Fagagna, 2012), and presbyopia (long-sightedness) from continued growth of the optical lens throughout life (Strenk et al., 2005). Notably, the pervasiveness of antagonistic pleiotropy may reflect the highly interconnected nature of biological systems, and resulting biological constraint (Gems and Kern, 2024).

These numerous, often-competing mechanistic theories of ageing reflect the relatively nascent state of the biogerontological field. No general consensus exists on which theory best explains ageing, and accepting multiple causes, what the relative importance of each is. This challenge is exacerbated by the striking variability in ageing between species, populations and even individuals, and in response to environmental differences and interactions between different ageing mechanisms. Attempts to relate different theories to one another in a broader theoretical framework have been made (López-Otín et al., 2013, Kennedy et al., 2014, López-Otín et al., 2023), though, it has been argued, with limited success (Gems and de Magalhães, 2021). Success here would require a model of ageing sufficiently broad to include relevant mechanisms of ageing, yet founded on adequately defined, primary causal mechanisms, and their interactions (Dilman, 1994, Gems, 2022). Most importantly, such a framework would help

direct further investigation into understanding the causes of ageing, by emphasising the relative importance of each mechanism for a particular organism and its environment.

# 1.2 – Ageing as a demographic phenomenon

The molecular revolution of the mid-20<sup>th</sup> century enabled rapid advances in biological research through adoption of principles from physics and chemistry (Olby, 1996). Biogerontology too was transformed, attaining new capacities to study the biological (particularly molecular) mechanisms of ageing, guiding the field towards its present emphasis on the molecular and cellular aspects of ageing. Prior to this, biogerontology was predominantly a study of systemic and organismal-scale biology, focusing on readily quantifiable, "downstream" measures of the ageing process, such as functional health and in particular, lifespan. Notably, these measures continue to be indispensable cornerstones of modern biogerontology, and are considered gold standard metrics of processes' involvement in the ageing process.

Despite a growing fashion to define and evaluate ageing research through health measures (Hansen and Kennedy, 2016), lifespan remains a more integrative metric of the ageing process. It is also generally more straightforward (albeit sometimes very time-consuming) to quantify, and more readily comparable between different types of organism. As a rule of thumb (with important exceptions that I will demonstrate), lifespan is usually a reliable metric of agerelated declines in health (which eventually cause the death event). As a very simple example, under laboratory conditions without extrinsic mortality, it would be reasonable to hypothesise that an individual that lives longer than another, has a slower or delayed ageing process.

While simple in principle, in practice the study of lifespan is surprisingly complex. Most notably, lifespan is a highly variable trait. For instance, in isogenic populations of the nematode *Caenorhabditis elegans* that are cultured in standard laboratory conditions and protected from extrinsic mortality, lifespan differs up to 3-fold between the shortest and longest-lived individuals (Kirkwood et al., 2005). The variability of lifespan within (and between) populations arises, seemingly, because it is a complex phenotype influenced by multiple factors, including genetics, epigenetics, environment, and their interactions (Govindaraju et al., 2015, Sutphin and Korstanje, 2016). In other words, lifespan is a function of the highly variable ageing phenotype. Understanding ageing through lifespan data is therefore most appropriate when sampling all individuals within a sufficiently large study population. With these considerations, the study of lifespan is an inherently demographic endeavour, that is, it adopts principles and practices from demography – the study of populations.

The work of demographers typically involves descriptive and/or predictive quantification of size and composition of human populations, their changes over time, and interactions with one another. Much of this information is captured through research on three core demographic processes: birth, migration, and death (including from ageing) (Harper, 2018). As a result, the application of demography to studying ageing, which will herein be referred to as "gerodemography", has relatively established roots in demography itself. A parallel subfield of demography is biodemography, wherein practitioners probe the biology of populations using demographic approaches, often merging with evolutionary and ecological disciplines (Gamelon and Froy, 2023). It is at the intersection of gerodemography and biodemography that the demography of the biology of ageing exists – the focal discipline of this thesis, which I will more simply refer to as "biogerodemography".

The origins of biogerodemography may be attributed to the 19<sup>th</sup> century British mathematician and actuary, Benjamin Gompertz, who noted that adult mortality rate (probability of dying in a given time interval) increases exponentially with age in human populations (Gompertz, 1825). This finding has since been so widely replicated in diverse animal populations, including humans, that it is often referred to as the "Gompertz law" (Jones et al., 2014). Despite the focus of Gompertz's publication on calculating insurance premiums, his discovery was a catalyst for biogerodemographic research, particularly in raising the question: what is the biological basis for the exponential increase in mortality rate?

As performed by Gompertz, representing lifespan data as mortality rate over age allows visualisation of how death risk changes with increasing age, which offers potential interpretations of how ageing progresses across these ages. These age patterns of mortality rate can be modelled by parametric functions, which describe the raw datapoints with a smoothened, continuous distribution that offers greater analytical power. For instance, the Gompertz law of mortality is described by a two-parameter exponential function (Eq. 1.1), where the scale and rate of mortality rate increase are respectively described by  $\alpha$  and  $\beta$ . These two parameters and their properties comprise a major focus of this thesis and will be introduced in greater detail in Chapter 2. With this Gompertz function (and that of other mortality models), predicted mortality rates can be obtained via interpolation and extrapolation, and changes in the mortality pattern between different populations can be quantified as changes in defined model parameters.

$$\mu(x) = \alpha e^{\beta x}$$
 Eq. 1.1

Mortality modelling has become a major component of biogerodemographic research, and numerous models beyond the Gompertz model have been developed to capture mortality

dynamics of different populations. Other commonly encountered models are listed below. In brief, the Gompertz-Makeham model adds a third, additive parameter, y, to the Gompertz model, to account for age-independent mortality (Eq. 1.2) (Makeham, 1860). This model has been found to better fit human mortality rates in the middle portion of lifespan distributions than the simpler Gompertz model. Meanwhile, the logistic model incorporates a different third parameter, s, which accounts for a deceleration of mortality rates at very late ages - a phenomenon observed in some human and model organism populations (Eq. 1.3) (Kannisto, 1994, Pletcher, 1999). The logistic-Makeham model, like in the Gompertz-Makeham model, adds the Makeham parameter as a fourth parameter to the logistic model to account for ageindependent mortality (Eq. 1.4) (Pletcher, 1999). Finally, the Weibull model describes mortality as a power rather than exponential function of time (Weibull, 1951), such that mortality increases at a slower rate than in the Gompertz model (a simple form of the Weibull model is shown in Eq. 1.5). It is worth noting that although models with more parameters tend to fit data more closely, it does not necessarily follow that these additional parameters reflect real mortality patterns within the population, unless the study population is sufficiently representative of the theoretical population. For this reason, simpler models with fewer parameters, yet sufficient in number to capture patterns of interest within the dataset, are preferable when selecting a mortality model to use.

$$\mu(x) = \alpha e^{\beta x} + \gamma$$

$$\mu(x) = \alpha s/[\alpha + e^{-\beta x}(s - \alpha)]$$

$$\mu(x) = \alpha s/[\alpha + e^{-\beta x}(s - \alpha)] + \gamma$$

$$\mu(x) = \alpha s/[\alpha + e^{-\beta x}(s - \alpha)] + \gamma$$

$$\mu(x) = \alpha s/[\alpha + e^{-\beta x}(s - \alpha)] + \gamma$$

$$\mu(x) = \alpha s/[\alpha + e^{-\beta x}(s - \alpha)] + \gamma$$

$$\mu(x) = \alpha s/[\alpha + e^{-\beta x}(s - \alpha)] + \gamma$$

$$\mu(x) = \alpha s/[\alpha + e^{-\beta x}(s - \alpha)] + \gamma$$

$$\mu(x) = \alpha s/[\alpha + e^{-\beta x}(s - \alpha)] + \gamma$$

$$\mu(x) = \alpha s/[\alpha + e^{-\beta x}(s - \alpha)] + \gamma$$

$$\mu(x) = \alpha s/[\alpha + e^{-\beta x}(s - \alpha)] + \gamma$$

$$\mu(x) = \alpha s/[\alpha + e^{-\beta x}(s - \alpha)] + \gamma$$

$$\mu(x) = \alpha s/[\alpha + e^{-\beta x}(s - \alpha)] + \gamma$$

$$\mu(x) = \alpha s/[\alpha + e^{-\beta x}(s - \alpha)] + \gamma$$

$$\mu(x) = \alpha s/[\alpha + e^{-\beta x}(s - \alpha)] + \gamma$$

$$\mu(x) = \alpha s/[\alpha + e^{-\beta x}(s - \alpha)] + \gamma$$

$$\mu(x) = \alpha s/[\alpha + e^{-\beta x}(s - \alpha)] + \gamma$$

$$\mu(x) = \alpha s/[\alpha + e^{-\beta x}(s - \alpha)] + \gamma$$

$$\mu(x) = \alpha s/[\alpha + e^{-\beta x}(s - \alpha)] + \gamma$$

$$\mu(x) = \alpha s/[\alpha + e^{-\beta x}(s - \alpha)] + \gamma$$

$$\mu(x) = \alpha s/[\alpha + e^{-\beta x}(s - \alpha)] + \gamma$$

$$\mu(x) = \alpha s/[\alpha + e^{-\beta x}(s - \alpha)] + \gamma$$

$$\mu(x) = \alpha s/[\alpha + e^{-\beta x}(s - \alpha)] + \gamma$$

$$\mu(x) = \alpha s/[\alpha + e^{-\beta x}(s - \alpha)] + \gamma$$

$$\mu(x) = \alpha s/[\alpha + e^{-\beta x}(s - \alpha)] + \gamma$$

$$\mu(x) = \alpha s/[\alpha + e^{-\beta x}(s - \alpha)] + \gamma$$

$$\mu(x) = \alpha s/[\alpha + e^{-\beta x}(s - \alpha)] + \gamma$$

$$\mu(x) = \alpha s/[\alpha + e^{-\beta x}(s - \alpha)] + \gamma$$

$$\mu(x) = \alpha s/[\alpha + e^{-\beta x}(s - \alpha)] + \gamma$$

$$\mu(x) = \alpha s/[\alpha + e^{-\beta x}(s - \alpha)] + \gamma$$

$$\mu(x) = \alpha s/[\alpha + e^{-\beta x}(s - \alpha)] + \gamma$$

$$\mu(x) = \alpha s/[\alpha + e^{-\beta x}(s - \alpha)] + \gamma$$

$$\mu(x) = \alpha s/[\alpha + e^{-\beta x}(s - \alpha)] + \gamma$$

$$\mu(x) = \alpha s/[\alpha + e^{-\beta x}(s - \alpha)] + \gamma$$

$$\mu(x) = \alpha s/[\alpha + e^{-\beta x}(s - \alpha)] + \gamma$$

$$\mu(x) = \alpha s/[\alpha + e^{-\beta x}(s - \alpha)] + \gamma$$

$$\mu(x) = \alpha s/[\alpha + e^{-\beta x}(s - \alpha)] + \gamma$$

$$\mu(x) = \alpha s/[\alpha + e^{-\beta x}(s - \alpha)] + \gamma$$

$$\mu(x) = \alpha s/[\alpha + e^{-\beta x}(s - \alpha)] + \gamma$$

$$\mu(x) = \alpha s/[\alpha + e^{-\beta x}(s - \alpha)] + \gamma$$

$$\mu(x) = \alpha s/[\alpha + e^{-\beta x}(s - \alpha)] + \gamma$$

$$\mu(x) = \alpha s/[\alpha + e^{-\beta x}(s - \alpha)] + \gamma$$

$$\mu(x) = \alpha s/[\alpha + e^{-\beta x}(s - \alpha)] + \gamma$$

$$\mu(x) = \alpha s/[\alpha + e^{-\beta x}(s - \alpha)] + \gamma$$

$$\mu(x) = \alpha s/[\alpha + e^{-\beta x}(s - \alpha)] + \gamma$$

$$\mu(x) = \alpha s/[\alpha + e^{-\beta x}(s - \alpha)] + \gamma$$

#### 1.3 – Mortality patterns in human populations

Given the origins of gerodemography in actuarial science, it is no surprise that extensive modelling of mortality patterns has been performed for human populations. These analyses have benefited from readily available death records collected by governments and other organisations throughout the world, with sample sizes that are ever-increasing. However, mortality modelling of human populations involves major challenges, such as the complexity of biological, social and economic factors influencing lifespan, their heterogeneity within populations, their changes over time, and the accuracy of death records. Yet, one could argue that these human-specific factors, which are largely controlled within laboratory culture of

model organisms, present a unique opportunity to understand the diversity of determinants affecting mortality model parameters; in other words, to separate biological and non-biological contributions to mortality rate trajectories.

Over the last two centuries, life expectancies have steadily yet dramatically increased throughout the world. For example, record mean female life expectancy from birth by country, was held by Sweden in 1840 at roughly 45 years, and by Japan in 2000 at about 85 years – a near doubling of life expectancy (Figure 1.1a) (Sierra et al., 2009). The magnitude of increase over the past two centuries is even greater when taking the global mean life expectancy: from about 25 years to 70 in women and 65 in men (Riley, 2001). This increase was primarily attributable to reductions in early-life mortality during the 19<sup>th</sup> and early 20<sup>th</sup> centuries, particularly from infant mortality and infectious diseases, through improvements in medicine, public healthcare, education, and economic welfare (Riley, 2001). In contrast, late-life mortality remained relatively static, reflecting a slower improvement in our ability to prevent and treat age-related diseases. The result was a redistribution of mortality into later ages but compressed against a stable age of maximum lifespan – a phenomenon known as "rectangularisation" of the survival curve (Figure 1.1b) (Fries, 1980, Riffe et al., 2020).

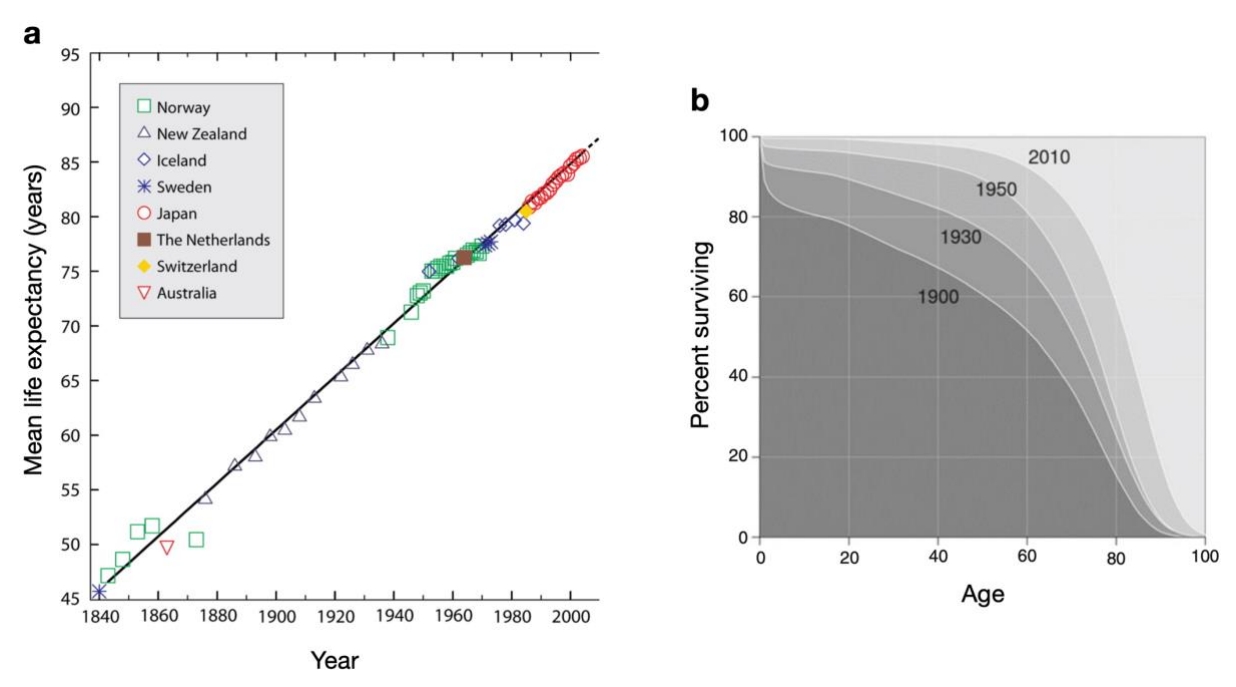


**Figure 1.1. Human mortality transitions over the years.** (a) Female life expectancy by record-holding countries from 1840 to 2000. Adapted from Sierra et al. (2009). (b) Survival curves of Swedish males dying in different years. Adapted from Riffe et al. (2020).

Rectangularisation has been viewed by some as suggestive of an upper limit to human longevity, consistent with the exponential rate of mortality increase described by Gompertz (Fries, 1980). However, since the second half of the 20<sup>th</sup> century, advances in medicine and

public health, specifically concerning age-related disease, have increased lifespan of those already longest-lived (Bongaarts, 2005, Christensen et al., 2009, Bergeron-Boucher et al., 2015), alongside continuing, but slowing reductions of early-life mortality (Christensen et al., 2009). This caused a different transformation of the survival curve: a shifting towards older ages, with little change in the variation of mortality ages, such that maximum lifespan also increased. This effect is visible in Figure 1.1b between the survival curves of 1950 and 2010.

In addition to increasing maximum lifespans, a deceleration of mortality rate increase has been observed at very old ages in some human populations (Vaupel et al., 1998). This is visible as a longer survival curve tail, which increases maximum lifespan. However, whether this observed deceleration reflects a slowing of biological ageing rate remains a topic of debate (Vaupel et al., 1998, Gavrilova and Gavrilov, 2014).

# 1.4 – Mortality patterns in Caenorhabditis elegans

Half a century ago, Sydney Brenner proposed to further develop the nematode worm Caenorhabditis elegans as a model organism for understanding the genetic basis of eukaryotic biology, particularly in relation to development and behaviour (Brenner, 1974). Since then, C. elegans has been applied to many other areas of biological research. For instance, it was used to develop RNA interference for gene silencing (Fire et al., 1998), GFP as an in-vivo biomarker (Martin et al., 1994), in the discovery of apoptosis genes (Hedgecock et al., 1983, Ellis and Horvitz, 1986), and was the first animal to have its entire genome sequenced (C. elegans Genome Consortium, 1998). C. elegans has also been a pioneering model in ageing research, in particular with the discovery of single gene mutations that greatly extend lifespan (Klass, 1983, Kenyon et al., 1993). Alongside dissection of the genetic regulation of nematode lifespan, molecular, anatomical and behavioural changes during ageing in C. elegans have also been characterised (Herndon et al., 2002, Zhao et al., 2017, Wang et al., 2018, Ezcurra et al., 2018, Son et al., 2019). These investigations have been aided by properties of *C. elegans* biology that render it ideal for biogerontological research, including a short lifespan (~20 days at 20°C), prolific reproductive output of hermaphrodites, population isogeneity and lack of inbreeding effects, ease of mass culture (~1 mm long, cultured on inexpensive agar-containing Petri dishes), and a transparent body (facilitating visualisation of internal anatomy and fluorescent markers).

Like in humans, the mortality rate of *C. elegans* has been found to increase exponentially during adulthood (Johnson, 1987). The ease of genetic, environmental and

pharmacological manipulation in this organism has allowed many studies to relate the Gompertz model parameters to specific culture or treatment conditions. For instance, compared to wild-type nematodes, long-lived insulin/IGF-1 signalling (IIS) pathway mutants typically exhibit a smaller  $\beta$  parameter value, reflecting a slower exponential increase in mortality rate (Johnson, 1990, Samuelson et al., 2007). In contrast, longevity from mild heat shock results from a smaller  $\alpha$  parameter value only, reflecting a postponement of mortality without change in the rate of exponential increase (Wu et al., 2008). The effects of different factors on the Gompertz parameters, particularly temperature, infection, and IIS, will be investigated in detail in Chapters 3–5.

Interestingly, most but not all life-extending conditions for *C. elegans* appear to reduce the rate of mortality rate increase ( $\beta$ ); the remainder increase lifespan by reducing the scale of mortality rate increase ( $\alpha$ ) (Yen et al., 2008, Hughes and Hekimi, 2016). This is in contrast to rodents (Yen et al., 2008, Hughes and Hekimi, 2016) and possibly humans (Finch, 1990), where longevity typically involves reductions in  $\alpha$  only, although this is controversial (de Magalhães et al., 2005, Simons et al., 2013). What this flexibility in reduction of both  $\alpha$  and  $\beta$  in *C. elegans* reflects about its ageing process and response to interventions remains unclear.

Although mortality rates rise exponentially during ageing in wild-type *C. elegans*, it has been widely recognised that this rise more accurately occurs in two phases, the first having a higher rate of increase than the second (Brooks et al., 1994, Johnson et al., 2001, Chen et al., 2007, Davies et al., 2015). This has been likened to the late-life mortality deceleration observed in other species, although in *C. elegans* the deceleration occurs much earlier, at around half the age of maximum lifespan. This deceleration has been proposed to result from intrapopulation heterogeneity, where the mixing of subpopulations with different mean lifespans can create the illusion of mortality deceleration (Brooks et al., 1994). More recently, this hypothesis was supported by the identification of two pathologically-distinct subpopulations (with and without pharyngeal infection); the shorter- and longer-lived subpopulations producing the first and second phases of the combined mortality rate trajectory, respectively (Zhao et al., 2017). However, in another study, preventing infection did not reduce the two stages to one (Baeriswyl et al., 2010), suggesting that other forms of heterogeneity, or entirely unrelated mechanisms, could also exist.

The presence of distinct mortality phases in *C. elegans* ageing has led some authors to prefer modelling nematode mortality with models that account for heterogeneity and/or mortality deceleration, such as the two-stage Gompertz, Weibull, and logistic family models (Vanfleteren et al., 1998, Johnson et al., 2001, Mulla et al., 2023). An alternative method is to deconvolve populations into subpopulations (Zhao et al., 2017), where possible, and perform

Gompertz modelling on the subpopulations separately. In some analyses described in this thesis, I will use this latter approach. However, where analysing full (non-deconvolved) populations, I will also use the Gompertz model, for several reasons: (1) a key aim is to explain the Gompertz parameters of full populations in terms of subpopulation heterogeneity, (2) the Gompertz model is sufficient to capture the major trends of nematode mortality, (3) the fewer parameters in the Gompertz model facilitates interpretation of potential biological mechanisms, (4) use of one model streamlines comparison and interpretation of model parameters between different populations, (5) the experimental protocols performed utilise smaller population sizes, which are more suited for modelling by models with fewer parameters, which give less weight to local noise. Additionally, I will show in Chapter 3 that the Gompertz model provides a strong empirical fit to the populations within my dataset.

# 1.5 – Between biological and demographic ageing

A primary objective of describing mortality rate data with mortality models is to discover biological information about the ageing process (which generates the observed mortality patterns). Indeed, Gompertz alluded in general terms, to a potential biological origin for his observed mortality pattern, writing that "if mankind be continually gaining seeds of indisposition, or in other words, an increased liability to death[,]... it would follow that the number of living... would decrease in a greater ratio than the geometrical progression" (Gompertz, 1825).

However, deriving biological truths about the ageing process from demographic mortality data is no simple task. Critically, in any attempt to do so, it must be acknowledged that the latter quantifies the timing of death (i.e. lifespan), whereas the desired former is about the ageing process *before* death. Additionally, demographic ageing (mortality rate) is a population-level property that emerges only in the presence of multiple individuals, whereas biological ageing is an individual-level property that exists *within* each individual of the population. These differences mean that demographic ageing is an *indirect* metric of biological ageing, and one that must rely on relatively strict assumptions: in particular, that there is little inter-individual variation in the ageing process, in exposure to lifespan interventions, and in responses to these interventions. However, as widely recognised and as I will demonstrate throughout this thesis, it is rarely true of real populations that they are so ideally homogeneous.

This distinction and gulf between demographic and biological phenomena are generally well-understood amongst biodemographers and statisticians working on (primarily human)

ageing (Vaupel and Yashin, 1985, Wilmoth and Horiuchi, 1999, Finkelstein, 2012), as well as other topics (van de Pol and Verhulst, 2006, Robinson, 2009). This view has been helpfully communicated in various forms, for instance: "for testing predictions about the 'rate of ageing' a distinction is made between biological and demographic (or actuarial) ageing" (Burger and Missov, 2016), "ageing rate based on the Gompertz slope parameter is often called an actuarial ageing rate in order to discriminate it from the true ageing rate related to the loss of function" (Gavrilov and Gavrilova, 2022), and "equating the demographic ageing rate of a population with the risk for individuals that compose is an ecological fallacy" (Hawkes et al., 2009).

However, this awareness of the complex relationship between demographic and biological ageing appears to be less well represented in broader biogerontology, particularly in model organism research. It is common practice to infer or even conclude biological properties about experimental populations, based solely upon their mortality rate trajectories. In section 2.3, I compile from a literature survey a representative list of studies that use the Gompertz parameters in this manner to draw conclusions about the biological ageing processes of their experimental model organism populations. This practice becomes of concern primarily due to the absence of empirical support for these now-widespread biological interpretations of mortality model parameters.

A possible origin of these issues is the interdisciplinary disconnect between gerodemographers and biogerontologists. Both disciplines attempt to understand the biology of ageing, but through different methodologies: addressing demographic ageing and biological ageing, respectively. Given the salient role of lifespan data in both disciplines, but more thorough understanding of its study in gerodemography, biogerontologists (i.e. biologists) may have attempted to adopt this demographic methodology with limited transfer of its conceptual foundations. Meanwhile, lesser access to biological (e.g. molecular and cellular) methodologies amongst gerodemographers may explain the scarcity of empirical attempts to confirm traditional biological interpretations of mortality model parameters. Similarly, the biogerontology field's preoccupation with biological data collected prior to death may have precluded simultaneous, time-consuming collection of lifespan data. These factors may have culminated in the present state of affairs: the commonplace interpretation of biological ageing from demographic ageing data, based on largely theoretical, unvalidated assumptions.

With limited data on the biological ageing of populations undergoing demographic mortality analysis, how are biological interpretations of these mortality patterns formed? Since Gompertz's description of exponentially increasing human mortality rates, many attempts at explaining this particular mortality pattern have been made. Some ideas emerged from the evolutionary biology of ageing: mutation accumulation and antagonistic pleiotropy resulting from Haldane's selection shadow are predicted to sharply raise mortality rates following the onset of reproduction (Vaupel, 1997, Yashin et al., 2000). However, neither theory predicts that this increase must be exponential, and caveats have been raised about the veracity of such causes of observed mortality rate accelerations (Partridge, 1997).

More mechanistic theories have also been put forward to explain Gompertzian mortality patterns. Numerous mathematical models, based on specific assumptions about individuals' physiology, some of which are supported by empirical data, have been developed. These include models that attribute exponentially increasing mortality to declining homeostatic capacity (ability to resist physiological fluctuations) (Strehler and Mildvan, 1960, Sacher and Trucco, 1962, Atlan, 1968), and mortality from wear-and-tear dynamics inspired by reliability theory (Gavrilov and Gavrilova, 2001), amongst others. Other physiological models have also been developed to explain more complex mortality models, such as those that incorporate late-life mortality decelerations and rectangularisation dynamics. For example, frailty models account for heterogeneity within populations (Vaupel et al., 1979), while phase-type distribution models and repair capacity models account for improvements in survival probability during ageing (Aalen, 1995, Yashin et al., 2000); these models can all to some extent explain mortality deceleration at very late ages.

Despite the increasingly complex physiological models now available to explain mortality rate patterns, their biological relevance remains uncertain and speculative. Indeed, any number of such models could theoretically recreate a given mortality distribution. An important limitation to developing biologically informed physiological models and mortality models, may be the biogerontological field's own uncertainty about the causes and mechanisms of ageing (Gems and de Magalhães, 2021), which would preclude development of appropriate model assumptions and collection of appropriate empirical data. For instance, proponents of a programmatic ageing paradigm may argue that many older models, based on the damagemaintenance paradigm, may be too specific (or tangential) to capture the determinants of mortality patterns.

Nonetheless, with improving understanding of the ageing process, researchers are now in a better position to develop and interpret biologically relevant models. An increasing number of studies are directly relating human mortality data to health data collected from the same populations. The majority of these studies compare mortality patterns between populations (or subpopulations) displaying different environmental, genetic or health profiles. For instance, medical records can be used to compare mortality patterns of patients living with or having died from different age-related diseases (Koopman et al., 2011, Koopman et al., 2015, Ismail et al., 2016) or to relate mortality parameters to metabolic rate trajectories in earlier life (Zuev et al., 2000). Similar approaches have been applied in model organisms. For instance, a recent study showed that in C. elegans, fruit flies, and mice, lifespan-extending interventions that steepen or shift the survival curve towards the right compress the mean population proportion of life spent in age-related decrepitude (Yang et al., 2025). This assessment was possible given the availability of health and lifespan data from the same individuals. Interestingly, another study using C. elegans directly compared mean population age-changes in health with the Gompertz parameters of those populations, reporting a disconnect between the two measures of biological ageing (Bansal et al., 2015).

However, these examples relate demographic ageing to population means of the relevant health measures, thus losing individual-level (i.e. biological) resolution and preventing a truly direct comparison of demographic and biological ageing. Such direct comparisons and their datasets are scarce, but on the rise in model organism research where the simultaneous, longitudinal collection and tracking of health and survival data for all population members is more practicable. Notably, these studies have mostly emerged outside of traditional gerodemography. Amongst others, they involve the longitudinal tracking of individual ageing rates and characterisation of within-population heterogeneity in senescent pathologies and ageing rates (Zhang et al., 2016, Zhao et al., 2017, Karin et al., 2019, Oswal et al., 2022, Zane et al., 2023, Yang et al., 2023, Eder et al., 2024). Adopting these individual-centric principles to interrogate mortality rates should prove fruitful for uncovering their biological bases.

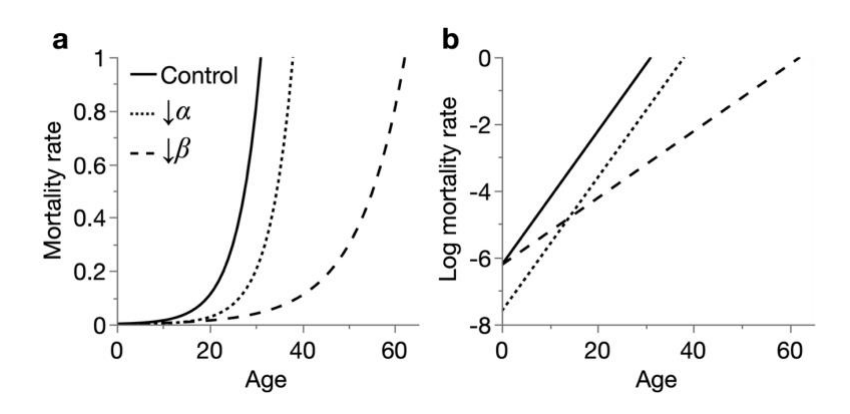
# Chapter 2 – A conceptual study of Gompertzian mortality

# 2.1 – Mathematical properties of the Gompertz parameters

The most commonly encountered parameterisation of the Gompertz model within gerodemography (Eq. 1.1, presented again below), models mortality rates as an exponential function of two parameters, denoted by  $\alpha$  and  $\beta$ , with age x and Euler's constant e.  $\alpha$  behaves as a scale parameter, affecting the magnitude of mortality increase with age, whereas  $\beta$  behaves as a rate parameter, affecting the rate of this mortality increase with age.

$$\mu(x) = \alpha e^{\beta x} \qquad Eq. 1.1$$

One can simulate how the Gompertz parameters  $\alpha$  and  $\beta$  affect the shape of the exponential function and other associated demographic measures. Changes to  $\alpha$  and  $\beta$  are reflected as vertical (along the y-axis) and horizontal (along the x-axis) stretches/compressions, respectively, of the exponential mortality function (Figure 2.1a). A common way to more easily visualise these parameter changes is through the log-transformation of mortality rate, which linearises the exponential function. In this semi-logarithmic plot, changes in  $\alpha$  result in parallel shifts of the function, while changes in  $\beta$  alter its gradient (Figure 2.1b). Although a simple means to visually distinguish between  $\alpha$  and  $\beta$  effects, such log-transformed plots can be misleading and lead to improper parameter estimation (Eakin et al., 1995, Mueller et al., 1995, Shouman and Witten, 1995, Rozing and Westendorp, 2008), as I will discuss in more detail in the next section.



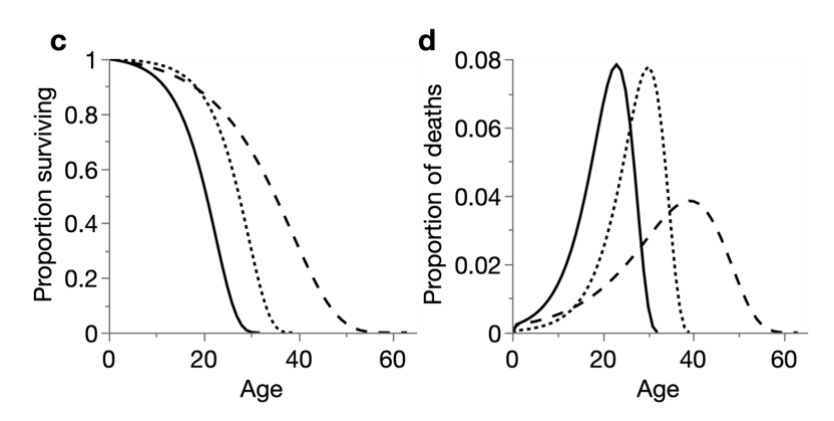


Figure 2.1. Effects of the Gompertz parameters on different demographic measures. Effects of reduction in  $\alpha$  or  $\beta$  on (a) mortality rate, (b) In-transformed mortality rate, (c) survival proportion, and (d) frequency distribution of deaths. In each panel, the Gompertz parameters values are: Control  $(\alpha, \beta: 0.002, 0.2)$ ;  $\downarrow \alpha$   $(\alpha, \beta: 0.0005, 0.2)$ ;  $\downarrow \beta$   $(\alpha, \beta: 0.002, 0.1)$ .

These Gompertz parameter changes may be more intuitively understood in terms of the equivalent survival function, which presents the data in a form more frequently encountered in lifespan studies, and from which the mortality data is derived. Here, changes to  $\alpha$  and  $\beta$  are reflected as approximate horizontal shifts and stretches/compressions, respectively, of the survival function (Figure 2.1c). Specifically, reductions in  $\alpha$  cause approximately parallel shifts of the survival curve towards the right (increasing lifespan), while reductions in  $\beta$  approximately stretch the survival curve along the (age) x-axis, leading to a greater extension of maximum than minimum lifespan. Throughout this thesis, I will predominantly understand and communicate about the Gompertz parameters in terms of their effects on the survival curve.

Finally, another way to represent mortality rate is as a mortality frequency distribution, which shows the concentration of deaths at different ages (Figure 2.1d). Populations with a Gompertzian mortality rate trajectory exhibit a mortality frequency distribution that roughly resembles a Gaussian distribution, but with a negative skew affecting the left tail. As in the survival curves, reductions in  $\alpha$  approximately shift the distribution towards later ages, whereas reductions in  $\beta$  stretch out the distribution considerably more, such that  $\beta$  is the primary determinant of lifespan variation (Tuljapurkar and Edwards, 2011). This correspondence between the Gompertz parameters (or any mortality model parameter) and lifespan variation will become a focal and recurring point in this thesis.

# 2.2 – Biological interpretation of the Gompertz parameters

In Chapter 1, I mentioned the gerodemography field's interest in explaining mortality models in terms of the underlying biology of ageing. Here, common biological interpretations of the

Gompertz model parameters are critically examined in greater detail, in preparation for the following chapters wherein the biological basis of the parameters will be experimentally investigated, and their traditional interpretations re-evaluated.

At their core, biological interpretations of the Gompertz parameters arise from their mathematical properties, and the biological intuitions associated with them. For instance, when age x is equal to zero, the Gompertz equation simplifies to  $\alpha$ , such that  $\alpha$  is in fact the y-axis intercept. Therefore,  $\alpha$  is often referred to as the initial mortality rate (IMR) (Finch, 1990). However, there can of course be no actual mortality at age zero, so  $\alpha$  is a theoretical approximation of mortality rate at the earliest age modelled, which is typically that of the onset of reproduction – when organisms are fully developed but not yet senescent. Because  $\alpha$  describes a mortality risk before the onset of ageing, this parameter has also been termed "intrinsic vulnerability" or "frailty", to denote a risk of death that occurs even in the absence of ageing (Sacher, 1977, Vaupel et al., 1979). For this reason,  $\alpha$  is sometimes considered to reflect the level of extrinsic mortality, such as deaths from infection, starvation, or injury.

On the other hand, as a measure of how rapidly mortality rate increases with age,  $\beta$  is widely interpreted to represent the rate of ageing and is also called "actuarial" or "demographic" senescence. In addition, mortality rate acceleration is sometimes expressed in a different form, as "mortality rate doubling time" (MRDT) (Eq. 2.1, derived from Eq. 1.1): the time taken for mortality rate to double, to allow comparison of ageing rates between populations in intuitive time units. For instance, MRDT of humans is about 8 years, but only 7 months for mice (Jones, 1956, Sacher, 1977). Therefore, in contrast to  $\alpha$  denoting extrinsic mortality,  $\beta$  is often thought to reflect levels of intrinsic mortality, specifically that arising from the internal and inevitable process of ageing.

$$MRDT = (\log_2 2)/\beta \qquad Eq. 2.1$$

However, this interpretation of  $\alpha$  and  $\beta$  as reflecting, respectively, extrinsic and intrinsic mortality has been criticised. For example, it was noted that deaths from causes typically considered extrinsic increase exponentially with age, just as they do for intrinsic deaths (Koopman et al., 2015). Furthermore, intrinsic and extrinsic mechanisms are highly interrelated in their contribution to age-related mortality. For instance, intrinsic immunological and neuromuscular ageing can increase susceptibility to death from infection and falls, while extrinsic pollutants and poor diets can promote pathogenesis of ageing-related cancers and cardiovascular disease (Koopman et al., 2015). This lack of clear distinction between extrinsic and intrinsic mortality suggests that there is no good basis for assigning  $\alpha$  and  $\beta$  to them,

respectively. Consistent with this, a somewhat common misconception promoting this assignment – that  $\alpha$  is age-independent, has been acknowledged and refuted elsewhere (Rozing and Westendorp, 2008). As  $\alpha$  varies, the resultant effect on mortality rate increases at a greater-than-linear rate with age, not unlike when  $\beta$  varies. This is illustrated in Figure 2.2a, which shows the differences in mortality rate across age, when each parameter is independently varied. This shows that only mortality described by the third parameter of the Gompertz-Makeham model (Eq. 1.2),  $\gamma$ , is truly age-independent.

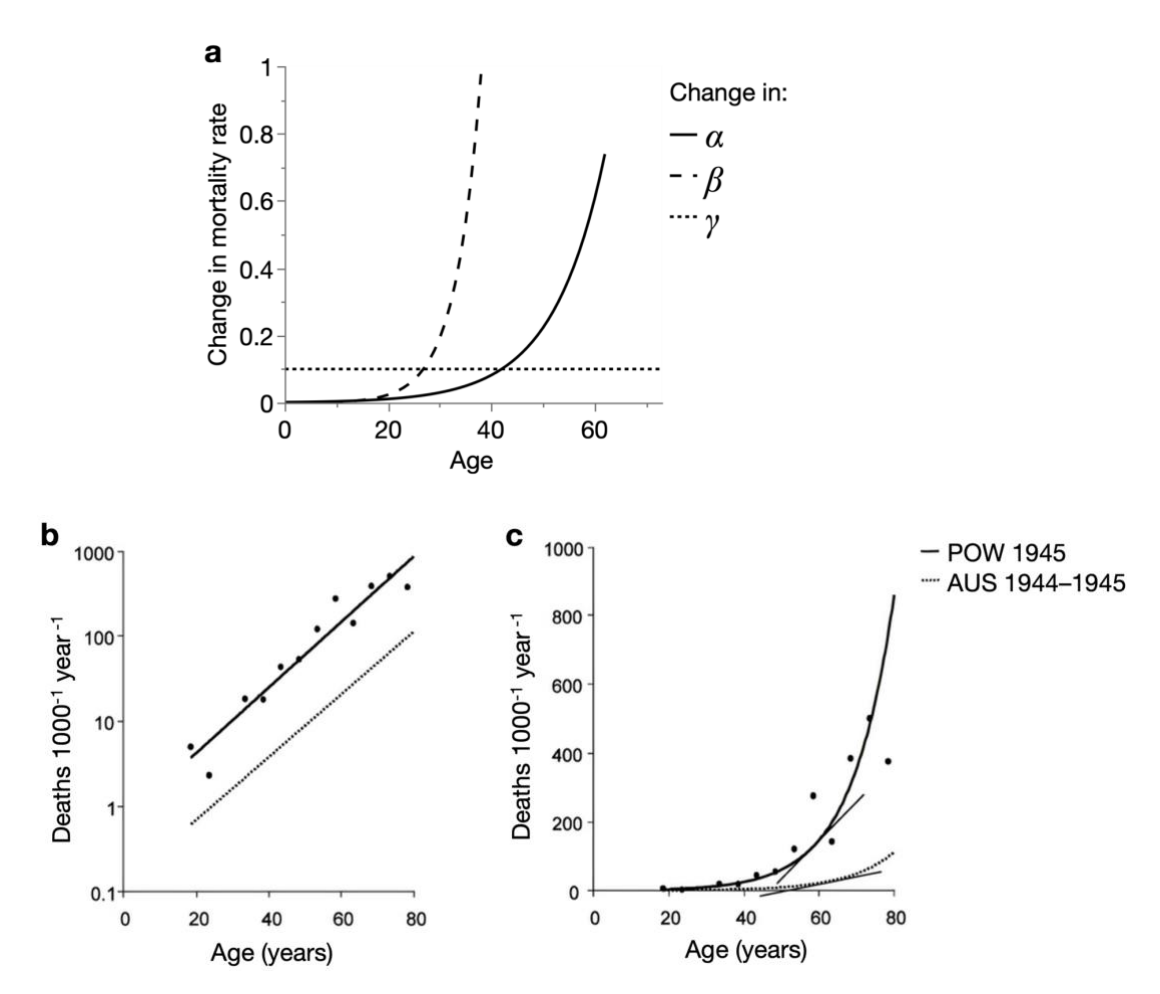


**Figure 2.2.** The scale parameter  $\alpha$  is not age-independent. (a) Age pattern of change in mortality rate when  $\alpha$ ,  $\beta$ , or  $\gamma$  are independently varied, obtained by subtracting mortality rates of a control population ( $\alpha$ =0.0005,  $\beta$ =0.1,  $\gamma$ =0) from one with a higher  $\alpha$  (solid line;  $\alpha$ =0.002,  $\beta$ =0.1,  $\gamma$ =0), higher  $\beta$  (dashed line;  $\alpha$ =0.0005,  $\beta$ =0.2,  $\gamma$ =0), or higher  $\gamma$  (dotted line;  $\alpha$ =0.0005,  $\beta$ =0.1,  $\gamma$ =0.1). (b) Log-transformed and (c) absolute mortality rates of Australian civilians (AUS) and prisoners of war (POW); adapted from Rozing and Westerndorp (2008), originally from Finch (1990).

One contributor to the misconception that  $\alpha$  is age-independent was proposed to be the practice amongst many gerodemographers to present Gompertzian mortality rate data with a logarithmic y-axis, such that the data fall along a straight line and can be modelled by least-squares linear regression (Sacher, 1977, Rozing and Westendorp, 2008). In this format, effects

of  $\alpha$  and  $\beta$  on mortality are simple to visualise:  $\alpha$  controls the position of the line, while  $\beta$  controls its gradient, as introduced in the previous section (Figure 2.1b, p. 25). A frequently cited example to illustrate this is a comparison of mortality rates between Australian civilians and Australian prisoners of war detained in concentration camps towards the end of the Second World War (Finch, 1990). Here, when plotted with a logarithmic mortality rate axis, the two populations form parallel lines, indicating constancy of  $\beta$  and change in only  $\alpha$  (Figure 2.2b). With this representation, one may mistakenly conclude that the higher  $\alpha$  of the prisoner cohort increases mortality rate equally across all ages (i.e. age-independent), but of course, the y-axis is logarithmic and the increase is far greater at older ages, as revealed by using an absolute y-axis scale (Figure 2.2c).

Rozing and Westerndorp (2008) argue that this reveals a fundamental flaw of the classical interpretations of  $\alpha$  as "not ageing" and  $\beta$  as "ageing", in addition to that of intrinsic versus extrinsic mortality. That  $\alpha$  is age-dependent, like  $\beta$ , suggests that it too models ageing, and if this is true, then the inability of  $\beta$  to capture  $\alpha$ -only effects (as in the above example) suggests that  $\beta$  is an inappropriate measure of ageing. Furthermore, the authors point out that any population only has one  $\beta$  value across all ages, which produces the potentially illogical conclusion that young and old individuals share the same rate of ageing. Although this is a clear conflation of demographic and biological ageing, it is possible that the authors use this extreme example to emphasise the overall ecological fallacy of attributing  $\beta$  to biological ageing rate. That said, they propose an alternative measure of ageing rate: the derivative of the Gompertz function (i.e. age-specific rate of change in mortality increase), which although likely more biologically relevant, remains an indirect measure of the ageing process. Notably, the conventional designation of  $\beta$  as the rate of ageing has also been criticised elsewhere (Driver, 2001, Yashin et al., 2002b, Driver, 2003, Rozing and Westendorp, 2008, Koopman et al., 2011, Hughes and Hekimi, 2016).

The uncertainty surrounding interpretation of the Gompertz parameters often goes unnoticed, and many researchers continue to use the classical interpretation ( $\alpha$ : "not ageing",  $\beta$ : "ageing") to draw conclusions about their data (see the next section for a literature survey of relevant studies). Another obstacle to reconciling gerodemography with biology, is a methodological weakness of modelling log-transformed mortality data. It is now widely accepted that performing least squares linear regression on such data leads to poor estimation of model parameters (Eakin et al., 1995, Mueller et al., 1995, Shouman and Witten, 1995). Better alternatives are non-linear regression and maximum likelihood estimation (MLE) on untransformed data, the latter of which is usually considered the gold standard (Pletcher, 1999, Yen et al., 2008). For this reason, mortality model fitting performed within this thesis will use

the MLE method (Pletcher, 1999). Similarly, instead of presenting data visually as log-mortality over age, I will show the equivalent survival curves (Figure 2.1c, p. 25), which I believe provide a more intuitive and biologically relevant view of the associated mortality model parameters.

An advantage of working from survival rather than mortality graphs, is that the former allows one to easily visualise the lifespan of every individual within a population and the rate at which they die as a population (by the slope of the survival curve). In contrast, mortality rate is a more abstract entity, especially as it is proportional to immediate population size (which changes as individuals die), rather than starting population size. A simple example of the intuitiveness of the survival plot, is that transformations of the survival function resulting from alterations in  $\alpha$  and  $\beta$  offer clues for underlying mechanisms, even without knowledge of the population's health structure. Changes in  $\alpha$  result in approximately parallel horizontal shifts of the survival function, indicating an advancement or postponement of all deaths within the population by the same additive factor, irrespective of survival time in the original population (Figure 2.3). On the other hand, changes in  $\beta$  result in an approximate horizontal stretch or compression of the survival curve, indicating advancement or postponement of deaths by a magnitude related (by a multiplicative factor) to survival time in the original population. One interpretation could therefore be that changes in  $\alpha$  and  $\beta$  reflect distinct biological effects, that respectively, do not and do interact with other lifespan-determining mechanisms.

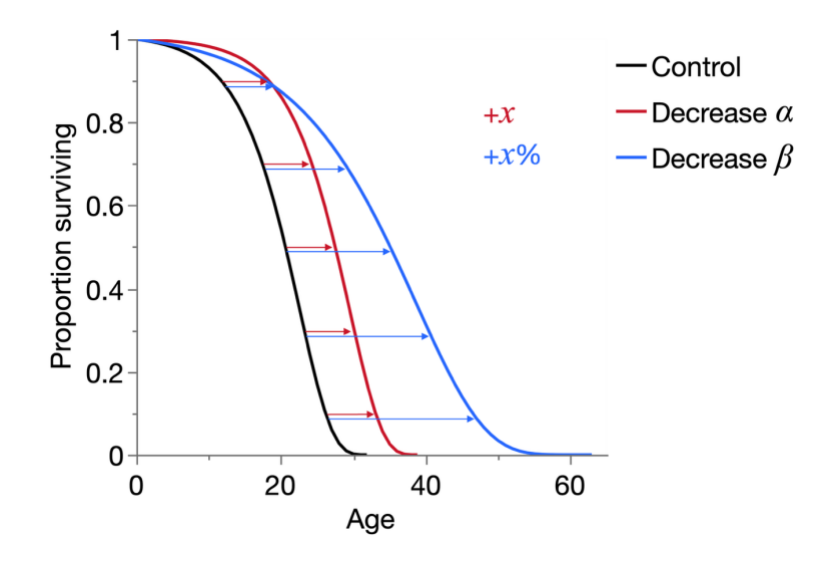


Figure 2.3.  $\alpha$  and  $\beta$  have distinct effects on lifespan. Changes in  $\alpha$  resemble (approximately) changes in lifespan of all individuals by an additive factor unrelated to original lifespan, whereas changes in  $\beta$  resemble (approximately) changes in lifespan of all individuals by a multiplicative factor.

Another way to conceive the above is that  $\beta$  reflects the degree of heterogeneity in individual ageing trajectories, given that it reflects the degree of lifespan variation (to a far greater extent than  $\alpha$ ) (Figure 2.1d, p. 25).  $\beta$  changes may therefore reflect differential effects

on different individuals within a population, such that they become more similar or dissimilar to one another in their survival time. In contrast,  $\alpha$  changes, which have smaller effects on lifespan variation, could reflect more similar effects on all individuals.

In summary, numerous biological interpretations of the Gompertz parameters have been proposed (Olshansky and Carnes, 1997, Kirkwood, 2015), yet most are theoretical in origin, and cogent critiques of them remain unaddressed by the wider field. In this thesis, I argue that truly informative biogerodemography requires approaches that emphasise the collection of biological information, particularly at the individual as well as the population level. In Chapters 3–6, I will demonstrate using *C. elegans* data, approaches that capture both survival and health data from the same populations, and associated analyses that allow one to draw experimentally-grounded biological interpretations of their Gompertz parameters. My findings and their implications are summarised in Chapter 6; in particular, Figure 6.1 (p. 155) in section 6.2.

# 2.3 – A literature survey of interpretations of the Gompertz parameters

To better understand the current biological interpretations of the Gompertz parameters, I conducted a survey of the literature from the past quarter century, focusing on model organism studies using the Gompertz parameters since the year 2000 (Table 2.1). These studies explore Gompertz parameter differences between different populations to evaluate the effects of interventions (e.g. drugs, environment, genetics) on the ageing process. This list currently includes 71 studies on over 23 species and is by no means exhaustive of the full relevant literature published during this period. In addition, the list excludes studies from the vast and older human literature, which deserve their own separate survey. Furthermore, the list excludes studies using mortality models outside of the immediate Gompertz family of models. Thus, this compilation of studies is intended to provide an objective overview of current and recent views about the Gompertz parameters in experimental gerodemography, as a representative snapshot of perspectives across the wider biogerodemography field.

Organism	Intervention or difference between populations	Reported effect on α	Authors' interpretation of effect on α	Reported effect on $\beta$	Authors' interpretation of effect on β	Reference
Rat, fruit fly	Dietary restriction, reduced temperature, selection for	Intervention/ organism- specific	Change in "baseline mortality" or susceptibility to early-life-specific mortality	Intervention/ organism- specific	Change in ageing rate	(Pletcher et al., 2000)

	longevity, inbreeding					
Fruit fly	Light exposure regimes	Regime- specific	Change in "age- independent mortality" or "early life mortality"	Regime- specific	Change in ageing rate	(Sheeba et al., 2000)
Fruit fly	Genetic reduction of IIS	Genotype- specific	Change in level of "premature mortality" or "sickness"	Genotype- specific	Change in ageing rate	(Clancy et al., 2001) <sup>c</sup>
Mouse	Genetic perturbation of growth hormone production	Decreased (visual assessment of log- mortality plots)	Delayed "effects of aging on lethal illness"	Unchanged (visual assessment of log- mortality plots)	Unchanged rate of increase in "effects of aging on lethal illness"	(Flurkey et al., 2001)
Nematode	Various genetic interventions (age-1, clk-1, spe-26)	Intervention- specific	No biological interpretation given	Intervention- specific	Change in ageing rate, possibly rate of "accumulation of toxic gene products"	(Johnson et al., 2001) <sup>a</sup>
Baboon	Inter-population differences	Population- specific	Change in "frailty" and "vulnerability"	Population- specific	Change in "demographic ageing rate", but implication of (biological) ageing rate	(Bronikowsk i et al., 2002)
Nematode	Hyperoxia	Unspecified	N/A	Decreased	Decreased ageing rate	(Honda and Honda, 2002)
Fruit fly	Species differences	Sex- dependent	"Baseline intrinsic mortality rate"	Sex- dependent	Change in ageing rate, although also referred to as "demographic ageing rate"	(Promislow and Haselkorn, 2002) <sup>c</sup>
Fruit fly	Antioxidant enzyme (MSRA) overexpression	Decreased	"Delayed onset of the mortality factors determining control lifespan"	Unspecified	N/A	(Ruan et al., 2002)
Fruit fly	Genetic reduction of IIS (chico mutations)	Sex- dependent	Change in level of "frailty"	Decreased	Decreased ageing rate, although also referred to as "demographic ageing rate"	(Tu et al., 2002)
Mouse	Antidiabetic biguanide treatment (phenformin and buformin)	Unspecified	N/A	Decreased	"Decreased demographic/popul ation ageing rate", but strong interpretation of decreased ageing rate	(Anisimov et al., 2003)
Fruit fly	Dietary restriction,	Intervention- specific	Change in "short-term risk of death"	Intervention- specific	Change in ageing rate, specifically "rate of	(Mair et al., 2003)

	reduced temperature				accumulation of aging-related	
F'+ (I	T. 1	TT. 1 1	NI. 1 1.1 1 1	D1	damage"	(M 1
Fruit fly	<i>Indy</i> mutation	Unchanged	No biological interpretation given	Decreased	Decreased ageing rate	(Marden et al., 2003)
Kissing	Sex difference	Unspecified	No biological	Increased (in	No biological	(Chaves et
bug	Sex difference	Olispecified	interpretation given	females)	interpretation given	al., 2004)
Bighorn	Sex difference,	Intervention-	Changes in	Intervention-	Change in ageing	(Gaillard et
sheep, roe	species	specific	extrinsic mortality	specific	rate	al., 2004)
deer	difference	Specific	(suggestion of	specific		di., 2001)
			dangerous mating			
			rituals and			
			associated energy			
			expenditure)			
Fruit fly	Dietary	Decreased	Decreased "initial	Sex-specific	No biological	(Magwere et
	restriction		intrinsic baseline		interpretation given	al., 2004)
			mortality rate"			
Nematode	RNAi of	Genotype	No biological	Genotype	No biological	(Ayyadevara
	glutathione	and	interpretation given	and	interpretation given	et al., 2005)
	transferase	environment		environment		
	CeGSTP2-2	-specific		-specific		
		(note		(note		
		statistical significance		statistical significance		
		unclear)		unclear)		
Fruit fly	Dietary	Unchanged	Unchanged "short-	Decreased	Decreased ageing	(Bross et al.,
Truit Hy	restriction	Chenangea	term risk"	Beereasea	rate	2005)
African	Sex difference	Unchanged	No biological	Unchanged	No biological	(Fonseca et
migratory			interpretation given		interpretation given	al., 2005) <sup>c</sup>
locust						
Mouse, rat	Various genetic	Intervention/	Change in age-	Intervention/	Change in ageing	(de
	interventions	organism-	independent	organism-	rate	Magalhães
	(~24)	specific	mortality, possibly	specific		et al., 2005)
			ageing-independent			
3.6	D' -	T	disease	T	CI :	(D
Mouse, rat	Dietary	Intervention/	Change in "acute risk of death"	Intervention/	Change in ageing	(Partridge et
	restriction	organism- specific	risk of death	organism- specific	rate	al., 2005)
Mouse	Mitochondrial	Decreased	Delayed onset of	Unchanged	No biological	(Schriner et
Wiouse	catalase	Decreased	ageing	Onenanged	interpretation given	al., 2005)
	overexpression		agemg		interpretation given	di., 2005)
Fruit fly	Natural genetic	Intervention-	Change in "baseline	Intervention-	Change in ageing	(Spencer and
,	variation,	specific	mortality rate" or	specific	rate	Promislow,
	genetic		"frailty"			2005)
	interactions, sex					
Mouse	Reduced core	Decreased	Decreased "ageing-	Unchanged	No biological	(Conti et al.,
	body		related frailty"		interpretation given	2006)
	temperature					
Mouse	Dietary	Increased	No biological	Decreased	Indirect statement	(Harper et
	restriction		interpretation given		of decreased ageing	al., 2006)
E '. A	NT / 11	D.1	C1	D 1	rate	(3.5.1.1.1
Fruit fly	Naturally ·	Polymorphis	Change in "frailty"	Polymorphis	Change in ageing	(Maklakov
	occurring	m-specific		m-specific	rate	et al., 2006)
	mitochondrial					

	DNA polymorphisms					
Nematode	Dietary restriction	Unspecified	N/A	Decreased	Decreased ageing rate, probably "slowed accumulation of molecular damage"	(Lenaerts et al., 2007)
Nematode	Altered IIS (genetic and RNAi)	Intervention- specific	Change in "risk of death throughout life" or "period of time prior to the onset of ageing" or "sickness"	Intervention- specific	Change in ageing rate	(Samuelson et al., 2007)
Alpine ibex	Sex difference	Modelling method- specific	Changes in extrinsic mortality (suggestion of dangerous mating rituals and associated energy expenditure)	Modelling method- specific	Change in ageing rate, and "intensity" of ageing	(Toïgo et al., 2007)
Fruit fly	Reduction of dietary protein to carbohydrate ratio	Decreased	No biological interpretation given	Decreased	Decreased ageing rate	(Lee et al., 2008) <sup>g</sup>
Nematode	T08D10.2 RNAi (to mimic lithium treatment)	Decreased	"Delayed onset of aging or lowered intrinsic mortality"	Unchanged	No biological interpretation given	(McColl et al., 2008)
Nematode	Early life heat shock	Heat shock severity- dependent	No biological interpretation given besides response to environmental stress	Heat shock severity- dependent	Change in ageing rate	(Wu et al., 2008)
Mouse, rat, nematode	Various genetic interventions (>20), dietary restriction, dietary restriction, reduced temperature, reduced IIS	Intervention/ organism- specific	Change in extrinsic hazard or "general physiologic robustness"	Intervention/ organism- specific	Change in ageing rate	(Yen et al., 2008)
Mouse	Mild impairment of mitochondrial respiration	Unspecified	N/A	Decreased	Decrease ageing rate	(Lapointe et al., 2009)
Fruit fly	Germline ablation	Decreased	Increased "beneficial effect on survival that is constant over the adult lifespan"	Unchanged	No biological interpretation given	(Shen et al., 2009) <sup>c</sup>
Nematode	Multiple heat shocks throughout life	Decreased	No biological interpretation given besides response to	Decreased	Decreased ageing rate	(Wu et al., 2009a)

			environmental			
Nematode	Reduced temperature, dietary restriction, altered IIS	Intervention- specific	Change in mortality "risk that is determined by current environment and genes"	Intervention- specific	Change in ageing rate	(Wu et al., 2009b)
Nematode	Reduced temperature, dietary restriction	Intervention and genotype- specific	No biological interpretation given	Intervention and genotype- specific	Change in "senescence"	(Yen and Mobbs, 2009)
Black field cricket	Sex difference	Decreased (in females)	Decreased "background mortality"	Unchanged	Unchanged rate of ageing	(Zajitschek et al., 2009)
Nematode	Altered (dietary/environ mental) bacterial pathogenicity	Bacterium- specific	No biological interpretation given	Bacterium- specific	Change in ageing rate	(Baeriswyl et al., 2010) <sup>a</sup>
Mouse	Mild impairment of mitochondrial respiration	Increased	Increased "intrinsic vulnerability to death"	Decreased	No biological interpretation given	(Hughes and Hekimi, 2011)
Mouse	Rapamycin treatment	Decreased	Rapidly decreased age-specific mortality	Decreased	No biological interpretation given	(Miller et al., 2011)
Fruit fly	Antioxidant (SkQ1) treatment	Decreased	Increased "quality of life", and "positive impact at an early age"	Increased	Unspecified, although conclusion of decreased ageing rate from increased slope of linear regression of $ln(\alpha)$ over $\beta$	(Krementsov a et al., 2012)
Mouse, rat, fruit fly, nematode, yeast	Dietary restriction	Intervention/ organism- specific	Change in age- independent mortality rate	Intervention/ organism- specific	No biological interpretation given	(Nakagawa et al., 2012)
Blowfly	Ambient temperature	Temperature regime-specific	No biological interpretation given	Temperature regime- and life-stage- specific	Change in ageing rate	(Shahrestani et al., 2012) <sup>a</sup>
Dog	Increased body size	Increased	Increased extrinsic- type mortality (suggestions of orthopedic diseases and growth-related degeneration.	Increased	Increased ageing rate	(Kraus et al., 2013)
Seed beetle	Paraquat stress	Increased	Increased "basal vulnerability to stresses"	Unchanged	Unchanged ageing rate, and "rate of increase in stress vulnerability"	(Lazarević et al., 2013)

Mouse, rat	Dietary	Intervention/	Change in	Intervention/	Change in ageing	(Simons et
	restriction	organism-	"vulnerability to the	organism-	rate	al., 2013)
		specific	ageing process"	specific		
Killifish	N. kunthae,	Decreased	No biological	Unchanged	Unchanged rate of	(Tozzini et
	compared to N.		interpretation given		ageing	al., 2013)
	furzeri					
Mosquito	Larval and adult	Temperature	No biological	Temperature	No biological	(Christianse
	ambient	-specific	interpretation given	-specific	interpretation given	n-Jucht et
	temperature					al., 2014)
Mouse	Rapamycin	Unchanged	No biological	Decreased	Decreased ageing	(Fok et al.,
	treatment		interpretation given		rate	2014)
Water flea	Level of	Intervention-	Change in ageing	Intervention-	Change in ageing	(Walsh et al.,
	extrinsic	specific	rate, but not	specific	rate, but not	2014) <sup>g</sup>
	mortality		specified whether		specified whether	
	(predation),		from $\alpha$ or $\beta$ , or		from $\alpha$ or $\beta$ , or	
	temperature		both.		both.	
Nematode	Various genetic	Intervention-	No biological	Intervention-	The authors argue	(Bansal et
	life-extending	specific	interpretation given	specific	that $\beta$ is a poor	al., 2015)
	interventions			(mostly	measure of ageing	
	(daf-2, ife-2,			decreased)	rate, by comparing	
	clk-1, eat-2)				$\beta$ changes to cross-	
					sectional health	
					changes	
Nematode	Genetic	Unspecified	N/A	Age-	Change in ageing	(Davies et
	reduction of IIS			dependent	rate	al., 2015) <sup>b</sup>
	(daf-2(m41))					
Water flea	Perceived threat	Species-	Change in ageing	Species-	Change in ageing	(Pietrzak et
	of predation	specific	onset age	specific	rate	al., 2015) <sup>d</sup>
Nematode	Mianserin	Age-	Change in "rate of	Age-	Change in rate of	(Rangaraju
	treatment	dependent	age-associated	dependent	"age-associated	et al., 2015) <sup>e</sup>
			physiological		physiological	
			change in young		change", and	
l l					change in mortality	
			adults"			
F 0					rate	(3)
Fruit fly	Trametinib	Decreased	Decreased	Unchanged	rate Unchanged	(Slack et al.,
Fruit fly	Trametinib treatment	Decreased	Decreased "demographic	Unchanged	rate Unchanged "duration of age-	(Slack et al., 2015)
Fruit fly		Decreased	Decreased "demographic frailty" and	Unchanged	rate Unchanged	
Fruit fly		Decreased	Decreased "demographic frailty" and "delayed onset of	Unchanged	rate Unchanged "duration of age-	,
Fruit fly		Decreased	Decreased "demographic frailty" and "delayed onset of mortality without	Unchanged	rate Unchanged "duration of age-	,
Fruit fly		Decreased	Decreased "demographic frailty" and "delayed onset of mortality without prolongation of the	Unchanged	rate Unchanged "duration of age-	
Fruit fly		Decreased	Decreased  "demographic frailty" and  "delayed onset of mortality without prolongation of the duration of age-	Unchanged	rate Unchanged "duration of age-	,
·	treatment		Decreased  "demographic frailty" and  "delayed onset of mortality without prolongation of the duration of age- related decline"		rate Unchanged "duration of age- related decline"	2015)
Mouse,	treatment  Various genetic	Intervention/	Decreased  "demographic frailty" and  "delayed onset of mortality without prolongation of the duration of age- related decline"  Change in "initial	Intervention/	rate Unchanged "duration of age- related decline"  Change in ageing	(Hughes and
·	treatment	Intervention/ organism-	Decreased  "demographic frailty" and  "delayed onset of mortality without prolongation of the duration of age- related decline"  Change in "initial vulnerability" or	Intervention/ organism-	rate Unchanged "duration of age- related decline"	(Hughes and Hekimi,
Mouse,	treatment  Various genetic	Intervention/	Decreased  "demographic frailty" and  "delayed onset of mortality without prolongation of the duration of age- related decline"  Change in "initial vulnerability" or  "aging-independent	Intervention/	rate Unchanged "duration of age- related decline"  Change in ageing	(Hughes and
Mouse,	treatment  Various genetic	Intervention/ organism-	Decreased  "demographic frailty" and  "delayed onset of mortality without prolongation of the duration of age- related decline"  Change in "initial vulnerability" or  "aging-independent physiological	Intervention/ organism-	rate Unchanged "duration of age- related decline"  Change in ageing	(Hughes and Hekimi,
Mouse, nematode	Various genetic interventions	Intervention/ organism- specific	Decreased  "demographic frailty" and  "delayed onset of mortality without prolongation of the duration of age- related decline"  Change in "initial vulnerability" or  "aging-independent physiological features"	Intervention/ organism- specific	rate Unchanged "duration of age- related decline"  Change in ageing rate	(Hughes and Hekimi, 2016)
Mouse, nematode Azara's	treatment  Various genetic	Intervention/ organism-	Decreased  "demographic frailty" and  "delayed onset of mortality without prolongation of the duration of agerelated decline"  Change in "initial vulnerability" or "aging-independent physiological features"  No biological	Intervention/ organism- specific	rate Unchanged "duration of age- related decline"  Change in ageing rate  No biological	(Hughes and Hekimi, 2016)
Mouse, nematode  Azara's owl	Various genetic interventions	Intervention/ organism- specific	Decreased  "demographic frailty" and  "delayed onset of mortality without prolongation of the duration of age- related decline"  Change in "initial vulnerability" or  "aging-independent physiological features"	Intervention/ organism- specific	rate Unchanged "duration of age- related decline"  Change in ageing rate	(Hughes and Hekimi, 2016)
Mouse, nematode  Azara's owl monkey	Various genetic interventions  Sex difference	Intervention/ organism- specific Unchanged	Decreased  "demographic frailty" and  "delayed onset of mortality without prolongation of the duration of agerelated decline"  Change in "initial vulnerability" or "aging-independent physiological features"  No biological interpretation given	Intervention/ organism- specific  Increased (in females)	rate Unchanged "duration of age- related decline"  Change in ageing rate  No biological interpretation given	(Hughes and Hekimi, 2016)  (Larson et al., 2016) <sup>d</sup>
nematode  Azara's owl	Various genetic interventions	Intervention/ organism- specific	Decreased  "demographic frailty" and  "delayed onset of mortality without prolongation of the duration of agerelated decline"  Change in "initial vulnerability" or "aging-independent physiological features"  No biological	Intervention/ organism- specific	rate Unchanged "duration of age- related decline"  Change in ageing rate  No biological	(Hughes and Hekimi, 2016)

	availability, and sex difference					
Fission yeast	N/A	Unspecified	N/A	Wholly decreased $(\beta \approx 0)$	No ageing	(Nakaoka and Wakamoto, 2017) <sup>h</sup>
Fruit fly, mouse	Mifepristone, p53 mutation, mTOR mutation, dietary restriction	Intervention/ organism- specific	Change in "health or vitality" and "environmental challenges"	Intervention/ organism- specific	Change in ageing rate, possibly of "accumulation of some as-yet unknown type of damage"	(Shen et al., 2017)
N/A	Fission yeast (vs budding yeast)	Unspecified	N/A	Wholly decreased $(\beta \approx 0)$	No ageing	(Spivey et al., 2017) <sup>h</sup>
N/A	Naked mole rat (vs other organisms)	Unspecified	N/A	Wholly decreased $(\beta \approx 0)$	No ageing	(Ruby et al., 2018) <sup>f</sup>
Mouse	IGF1 overexpression	Unchanged	No biological interpretation given	Increased	Increased ageing rate	(Anisimov et al., 2019)
Mouse	Polyphenol treatments	Polyphenol- specific	No biological interpretation given	Polyphenol- specific	Change in ageing rate	(Panchenko et al., 2019)
Mouse	Neonatal melatonin treatment	Unchanged	Unchanged "initial viability"	Unchanged	Unchanged ageing rate	(Yurova et al., 2019)
Mouse	Senolytic treatment	Decreased	No biological interpretation given	Increased	Increased "side effects", possibly "impaired damage repair capacity"	(Kowald and Kirkwood, 2021)
Fruit fly	Genetic variation (20 inbred strains from a single, original wild population)	Strain- specific	No biological interpretation given	Strain- specific	Change in ageing rate	(Zhao et al., 2022) <sup>c</sup>
Mouse	Dietary restriction regimes	Unspecified	N/A	Intervention- specific	Change in ageing rate	(Di Francesco et al., 2024)
N/A	Naked mole rat and Fukomys species (vs other organisms)	Unspecified	N/A	Wholly decreased $(\beta \approx 0)$	No biological interpretation given, but suggestion of "slow ageing (rate) mechanisms"	(Ruby et al., 2024) <sup>f</sup>

Table 2.1. Interpretations of the Gompertz parameters in model organism studies. A non-exhaustive list of model organism studies published since 2000 utilising the Gompertz (or Gompertz family, but excluding logistic) model, explicitly or implicitly (e.g. linear regression analysis of log-transformed mortality rates). Phrases within quotation marks may not match exactly with those in the articles, but have been presented as faithfully as possible, retaining key words and changing only grammar and syntax.

<sup>&</sup>lt;sup>a</sup> These studies used a two-stage Gompertz model.

<sup>&</sup>lt;sup>b</sup> This study compared  $\beta$  between a one stage (for control) and two stage (for *daf-2(m41)*) Gompertz model.

- <sup>c</sup> These studies used the Gompertz-Makeham model.
- <sup>d</sup> These studies used a different parameterisation of the standard Gompertz-Makeham model.
- <sup>e</sup> This study graphically compares the linear regressions of log-mortality rate over age, but conceptually interprets this analysis as though using a two stage Gompertz model, using day 12 of adulthood to separate early and later life.
- <sup>f</sup> These studies does not directly fit a Gompertz model, but rather demonstrates the inability to fit one (given lack of exponential mortality rate increase), therefore indirectly measuring  $\beta$  as 0 (i.e. constant mortality rate over time).
- <sup>g</sup> This study used a three-parameter Gompertz model, where  $x_0$  and b are functional equivalents of  $\alpha$  and  $\beta$ , respectively.
- <sup>h</sup> These studies performed survival/mortality rate analyses on replicative lifespan (of fission yeast), and do not directly fit a Gompertz model given that they demonstrate the *lack* of a Gompertzian mortality pattern.

Notably, almost all studies (55/58) that gave a biological interpretation of  $\beta$  attributed it directly or indirectly to biological ageing rate or other property of the ageing process. That is, that reductions in  $\beta$  reflect the slowing or amelioration of ageing in their intervention cohorts. 13 other studies gave no biological interpretation of  $\beta$ , describing its changes in only mathematical terms. The remaining 3 studies (summing up altogether to 71 studies) either did not specify  $\beta$  values (Ruan et al., 2002), concluded changes in ageing rate but did not attribute them specifically to either Gompertz parameter (Walsh et al., 2014), or presented data arguing against the suitability of  $\beta$  as a measure of ageing rate (Bansal et al., 2015). Importantly, these majority views of  $\beta$  as ageing rate were not supported by direct measurements of biological ageing rate within individuals.

About half of all studies (36/71) reported a mix of effects on  $\beta$  (intervention-specific increases and decreases), while 17 reported only decreases in  $\beta$ , 11 reported no change in  $\beta$ , and only 6 reported increases in  $\beta$ . A possibility is that these frequencies of different effects on  $\beta$  may reflect not the true biology of this parameter across the surveyed populations, but rather publication bias influenced by traditional views of this parameter (that reductions in  $\beta$  reflect slowed ageing and are therefore more publishable). Consistent with this, 15/17 (88%) of studies reporting only decreases in  $\beta$  interpreted this as slowed ageing rate, but only 2/6 (33%) of studies reporting only increases in  $\beta$  interpreted this as accelerated ageing rate (Kraus et al., 2013, Anisimov et al., 2019). Half of these 6 studies reporting increases provided no biological interpretation of the change (Chaves et al., 2004, Krementsova et al., 2012, Larson et al., 2016), while the remaining study suggested an increase in deleterious "side effects", for instance, through "impaired damage repair capacity", despite an increase in mean lifespan (Kowald and Kirkwood, 2021).

Intriguingly, no clear consensus on the biological interpretation of  $\alpha$  existed across the 71 studies. 10 studies did not measure/specify  $\alpha$  (potentially reflecting the weaker interest in

this supposedly ageing-independent parameter), 19 studies gave no biological interpretation of  $\alpha$ , while the remaining 42 studies offered a remarkable diversity of interpretations and phraseologies of the meaning of this parameter for their intervention cohorts. These interpretations tended to belong to one of several distinct categories, with 10 studies giving multiple interpretations from more than one category:

- 1. "Frailty"/"vulnerability"/"vitality"/"viability": 12 studies
- 2. "Extrinsic"/"environmental" mortality: 7 studies
- 3. "Onset of ageing": 7 studies
- 4. "Baseline"/"background" mortality: 5 studies
- 5. "Early-life"/"premature" mortality: 4 studies
- 6. "Short-term"/"acute" risk of death: 4 studies
- 7. "Age-independent" mortality: 3 studies

7 studies gave interpretations of  $\alpha$  that did not easily fit into the above categories. These were:

- "Risk of death throughout life" or "sickness" (Samuelson et al., 2007)
- "Beneficial effect on survival that is constant over the adult lifespan" (Shen et al., 2009)
- Mortality "risk that is determined by current environment and genes" (Wu et al., 2009b)
- "Quality of life" (Krementsova et al., 2012)
- "Rate of age-associated physiological change in young adults" (Rangaraju et al., 2015)
- "Ageing-independent physiological features" (Hughes and Hekimi, 2016)
- "Health" (Shen et al., 2017)

It is readily apparent that the biological conception of  $\alpha$  is a point of confusion and disagreement within the field. Besides the great diversity of interpretation, this is evident in several ways, the most prominent of which is the use of mechanistically generic phraseology to describe causes/types of mortality, such as "frailty", "vulnerability", "baseline", and "acute". Although these terms do have appropriate, specialised uses within biology and gerodemography, in these surveyed studies they are used without sufficient explanation or context. Additionally, their original definitions themselves derive from primarily theoretical research, and lack clear mechanistic (biological) descriptions. It is likely therefore that the mechanistic ambiguity of the original terminology used to describe the  $\alpha$  parameter has since been propagated afield, exacerbating the uncertainties concerning its biological interpretation.

Mechanistically, the 7 categories of interpretation listed above also differ amongst themselves. The most common category (1) views  $\alpha$  as a measure of intrinsic, ageing-independent biological states that determine an individual's risk of death (possibly, for instance, genetic mutations), whereas category 2 views  $\alpha$  as a measure of environmental, extrinsic forces external to organism. In contrast again, category 3 interprets  $\alpha$  to reflect the age at which the ageing process begins, which is mechanistically unrelated to either of the former categories. Finally, category 7 is erroneous, since  $\alpha$  effects upon mortality rate are age-dependent (as explained in the previous section, Figure 2.2, p. 28).

In summary, this literature survey highlights the limited empirical and conceptual foundations beneath recent model organism biogerodemographic studies using the Gompertz model. Although mostly identical between different researchers, biological interpretations of  $\beta$  are made without direct empirical support, while interpretations of  $\alpha$  are limited in both conceptual consensus and empirical backing. Therefore, empirical studies of the Gompertz (and other mortality model) parameters would be greatly helpful in re-evaluating and guiding existing and incoming biogerodemographic research.

## Chapter 3 – An empirical investigation of Gompertzian mortality in C. elegans

# 3.1 – Introduction and experimental design

In the coming chapters, I will present the results (summarised in section 6.2) of an empirical investigation into the biological basis of the Gompertz parameters, using *C. elegans*. To the best of my knowledge, this is the first direct attempt to explain the Gompertz parameters in terms of *population-wide* biological ageing (i.e. direct comparison of demographic and biological ageing). As such, a number of conceptual and analytical approaches presented here have been developed specifically for this investigation. The general strategy employed is the simultaneous characterisation of demographic and individual biological ageing across different lifespan conditions, allowing changes in one to be explained in terms of changes in the other.

Three classes of intervention that increase *C. elegans* lifespan were examined:

- (i) Reduction of ambient temperature, from 25°C to 20°C or 15°C.
- (ii) Prevention of late-life infection (by dietary E. coli) using the antibiotic carbenicillin.
- (iii) Reduction-of-function (*rf*) mutations of the *daf-2* insulin/IGF-1 receptor, specifically the class 1 alleles *daf-2(m577)* and *daf-2(e1368)*, and the class 2 (more pleiotropic) allele *daf-2(e1370)*. These three genotypes were compared to the wild-type control, N2.

These life-extending interventions were selected on the basis of having robust, reproducible effects on lifespan, having mechanistic and genetic relevance to ageing, including across species, and being subjects of existing interest within the ageing research field. For instance, *C. elegans* longevity correlates inversely with ambient temperature (Klass, 1977), and temperature affects ageing in other species, both poikilotherms and mammals (Keil et al., 2015). Proposed mechanisms for temperature effects on longevity include thermodynamic pacing of ageing (Hayflick, 2007), effects of this "rate-of-living" on metabolic exhaustion (Pearl, 1928), and temperature-regulated genetic programmes (Xiao et al., 2013, Palani et al., 2023), amongst others.

Similarly, protecting *C. elegans* from infection by their *E. coli* food source increases lifespan (Gems and Riddle, 2000, Garsin et al., 2003), and bacterial infection (including by *E. coli*) is perhaps the best characterised cause of ageing-related death in *C. elegans* currently known (Garigan et al., 2002, Zhao et al., 2017, Podshivalova et al., 2017, Zhao et al., 2021).

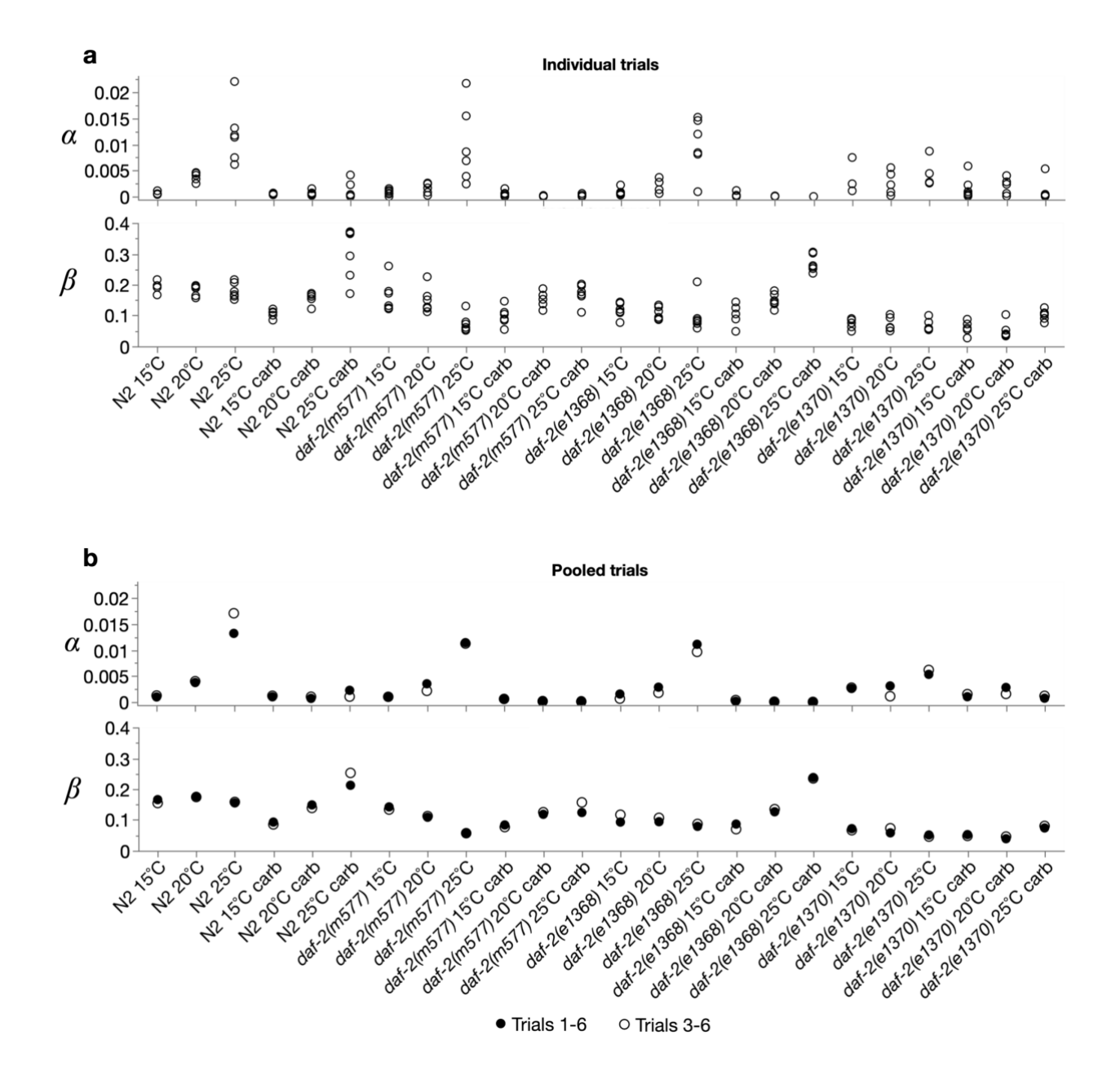
Finally, one of the most effective known longevity interventions in *C. elegans* is genetic reduction of IIS, which in several other species also increases lifespan (Kenyon, 2011, Vitale et al., 2019). In *C. elegans*, lowering IIS can be achieved by various mutations affecting the DAF-2 receptor including, in order of increasing severity of IIS reduction and longevity magnitude, those used here: daf-2(m577), daf-2(e1368) and daf-2(e1370) (Gems et al., 1998, Zhao et al., 2021). Moreover, these three treatment targets (temperature, infection and IIS) often show additive effects on lifespan, such that investigating them in different combinations should prove informative about their interactions, and how this affects mortality patterns.

Lifespan was therefore measured for all 24 combinations of these treatment conditions (3 temperatures, ± carbenicillin, 4 genotypes) in 6 successive trials. To relate the Gompertz parameters to individual-level biological ageing features, in 4/6 trials, all animals were tracked individually and their locomotory health assessed every 2–3 days from the start of adulthood until death. As adapted from a well-established protocol (Hosono et al., 1980, Herndon et al., 2002) (see Methods for further details), animals were scored as either youthful (healthy, sinusoidal locomotion) or decrepit (non-sinusoidal/uncoordinated locomotion, or immotility) following controlled physical stimulation with a platinum wire; this induces an escape response that reveals true locomotory capacity rather than behavioural locomotory preference (Hahm et al., 2015). I will refer to absolute and relative healthspan (H-span<sup>abs</sup>, H-span<sup>rel</sup>) and gerospan (G-span<sup>abs</sup>, G-span<sup>rel</sup>) to describe, respectively, the total number of days or proportion of life spent in youthfulness or decrepitude (morbidity). In other words, for every individual, H-span<sup>abs</sup> + G-span<sup>abs</sup> = lifespan, and H-span<sup>rel</sup> + G-span<sup>rel</sup> = 1.

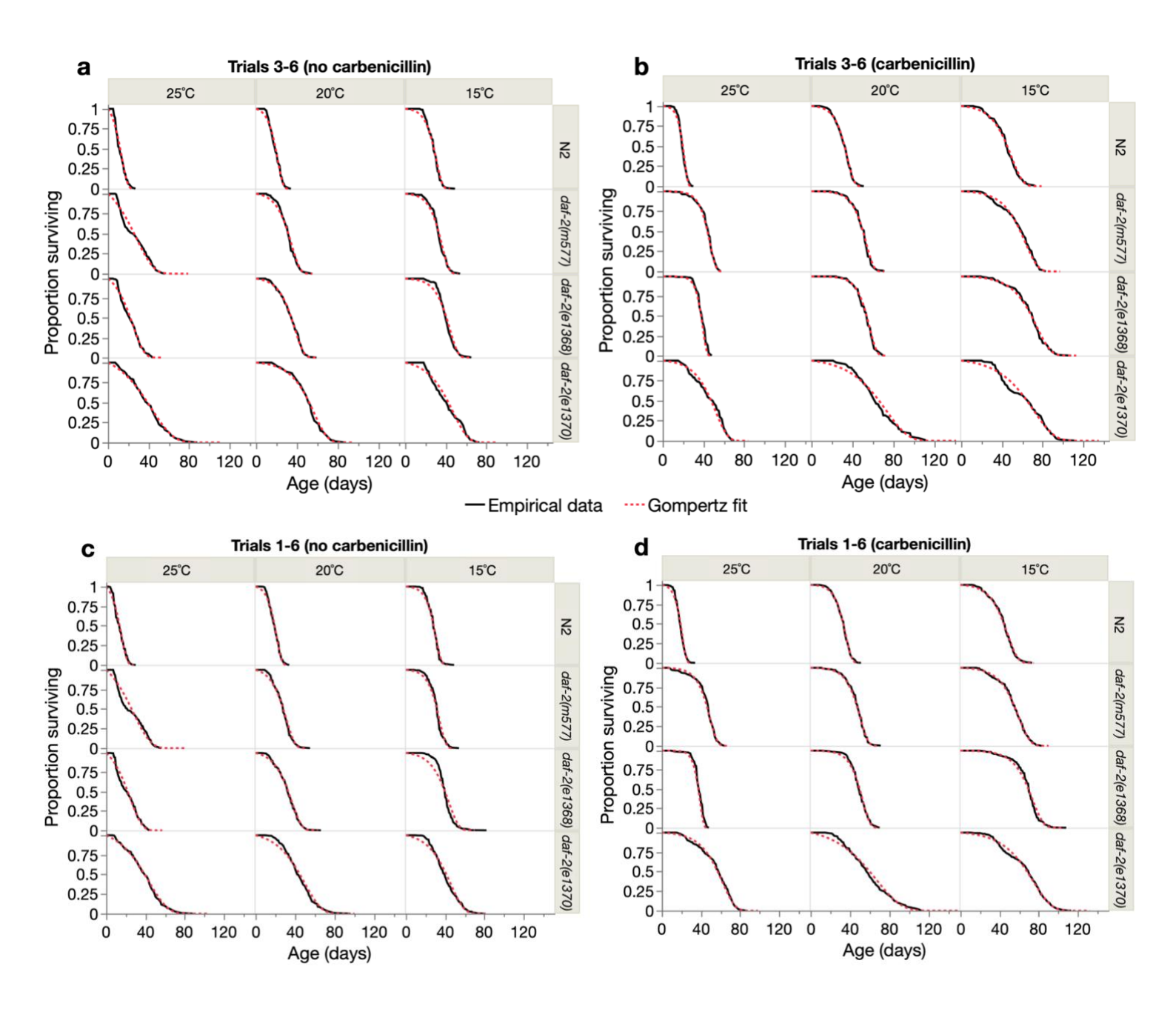
Necropsies were also performed to determine the mode of death of all animals in these 4 trials, using an extended version of an earlier protocol (Zhao et al., 2017, Zhao et al., 2021) (see Methods for further details). In brief, infection-related (by dietary *E. coli*) pathologies were scored visually in recently-deceased corpses, identifying two distinct anatomical sites of infection/colonisation, namely the pharynx and intestine, with corpses presenting with one, both or neither pathology.

Unless indicated otherwise, I will characterise the relationship between demographic and biological ageing using the combined pool of these 4 trials described above (n=116–179/cohort), as they collected both lifespan and health data. Mean lifespan and the Gompertz parameters, calculated by maximum likelihood estimation (Pletcher, 1999), were stable between these 4 trials (Figure 3.1a, Table 3.1), and the Gompertz model provided an excellent fit to their combined pooling, predicting mean, median, and first and third quartile lifespans across the 24 cohorts with R<sup>2</sup>=0.98–1.00 (Figure 3.2a, b, e–h). To confirm that sample sizes are sufficient for model fitting, and that these Gompertz parameters are representative of these

cohorts, I ran two additional larger trials (measuring lifespan only), increasing total pooled sample sizes by 2–3-fold to 326–396/cohort (Table 3.1). Notably, the Gompertz fit remained very strong, predicting the above lifespan measures with R<sup>2</sup>=0.97–0.99 (Figure 3.2c, d, e–h). The Gompertz parameters were also near-identical to those calculated from the pool of the 4 smaller trials (Figure 3.1b). These data are therefore highly consistent between trials and are robustly fitted by the Gompertz model. Importantly, although more complex mortality models can better fit *C. elegans* populations (Vanfleteren et al., 1998, Johnson et al., 2001, Stroustrup et al., 2016, Mulla et al., 2023), my aim is not to find the best-fitting model but to study the larger mortality patterns that are readily captured by this mathematically parsimonious and widely employed Gompertz model. Additional reasons for preferring the simpler Gompertz model for this work are described in section 1.4 (p. 21).



**Figure 3.1.** The Gompertz parameters are stable between trials. The Gompertz parameters for each of the (a) individual 6 trials and (b) combined pool of Trials 1-6 or 3-6, for each of the 24 cohorts. Trials 3-6 (n=116-179/cohort) are those in which both lifespan and health were measured, while Trials 1-6 (n=326-396/cohort) include 2 additional larger trials in which only lifespan was measured. All primary analyses in Chapters 3 and 4 compare mortality and health data from the pool of Trials 3-6. Statistical details of each trial are provided in Table 3.1.



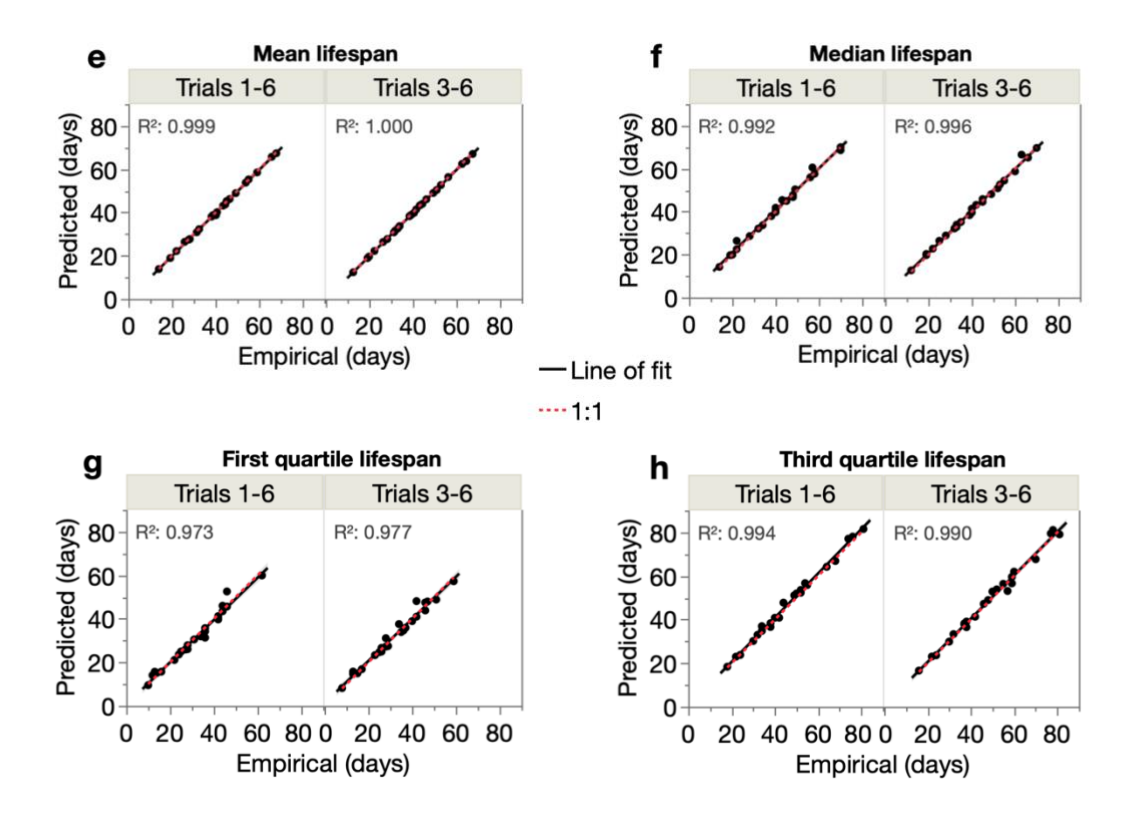


**Figure 3.2.** The Gompertz model fits the data closely. (a–d) Overlay of empirical and idealised Gompertz curves for each of the 24 cohorts, for the pool of Trials 3–6 (a: non-carbenicillin cohorts, b: carbenicillin cohorts) and pool of Trials 4–6 (c: non-carbenicillin cohorts, d: carbenicillin cohorts). (e–h) Linear regressions between true (empirical) and predicted (from the Gompertz fit) lifespan measures, across the 24 cohorts. First quartile, median and third quartile lifespans are the ages at which survival proportion equals, respectively, 0.75, 0.5 and 0.25; the strong regression relationships for each of these indicates a robust prediction of overall survival curve shape by the Gompertz model for these 24 cohorts. 95% confidence regions around the regression fits are shaded (barely visible). Trials 3–6 (*n*=116–179/cohort) are those in which both lifespan and health were measured, while Trials 1–6 (*n*=326–396/cohort) include 2 additional larger trials in which only lifespan was measured. All primary analyses in Chapters 3 and 4 compare mortality and health data from the pool of Trials 3–6. Statistical details of each trial are provided in Table 3.1.

			Effect of reduci	ng temperature	Effect of ca	arbenicillin	Effect of	daf-2(rf)
Cohort	No. dead/	Mean lifespan	% change vs.	p vs. 25°C	% change vs.	p vs. no carb.	% change	p vs. N2
N2 25 °C	censors	(days since L4)	25 °C	(Log-Rank)	no carb.	(Log-Rank)	vs. N2	(Log-Rank)
N2 25 C	<b>[C] 340/46</b> [1] 95/10	<b>13.9</b> 16.4						
	[2] 76/29 [3] 70/1	13.8 11.3						
	[4] 33/2	13.7						
	[5] 31/4 [6] 35/1	11.6 14.9						
N2 20 °C	[C]358/27	19.3	38.9	<0.0001				
	[1] 96/9 [2] 93/12	19.7 19.3	19.7 39.8	0.0001 <0.0001				
	[3] 67/2	19.9	76.1	<0.0001				
	[4] 33/3 [5] 33/3	20.6 18.1	50.5 55.7	<0.0001 <0.0001				
NO 45 °C	[6] 36/0	17.4	16.9	0.0663				
N2 15 °C	<b>[C] 328/51</b> [1] 83/22	<b>28.1</b> 28.8	<b>102.3</b> 75.5	< <b>0.0001</b> <0.0001				
	[2] 86/19 [3] 62/8	27.3 27.4	98.4 142.7	<0.0001 <0.0001				
	[4] 33/3	33.5	145.4	<0.0001				
	[5] 30/5 [6] 34/2	25.2 27.3	116.0 83.0	<0.0001 <0.0001				
N2 25 °C carb.	[C]341/46	19.2			38.0	<0.0001		
	[1] 85/20 [2] 83/22	19.2 18.0			16.8 30.3	0.0025 <0.0001		
	[3] 70/2	18.2 20.8			61.9 52.4	<0.0001 <0.0001		
	[4] 34/1 [5] 35/1	24.0			106.1	<0.0001		
N2 20 °C carb.	[6] 34/2 [C] 350/38	17.6 <b>32.6</b>	69.8	<0.0001	18.1 <b>68.7</b>	0.0235 < <b>0.0001</b>		
INVE ZU G GAID.	[1] 85/20	32.7	70.3	<0.0001	66.2	<0.0001		
	[2] 92/13 [3] 70/1	34.0 29.0	89.6 59.1	<0.0001 <0.0001	76.7 46.2	<0.0001 <0.0001		
	[4] 33/3	32.2	54.4	<0.0001	56.5	<0.0001		
	[5] 35/1 [6] 35/1	32.4 36.4	34.9 106.8	<0.0001 <0.0001	78.5 108.8	<0.0001 <0.0001		
N2 15 °C carb.	[C] 337/43	43.5	126.4	<0.0001	54.5	<0.0001		
	[1] 81/24 [2] 95/10	42.0 43.3	118.9 141.0	<0.0001 <0.0001	45.7 58.2	<0.0001 <0.0001		
	[3] 62/1 [4] 32/4	38.2 50.2	109.3 141.2	<0.0001 <0.0001	39.6 49.8	<0.0001 <0.0001		
	[5] 34/2	47.0	95.8	<0.0001	86.8	<0.0001		
daf-2(m577) 25°C	[6] 33/3 [C] 248/100	47.3 <b>25.8</b>	168.7	<0.0001	73.4	<0.0001	85.4	<0.0001
dar 2(morr) 20 0	[1] 71/34	27.8					68.9	<0.0001
	[2] 52/53 [3] 21/0	21.9 26.6					58.7 N/A	<0.0001 N/A
	[4] 32/2 [5] 31/5	34.7 26.8					153.9 129.9	<0.0001 <0.0001
	[6] 41/6	19.1					27.7	0.0358
<i>daf-2(m577)</i> 20°C	[C] 253/98 [1] 66/39	<b>27.7</b> 24.7	<b>7.4</b> -10.8	<b>0.164*</b> 0.002			<b>43.3</b> 25.8	<0.0001 <0.0001
	[2] 68/37	24.0	9.7	0.6874			24.6	<0.0001
	[3] 32/4 [4] 26/7	36.0 33.2	35.3 -4.4	<0.0001 0.057			N/A 61.3	N/A <0.0001
	[5] 29/7	28.3	5.8	0.1731			56.2	<0.0001
daf-2(m577) 15°C	[6] 32/4 [C] 316/35	27.7 <b>31.4</b>	45.2 <b>21.6</b>	0.0126 <b>0.9435</b> *			58.6 <b>11.4</b>	<0.0001 < <b>0.0001</b>
	[1] 84/21 [2] 96/9	30.0 30.3	7.9 38.4	0.0411 0.1722			3.9 10.8	0.0699 0.0008
	[3] 35/1	34.2	28.5	0.0022			N/A	N/A
	[4] 30/3 [5] 35/1	33.4 32.7	-3.7 22.1	0.0205 0.9711			-0.4 29.9	0.1267 <0.0001
	[6] 36/0	31.8	67.0	0.0002			16.6	0.0045
<i>daf-2(m577)</i> 25 °C carb.	<b>[C] 238/88</b> [1] 78/27	<b>45.0</b> 41.8			<b>74.7</b> 50.6	< <b>0.0001</b> <0.0001	<b>134.6</b> 117.8	< <b>0.0001</b> <0.0001
	[2] 56/49	52.5			139.9 34.4	<0.0001 0.0005	192.3	<0.0001
	[3] 18/1 [4] 29/2	35.8 45.8			31.9	0.0032	N/A 119.7	N/A <0.0001
	[5] 22/8 [6] 35/1	41.9 45.6			56.4 139.3	<0.0001 <0.0001	74.4 158.8	<0.0001 <0.0001
<i>daf-2(m577)</i> 20 °C carb.	[C] 232/103	46.4	3.1	0.1588	67.7	<0.0001	42.5	<0.0001
	[1] 63/42 [2] 46/44	41.1 45.9	-1.8 -12.5	0.0145 <0.0001	65.9 91.3	<0.0001 <0.0001	25.6 34.9	<0.0001 <0.0001
	[3] 30/2	47.5	32.7	<0.0001	31.8	<0.0001	N/A	N/A
	[4] 27/9 [5] 33/3	53.7 46.4	17.4 10.7	<0.0001 0.0005	62.1 63.6	<0.0001 <0.0001	67.1 43.1	<0.0001 <0.0001
d-60(577) 45°0	[6] 33/3	50.3	10.3	0.0003	81.8	<0.0001	38.1	<0.0001
<i>daf-2(m577)</i> 15 °C carb.	<b>[C] 308/46</b> [1] 83/22	<b>53.8</b> 50.4	<b>19.5</b> 20.5	< <b>0.0001</b> <0.0001	<b>71.6</b> 68.1	< <b>0.0001</b> <0.0001	<b>23.8</b> 19.9	< <b>0.0001</b> <0.0001
	[2] 96/9	53.7	2.3	0.0041	77.2 51.2	<0.0001	24.0 N/A	<0.0001
	[3] 32/4 [4] 30/6	51.7 56.9	44.6 24.4	<0.0001 0.0033	70.4	<0.0001 <0.0001	13.3	N/A 0.0029
	[5] 34/2 [6] 33/3	63.6 52.8	52.0 15.9	<0.0001 <0.0001	94.7 66.0	<0.0001 <0.0001	35.4 11.6	<0.0001 0.0098
	[0] 33/3	52.8	15.9	<0.0001	66.0	<0.0001	11.6	0.0098

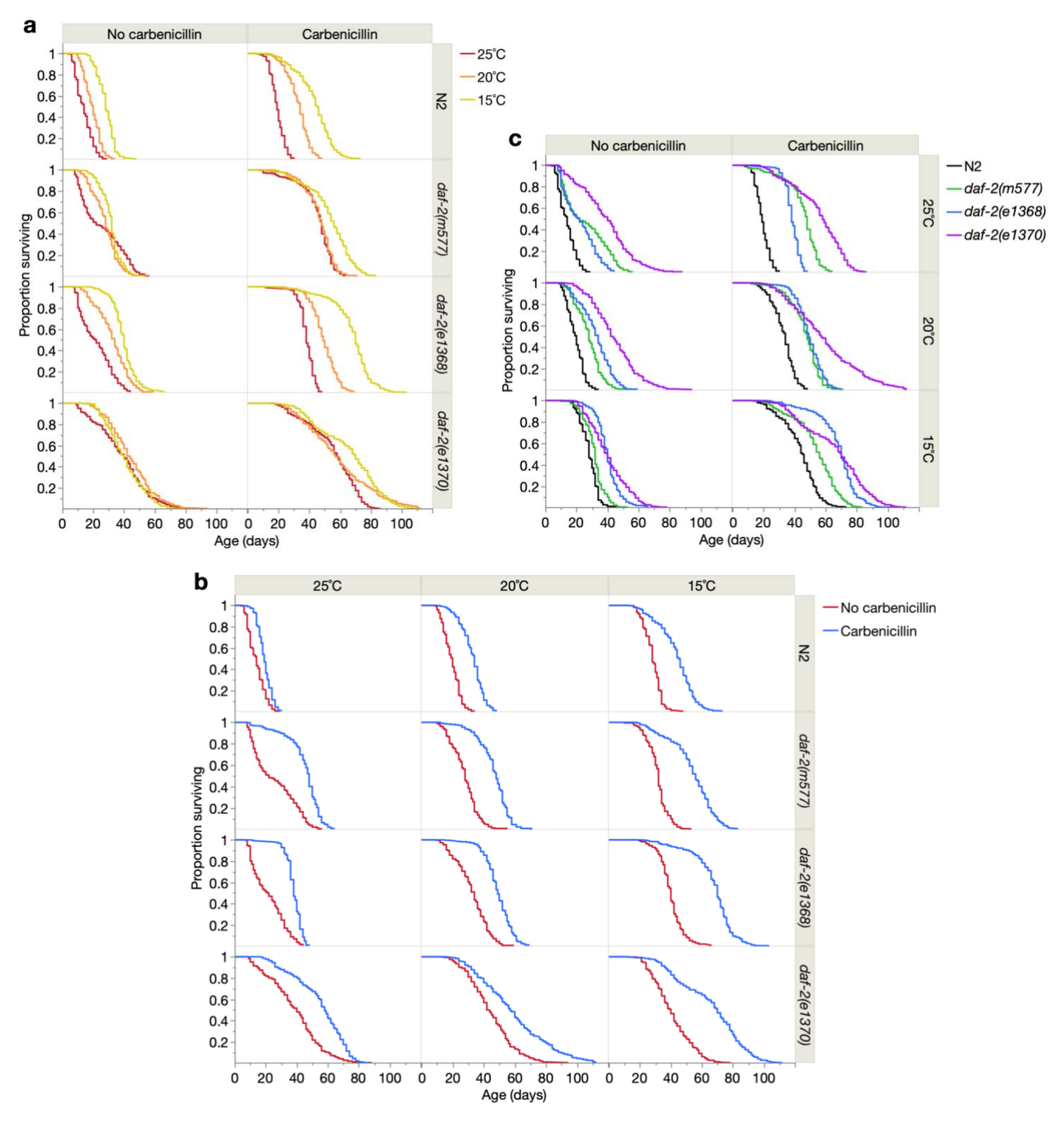
			Effect of reduci	ng temperature	Effect of ca	arbenicillin	Effect of	daf-2(rf)
Cohort	No. dead/ censors	Mean lifespan (days since L4)	% change vs. 25°C	p vs. 25°C (Log-Rank)	% change vs. no carb.	p vs. no carb. (Log-Rank)	% change vs. N2	p vs. N2 (Log-Rank)
daf-2(e1368) 25°C	[C] 326/70	22.0	200	(==8)		(==8 :)	58.2	<0.0001
	[1] 100/20 [2] 85/35	19.6 24.2					N/A 75.4	N/A <0.0001
	[3] 35/1 [4] 34/2	23.2 23.3					N/A 70.6	N/A <0.0001
	[5] 30/6 [6] 42/6	22.8 20.7					95.3 38.8	<0.0001 0.0006
daf-2(e1368) 20°C	[C] 273/110	32.4	47.4	<0.0001			67.9	<0.0001
	[1] 78/42 [2] 77/44	30.7 31.9	56.3 32.0	<0.0001 0.0003			N/A 65.6	N/A <0.0001
	[3] 31/5 [4] 26/8	34.6 37.5	49.3 61.1	<0.0001 <0.0001			N/A 82.7	N/A <0.0001
	[5] 32/4 [6] 29/7	30.8 33.2	35.3 60.4	0.0666 <0.0001			69.7 90.4	<0.0001 <0.0001
daf-2(e1368) 15°C	[C] 345/39	40.1	82.4	<0.0001			42.6	<0.0001
	[1] 105/15 [2] 108/12	41.4 38.5	110.8 59.2	<0.0001 <0.0001			N/A 40.8	N/A <0.0001
	[3] 34/2 [4] 33/3	39.3 41.0	69.6 75.7	<0.0001 <0.0001			N/A 22.2	N/A <0.0001
	[5] 34/2 [6] 31/5	41.5 40.1	82.3 93.9	<0.0001 <0.0001			64.9 47.0	<0.0001 <0.0001
<i>daf-2(e1368)</i> 25 °C carb.	[C] 336/48	38.1			73.3	<0.0001	98.6	<0.0001
	[1] 108/12 [2] 101/19	36.8 39.2			87.3 62.2	<0.0001 <0.0001	N/A 118.5	N/A <0.0001
	[3] 33/3 [4] 32/4	35.6 37.1			53.7 59.1	<0.0001 <0.0001	N/A 78.1	N/A <0.0001
	[5] 34/2 [6] 28/8	40.4 40.2			77.6 94.3	<0.0001 <0.0001	68.3 128.3	<0.0001 <0.0001
daf-2(e1368) 20°C carb.	[C] 263/114 [1] 67/54	<b>49.3</b> 45.5	<b>29.2</b> 23.7	< <b>0.0001</b>		< <b>0.0001</b> <0.0001	<b>51.1</b> N/A	< <b>0.0001</b> N/A
	[2] 92/28	47.9	22.0	<0.0001	50.0	<0.0001	40.6	<0.0001
	[3] 25/5 [4] 19/15	52.3 56.3	46.8 51.7	<0.0001 <0.0001	51.2 49.8	<0.0001 <0.0001	N/A 74.9	N/A <0.0001
	[5] 29/7 [6] 31/5	50.6 53.1	25.1 32.1	<0.0001 <0.0001	64.2 60.0	<0.0001 <0.0001	56.1 45.8	<0.0001 <0.0001
daf-2(e1368) 15°C carb.	[C] 342/42 [1] 108/12	<b>67.9</b> 69.1	<b>78.0</b> 88.0	< <b>0.0001</b> <0.0001	<b>69.1</b> 67.0	< <b>0.0001</b> <0.0001	<b>56.2</b> N/A	<0.0001 N/A
	[2] 111/9	67.3	71.5	<0.0001	74.8	<0.0001	55.5	<0.0001
	[3] 30/6 [4] 30/6	60.6 66.8	70.0 80.0	<0.0001 <0.0001	54.1 63.0	<0.0001 <0.0001	N/A 33.0	N/A <0.0001
	[5] 35/1 [6] 28/8	70.3 71.1	73.9 76.8	<0.0001 <0.0001	69.3 77.1	<0.0001 <0.0001	49.5 50.2	<0.0001 <0.0001
daf-2(e1370) 25°C	[C] 241/123 [1] 45/61	<b>38.7</b> 38.0					<b>178.6</b> N/A	< <b>0.0001</b> N/A
	[2] 53/52 [3] 36/0	37.9 32.2					174.7 N/A	<0.0001 N/A
	[4] 31/2 [5] 34/2	48.6 29.3					255.8 151.9	<0.0001 <0.0001
	[6] 42/6	46.3					210.2	<0.0001
daf-2(e1370) 20°C	<b>[C] 304/52</b> [1] 90/19	<b>44.4</b> 39.3	<b>14.7</b> 3.4	<b>0.0017</b> 0.9323			<b>130.0</b> N/A	< <b>0.0001</b> N/A
	[2] 84/21 [3] 33/1	39.9 55.8	5.3 73.4	0.8815 <0.0001			107.0 N/A	<0.0001 N/A
	[4] 30/6 [5] 31/5	58.8 41.6	21.0 41.7	0.0269 0.0037			186.0 129.3	<0.0001 <0.0001
4.624.4222.4232	[6] 36/0	47.8	3.3	0.7321			174.0	<0.0001
daf-2(e1370) 15°C	[ <b>C]310/48</b> [1]94/13	<b>40.6</b> 40.1	<b>4.8</b> 5.5	<b>0.8437</b> 0.6179			<b>44.4</b> N/A	<0.0001 N/A
	[2] 90/17 [3] 30/6	40.1 44.3	5.8 37.8	0.5505 0.0002			46.6 N/A	<0.0001 N/A
	[4] 34/2 [5] 33/3	34.9 43.1	-28.1 46.9	0.0051 0.0002			4.2 71.4	0.6074 <0.0001
<i>daf-2(e1370)</i> 25 °C carb.	[6] 29/7 [C] 257/101	44.2 <b>55.2</b>	-4.4	0.2229	42.3	<0.0001	62.0 <b>187.3</b>	<0.0001 <0.0001
Com 2   Coto / Co / Co	[1] 75/30	63.1			66.0	<0.0001	N/A	N/A
	[2] 70/35 [3] 32/4	61.2 31.1			61.5 -3.3	<0.0001 0.5667	240.7 N/A	<0.0001 N/A
	[4] 22/8 [5] 30/6	53.3 48.0			9.7 63.6	0.4664 <0.0001	156.1 99.9	<0.0001 <0.0001
<i>daf-2(e1370)</i> 20 °C carb.	[6] 28/18 [C] 291/65	52.9 <b>59.1</b>	7.1	<0.0001	14.3 <b>32.9</b>	0.6046 < <b>0.0001</b>	200.3 <b>81.2</b>	<0.0001 < <b>0.0001</b>
	[1] 87/21 [2] 78/27	56.1 53.1	-11.0 -13.2	0.5666 0.4668	42.8	<0.0001 <0.0001	N/A 55.9	N/A <0.0001
	[3] 33/3	62.7	101.4	<0.0001	12.3	0.0095	N/A	N/A
	[4] 28/7 [5] 33/3	76.1 58.1	42.6 21.1	<0.0001 0.0322		<0.0001 0.0001	136.5 79.4	<0.0001 <0.0001
<i>daf-2(e1370)</i> 15 °C carb.	[6] 32/4 [C] 299/46	61.5 <b>65.8</b>	16.2 <b>19.3</b>	0.0043 <0.0001	28.6 <b>61.9</b>	0.0006 < <b>0.0001</b>	68.7 <b>51.3</b>	<0.0001 < <b>0.0001</b>
	[1] 86/21 [2] 89/16	70.3 65.8	11.4 7.6	<0.0001 0.0002	75.3 64.2	<0.0001 <0.0001	N/A 52.1	N/A <0.0001
	[3] 20/5 [4] 34/2	51.6 53.3	65.9 -0.1	<0.0002 <0.0001 0.8327	16.4	0.0785 0.0003	N/A 6.1	0.4075
	[5] 34/2	73.4	52.8	< 0.0001	52.5 70.1	<0.0001	56.1	<0.0001
	[6] 36/0	67.4	27.4	<0.0001	52.4	<0.0001	42.3	<0.0001

Table 3.1. Lifespan data for all cohorts and trials, and effect on lifespan of reducing temperature, antibiotic treatment and daf-2(rf). N2: wild-type, [C]: combined (pooled) data from all trials, [n]: trial number, carb.: carbenicillin, \*: cohorts where log-rank p>0.05 due to crossing survival curves and greater changes in early than late mortality; the Wilcoxon test is more appropriate to detect lifespan differences in these conditions (p<0.0015; data not shown). The 6 trials were performed sequentially over 34 months. In Trials 1–3, experiments for the 24 cohorts were not always performed together due to practical constraints. In this table, intra-trial comparisons between such cohorts were therefore withheld, and these exclusions (affecting a small proportion of within-trial comparisons: 30/276) are labelled (N/A). However, most analyses performed in this study utilise pooled data (Trials 3–6) from multiple trials (see Methods); in these analyses, the above-excluded comparisons were included, given that pooled analyses by nature compare different trials, and additionally dilute inter-trial noise.

In summary, I will attempt to use individual-specific profiles of biological ageing (locomotory decline and ageing-related bacterial pathologies) to provide a biological explanation of the Gompertz parameters across differently longevous *C. elegans* populations. Given the 24 different cohorts for which I collected this lifespan and health data, I will refer to this dataset as the "24-cohorts dataset".

# 3.2 – Three life-extending intervention classes disproportionately extend gerospan

From the 24 cohorts, I will focus on a total of 46 treatments (i.e. comparisons) of interest: 16 lower temperature treatments (20°C and 15°C, vs 25°C, across antibiotic and genotype backgrounds) + 12 antibiotic treatments (carbenicillin vs no carbenicillin, across temperature and genotype backgrounds) + 18 *daf-2(rf)* treatments (3 *daf-2(rf)* alleles vs the N2 wild-type, across temperature and antibiotic backgrounds). As expected (Klass, 1977, Kenyon et al., 1993, Garigan et al., 2002), almost all (44/46) treatments increased mean lifespan (average class effects for lower temperature, antibiotic and *daf-2(rf)* treatments: +42.0%, +58.9%, +77.1%, respectively; Figure 3.3, Table 3.1).



**Figure 3.3. Kaplan-Meier survival curves for all cohorts.** Effects of (a) reducing temperature, (b) antibiotic treatment, and (c) *daf-2(rf)*. N2: wild-type. Pool of all 6 trials. Statistical comparisons (*p-values*, log-rank test) are presented in Table 3.1. A previous study found that culture of *daf-2(e1370)* on a different antibiotic (gentamycin) did not increase lifespan, and even slightly shortened it, suggesting that this mutation might confer full resistance to life-shortening effects of live *E. coli* (Podshivalova et al., 2017). My finding that carbenicillin (b) increases lifespan in all three *daf-2* mutants suggests that they do in fact succumb to effects of proliferating *E. coli* in later life, likely reflecting inevitable, eventual immunosenescence.

I next examined effects of these life-extending treatments on G-span<sup>rel</sup> (the proportion of life spent in gerospan). Against possible expectations of improved health, 12/16 lower temperature treatments increased G-span<sup>rel</sup> (Figure 3.4a). Furthermore, all (12/12) carbenicillin treatments increased G-span<sup>rel</sup> (Figure 3.4b), but in line with an earlier report of antibiotic-elicited morbidity expansion (Podshivalova et al., 2017). Similarly, 9/18 *daf-2(rf)* treatments increased G-span<sup>rel</sup> compared to only 2/18 that decreased it (Figure 3.4c).

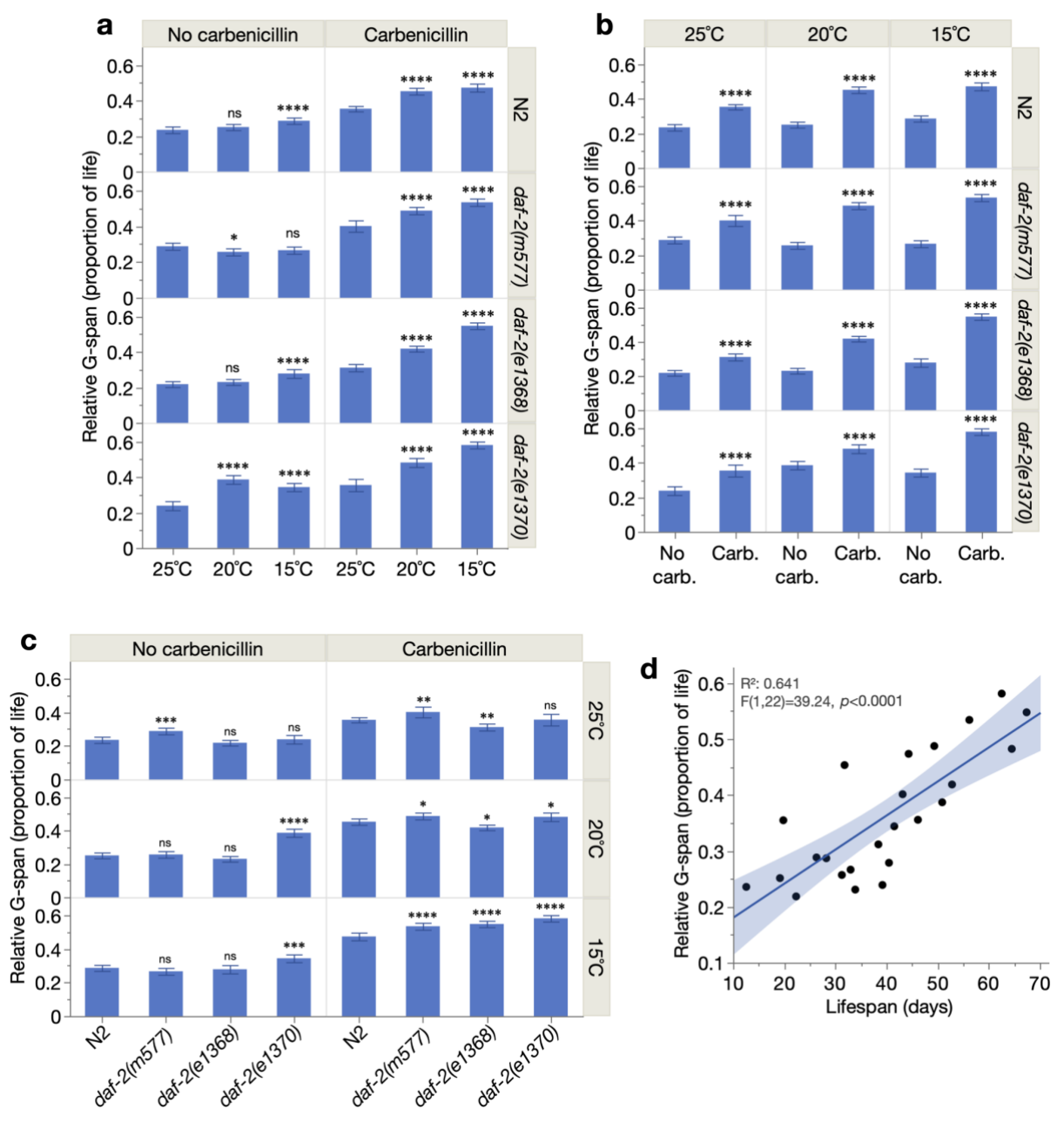


**Figure 3.4. Life-extending treatments disproportionately extend gerospan.** Effects of (a) reduced temperature, (b) carbenicillin, and (c) daf-2(rf) on mean relative gerospan (G-span<sup>rel</sup>). daf-2(e1368) was previously observed to increase G-span<sup>rel</sup> at 20°C (Podshivalova et al., 2017); that I did not see this could reflect differences in how G-span was measured. N2: wild-type. Statistical significance of G-span<sup>rel</sup> differences were assessed by two-tailed Student's t-tests, showing 95% confidence intervals; ns p > 0.05, \* $p \le 0.05$ , \*\* $p \le 0.01$ , \*\*\*\*  $p \le 0.001$ , \*\*\*\*  $p \le 0.0001$ . (d) Mean G-span<sup>rel</sup> is positively related to mean

lifespan across the 24 cohorts. The relationship was assessed using least-squares linear regression and an F-test, with the 95% confidence region shaded.

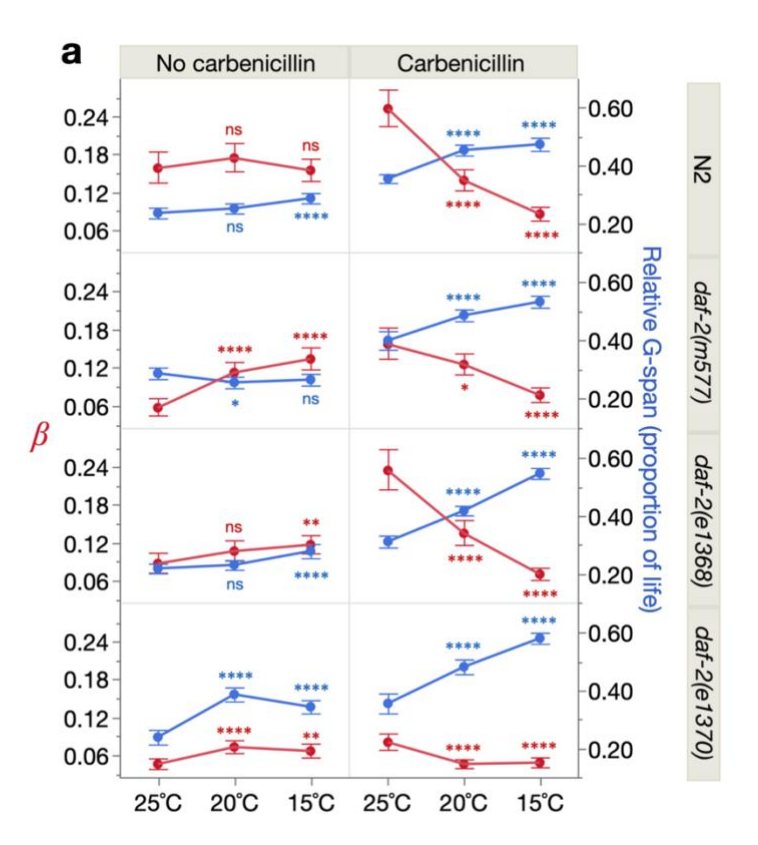
These daf-2(rf) results are broadly consistent with previous reports of morbidity expansion in daf-2(e1368) and daf-2(e1370) (Huang et al., 2004, Bansal et al., 2015, Podshivalova et al., 2017), including the finding that this expansion results from greater infection resistance (against the E. coli food) than wild-type animals (Podshivalova et al., 2017, Statzer et al., 2022). For instance, at the standard culture temperature of 20°C, daf-2(e1370) increased Gspan<sup>rel</sup>, and this increase was largely suppressed by carbenicillin (Figure 3.4c). However, among other daf-2(rf) allele/temperature combinations, G-span<sup>rel</sup> patterns varied markedly. For instance, at 15°C, daf-2(e1370) G-span<sup>rel</sup> increase was not suppressed on carbenicillin, while at 25°C, Gspan<sup>rel</sup> of this mutant was unchanged regardless of bacterial pathogenicity. And G-span<sup>rel</sup> of class 1 mutants (daf-2(m577) and daf-2(e1368)) increased more on carbenicillin, although in daf-2(e1368) it was decreased at the two higher temperatures. These data therefore reveal more complex allelic and environmental effects of daf-2(rf) on the relationship between health and lifespan than previously reported. This condition-dependency, and inter-study differences in detection and definition of gerospan, may explain disagreements in the literature about daf-2(rf) effects on relative morbidity; for instance, some studies have reported a proportional scaling of gerospan between daf-2(rf) and wild-type animals (Hahm et al., 2015, Statzer et al., 2022).

Overall, the longevity interventions tested here mostly increase the proportion of life in poor (aged) health. Indeed, direct regression of G-span<sup>rel</sup> against lifespan for the 24 cohorts revealed a strong positive relationship (Figure 3.4d). Thus, against expectation, in these cohorts, longer life is frequently accompanied by a disproportionate expansion of decrepitude.

Importantly, while gerospan here is necessarily simplified to a single portion of life, its definition (non-sinusoidal locomotion or immotility, after stimulation) captures well-characterised stages of nematode ageing and is a physiologically integrative measure of overall health (Hosono et al., 1980, Herndon et al., 2002). Accordingly, the age of this gerospan onset provides a measure of the overall rate of change in health, or equivalently, a simple estimate of an individual's overall rate of ageing. In this view, the G-span<sup>rel</sup> increases observed across these life-extending treatments argue against a simple deceleration of ageing, which may be expected to stretch H-span<sup>abs</sup> and G-span<sup>abs</sup> proportionally, leaving G-span<sup>rel</sup> unchanged.

Next, I considered the central question of this study: the relationship between biological and demographic ageing. To this end, I examined the relationship between effects on G-span<sup>rel</sup> and the Gompertz parameters across the 46 life-extending treatments; I start with the rate parameter  $\beta$ , reduction of which has often been equated with decelerated biological ageing.

First, I considered the effects of reducing temperature. On carbenicillin, this decreased  $\beta$  in all genotypes (Figure 3.5a), which would be consistent with a general slowing of the rate of living. However, without carbenicillin,  $\beta$  was unchanged in wild-type and even increased in *daf-*2 mutants, suggesting complex effects of genotype and temperature on host-*E. coli* interactions. Surprisingly,  $\beta$  reduction by lowered temperature (on carbenicillin) consistently co-occurred with G-span<sup>rel</sup> increase (Figure 3.5a, right), suggesting that  $\beta$  reduction here reflects neither simply slowed ageing rate nor improved overall quality of life.



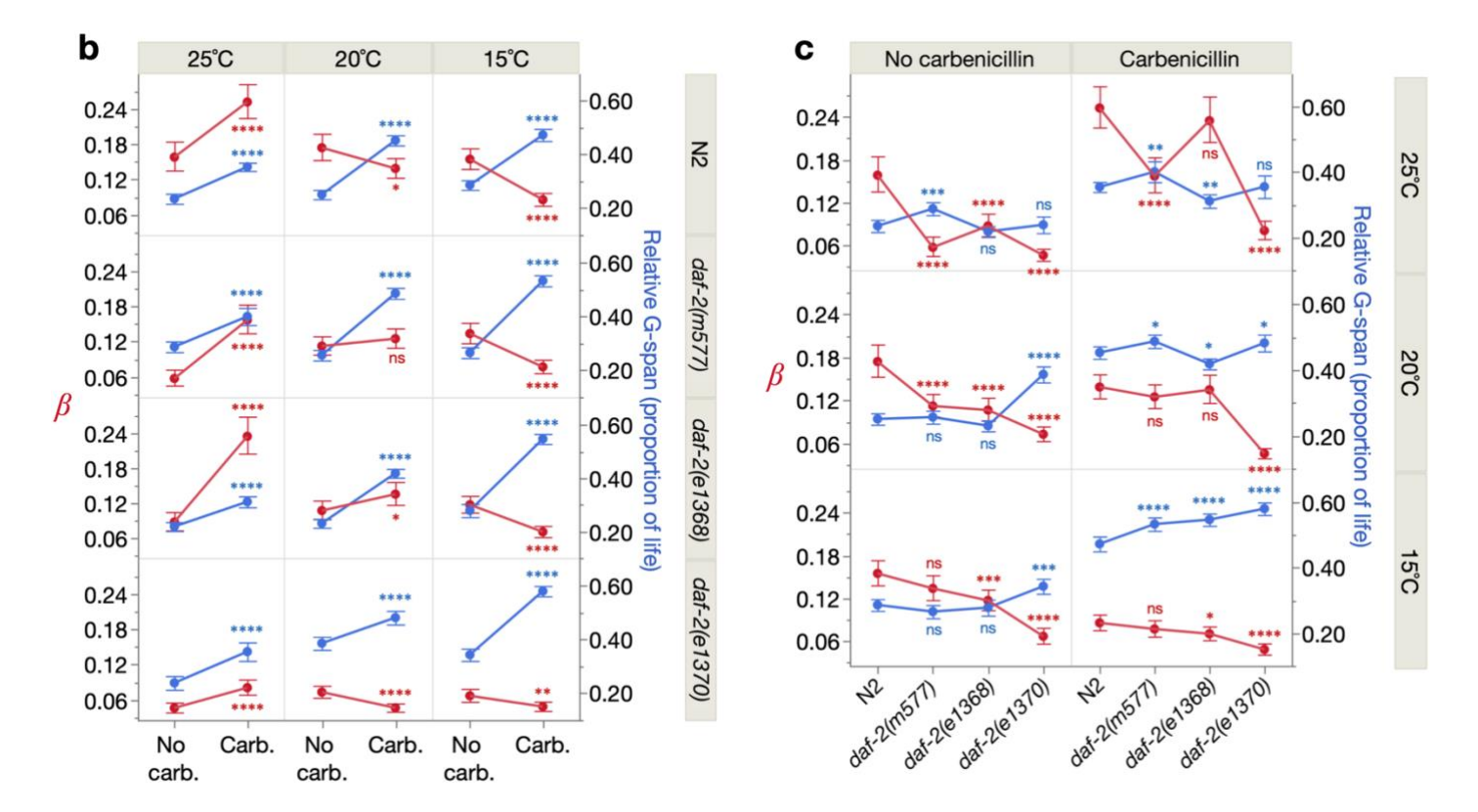


Figure 3.5. Correspondence between reduced  $\beta$  and increased relative gerospan. Effects of (a) reduced temperature, (b) carbenicillin, and (c) daf-2(rf) on  $\beta$  and relative gerospan (G-span<sup>rel</sup>). N2: wild-type. G-span<sup>rel</sup> values, 95% confidence intervals and statistical significance symbols are replotted from Figure 3.4, and  $\beta$  calculated by maximum likelihood estimation, and statistical significance of  $\beta$  differences assessed by likelihood ratio tests, showing 95% confidence intervals.

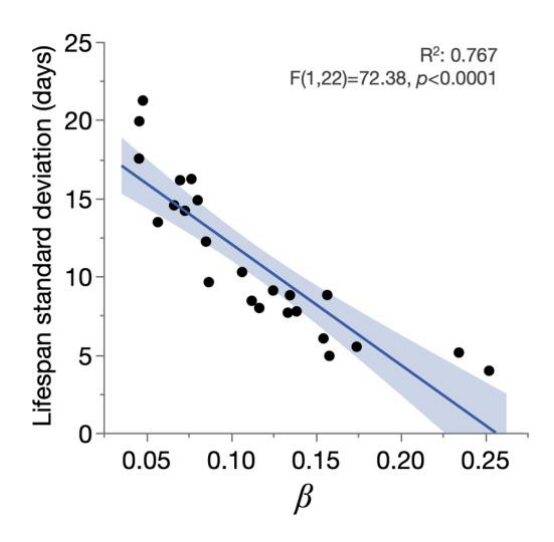
I similarly evaluated the effects of the antibiotic treatments. Against the expectation that preventing infection (a largely extrinsic insult) would reduce  $\alpha$  alone, carbenicillin decreased  $\beta$  in all genotypes at 15°C, and in wild-type and daf-2(e1370) at 20°C (Figure 3.5b). In each case, G-span<sup>rel</sup> was again increased. In the remaining carbenicillin treatments, both  $\beta$  and G-span<sup>rel</sup> increased, suggesting that  $\beta$  reduction may require G-span<sup>rel</sup> increase, but not vice versa.

Finally, I assessed the daf-2(rf) mutations. daf-2(e1370), the severest (and longest-lived) allele, also lowered  $\beta$  while increasing G-span<sup>rel</sup>, both off and on carbenicillin, at 15°C and 20°C (Figure 3.5c). At 25°C,  $\beta$  was decreased without change in G-span<sup>rel</sup>, as an exception to the pattern; similarly, only 3/7 class 1 daf-2(rf) treatments (daf-2(m577)) and daf-2(e1368)) that reduced  $\beta$  increased G-span<sup>rel</sup>.

Despite these exceptions, 21/27 (78%) of all treatments that significantly reduced  $\beta$  simultaneously increased G-span<sup>rel</sup>. Thus, amongst these life-extending interventions, reduction of  $\beta$  largely reflects expanded decrepitude rather than a simple deceleration of biological ageing. Of course, this does not preclude more complex forms of ageing deceleration, as I will demonstrate later in section 3.5.

A notable feature of the demography of ageing is the high degree of inter-individual variability in lifespan. This is true of *C. elegans*, despite their being isogenic and maintained under identical conditions (Vaupel et al., 1998, Kirkwood et al., 2005). An often-overlooked property of the Gompertz rate parameter  $\beta$  is its inverse relation to lifespan variation, which in comparison is only marginally affected by the  $\alpha$  parameter (Figure 2.1d, p. 25) (Tuljapurkar and Edwards, 2011).

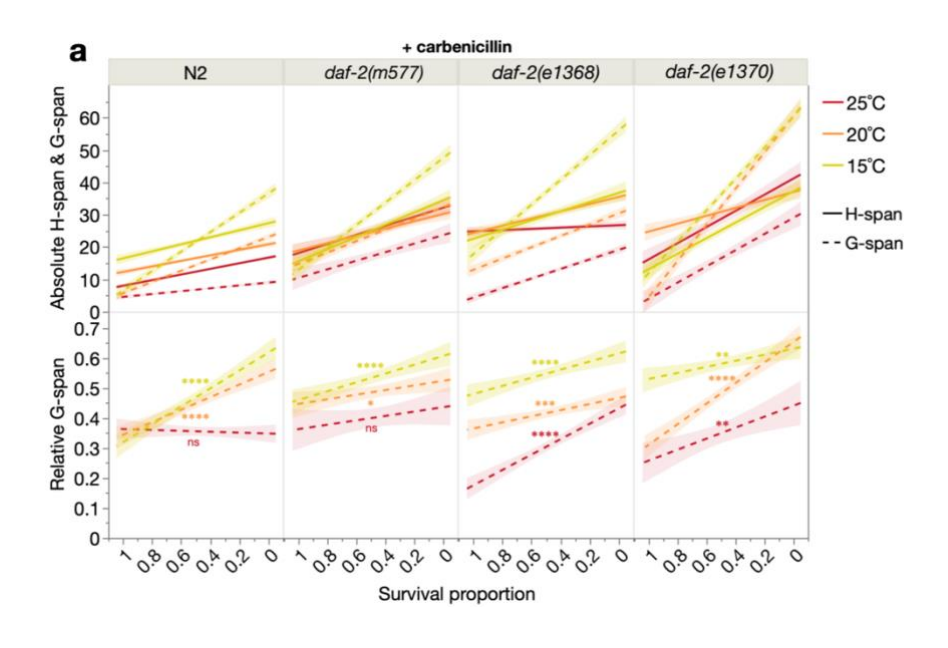
I therefore wondered about the relation of  $\beta$  to inter-individual differences in ageing. As expected, across my 24 cohorts,  $\beta$  showed a strong inverse correlation with the standard deviation of lifespan (Figure 3.6). According to a previous estimate, G-span differences account for most (~67%) inter-individual lifespan variation in a normal-lived sterile strain of *C. elegans* (Zhang et al., 2016). Thus, the correspondence between reduced  $\beta$  and increased G-span<sup>rel</sup> in my cohorts might reflect inter-individually variable G-span expansion. To investigate this, I assessed H-span<sup>abs</sup> and G-span<sup>abs</sup> for all individuals in the 21 treatments displaying an inverse  $\beta$ -G-span<sup>rel</sup> relationship, as explained next.

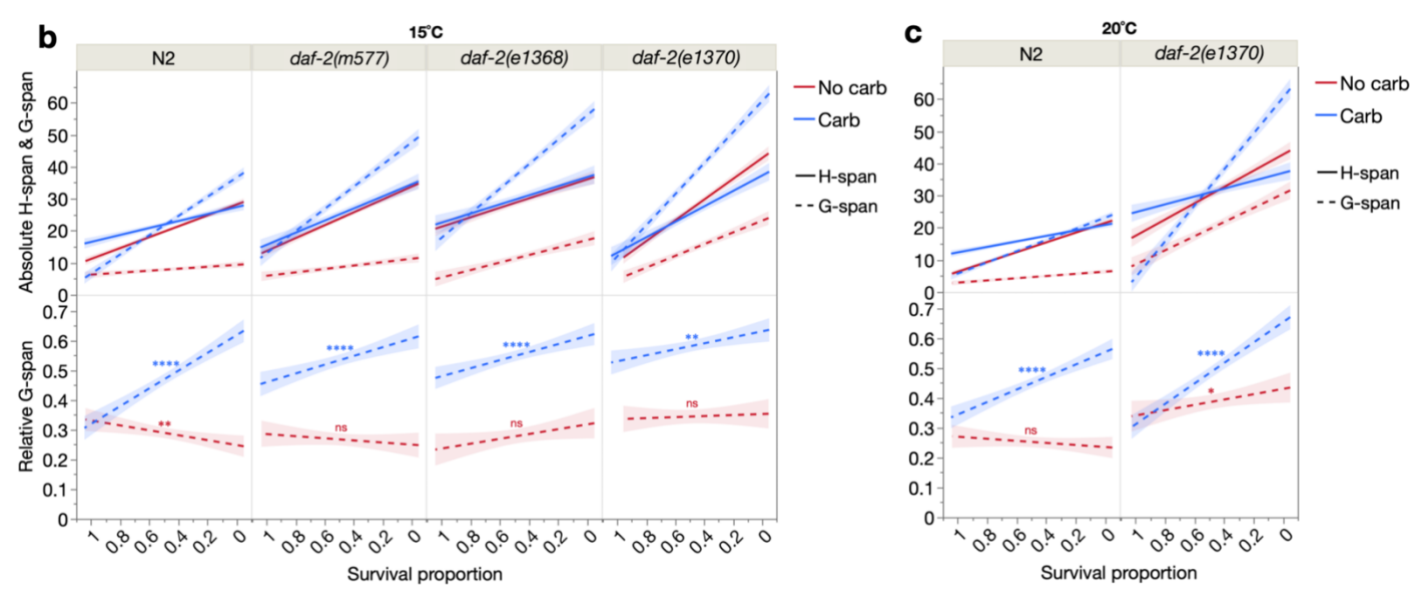


**Figure 3.6.**  $\beta$  reflects lifespan variation.  $\beta$  is an inverse measure of lifespan standard deviation, across the 24 cohorts. The relationship was assessed using least-squares linear regression and an F-test, with the 95% confidence region shaded.

To visualise the variation in H-span<sup>abs</sup> and G-span<sup>abs</sup> in each cohort population, I regressed individuals' H-span<sup>abs</sup> and G-span<sup>abs</sup> values over their "survival proportion" (Figure 3.7; upper boxes in each panel). In this form of representation, the x-axis orders individuals by survival order (i.e. left: shorter-lived individuals, right: longer-lived individuals), therefore allowing H-span and G-span of individuals from different cohorts to be compared. This is akin to the y-axis of survival curve plots which allow comparison of lifespans between cohorts for the same

survival proportion (e.g. 0.5 for median lifespan). These linear regression fits reveal a striking positive linearity in the relationships of both H-span<sup>abs</sup> and G-span<sup>abs</sup> against survival proportion, indicating a robust scaling between H-span<sup>abs</sup> and G-span<sup>abs</sup> in all individuals, regardless of lifespan and cohort identity.





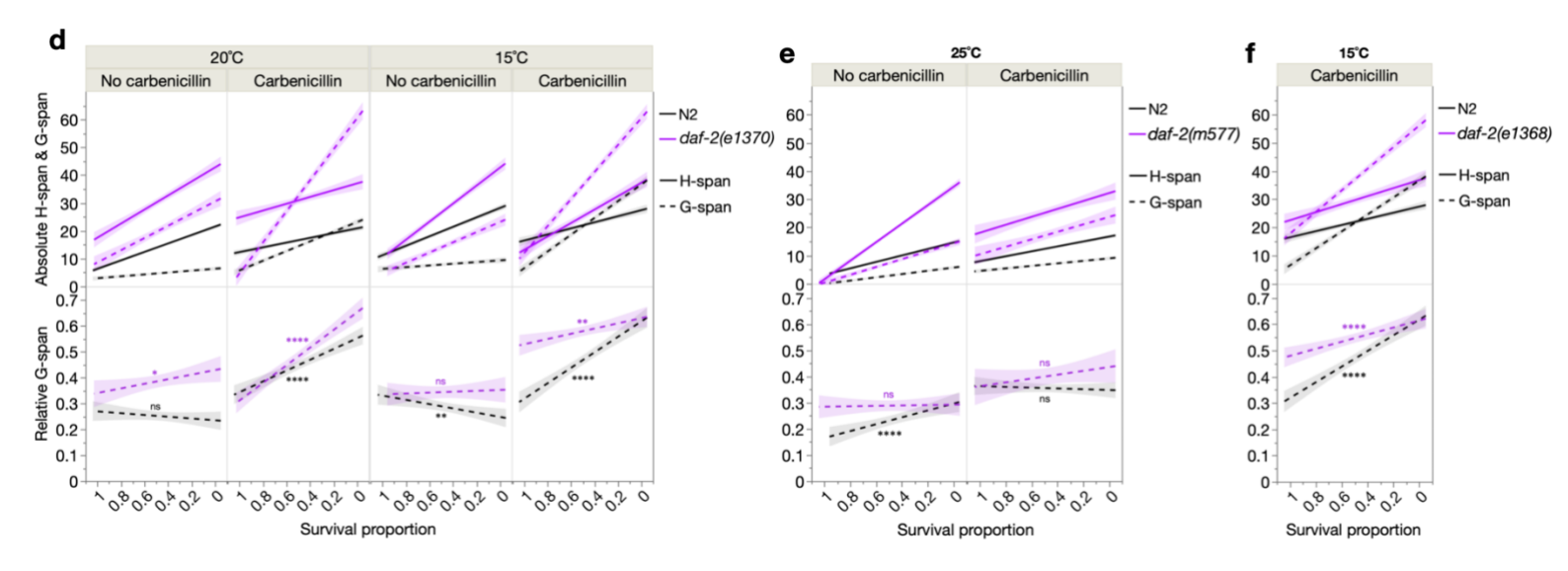


Figure 3.7. Reduced  $\beta$  reflects inter-individually variable gerospan expansion. Effects of low (a) temperature, (b-c) carbenicillin, and (d-f) *daf-2(rf)* on absolute healthspan and gerospan (top boxes) and relative gerospan (bottom boxes), plotted over survival proportion (i.e. x-axis left: shorter-lived individuals, x-axis right: longer-lived individuals). All panels show least-squares linear regressions with shaded 95% confidence regions, whose relationships were assessed by F-tests; statistical significance indicated for relative G-span regressions (bottom boxes): ns p > 0.05, \*  $p \le 0.05$ , \*\*  $p \le 0.01$ , \*\*\*\*  $p \le 0.001$ , \*\*\*\*  $p \le 0.0001$ .

I first used this dataset to assess reduced temperature effects. On carbenicillin, reducing temperature to  $20^{\circ}$ C in wild-type, daf-2(m577), and daf-2(e1370) increased G-span<sup>abs</sup> disproportionately more than H-span<sup>abs</sup> in longer-lived individuals (Figure 3.7a top, 3.9a top and middle). As a result, G-span<sup>rel</sup> was increased in longer-lived individuals (Figure 3.7a bottom, 3.9a bottom). This illustrates how life-extending interventions can act by introducing or amplifying the extended "twilight" (Zhang et al., 2016) (greater G-span<sup>rel</sup>) of longer-lived individuals within a population, which I will refer to as *extended twilight longevity* (ETL) (see Glossary, p. 10). A critical implication of this ETL is that the  $\beta$  reduction and associated extension of the survival curve tail arises from the disproportionate expansion of decrepitude in longer-lived population members (Figure 3.8). This finding is a key component of the understanding that this thesis presents, and one that I will return to regularly. Notably however, in the remaining minority of treatments ((daf-2(e1368)) and  $15^{\circ}$ C in daf-2(e1370)), G-span<sup>rel</sup> increased more in shorter-lived individuals (Figure 3.7a); the significance of this will be discussed later.

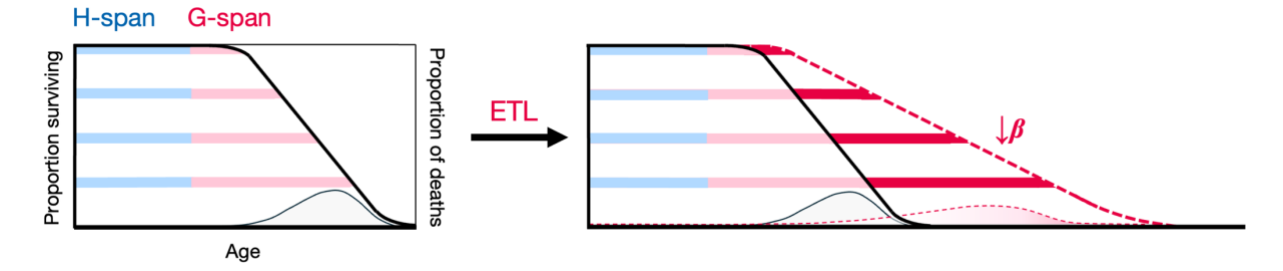
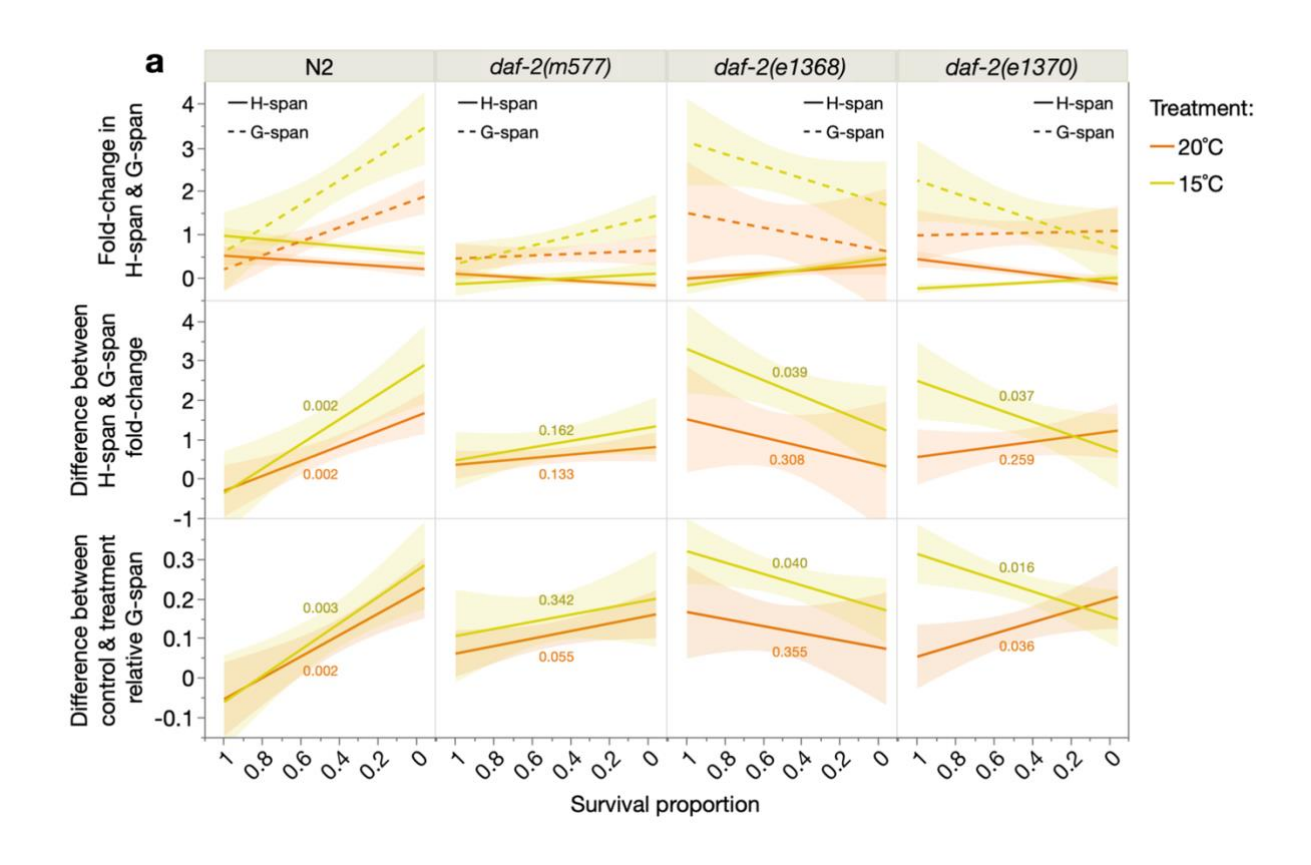
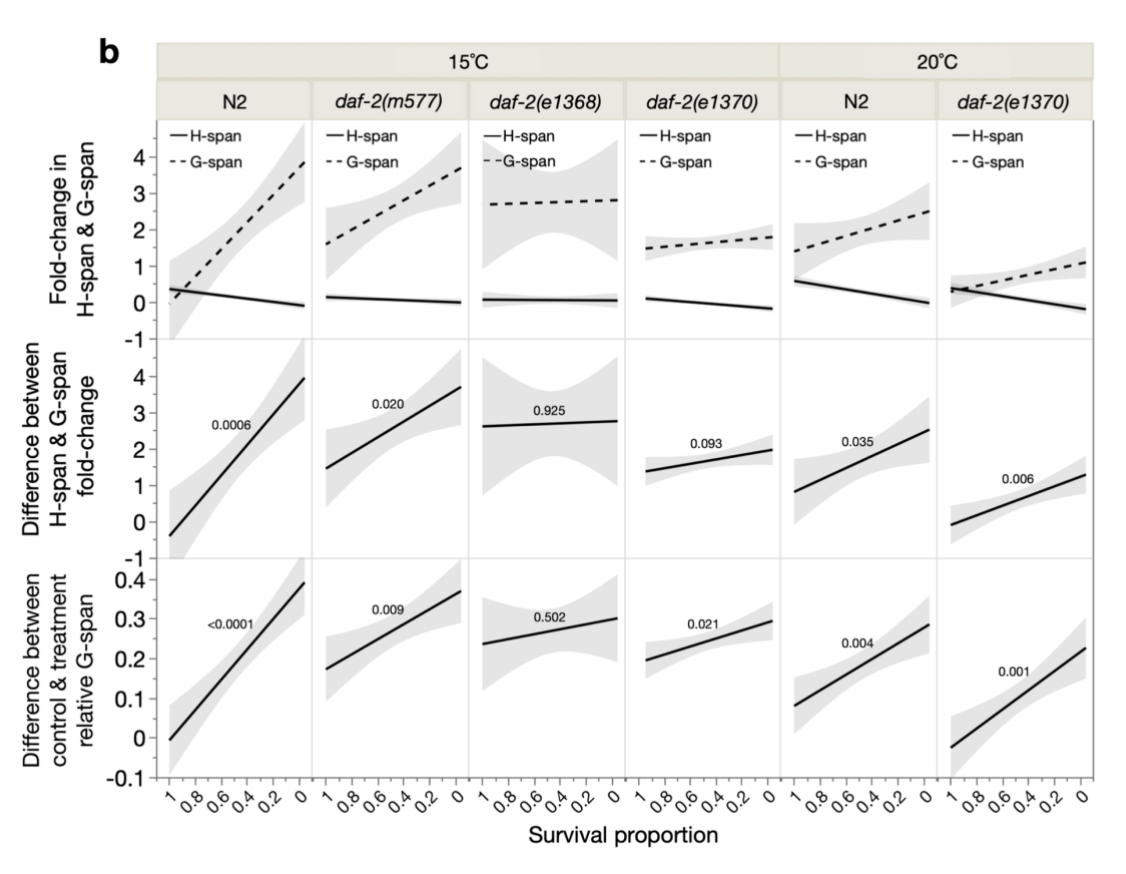


Figure 3.8.  $\beta$  reduction reflects increased gerospan variation. Summary schematic of the biological basis of  $\beta$  across my experimental cohorts, depicting a hypothetical intervention that reduces  $\beta$ . Each panel depicts healthspan (H-span; blue bar segment) and gerospan (G-span, red bar segment) for four individuals representative of their depicted lifespan within the population as bordered by the survival curves (left y-axis, bold data lines).  $\beta$  reduction arises from inter-individually variable G-span expansion (greater in longer-lived individuals), causing the approximate horizontal stretch of the survival curve (dashed red) that occurs in  $\beta$  reduction. In both panels, probability distributions of death times corresponding to the survival curves, are overlaid (right y-axis, thin data lines), showing that  $\beta$  reduction stretches this distribution, increasing lifespan variation. The area under these probability distributions is shaded to reflect the level of inter-individual variation in G-span:  $\beta$  reduction involves greater G-span expansion in longer-lived individuals (red gradient). Therefore,  $\beta$  describes the degree of inter-individual variation in health and lifespan, and not intra-individual biological ageing rate.

Next, in all carbenicillin treatments that yielded the inverse  $\beta$ -G-span<sup>rel</sup> relationship, G-span<sup>abs</sup> again increased disproportionately more than H-span<sup>abs</sup> in longer-lived individuals, thus increasing G-span<sup>rel</sup> in these individuals (Figure 3.7b–c, 3.9b). Therefore, carbenicillin too is an ETL treatment that lowers  $\beta$  via variable G-span expansion. This shows that extrinsic mortality (here, infection) can also affect  $\beta$  through ETL.

Finally, I asked if  $\beta$  reduction in daf-2(rf) reflects ETL. At 20°C, and 15°C without carbenicillin, daf-2(e1370) indeed increased G-span<sup>abs</sup> more than H-span<sup>abs</sup>, and therefore G-span<sup>rel</sup>, in longer-lived individuals (Figure 3.7d, 3.9c). However, on carbenicillin at 15°C, daf-2(e1370) increased G-span<sup>rel</sup> more in shorter-lived individuals. This was also true for 2/3 of the daf-2(m577) and daf-2(e1368) treatments with an inverse  $\beta$ -G-span<sup>rel</sup> relationship, although the remaining treatment exhibited modest ETL (Figure 3.7e–f, 3.9c). This thus reveals a more complex picture in the effects of daf-2(rf).





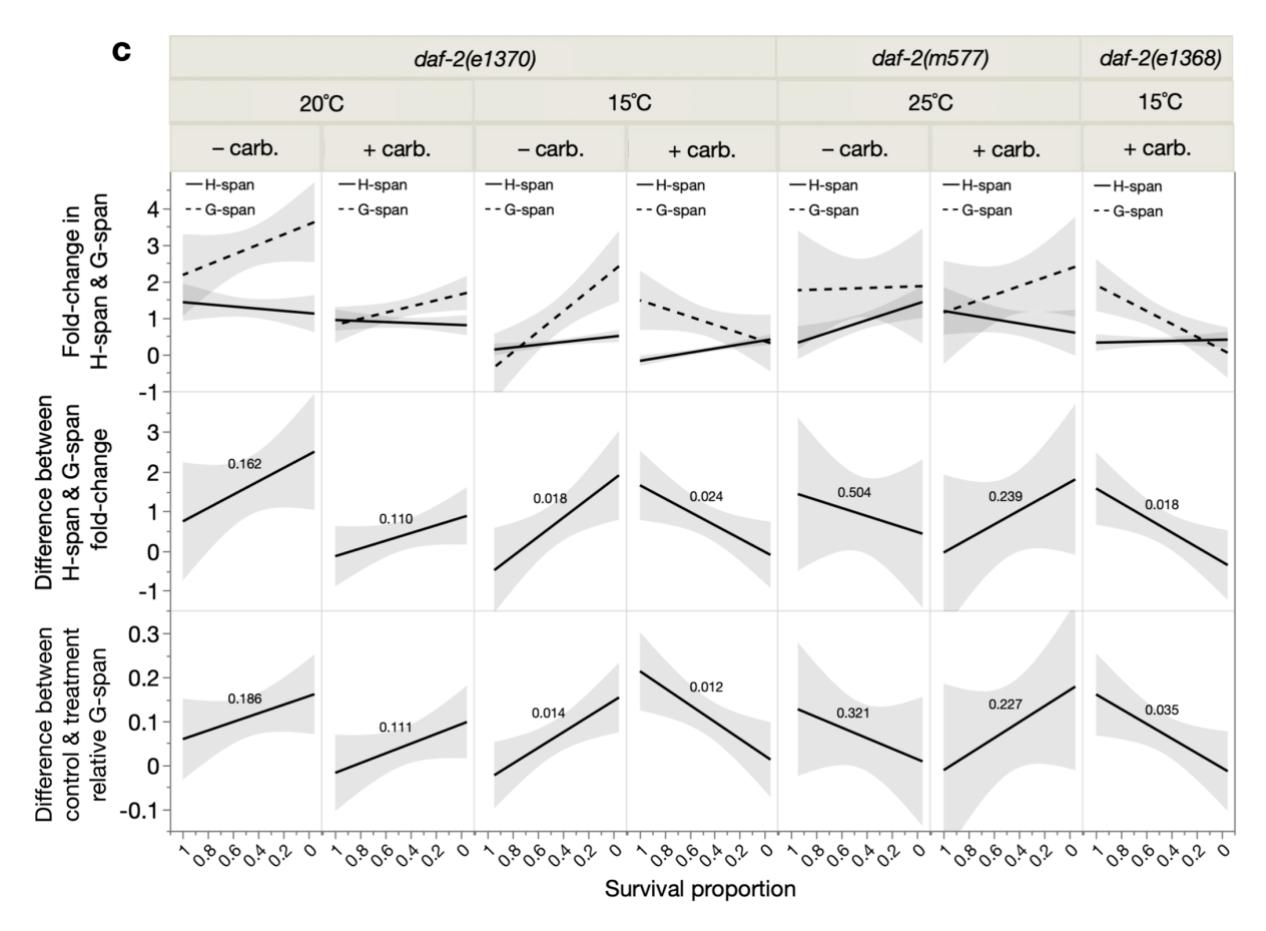
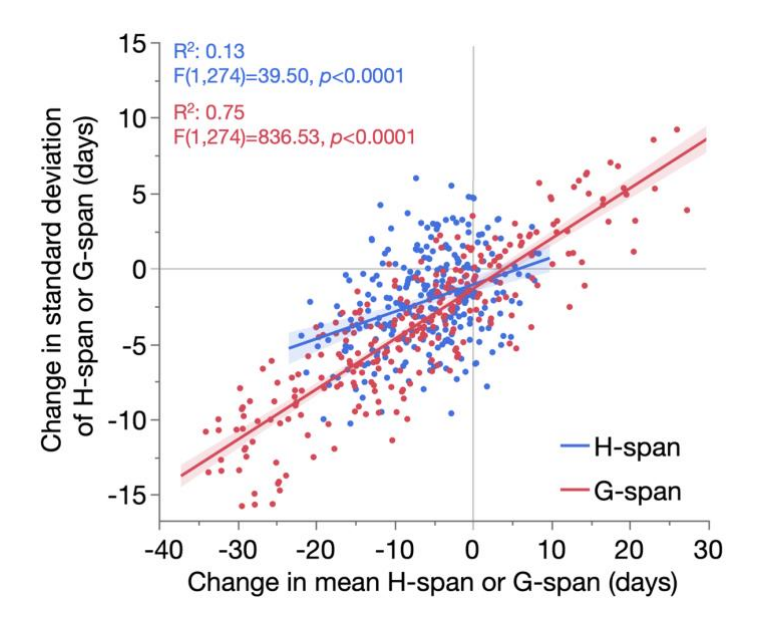


Figure 3.9. Extended twilight longevity (ETL) increases gerospan in longer-lived individuals. All longevity treatments causing simultaneous  $\beta$  decrease and G-span<sup>rel</sup> increase are presented, from three treatment categories: low temperature (a), carbenicillin (b) and daf-2(rf) (c). N2: wild-type. The top row of panels plots the fold-change of absolute H-span and G-span (in response to treatment), over survival proportion; in ETL, G-span fold-change is greater than H-span fold-change at lower survival proportions (longer-lived individuals). This difference between G-span and H-span fold-change across survival proportions is plotted and statistically evaluated in the middle row of panels; in ETL, this yields a positive relationship. The **bottom row of panels** plots and statistically evaluates the difference between control and treatment G-span<sup>rel</sup> (from Figure 3.7 bottom boxes), over survival proportion; in ETL, this yields a positive relationship. All panels show least-squares linear regressions with shaded 95% confidence regions, and associated F-test p-values overlaid for middle and bottom panels. These regressions may be limited in power by sample size  $(8 \le n \le 20)$ , due to binning and averaging of individual survival proportions (0.05 survival proportion bins) and inclusion of only those bins represented in both control and treatment cohorts. This may explain the statistical non-significance of some relationships; however, all relationship directions (positive or negative) agree with those in Figure 3.7, which perform regressions using all (unbinned) individuals ( $104 \le n \le 173$ ).

In summary,  $\beta$  reduction reflected ETL in 5/8 reduced temperature, 6/6 antibiotic, and 4/7 daf-2(rf) treatments (15/21 or 71%, in total) where  $\beta$  reduction co-occurred with G-span<sup>rel</sup> increase. Notably, in all 6 exceptions, control cohorts already exhibited extended relative twilight (G-span<sup>rel</sup>) in long-lived population members (Figure 3.7a, d–f), perhaps limiting further amplification (via ETL) of this existing variation. Importantly, in most (4/6) of these exceptions,

 $\beta$  was still primarily a function of greater G-span<sup>abs</sup> expansion in longer-lived population members (Figure 3.7a, d–f), whose ETL effect on G-span<sup>rel</sup> was obscured by simultaneous H-span<sup>abs</sup> changes and/or especially short G-span<sup>abs</sup> in short-lived members, to which G-span<sup>rel</sup> is sensitive. Thus, in 19/21 (90%) of treatments with reduced  $\beta$  and increased G-span<sup>rel</sup>, this  $\beta$  reduction arose primarily from G-span<sup>abs</sup> expansion in longer-lived population members. However, for simplicity, I will focus on the subset of 15 ETL treatments.

As a further probe of whether  $\beta$  reduction arises from ETL in these 15 treatments, I compared contributions of H-span<sup>abs</sup> and G-span<sup>abs</sup> changes to  $\beta$  reduction, and to lifespan variation (standard deviation) increase. Indeed, G-span<sup>abs</sup> changes decreased  $\beta$  more than H-span<sup>abs</sup> changes in 13/15 treatments (compared to 0/6 non-ETL treatments) (Table 3.2), and increased lifespan standard deviation more in 14/15 interventions (compared to 3/6 exceptions) (Table 3.3). Consistent with these findings, across the 24 cohorts, G-span variation increased more rapidly with mean G-span than H-span variation with mean H-span, while mean length and variability of G-span had a wider range than those of H-span (Figure 3.10). This shows that across these cohorts, inter-individually variable expansion of G-span rather than H-span (i.e. ETL), is the primary mode of life extension.



**Figure 3.10. G-span expansion is more inter-individually variable than H-span expansion.** Assessed across all possible pairs of the 24 cohorts. In addition to a considerably higher R<sup>2</sup>, the steeper gradient of the G-span linear fit indicates a greater increase in variation for a given increase in span length; i.e. G-span variation increases faster than H-span variation under life-extending conditions. Consistent with this, the range of values for mean H-span and H-span standard deviation is notably less than that for G-span. The relationships were assessed using F-tests, and the 95% confidence regions are shaded.

Control (25°C + carbenicillin) a Effect of low temperature N2 daf-2(m577) daf-2(e1368) daf-2(e1370) on  $\beta$ H-span G-span H-span G-span H-span G-span H-span G-span Abs. -0.06 -0.24 20°C Rel. -19.7 -62.1 -0.14 -0.30 15°C Treatment (20 or 15°C + carbenicillin) Rel. -47.0 -78.5 Abs. 0.02 0.01 20°C 23.1 14.5 Abs. -0.03 -0.01 15°C Rel. -28.3 -6.6 Abs. -0.12 0.01 20°C Rel. -38.3 9.2 Abs. -0.19 -0.06 15°C Rel. -63.7 -45.0 0.048 -0.005 Abs. 20°C Rel. 67.3 -12.4 0.001 0.016 15°C Rel. 8.0 44.0

						Con	trol (– c	arbenici	llin)				
1	ffect of benicillin		N	12		daf-2(i	m577)	daf-2(e	e1368)		daf-2(e	1370)	
	on $\beta$	20	°C	15	°C	15	°C	15	°C	20	°C	15	°C
	,	H-span	G-span	H-span	G-span	H-span	G-span	H-span	G-span	H-span	G-span	H-span	G-spa
	Abs.	0.06	-0.13										
	Rel.	33.2	-46.5										
	Abs.			0.01	-0.15	]							
Treatment (+ carbenicillin)	Rel.			10.6	-63.9								
enic	Abs.					-0.058	-0.063						
carb	Rel.					-43.7	-43.3						
nt (+	Abs.							-0.028	-0.005				
tme	Rel.							-19.9	-6.5				
Trea	Abs.									0.028	-0.029		
	Rel.									31.6	-47.5		
	Abs.											-0.01	-0.0
	Rel.											-7.5	-27.

c									Contr	ol (N2)					
	E	Effect of daf-2(r	f)			– carbe	nicillin					+ carbe	nicillin		
		on $oldsymbol{eta}$		25	°C	20	°C	15	°C	25	°C	20	°C	15	°C
				H-span	G-span	H-span	G-span	H-span	G-span	H-span	G-span	H-span	G-span	H-span	G-span
		daf-2(m577)	Abs.	-0.17	-0.08					-0.18	-0.30				
		uai-2(111577)	Rel.	-71.2	-47.5					-64.1	-77.1				
	on)	daf-2(e1368) Abs.												-0.04	-0.01
	daf-2(e1368)	Rel.											-27.6	-17.7	
	m	<u> </u>	Abs.			-0.08	-0.21								
	ıf-2		Rel.			-48.3	-77.5								
	t (dê		Abs.					-0.06	-0.16						
	ent	dof 2(a1270)	Rel.					-44.3	-68.0						
	atr	daf-2(e1370) Abs. Rel.	Abs.									-0.113	-0.115		
	Tre		Rel.									-48.9	-77.9		
			Abs.											-0.08	-0.03
			Rel.											-53.4	-35.9

Table 3.2. Effect of changes in H-span and G-span on the  $\beta$  parameter. All longevity treatments causing simultaneous  $\beta$  decrease and G-span<sup>rel</sup> increase are presented, from three treatment categories: low temperature (a), carbenicillin (b), and daf-2(rf) (c). N2: wild-type. Blue cells indicate treatments causing extended twilight longevity (ETL), and pink cells indicate non-ETL treatments. Treatments where G-span causes greater reduction in  $\beta$  than H-span have a bold border. Both absolute (Abs.) and relative percentage (Rel.) effects are shown, with the sign (positive/negative) indicating direction of change. For this analysis,  $\beta$  was obtained for H-span and G-span (instead of lifespan), for control and treatment cohorts, and the change (between control and treatment) quantified to estimate the separate contributions of H-span and G-span to lifespan  $\beta$  (H-span and G-span sum to lifespan and have approximately additive effects on  $\beta$ ).

	450	ffect of l	7.55			Contro	l (25°C	+ carben	icillin)		
		nperatur span star		N	2	daf-2(i	m577)	daf-2(e	e1368)	daf-2(e	1370)
		deviatio	n	H-span	G-span	H-span	G-span	H-span	G-span	H-span	G-span
		20°C	Abs.	0.8	3.7						
		20 0	Rel.	23.6	153.0						
		15°C	Abs.	2.3	7.8						
	(lin	15 C	Rel.	69.8	324.1						
	nici	20°C	Abs.			-1.8	-0.5				
	Treatment (20 or 15 °C + carbenicillin)  15 °C + carbenicillin)  15 °C + carbenicillin)	Rel.			-20.5	-5.9					
		15°0	Abs.			0.05	3.80				
	င်္ခ	15 C	Rel.			0.5	44.6				
	or 15	20°C	Abs.					1.8	1.1		
	(20	20 C	Rel.					45.2	20.2		
	ent	15°0	Abs.					4.7	7.5		
	atm	15°C	Rel.					120.0	136.7		
	Tre	20°C	Abs.							-3.3	6.1
		20°C	Rel.							-29.1	51.3
		15°C	Abs.							-1.0	3.9
		15°C	Rel.							-9.0	32.4

b	1	ect of					Cor	itrol (– ca	arbenici	llin)				
	1	enicillin ifespan		N	12		daf-2(	m577)	daf-2(e	e1368)		daf-2(e	e1370)	
	1	ndard	20	°C	15	°C	15	°C	15	°C	20	°C	15	°C
	dev	/iation	H-span	G-span	H-span	G-span	H-span	G-span	H-span	G-span	H-span	G-span	H-span	G-span
		Abs.	-0.9	3.7										
		Rel.	-19.0	157.0										
		Abs.			-0.5	6.9								
	illin)	Rel.			-8.6	208.2								
	enic	Abs.					1.5	8.1						
	carb	Rel.					21.1	188.1						
	+ +	Abs.							1.4	6.1				
	tmer	Rel.							19.2	87.4				
	Treatment (+ carbenicillin)	Abs.									-2.4	8.1		
		Rel.									-23.5	81.8		
		Abs.											-0.5	8.0
		Rel.											-4.9	104.4

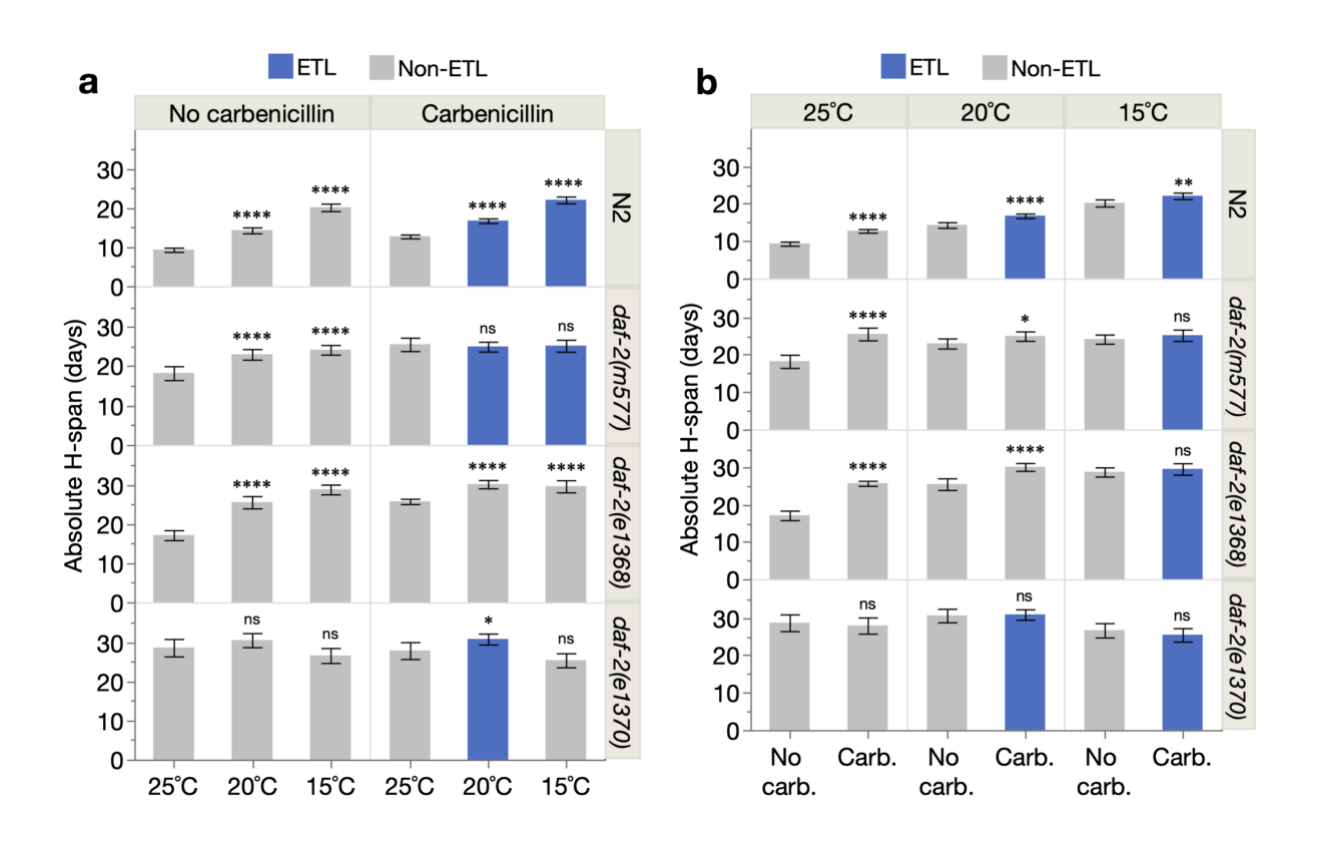
C	E#	fect of <i>daf-2(rf</i> )	on						Contro	ol (N2)					
		ifespan standar				- carbe	nicillin					+ carbe	enicillin		
	•	deviation	-	25	°C	20	°C	15	°C	25	°C	20	°C	15	°C
				H-span	G-span	H-span	G-span	H-span	G-span	H-span	G-span	H-span	G-span	H-span	G-span
		dof 2(mE77)	Abs.	6.4	2.9					5.4	6.1				
		daf-2(m577)	Rel.	180.3 127.9					166.0	256.4					
	daf-2(e1368)	Abs.											3.1	2.9	
		uai-2(e1368)	Rel.											56.4	28.4
			Abs.			5.4	7.5								
	1f-2		Rel.			108.9	319.5								
	g		Abs.					4.7	4.4						
	ent	def 0(e1070)	Rel.					77.0	133.6						
	atu	daf-2(e1370) Rel	Abs.							,		3.9	11.9		
	Trea		Rel.									97.3	196.7		
			Abs.											4.7	5.6
			Rel.											84.1	54.9

Table 3.3. Effect of changes in H-span and G-span on lifespan standard deviation. All longevity treatments causing simultaneous  $\beta$  decrease and G-span<sup>rel</sup> increase are presented, from three treatment categories: low temperature (a), carbenicillin (b), and daf-2(rf) (c). N2: wild-type. Blue cells indicate treatments causing extended twilight longevity (ETL), and pink cells indicate non-ETL treatments. Treatments where G-span causes greater increase in lifespan standard deviation than H-span have a bold border. Both absolute (Abs.) and relative percentage (Rel.) effects are shown, with the sign (positive/negative) indicating direction of change (positive changes are related to  $\beta$  reduction). For this analysis, standard deviation was obtained for H-span and G-span, for control and treatment cohorts, and the change (between control and treatment) quantified to estimate the separate contributions of H-span and G-span to lifespan standard deviation (H-span and G-span sum to lifespan and have approximately additive effects on lifespan standard deviation).

In summary, these findings argue that expanded decrepitude not only correlates with a lower  $\beta$  value, but causes it. That is, gerospan expansion in longer-lived population members further increases their lifespan, thus extending the survival curve tail in the manner characteristic of a lower  $\beta$  value (Figure 3.8). Therefore,  $\beta$  here is not a measure of intra-individual, biological ageing rate as commonly understood, but rather of inter-individual heterogeneity in late-life decrepitude.

## 3.5 – Reduced α reflects slowed biological ageing

Because healthspan expansion may be considered a reliable indicator of slowed biological ageing (given more time to G-span onset), I wondered if  $\beta$  reduction could at least indirectly reflect decelerated ageing, should G-span<sup>abs</sup> and H-span<sup>abs</sup> expansions be coupled. Indeed, H-span<sup>abs</sup> was increased in 9/15 ETL treatments (Figure 3.11).



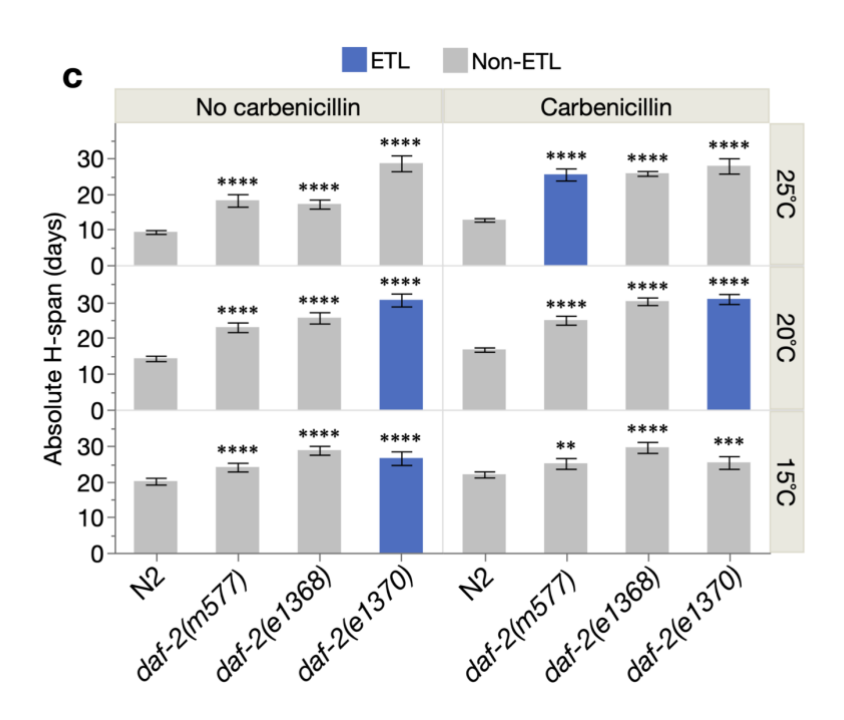


**Figure 3.11. Absolute H-span is increased in ETL and non-ETL treatments.** Effects of (a) low temperature, (b) carbenicillin, and (c) *daf-2(rf)* on mean absolute healthspan (H-span<sup>abs</sup>). N2: wild-type, ETL: extended twilight longevity. Statistical significance of H-span<sup>abs</sup> differences was assessed by two-tailed Student's t-tests, showing 95% confidence intervals.

I therefore examined the effect of H-span<sup>abs</sup> expansion on the Gompertz parameters in these 9 treatments. H-span<sup>abs</sup> expansion significantly decreased  $\beta$  in 4/9 treatments but, strikingly, significantly decreased  $\alpha$  in 8/9 (Figure 3.12a, Table 3.4). This suggests that  $\alpha$ , though not traditionally associated with biological ageing, may in fact be a better measure of it than  $\beta$ .

To assess if this unexpected finding is idiosyncratic to ETL, I also examined the non-ETL treatments, of which 27/31 significantly extended H-span<sup>abs</sup> (Figure 3.11). However, again, H-span<sup>abs</sup> expansion decreased  $\alpha$  in 22/27 (81%) of these non-ETL treatments, but decreased  $\beta$  in only 13/27 (48%) (Figure 3.12a, Table 3.4). Additionally, H-span<sup>abs</sup> expansion *increased*  $\beta$  in 9/27 treatments, including in all carbenicillin treatments; thus, slowing biological ageing can even increase  $\beta$ . Considering all treatments together (ETL plus non-ETL), H-span<sup>abs</sup> expansion decreased  $\alpha$  in 30/36 (83%) cases, decreased  $\beta$  in 16/36 (44%), and increased  $\beta$  in 12/36 (33%). This suggests that  $\alpha$  should better predict H-span<sup>abs</sup> than  $\beta$  amongst the 24 cohorts, and this indeed proved to be the case (Figure 3.12b).

а	Ψ	α	4	β	1	β
	ETL	Non-ETL	ETL	Non-ETL	ETL	Non-ETL
Low temperature	3/3	6/8	0/3	5/8	1/3	3/8
Carbenicillin	2/2	5/5	0/2	0/5	2/2	5/5
daf-2(rf)	3/4	11/14	3/4	8/14	0/4	1/14
Total	8/9	22/27	3/9	13/27	3/9	9/27
Total (ETL + non-ETL)	30/36	(83%)	16/36	(44%)	12/36	(33%)

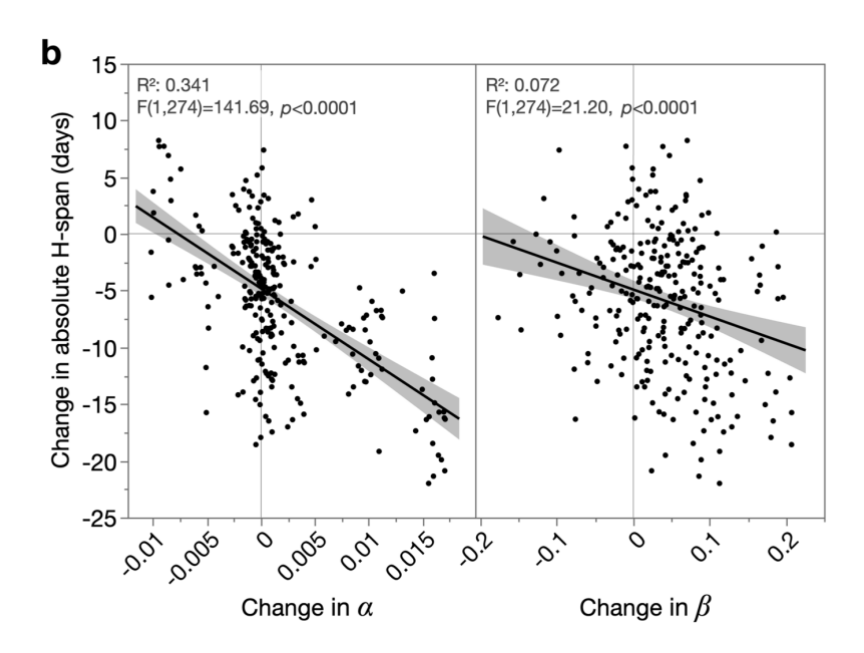


Figure 3.12.  $\alpha$  outperforms  $\beta$  as a measure of absolute healthspan. (a) Table summarising fractions of ETL and non-ETL cohorts in which H-span<sup>abs</sup> increase causes the specified Gompertz parameter change, for each life-extending treatment class. (b) Least-squares linear regressions of the changes in H-span<sup>abs</sup> between all possible pairs of all 24 cohorts, over the corresponding change in  $\alpha$  or  $\beta$  for those pairs. This shows that  $\alpha$  is the better predictor of H-span<sup>abs</sup>. The relationships were assessed by F-tests, with the 95% confidence regions shaded.

a Control (25°C) Effect of H-span N2 daf-2(m577) daf-2(e1368) daf-2(e1370) expansion in low temperature -carb. + carb. -carb. -carb. + carb. + carb. treatment β α β β β α β β α  $\alpha$  $\alpha$ α 20°C -98 -33 15°C -250 -49 20°C -53 2 Treatment (20 or 15°C) 15°C -105 -25 20°C -586 30 15°C -691 39 20°C -198 -6 15°C -437 42 20°C 0.5 -525 15°C 10 -725 20°C -46 45

Effect of						Con	itrol (– c	arbeni	cillin)					
H-span			N	2				daf-2(	m577)			daf-2(	e1368)	
expansion in carbenicillin	25	°C	20	°C	15	s°C	25	°C	20	°C	25	°C	20	°C
treatment	α	β	α	β	α	β	α	β	α	β	α	β	α	β
	-152	24												
(lin)			-95	44										
benici					-47	36								
Treatment (+ carbenicillin)							-951	57						
tment									-62	53				
Trea											-527	93		
													-110	60

C	Effect of	H-span						Contr	ol (N2)					
	expans	sion in		-	- carbe	nicillir	1				+ carbe	nicillir	1	
	daf		25	°C	20	°C	15	°C	25	°C	20	°C	15	°C
	treat	ment	α	β	α	β	α	β	α	β	α	β	α	β
			46	-185										
					-88	-51								
		157					-22	-18						
		daf-2(m577)							-127	-60				
		dai									-57	-28		
	(uoi												6	-75
	Treatment ( <i>daf-2(rf)</i> mutation)		-24	-127										
	m ()	86			-86	-81								
	2(ri	136					-89	12						
	(daf	daf-2(e1368)							-208	80				
	ent	da									-100	-29		
	atu												-35	-33
	Tre		-179	-240										
		(0,			-177	-67								
		137					7	-89						
		daf-2(e1370)							-115	-157				
		dai									-105	-44		
													20	-123

Table 3.4. Effect of absolute H-span increase on  $\alpha$  and  $\beta$ . All longevity treatments causing H-span increase are presented, from three treatment categories: low temperature (a), carbenicillin (b), and  $daf^2(rf)$  (c). N2: wild-type. Blue cells indicate treatments causing extended twilight longevity (ETL). Relative percentage effects are shown, with the sign (positive/negative) indicating direction of change, and statistically significant (p < 0.05) effects are coloured red. Effects on  $\alpha$  and  $\beta$  are respectively estimated as changes in the y-intercept and gradient of the least-squares linear regression model of H-span abs over survival proportion (as plotted in Figure 3.7). Increases in y-intercept and gradient correspond, respectively, to decreases in  $\alpha$  and  $\beta$ . Statistical significance was assessed by two-tailed regression t-tests on model parameter estimates (y-intercept: treatment term; gradient: interaction term between treatment and survival proportion).

In summary, healthspan expansion, a plausible metric of slowed biological ageing, more consistently reduces  $\alpha$  than  $\beta$ , and even increases  $\beta$ . This occurs because H-span increases relatively equally in all population members and in some cases preferentially in shorter-lived population members; in both scenarios,  $\alpha$  reflects H-span length primarily in shorter-lived population members (whose lifespans determine mortality onset age). In contrast, gerospan increases primarily in longer-lived population members, as demonstrated in the previous section. Thus, overall, my empirically-based findings invert traditional interpretations of the biological meaning of the two Gompertz parameters:  $\alpha$  is a metric of biological ageing rate, while  $\beta$  is not (Figure 3.13).

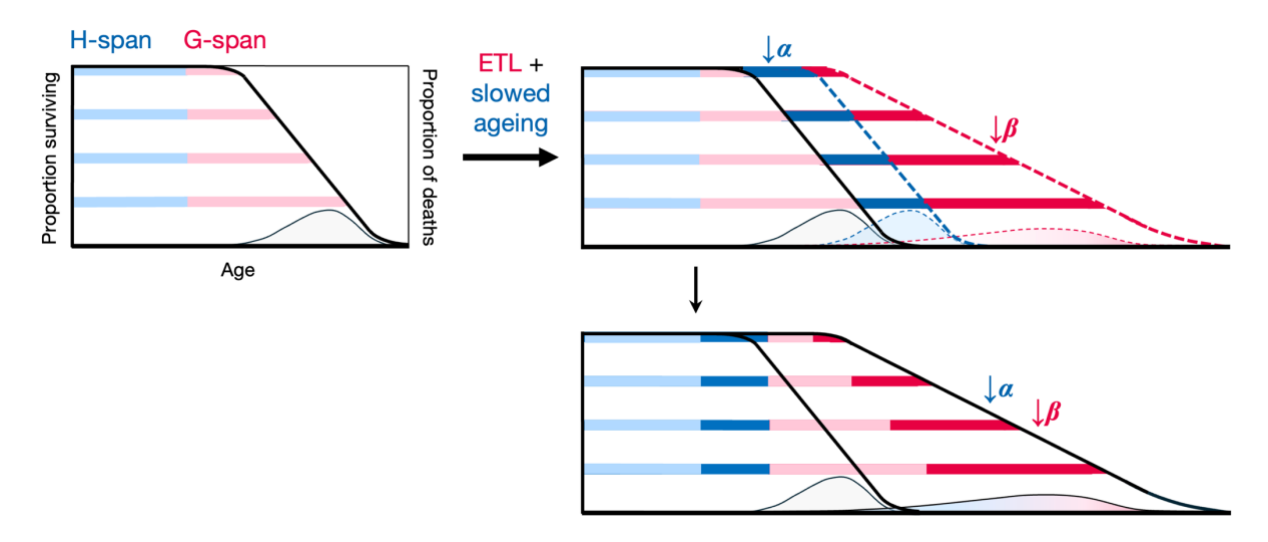


Figure 3.13.  $\alpha$  reflects healthspan and  $\beta$  reflects gerospan variation. Summary schematic of the biological basis of the Gompertz parameters across my experimental cohorts, depicting a hypothetical intervention that reduces both  $\alpha$  and  $\beta$ .  $\alpha$  reduction arises from H-span expansion (equally across individuals in this simplified depiction, noting that expansion can also be greater in shorter-lived individuals), causing the approximately parallel right-shift of the survival curve (middle panel, dashed blue) that occurs in  $\alpha$  reduction.  $\beta$  reduction arises from inter-individually variable G-span expansion (greater in longer-lived individuals), causing the approximate horizontal stretch of the survival curve (middle panel, dashed red) that occurs in  $\beta$  reduction. Bottom panel: overall effect of this hypothetical intervention with H-span and G-span arranged in order. In all panels, probability distributions of death times corresponding to the survival curves, are overlaid (right y-axis, thin data lines), showing that  $\alpha$ reduction causes an approximate right-shift of death ages, whereas  $\beta$  reduction causes an additional stretch that increases lifespan variation more. The area under these probability distributions is shaded to reflect the level of inter-individual variation in H-span/G-span: α reduction involves similar expansion of H-span in all individuals (solid blue shading), whereas  $\beta$  reduction involves greater G-span expansion in longerlived individuals (red gradient shading). Therefore,  $\beta$  describes the degree of inter-individual variation in health and lifespan, and not biological ageing rate, which is better captured by  $\alpha$  as H-span length.

#### $3.6 - \alpha$ and $\beta$ describe inter-individual heterogeneity in age-related infection

To further understand the biological mechanisms underpinning the Gompertz parameters, I performed necropsies on all corpses, building upon established mortality deconvolution methodology developed in the Gems laboratory (Zhao et al., 2017). Specifically, I scored for ageing-related bacterial colonisation of the pharynx and intestine which, as expected, was abolished in the 12 carbenicillin-treated cohorts (Figure 3.14b). In the following analyses, I therefore focus on these pathologies in the 12 cohorts cultured without carbenicillin. Notably, almost all corpses with a swollen, infected pharynx (P or "big P", as opposed to p or "small p" with an atrophied, uninfected pharynx) (Zhao et al., 2017) also had intestinal colonisation, but not vice versa (Figure 3.14a,c). This suggests that P animals are a subset of those with intestinal colonisation. Death type was accordingly used to define three biologically-distinct

subpopulations: P, pIC (<u>p</u> with <u>intestinal colonisation</u>), and pnIC (<u>p</u> with <u>no intestinal colonisation</u>) (Figure 3.14a).

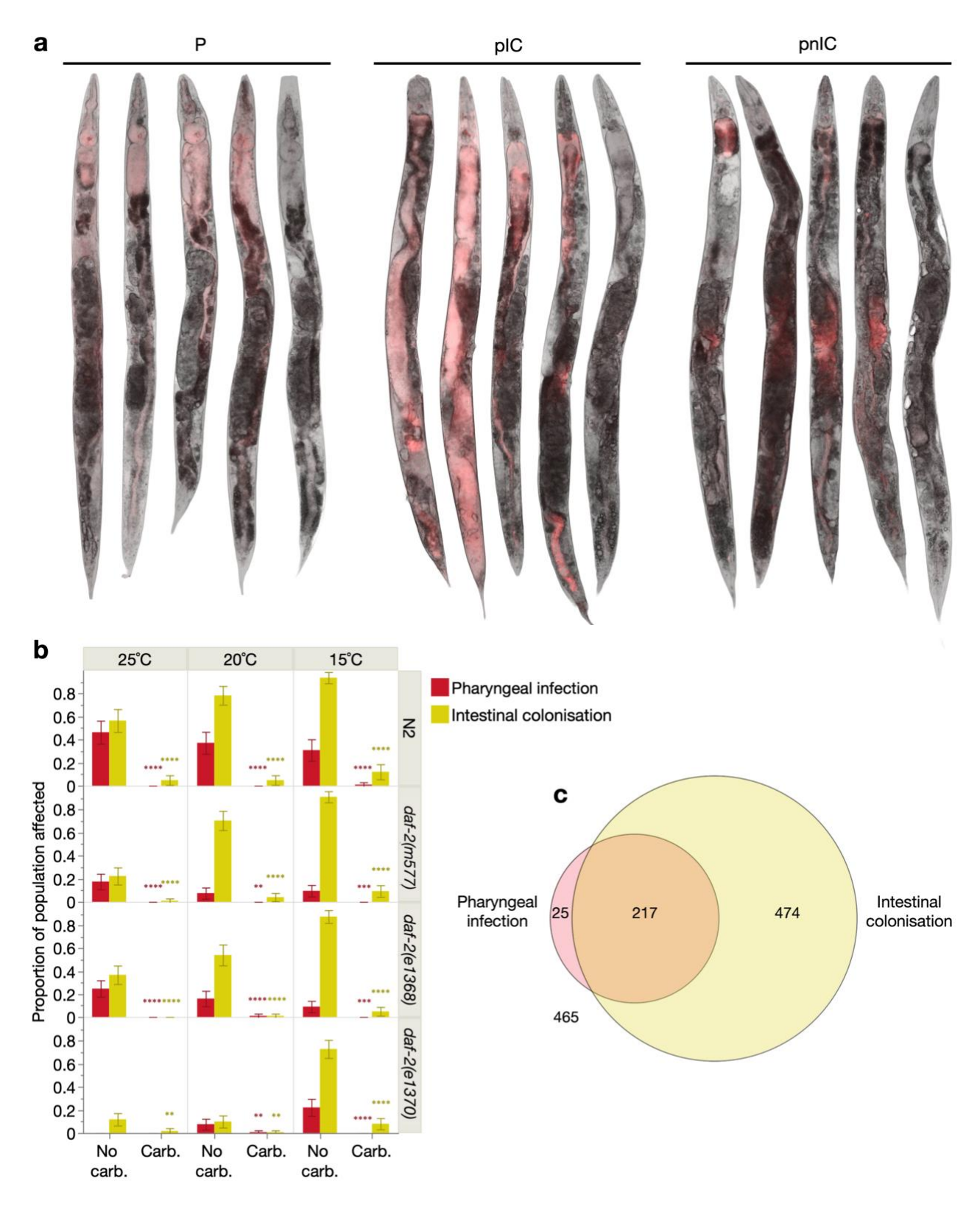
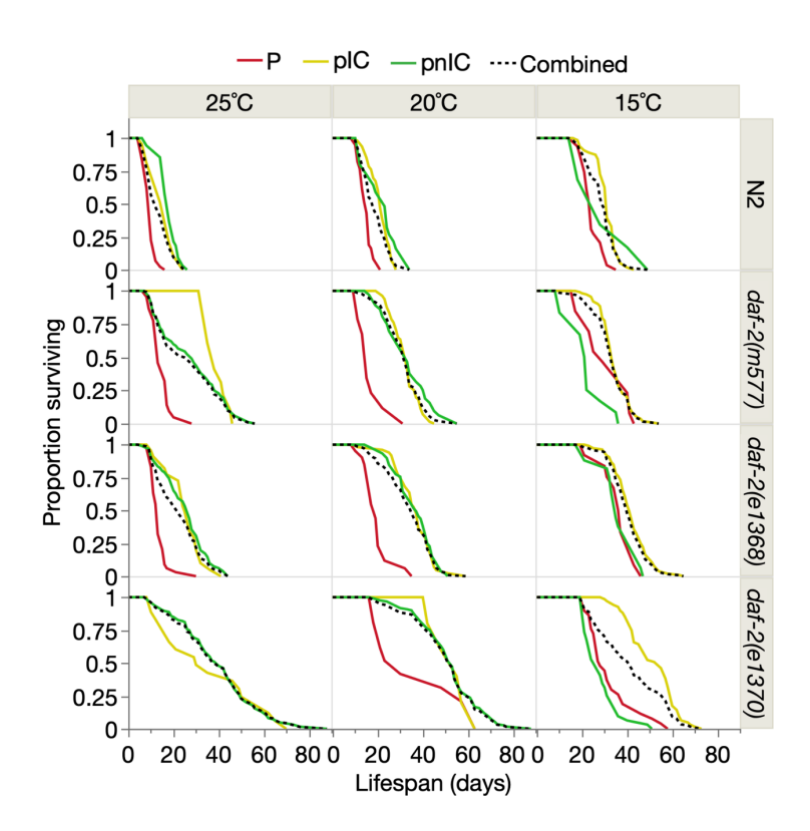


Figure 3.14. Pharyngeal and intestinal tissues are colonised by dietary E. coli during ageing. (a) Representative images of the range of corpse presentations for each subpopulation (P, pIC, pnIC), taken from a single population (n=45) of nematodes fed throughout life with and colonised by RFP-expressing E. coli (first four examples in each subpopulation). The last (fifth) example in each subpopulation is of

individuals fed standard *E. coli* (lacking RFP expression) throughout life, showing that RFP signal is attributable to bacteria rather than nematode autofluorescence, and that presentation of the described pathologies does not differ between standard and RFP-expressing *E. coli* diets. From left to right, lifespan in days for these specific individuals: P (12, 14, 16, 20, 16), pIC (12, 14, 20, 22, 26), pnIC (16, 20, 24, 34, 30). See Methods for detailed microscopy methodology. Interestingly, epifluorescence microscopy of RFP-expressing *E. coli* reveals its uterine and/or tumoural colonisation in pnIC individuals, which is less readily visible under a dissecting stereomicroscope than pharyngeal and intestinal colonisation. (b) Antibiotic (carbenicillin) treatment abolishes pharyngeal and intestinal colonisation, as scored visually under a Leica MZ8 stereomicroscope (50x total magnification), based on tissue colour, texture and morphology, as described in the methods and performed previously (Zhao et al., 2017). 95% confidence intervals are shown. Differences in proportion of the population affected were assessed by Pearson's chi-squared test; ns p > 0.05, \* $p \le 0.05$ , \*\* $p \le 0.01$ , \*\*\*\*  $p \le 0.001$ , \*\*\*\*  $p \le 0.001$ . (c) Venn diagram showing that most P individuals simultaneously have intestinal colonisation by bacteria.

Consistent with prior findings (Zhao et al., 2017), lifespan was shorter for P than p (pIC and pnIC) subpopulations for most treatments (Figure 3.15, Table 3.5). Lifespan was also shorter for pIC than pnIC populations (at 15°C and 25°C, but not 20°C). Thus, the three subpopulations exhibit distinct ageing trajectories.



**Figure 3.15. Survival curves of P, pIC and pnIC subpopulations and whole population.** Log-rank *p*-values of depicted comparisons are presented in Table 3.5. Survival proportions were obtained from Kaplan-Meier lifespan analysis using pseudofrequencies (in place of frequency) to account for censors (see Methods for details).

								Effect of reduc	ng temperature	Effect of	daf-2(rf)
O - v - diti - v	0 - 1	No. dead/	Mean lifespan	% change	p vs. P	% change	p vs. pIC	% change	<i>p</i> vs. 25°C	% change	p vs. N2
Condition	Cohort	censors	(days since L4)	vs. P	(Log-Rank)	vs. pIC	(Log-Rank)	vs. 25°C	(Log-Rank)	vs. N2	(Log-Rank)
N2 25 °C	P	46	9.5								
112 20 0	pIC	20	14.7	54.4	<0.0001						
	pnIC	33	17.9	87.6	<0.0001	21.5	0.0770*				
	Combined	99/7	13.4	07.0	10.0001	21.5	0.0770				
N2 20 °C	P	38	14.6					53.4	<0.0001		
	pIC	45	20.8	42.3	<0.0001			41.3	<0.0001		
	pnIC				<0.0001	2.0	0.1005				
	-	19	21.6	47.4	<0.0001	3.6	0.1225		0.0037		
NO 15°0	Combined	102/6	18.7					39.1	<0.0001		
N2 15 °C	P	30	24.2					153.2	<0.0001		
	pIC	61	30.9	27.7	<0.0001			109.5	<0.0001		
	pnIC	6	30.2	24.9	0.0739	-2.3	0.3779		0.0008		
	Combined	97/10	28.8					114.0	<0.0001		
' '	Р	22	14.6							52.5	<0.0001
	pIC	10	38.7	166.0	<0.0001					162.7	<0.0001
	pnIC	93	27.6	89.5	<0.0001	-28.8	0.3309*			54.0	<0.0001
	Combined	125/13	26.3							95.6	<0.0001
daf-2(m577) 20°C	P	9	16.8					15.6	0.3766	15.0	0.2530
	pIC	76	32.1	91.0	<0.0001			<del>-</del> 17.0	0.0130	54.3	<0.0001
	pnIC	34	32.8	95.2	<0.0001	2.2	0.1298	19.1	0.3506	52.2	<0.0001
	Combined	119/22	31.3					18.9	0.6186*	67.2	<0.0001
daf-2(m577) 15°C	P	13	30.9					112.0	<0.0001	27.7	0.0088
	pIC	111	34.4	11.4	0.6031			-11.2	0.1587	11.3	0.0002
	pnIC	12	22.2	-28.2	0.0306	-35.5	<0.0001	-19.6	0.0976	-26.5	0.1409
	Combined	136/5	33.0					25.4	0.3171*	14.6	<0.0001
daf-2(e1368) 25°C		35	13.3							39.9	<0.0001
, ,	pIC	21	25.2	88.6	<0.0001					70.8	<0.0001
	pnIC	85	25.1	88.0	<0.0001	-0.3	0.6036			40.2	<0.0001
	Combined	141/15	22.3							65.9	<0.0001
daf-2(e1368) 20°C	Р	19	19.5					46.3	0.0003	33.4	0.0007
44, 2(01000) 20 0	pIC	45	36.5	87.1	<0.0001			45.1	<0.0001	75.4	<0.0001
	pnIC	54	36.2	85.5	<0.0001	-0.9	0.893		<0.0001	67.9	<0.0001
	Combined	118/24	33.9	00.0	10.0001	0.5	0.000	51.9	<0.0001	81.2	<0.0001
<i>daf-2(e1368)</i> 15°C	P	12	36.0					169.6	<0.0001	48.9	<0.0001
dai-2(e1300) 13 C	pIC	104	41.8	16.0	0.0094			65.9	<0.0001	35.3	<0.0001
	pnIC	16	35.5	-1.2	0.8754	-14.9	0.0078		0.0026		0.9213
	Combined		40.5	-1.2	0.6754	-14.9	0.0076			40.7	
def 0(e1270) 05°C		132/12 0						81.5	<0.0001		<0.0001
<i>daf-2(e1370)</i> 25°C		-	N/A	N1/A	NI/A					N/A	N/A
	pIC	17	35.9	N/A	N/A		0.0155			143.3	0.0003
	pnIC	126	39.7	N/A	N/A	10.6	0.8136			121.5	<0.0001
1 (0/ 10==: ====	Combined		39.2							191.6	
daf-2(e1370) 20°C		10	36.9					N/A	N/A		<0.0001
	pIC	5	53.0	43.8	0.5439			47.8	0.5539		0.0002
	pnIC	115	52.0	41.1	0.0877*	-1.9	0.8634		0.0001	140.9	<0.0001
	Combined	130/12	50.9					29.8	0.0001	172.2	<0.0001
<i>daf-2(e1370)</i> 15°C		28	32.4					N/A	N/A	34.1	0.0004
	pIC	65	51.5	58.8	<0.0001			43.5	0.1455*	66.7	<0.0001
	pnIC	33	28.2	-13.0	0.1303	<del>-</del> 45.2	<0.0001	-28.9	<0.0001	<del>-</del> 6.5	0.6324
	Combined	126/18	41.5					5.9	0.9204	44.3	< 0.0001

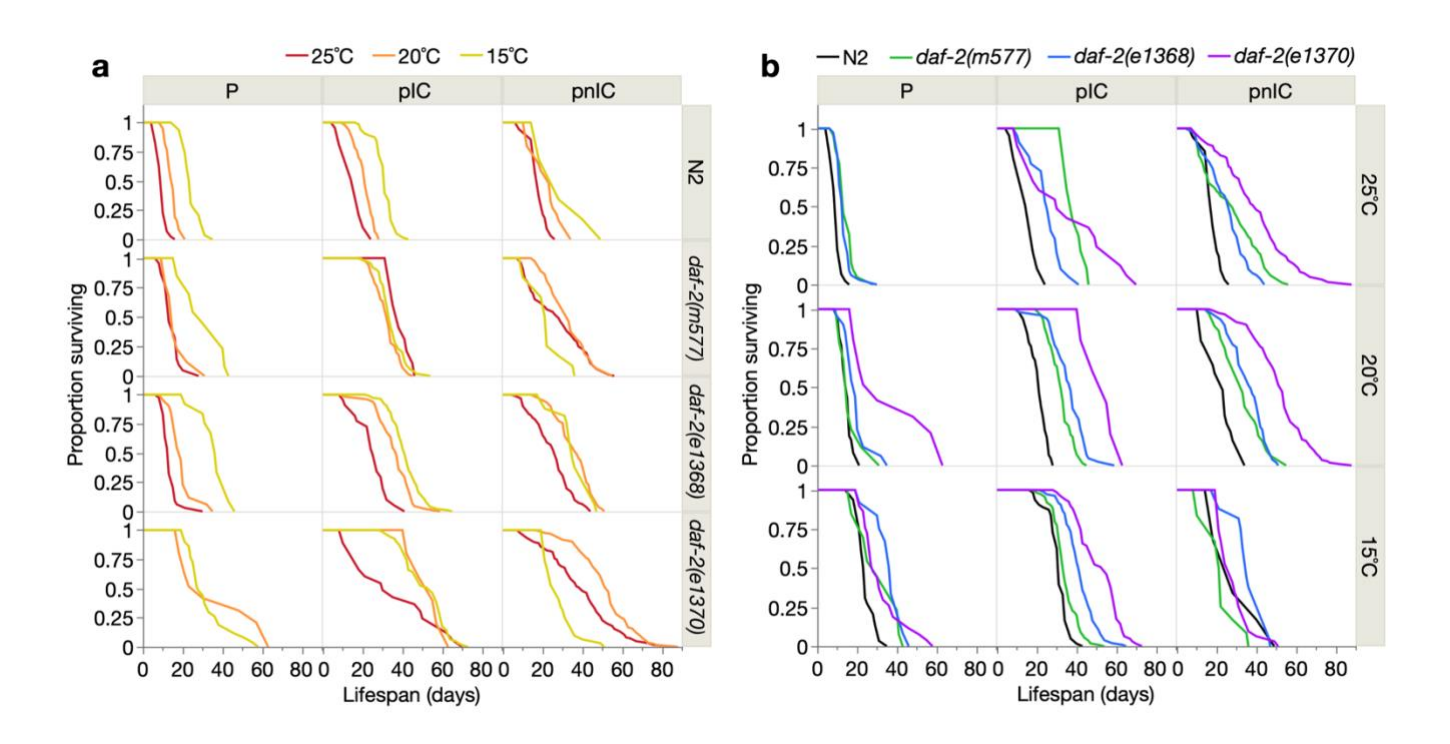
Table 3.5. Lifespan data for P, pIC and pnIC subpopulations in non-carbenicillin cohorts, their differences and effect upon them of low temperature and daf-2(rf) treatment. N2: wild-type. Mean lifespans of the subpopulations and combined population were obtained by Kaplan-Meier analysis using age-specific mortality pseudofrequencies, to allow unbiased incorporation of censors in subpopulation analyses (see Methods). \*: cohorts where log-rank p>0.05, due to crossing survival curves and/or greater changes in early than late mortality; the Wilcoxon test is more appropriate to detect lifespan differences in these conditions (0.01 for inter-subpopulation comparisons, and <math>0.0002 for treatment effects; data not shown).

I then asked how this inter-subpopulation heterogeneity affects  $\beta$ . Notably,  $\beta$  was consistently smaller in whole populations than in subpopulations (Table 3.6). This illustrates how  $\beta$  can underestimate demographic ageing rate in the presence of hidden subpopulation heterogeneity, and provides empirical evidence for this known concern (Yashin et al., 2002b). Moreover, the traditional interpretation of  $\beta$  would paradoxically predict that subpopulations age biologically faster than their combination (whole population). This further underscores how even in these isogenic populations maintained in controlled environments,  $\beta$  is primarily a measure of inter-individual heterogeneity in ageing, rather than of biological ageing rate itself.

		No. dead/	0	% change vs.	p vs. combined	
Condition	Cohort	censors	β	combined	, (LRT)	
N2 25 °C	Р	46	0.38456	135.2	<0.0001	
	pIC	20	0.18510	13.2	0.6039	
	pnIC	33	0.27666	69.2	0.0032	
	Combined	99/7	0.16350			
N2 20 °C	Р	38	0.33946	107.7	<0.0001	
	pIC	45	0.26673	63.2	0.0018	
	pnIC	19	0.14675	-10.2	0.6207	
	Combined	102/6	0.16346			
N2 15 °C	Р	30	0.21114	45.2	0.0246	
	pIC	61	0.21046	44.7	0.0025	
	pnIC	6	0.07728	-46.9	0.0574	
	Combined	97/10	0.14543			
daf-2(m577) 25°C	Р	22	0.16444	190.2	0.0028	
	pIC	10	0.23111	307.8	0.0004	
	pnIC	93	0.05929	4.6	0.8180	
	Combined	125/13	0.05667			
daf-2(m577) 20°C	Р	9	0.11551	4.9	0.9034	
	pIC	76	0.17480	58.8	0.0003	
	pnIC	34	0.08814	-19.9	0.1969	
	Combined	119/22	0.11009			
daf-2(m577) 15°C	Р	13	0.11613	-13.0	0.6464	
	pIC	111	0.14486	8.6	0.4538	
	pnIC	12	0.11676	-12.5	0.8922	
	Combined	136/5	0.13341			
daf-2(e1368) 25°C	Р	35	0.14304	66.3	0.0437	
	pIC	21	0.13201	53.5	0.1202	
	pnIC	85	0.10012	16.4	0.3649	
	Combined	141/15	0.08599			
daf-2(e1368) 20°C	Р	19	0.12294	15.9	0.5731	
	pIC	45	0.11665	10.0	0.5193	
	pnIC	54	0.13545	27.7	0.1064	
	Combined	118/24	0.10606			
daf-2(e1368) 15°C	Р	12	0.19005	63.9	0.1030	
	pIC	104	0.11830	2.0	0.8546	
	pnIC	16	0.15642	34.9	0.2487	
	Combined	132/12	0.11598			
daf-2(e1370) 25°C	Р	0	N/A	N/A	N/A	
	pIC	17	0.03747	-17.9	0.6227	
	pnIC	126	0.04657	2.1	0.8985	
	Combined	143/10	0.04563			
daf-2(e1370) 20°C	P	10	0.04380	-39.7	0.1972	
	pIC	5	0.15907	118.9	0.1117	
	pnIC	115	0.07471	2.8	0.8123	
1.624.42=21.4=2=	Combined	130/12	0.07268	4.5		
<i>daf-2(e1370)</i> 15°C	P	28	0.07444	13.0	0.5900	
	pIC	65	0.10575	60.6	0.0015	
	pnIC	33	0.09422	43.1	0.0951	
	Combined	126/18	0.06586			

Table 3.6.  $\beta$  parameters for P, pIC and pnIC subpopulations in non-carbenicillin cohorts, and their differences. N2: wild-type.  $\beta$  parameters were obtained by maximum likelihood estimation using mortality pseudofrequencies (in place of standard mortality frequencies) (see Methods). LRT: likelihood ratio test, used here to assess statistical significance of  $\beta$  differences between subpopulations and whole populations (Combined).

I next examined how life-extending interventions (here low temperature and *daf-2(rf)*, without carbenicillin) affect subpopulation lifespan and prevalence. While both treatments increased lifespan in most subpopulations, increases were generally greater for P by low temperature, and pIC by *daf-2(rf)* (Figure 3.16a–b; Table 3.5). Lower temperature modestly decreased P prevalence in all genotypes except *daf-2(e1370)*, suggesting reduced bacterial pathogenicity and/or enhanced host immunity, and allele-specific temperature sensitivity in *daf-2(e1370)* (Zhao et al., 2021) (Figure 3.16c). Interestingly, however, low temperature strongly increased pIC prevalence (concomitantly decreasing pnIC prevalence). Thus, reducing temperature acts antagonistically on terminal infection, respectively decreasing and increasing pharyngeal and intestinal colonisation by pathogenic *E. coli*. Meanwhile, *daf-2(rf)* treatment also decreased P prevalence as previously seen (Zhao et al., 2021), and affected pIC prevalence in an allele- and temperature-specific manner (Figure 3.16d), largely consistent with known *daf-2(rf)* infection resistance (Podshivalova et al., 2017).



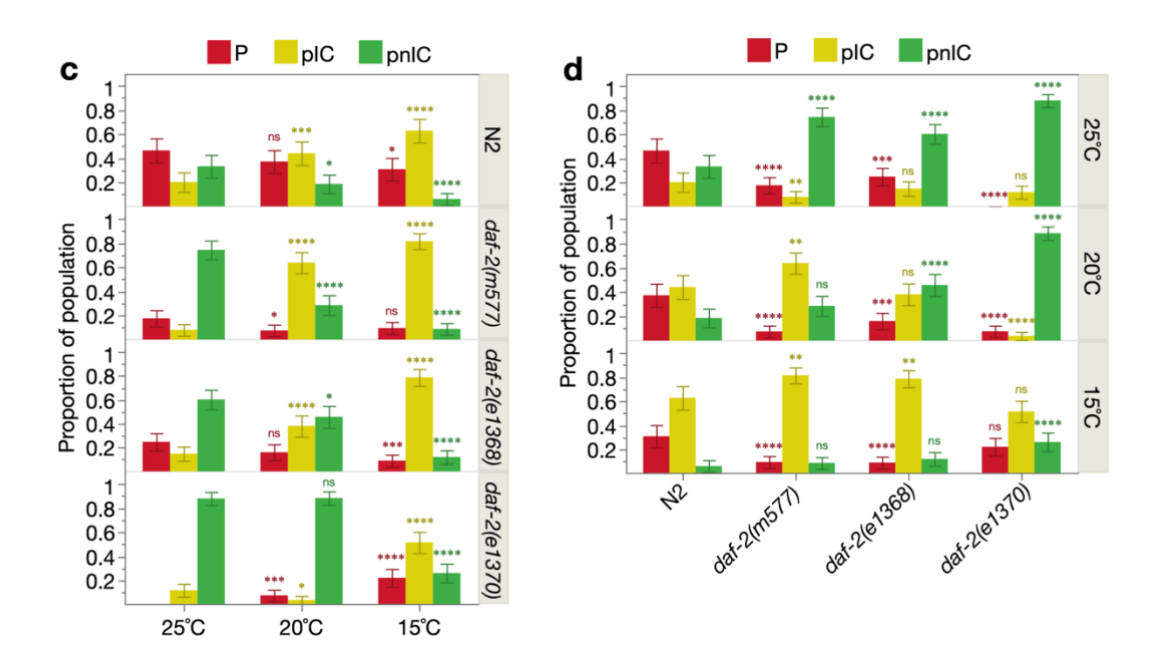


Figure 3.16. Life-extending interventions change lifespan and prevalence of pathological subpopulations. (a-b) Effect of (a) low temperature and (b) daf-2(rf) treatments on subpopulation lifespan. Log-rank p-values of depicted survival curve comparisons are presented in Table 3.5. Survival proportions were obtained from Kaplan-Meier lifespan analysis using pseudofrequencies (in place of mortality frequency) to account for censors (see Methods). (c-d) Effects of (c) low temperature and (d) daf-2(rf) on subpopulation prevalence. Differences in prevalence was assessed by Pearson's chi-squared test; ns p > 0.05, \*  $p \le 0.05$ , \*\*  $p \le 0.01$ , \*\*\*\*  $p \le 0.001$ .

Finally, I determined the relative contribution of these changes in subpopulation lifespan and prevalence to the Gompertz parameters. Effects of low temperature on  $\beta$  proved to be determined mainly by changes in pnIC lifespan (Figure 3.17a). In wild-type and daf-2(e1368), low temperature increased lifespan of this longer-lived subpopulation (and pIC) (Figure 3.15, 3.16a; Table 3.5), therefore extending the survival curve tail (i.e. reducing  $\beta$ ) (Figure 3.18a). However, in daf-2(m577) and daf-2(e1370), pnIC survival either decreased (15°C) or rectangularised (20°C) (Figure 3.15, 3.16a; Table 3.5), thus compressing the survival curve (i.e. increasing  $\beta$ ) (Figure 3.18a). Interestingly, P lifespan and subpopulation prevalence contributed little to  $\beta$ , except for an increase in pIC to pnIC ratio (i.e. "pnIC  $\rightarrow$  pIC") in daf-2(m577), which further increased  $\beta$  (Figure 3.17a, 3.18a).

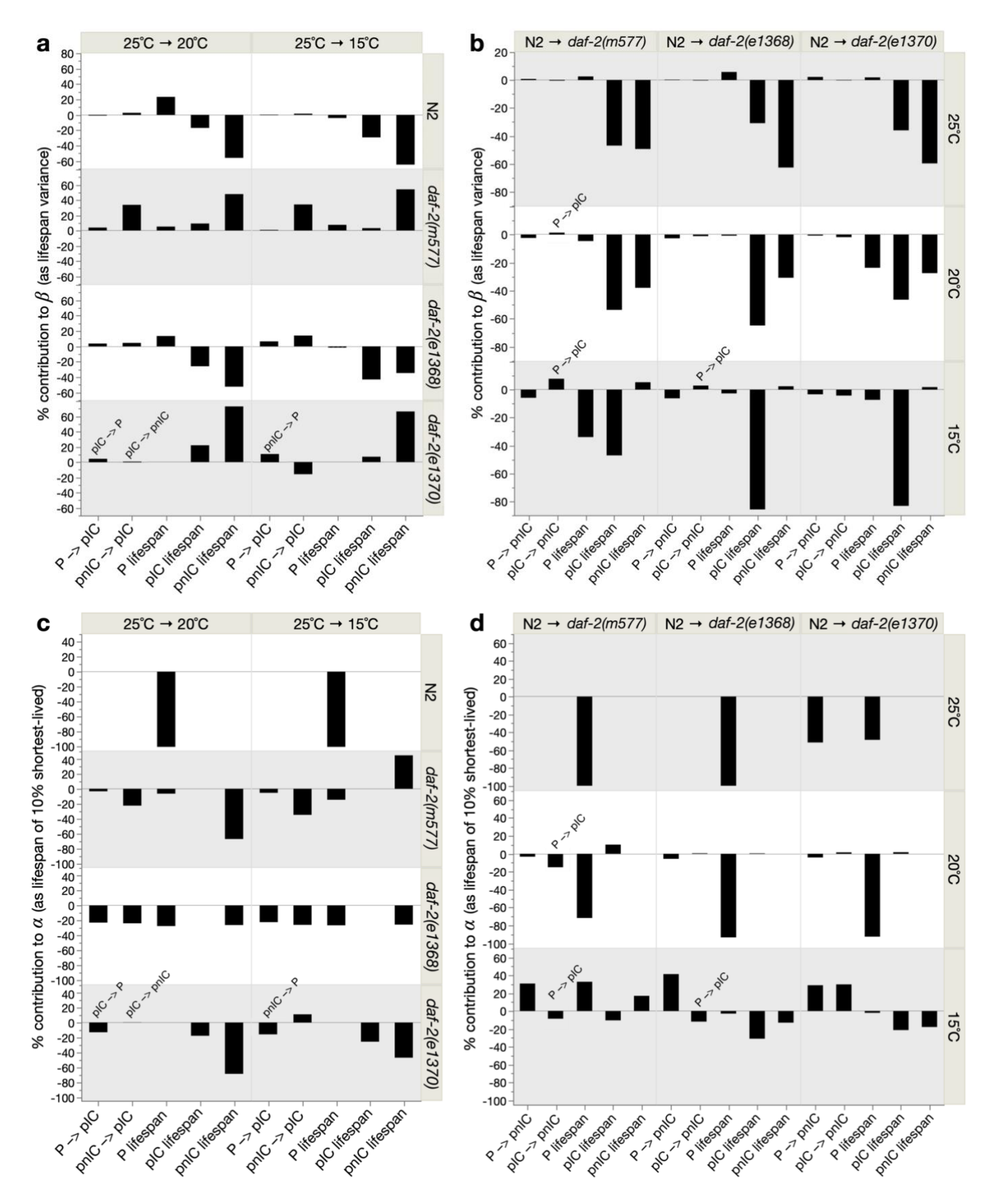


Figure 3.17.  $\alpha$  and  $\beta$  reflect subpopulation-specific changes in lifespan and prevalence. Relative contributions (summing to 100%) of changes in subpopulation prevalence and lifespan to overall change in population  $\beta$  (**a**-**b**) and  $\alpha$  (**c**-**d**) in lower temperature (**a**, **c**) and daf-2(rf) (**b**, **d**) treatments. Bar height indicates contribution magnitude (%) and bar direction (+/-) contribution direction (increase/decrease Gompertz parameter). The first two x-axis items are component contributions of changing control

subpopulation prevalence to that of the treatment cohort (e.g. daf-2(rf)) generally converts P and pII to pnII), based on principles of parsimony (Figure 3.16c–d), while retaining control subpopulation lifespans. Overlaid angled labels reflect different subpopulation prevalence changes for those specific treatments, similarly based on principles of parsimony. The remaining x-axis items are contributions of changing control subpopulation lifespan to that of the treatment cohort, while retaining control subpopulation prevalence, for P, pIC and pnIC, chronologically. See Methods for full analysis details; in brief, simulated survival data was generated for each component change (in subpopulation prevalence or lifespan), by accordingly combining control and treatment subpopulations, generated using agespecific mortality pseudofrequencies (in place of frequency) to account for censors. The sum of these component changes closely predicts the true change between control and treatment cohorts (Figure 3.19a). Contributions of component changes to  $\alpha$  and  $\beta$  were then estimated as the change in, respectively, lifespan of the 10% shortest-lived individuals and lifespan variance, which strongly predict  $\alpha$  and  $\beta$  across these 12 non-antibiotic cohorts (Figure 3.19b–c) and whose component sum of these measures predicts their true change between control and treatment cohorts (Figure 3.19d–e).

In daf-2(rf),  $\beta$  was also primarily determined by pIC and/or pnIC lifespan (Fig. 3.17b), whose already-longer lifespans are further increased (Figure 3.15, 3.16b; Table 3.5), extending the survival curve tail and decreasing  $\beta$  (Figure 3.18b). Again, P lifespan and subpopulation prevalence contributed little to  $\beta$  (Figure 3.17b). In summary,  $\beta$  is largely a function of p lifespan, where increases and decreases in  $\beta$  result respectively from decreased and increased p (pIC and/or pnIC) longevity. These findings further demonstrate that  $\beta$  is not a measure of biological ageing rate but inter-individual heterogeneity, here as subpopulation-specific responses to longevity interventions.

I similarly deconvolved the determinants of  $\alpha$ , starting with lower temperature treatments (Figure 3.17c). In wild-type,  $\alpha$  was wholly determined by increased lifespan of short-lived P animals (Figure 3.15, 3.16a; Table 3.5), which delayed population mortality onset (i.e. decreasing  $\alpha$ ) (Figure 3.18a). In daf-2(m577) and daf-2(e1370),  $\alpha$  was primarily determined by pnIC individuals, whose mortality onset was generally delayed at the lower temperatures (Figure 3.16a, 3.18a). In daf-2(e1368),  $\alpha$  was equally decreased by several determinants, including subpopulation prevalence changes, which all weakly delayed mortality onset (Figure 3.18a).

In daf-2(rf) treatments,  $\alpha$  was primarily determined by P lifespan at 25°C and 20°C (Figure 3.17d), where increased lifespan of this short-lived subpopulation postponed mortality onset (Figure 3.15, 3.16b, 3.18b; Table 3.5). At 15°C, several determinants were important, but in common was the increase in pnIC to P ratio (i.e. "P  $\rightarrow$  pnIC") (Figure 3.17d), with the latter having earlier mortality onset, therefore increasing  $\alpha$  (Figure 3.16d, 3.18b).

Therefore, in contrast to  $\beta$ ,  $\alpha$  is largely a function of P lifespan and subpopulation prevalence, but like  $\beta$ , reflects subpopulation-specific responses to life-extending interventions. Taken together, these findings provide further evidence that being demographic measures, the Gompertz parameters can often reflect inter-individually variable biological changes, whose

complexity is unlikely to be captured by the traditional, theoretical interpretations of the parameters.

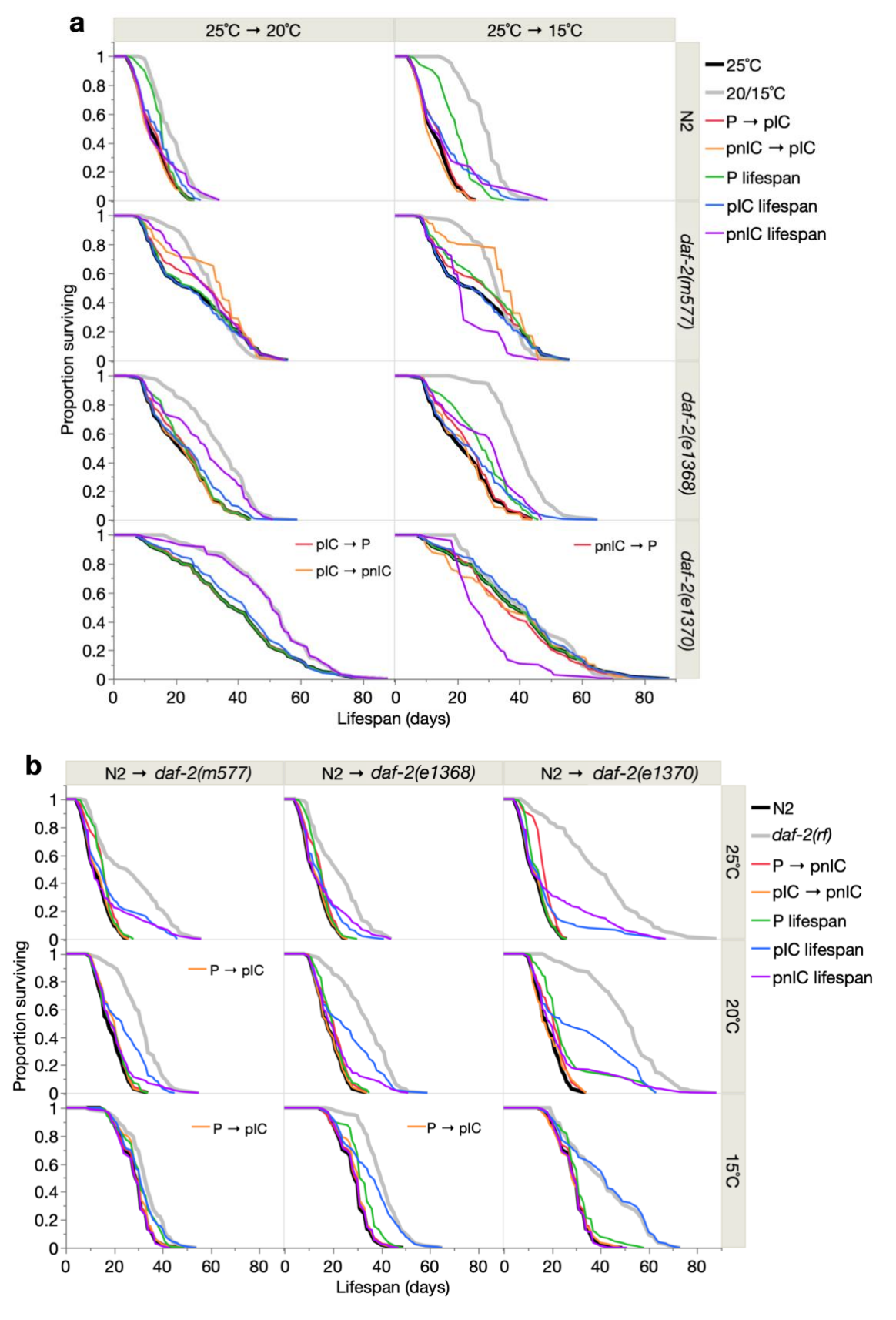
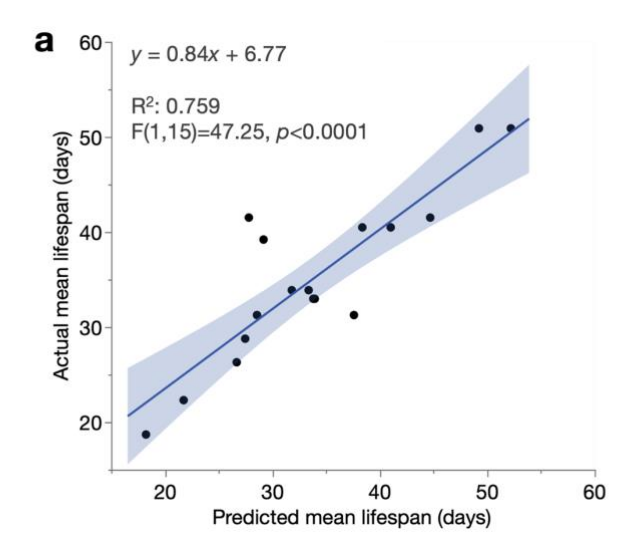
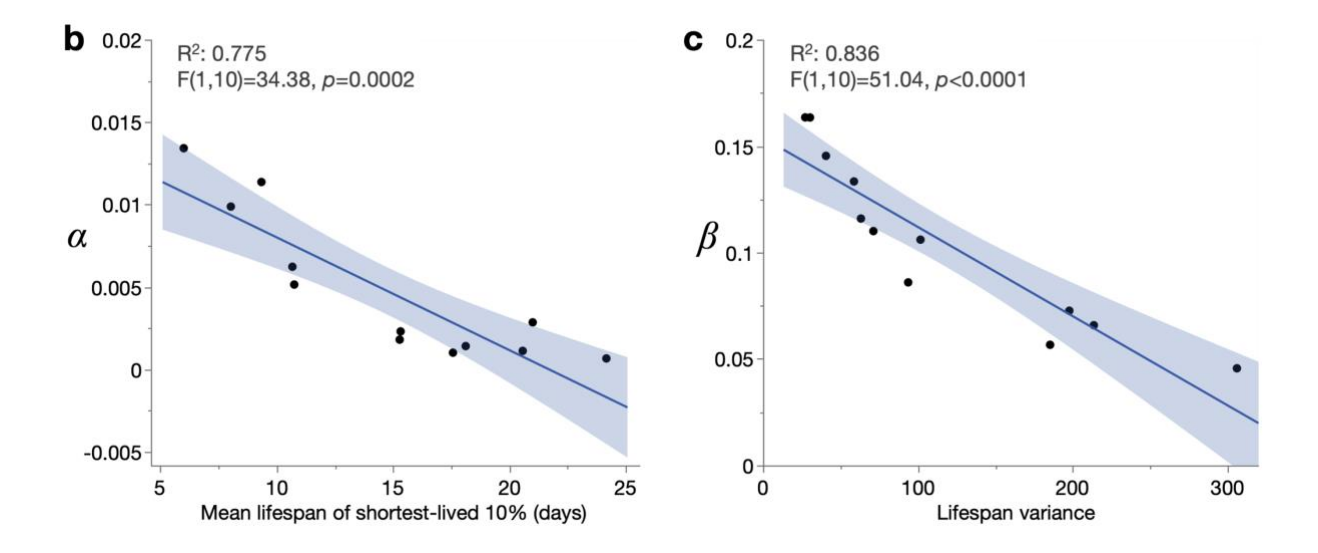


Figure 3.18. Effect of life-extending treatments on subpopulation prevalence and lifespan. Effect of (a) low temperature and (b) daf-2(rf) treatments. Black and grey cohorts are control and treatment

cohorts, respectively. Red and orange cohorts are the component effects of changing control subpopulation prevalence to that of the treatment cohort, based on principles of parsimony (see Figure 3.16c–d), while retaining control subpopulation lifespans. Green, blue and purple cohorts are the effects of changing control subpopulation lifespan to that of the treatment cohort, while retaining control subpopulation prevalence, for P, pIC and pnIC, respectively. Survival proportions were obtained from Kaplan-Meier lifespan analysis using pseudofrequencies (in place of mortality frequency) to account for censors (see Methods). Sub-legends reflect different subpopulation prevalence changes for those specific treatments, similarly based on principles of parsimony.





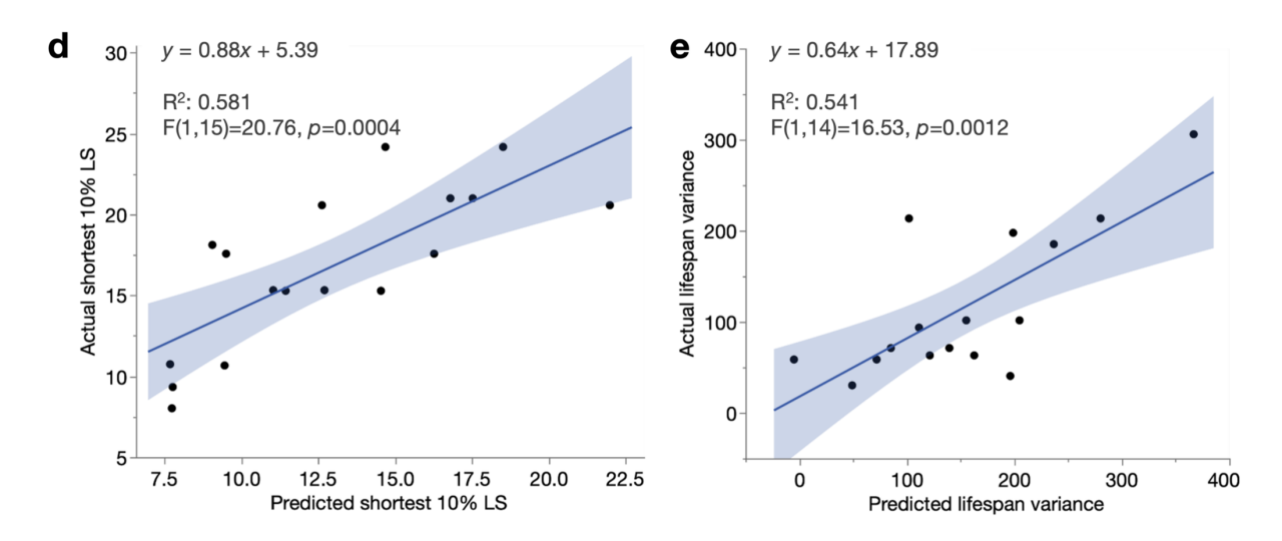


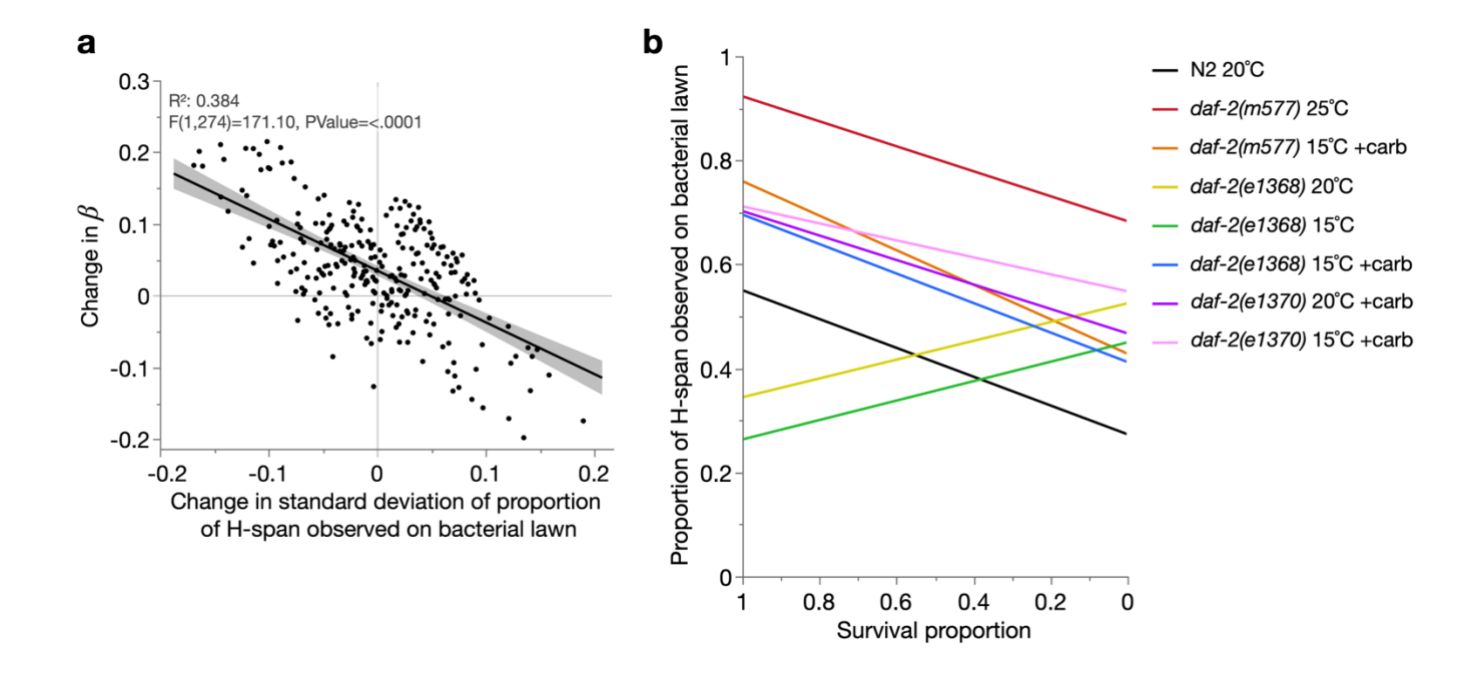
Figure 3.19. Methodological background of determining relative contributions to the Gompertz parameters of subpopulation changes. (a) Mean lifespan in the 17 treatments (low temperature and daf-2(rf); non-antibiotic background) is strongly predicted by the sum of simulated component changes (in subpopulation prevalence and lifespan) (see Methods for analysis details). (b-c) Mean lifespan of 10% shortest-lived individuals and lifespan variance are strong respective predictors of  $\alpha$  and  $\beta$  in the 12 non-antibiotic cohorts under analysis. (d-e) Simulated component changes (in subpopulation prevalence and lifespan) predict true changes in mean lifespan of the 10% shortest-lived individuals, and lifespan variance, in the 17 treatments (low temperature and daf-2(rf); non-antibiotic background). In e, one outlier treatment (daf-2(e1370)) at 20°C) was excluded, with datapoints x=754, y=198 (determined by the Robust Fit Outliers analysis in JMP Pro, Huber method, K=4).

#### $3.7 - \beta$ reflects inter-individual heterogeneity in bacterial contact during early adulthood

Thus far, I have shown that  $\beta$  reflects inter-individual differences in the ageing process, relating to locomotory decline and E. coli-associated terminal pathologies. A possibility is that interindividual variation in earlier life may also contribute to  $\beta$ . For instance, various early-life predictors of individual mortality (within populations) have been identified: ROS levels in L2 larvae (Bazopoulou et al., 2019), nucleolus size in day 1 adults (Tiku et al., 2017), lipid droplet number in day 1 and 6 adults (Papsdorf et al., 2023), mitochondrial superoxide generation frequency in day 3 adults (Shen et al., 2014), and intestinal E. coli content in day 3 adults (Baeriswyl et al., 2010), amongst others. Causally or correlatively, these early-life traits predict individual lifespan (i.e. lifespan variation), and therefore  $\beta$ . To my knowledge, the possible relationship between pre-senescent individual differences and demographic ageing rate has not been directly considered before with the intention of explaining mortality and survival curve shape.

Given the close association of *C. elegans* lifespan with dietary *E. coli*, whose intestinal load in early adulthood can predict nematode lifespan (Baeriswyl et al., 2010), I wondered

whether bacterial contact in earlier life might predict individual lifespan, and therefore  $\beta$ . To test this, bacterial contact was quantified by regular, longitudinal scoring of nematode contact with the bacterial lawn, for the 24 cohorts. To avoid confounding effects of ageing-related locomotory decline on lawn contact, contact time was quantified only for the duration of (locomotory) H-span, during which animals can move on and off the lawn unhindered. Bacterial contact was therefore defined as the proportion of H-span observed to be in contact with the bacterial lawn, for each individual. Strikingly, across the 24 cohorts, the standard deviation of individual bacterial contact (for each cohort) indeed predicted  $\beta$ , with greater variation in bacterial contact predicting a smaller  $\beta$  value (Figure 3.20a). This again demonstrates that  $\beta$  is a function of interindividual variation, whose determinants are to some extent operative even in early adulthood.



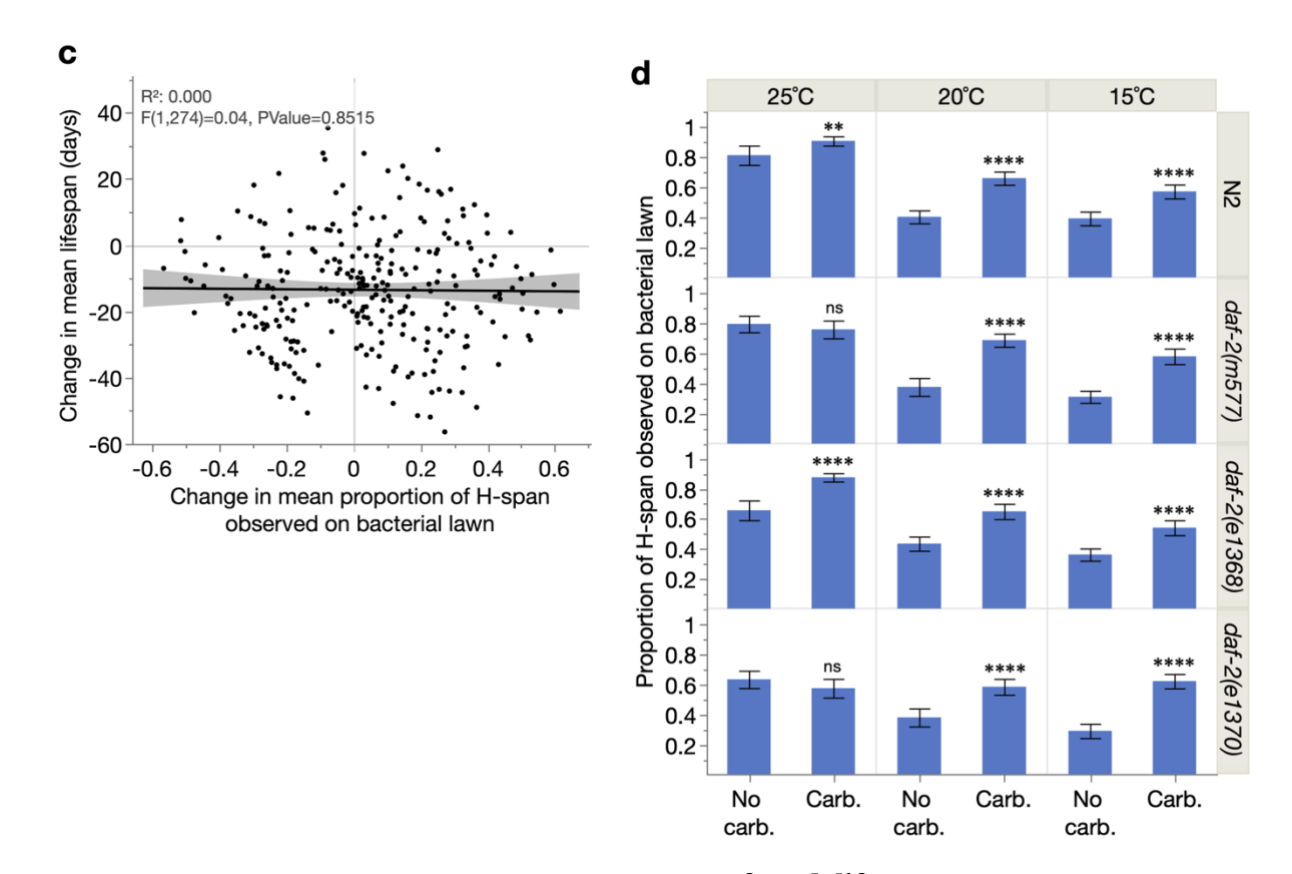


Figure 3.20. Pre-senescent bacterial contact predicts  $\beta$  and lifespan. (a) Least-squares linear regression of the changes in standard deviation of bacterial contact between all possible pairs of the 24 cohorts, over the corresponding change in  $\beta$  for those pairs. This shows that increased bacterial contact predicts a decreased  $\beta$ ; assessed by an F-test, 95% confidence region shaded. (b) Least-squares linear regressions of bacterial contact over survival proportion (i.e. x-axis left: shorter-lived individuals, x-axis right: longer-lived individuals) for specific cohorts, showing only those with statistically significant relationships (F-test p<0.05). (c) Least-squares linear regression of the changes in mean bacterial contact between all possible pairs of the 24 cohorts, over the corresponding change in mean lifespan for those pairs. This does not detect a relationship between bacterial contact and lifespan; assessed by an F-test, 95% confidence region shaded. (d) Effect of carbenicillin on mean bacterial contact, assessed by two-tailed Student's t-tests, showing 95% confidence intervals; ns p > 0.05, \* p ≤ 0.05, \*\* p ≤ 0.01, \*\*\*\* p ≤ 0.001. These figures present data pooled from Trials 4–6 (rather than Trials 3–6 as in most figures of this chapter), except for N2 at 20°C ± carbenicillin (Trials 3–6), due to the scoring of bacterial contact in only these trials.

This finding suggests that bacterial contact should predict lifespan. However, individual bacterial contact only significantly predicted individual lifespan in 8/24 cohorts (Figure 3.20b), while across the 24 cohorts, mean bacterial contact (of cohorts) failed to predict mean lifespan (Figure 3.20c). However, in 6/8 cohorts within which individual bacterial contact did predict individual lifespan (Figure 3.20b), and 10/16 cohorts exhibiting a non-significant trend (data not shown) (i.e. 16/24 or two-thirds of all cohorts), increased bacterial contact was correlated with decreased lifespan. This suggests that increased bacterial contact during early-adulthood is on the whole modestly life-limiting (or correlated with a life-limiting process), and in some but not all conditions. Automated quantification of bacterial contact based on existing protocols

(Stroustrup et al., 2013, Churgin et al., 2017) could yield higher resolution data to verify this lifespan–bacterial contact relationship.

In those cohorts where bacterial contact was associated with decreased lifespan, a possibility is that increased contact with the mildly pathogenic *E. coli* increases the severity of associated infection, thus reducing lifespan. Indeed, it was shown before that the intestinal content of live *E. coli* on day 3 of adulthood (during locomotory H-span) predicts lifespan (Baeriswyl et al., 2010). Consistent with this hypothesis, here, carbenicillin treatment increased bacterial contact in almost all cohorts, showing that nematodes actively avoid proliferating *E. coli* (Figure 3.20d). However, that the relationship between individual bacterial contact and lifespan was still present in carbenicillin cohorts (4/8 cohorts showing this relationship; Figure 3.20b) suggests that infection may not be the only mechanism by which increased bacterial contact limits lifespan. One possible but untested explanation could be that individuals with reduced bacterial contact also consume less bacteria, therefore undergoing dietary restriction-mediated longevity.

To summarise, I have shown that inter-individual variation in a pre-ageing trait can predict lifespan variation and  $\beta$ . This finding is particularly striking given that these *C. elegans* populations are comprised of isogenic individuals raised under identical environmental conditions. Discovering the source and mechanistic determinants of this seemingly stochastic yet predictable lifespan variation would be key to understanding the biodemography of ageing, and in particular the biological meaning of  $\beta$ , which is a metric of lifespan variation. I will discuss these ideas further in section 6.5.

In conclusion, in this chapter I investigated the relationship between population-level demographic ageing and individual-level biological ageing. By assessing this relationship for *all* population members, it was possible to explain demographic measures (such as the Gompertz parameters) in terms of the distribution of inter-individual variation in biological traits. I found that the Gompertz scale parameter  $\alpha$  reflects a metric of biological ageing rate (healthspan *length*) in short-lived population members, whereas the rate parameter  $\beta$  reflects the degree of inter-individual *variation* in ageing (particularly in gerospan length), rather than biological changes within individuals (summary diagram: Figure 3.13, p. 69). This inverts and challenges long-standing (but largely untested) views of the two parameters, showing that it is  $\alpha$ , rather than  $\beta$ , that better represents the biological rate of ageing.

### Chapter 4 – An empirical investigation of the Strehler-Mildvan correlation in C. elegans

In this chapter, I will investigate the biological basis of the Strehler-Mildvan correlation, an inverse correlation between  $\alpha$  and  $\beta$  that is often observed between populations. I will show that this correlation exists in my 24-cohorts dataset as two main types of change in the survival curve, rectangularisation and triangularisation, both of which can be explained by my reinterpretation of the Gompertz parameters in Chapter 3. Specifically, I will demonstrate that rectangularisation arises from expansion of healthspan (one metric of slowed ageing) in shorter-lived population members, and triangularisation from expansion of decrepitude in longer-lived population members (i.e. ETL). Additionally, I will show how rectangularising S-M correlations can be readily explained by a differential heterogeneity view of population ageing.

## 4.1 – Reinterpretation of the Gompertz parameters resolves paradoxes of the S-M correlation

A frequently observed pattern within studies of Gompertzian mortality is that the two Gompertz parameters vary antagonistically, that is, in opposite directions. This relationship is known as the Strehler-Mildvan (S-M) correlation (Strehler and Mildvan, 1960), and elsewhere in modified form, as the compensation law of mortality (Gavrilov and Gavrilova, 1991). The S-M correlation arises as a mathematical property of the Strehler-Mildvan general theory of ageing and mortality (Strehler and Mildvan, 1960), which proposes a theoretical model of physiological ageing that can produce exponential, Gompertzian mortality rates. Here, in brief, the S-M correlation takes the form of a linear relationship between  $\alpha$  and  $\beta$ , where  $\beta$  and  $\beta$  are constants describing the rates of biological physiological decline and occurrence of stressor events, respectively (Equation 4.1, note that this is the S-M *correlation*, derived from the S-M model).

$$\ln \alpha = -1/B \cdot \beta + \ln K \qquad Eq. 4.1$$

Importantly, this mathematical relationship arises *specifically* from the S-M model of ageing, which is only one of numerous physiological models that can produce Gompertzian mortality patterns. However, the S-M correlation has proven to be well supported by empirical mortality data, and has been observed in comparisons of populations within various species, particularly humans (Figure 4.1).

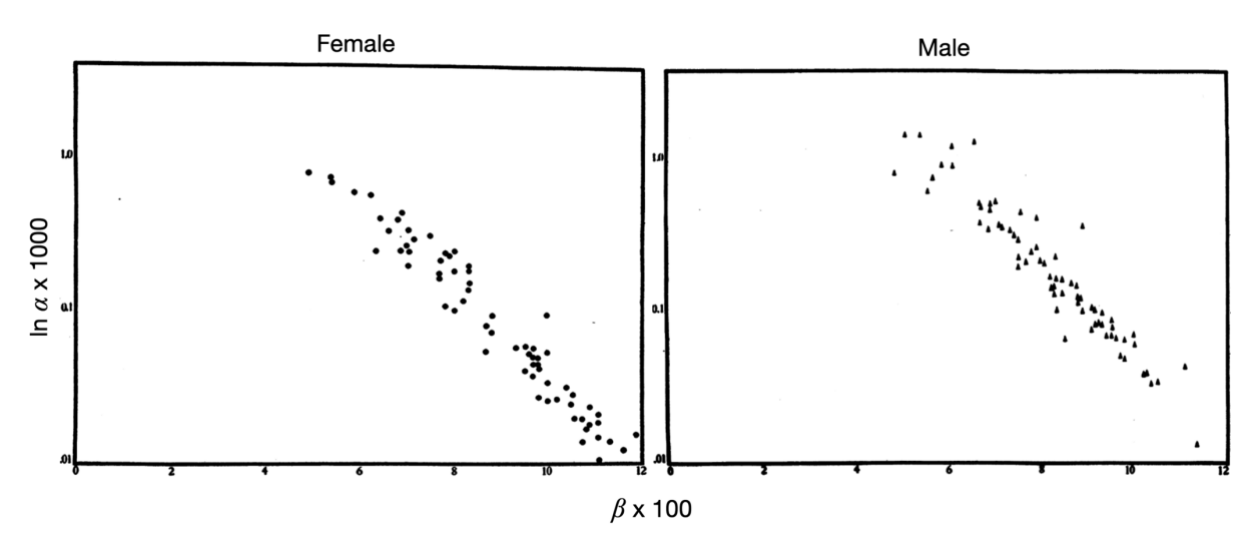


Figure 4.1. The S-M correlation is observed across human populations. Linear inverse relationships between  $\beta$  and the natural logarithm of  $\alpha$ , for both sexes. Each datapoint represents a different country, whose Gompertz parameters were calculated from data from the United Nations Demographic Yearbook for 1955. Figure adapted from Strehler and Mildvan (1960).

Consequently, many demographers have grown to view the S-M correlation as a universal law of mortality, much like the Gompertz model itself. Further sampling of populations however, particularly of human mortality transitions over the last century, revealed frequent exceptions where the Gompertz parameters varied independently of one another (Myers and Manton, 1984, Zheng et al., 2011, Li and Anderson, 2015). It has also been argued that S-M correlations can arise as statistical artefacts (Lestienne, 1988, Burger and Missov, 2016, Tarkhov et al., 2017), although these claims do not rule out the possibility of real biological (or other) phenomena underlying the correlation, which certainly exist where large effects on mortality and survival are observed.

Where non-artefactual S-M correlations occur, what might this reflect in terms of underlying biology? The S-M general theory of ageing and mortality itself suggests that the correlation results from changes in either of two model constants, V<sub>0</sub> (initial vitality) and D (energy demand to overcome stressor events) (Strehler and Mildvan, 1960, Yashin et al., 2002a). However, as with the traditional interpretations of  $\alpha$  and  $\beta$  (Chapter 3), the biological assumptions of the S-M physiological model have yet to be empirically validated. A limitation of such physiological models is that they rely on theoretical assumptions about specific biological mechanisms, yet have limited ability to capture individual variation in them. The latter, as we have seen, is critical to understand gerodemography in terms of biology.

In this chapter, I will use my individual-focused biogerodemographic methodology to attempt to explain the biological basis of the S-M correlations observed within my *C. elegans* data (the 24-cohorts dataset introduced in Chapter 3). Notably, I will show empirically how these S-M correlations are fully consistent with, and intelligible in terms of my reinterpretation

of the Gompertz parameters. However, in this section, I will first demonstrate with a conceptual approach how even without further empirical investigation, the new view of the parameters can parsimoniously resolve two paradoxes of the S-M correlation (summarised in Figure 4.2), which arise from traditional interpretations of  $\alpha$  and  $\beta$ .

When  $\alpha$  and  $\beta$  vary in opposite directions (as in the S-M correlation), antagonistic effects on lifespan occur, because both parameters affect lifespan in the same direction (Figure 2.1c, p. 25; showing that reduction of either parameter extends lifespan). Therefore, S-M correlations produce antagonistic effects on lifespan. In the extreme case these diametric changes can negate each other's effects, thereby having no effect on mean lifespan, as can happen with intersecting survival curves. I propose to refer to this phenomenon with the term "mortality parameter antagonism", or more succinctly, "parametric antagonism", to describe such antagonistic effects of mortality model parameters (e.g. of the Gompertz model) upon lifespan.

The parametric antagonism arising from S-M correlations presents an intriguing question: given that lifespan is simultaneously increased and decreased by  $\alpha$  and  $\beta$  changes, is biological ageing correspondingly ameliorated or exacerbated (or changed at all)? Importantly, this becomes paradoxical in the light of the traditional interpretations of the Gompertz parameters ( $\alpha$ : ageing-independent mortality,  $\beta$ : biological ageing rate), which assume that the parameters reflect the effects of specific and distinct mechanisms upon lifespan. Thus, S-M correlations can appear paradoxical because they indicate the simultaneous action of opposite effects on lifespan.

Such traditional views of the Gompertz parameters have also been suggested to present a problem for reconciling the S-M correlation with evolutionary theory. Medawar's mutation accumulation and Williams' antagonistic pleiotropy theories predict that higher ageing-independent mortality rates should lead to the evolution of faster biological ageing rates (Medawar, 1952, Williams, 1957). In traditional demographic terms (of the Gompertz model), this has been viewed as corresponding to unidirectional changes in  $\alpha$  and  $\beta$ , respectively. However, S-M correlations, which have also been observed between genetically distinct populations of humans and other animals, involve inverse changes in the two parameters.

A traditional interpretation would suggest that in these evolutionary S-M correlations, higher ageing-independent mortality leads to slower biological ageing (and lower ageing-independent mortality to faster ageing), in clear contradiction to evolutionary theory as described above. This problem, for parameters of the Gompertz and other mortality models, has been raised by several authors comparing free-living populations evolved in environments with different levels of extrinsic mortality, including hunter-gather populations (Ricklefs, 1998, Hawkes et al., 2009, Burger and Missov, 2016). An implicit assumption of these claims is that the current environments of these populations do not differ greatly from those in which they evolved.

Note that I do not include in this list a study of guppies in the wild (Reznick et al., 2004), despite a claim by Burger and Missov (2016) that Reznick et al. reported this evolutionary paradox based on an inverse relationship between the Gompertz parameters. Reznick et al. in fact defined extrinsic mortality as predation level, not  $\alpha$ , and biological ageing rate was derived from a derived measure of both Gompertz parameters, not  $\beta$  alone; the evolutionary paradox reported by Reznick et al. therefore does not arise from conflicting interpretations of the parameters of a single model, in contrast to the other studies listed above.

Attempts to resolve these two paradoxes of the S-M correlation have been made, typically falling into two categories. The first explains the correlation as a real, biological property of individuals, usually as arising from an antagonistically pleiotropic trait with opposite effects on early and late life mortality over the course of an individual's life. For example, Yashin et al. (2001) proposed a model in which frailer individuals that survive past early adulthood have greater late-life survival and stress resistance than those more robust in earlier life, due to escaping the metabolic costs of maintaining robustness, or being better "trained" to handle stressor events (given greater susceptibility to and experience of homeostatic fluctuation in earlier life).

More specific though hypothetical examples were also offered, such as the 4G4G genotype (enriched in centenarians (Mannucci et al., 1997)) of the PAI-1 gene. This causes elevated plasma levels of plasminogen activator inhibitor (promoting blood coagulation), which increases atherothrombosis and myocardial infarction risk, yet reduces bleeding complications that may be more harmful in later life (Yashin et al., 2001). Therefore, these antagonistic pleiotropy-based interpretations of the S-M correlation argue that early mortality and ageing rate can indeed vary inversely, simultaneously, within individuals.

The second category of solution to the S-M paradoxes suggests that the S-M correlation is an artefact of demography rather than a strictly biological phenomenon. This "differential heterogeneity" (DH) view argues that rectangularisation/de-rectangularisation of survival (a type of S-M correlation) arises from selective mortality of frailer individuals or subpopulations. Here, Yashin et al. (2001) provide further insight with their model, which additionally includes an element of hidden heterogeneity. They propose two subpopulations, one frail and one robust, with longevity interventions having greater effect on the frail, shorter-lived subpopulation. This rectangularises the full population survival curve due to smaller increases in maximum lifespan, which is determined by the already-long-lived robust subpopulation. Similar arguments have been made (Vaupel and Yashin, 1985, Hawkes et al., 2012), and all view  $\beta$  as a measure of subpopulation heterogeneity in frailty (mortality risk), rather than of biological ageing within individuals. Note however, that this DH hypothesis is usually used to explain intraspecific

rectangularising S-M correlations (e.g. in lifespan intervention experiments) and so is considered a solution to the lifespan paradox (concerning parametric antagonism), but not necessarily the evolutionary paradox. For example, Hawkes et al. (2012) state this precisely:

"Of particular importance, the differential heterogeneity hypothesis also highlights the likelihood that variation in actuarial aging rates among populations *of the same species* are unrelated to the rates of physiological senescence among individuals." (italics added)

My experimental findings in the previous chapter offer support to the latter (DH) category of solution to the S-M paradoxes described. That is, where these paradoxes are resolved by disassociating  $\beta$  from biological ageing rate, so that changes in mortality onset (i.e.  $\alpha$ ) need not co-occur with inverse changes in ageing rate. Specifically, section 3.4 showed that  $\beta$  is a measure of inter-individual gerospan variation, section 3.6 that  $\beta$  can additionally be an artefactual composite of subpopulations with different mortality patterns and their differential responses to treatments, and section 3.7 that  $\beta$  also reflects inter-individual variation in bacterial contact during early adulthood. These findings thus offer a solution to the S-M paradoxes, and provide empirical evidence for DH resolutions proposed by other authors (Vaupel and Yashin, 1985, Yashin et al., 2001, Hawkes et al., 2012). However, my solution differs from other heterogeneity resolutions in several ways:

- 1. It defines specific mechanistic bases for this heterogeneity (i.e. locomotory gerospan and/or bacterial pathologies), rather than the general, theoretical concept of frailty.
- 2. Critically, it demonstrates heterogeneity between not only discrete subpopulations, but each individual (i.e. inter-individual rather than only inter-subpopulation heterogeneity).
- 3. Based on the above, it predicts that  $\beta$  is a measure of heterogeneity (not biological ageing rate) even within supposedly homogeneous subpopulations. That is,  $\beta$  likely reflects inter-individual variation in even populations without subpopulations, such that  $\beta$  may rarely be a direct measure of biological ageing rate.
- 4. The above implies that  $\beta$  could reflect inter-individual variation (rather than ageing rate) not only in comparisons between populations of the same species (e.g. as quoted above from Hawkes *et al.*), but also between different species.

This account of  $\beta$  has implications for our expectations regarding the S-M correlation. For one,  $\beta$  reflecting inter-individual as well as inter-subpopulation heterogeneity may explain why the S-M correlation occurs so frequently. Additionally, one might expect to observe S-M correlations between populations of *different* species, as suggested in point 4 above. However, to my knowledge, an interspecific S-M correlation has not been reported before, and it has even been proposed that the Gompertz parameters should change unidirectionally between species (in contrast to inversely within species) (Hawkes et al., 2009). Such interspecific S-M correlations would exemplify the evolutionary S-M paradox, which thus far, to my knowledge, has only been described between genetically-diverged, free-living populations of the same species (Ricklefs, 1998, Hawkes et al., 2009, Burger and Missov, 2016). However, if interspecific S-M correlations are *not* paradoxical (as my reinterpretation of  $\beta$  implies), then why have they not been widely reported?

One possibility is that many interspecific comparisons (e.g. Sacher, 1977, Finch et al., 1990) are confounded by large differences in mean lifespan between the species examined (e.g. mouse versus human). A clear expectation is that  $\beta$ , being a measure of lifespan variation, will be reduced (i.e. reflecting greater variation) when lifespan is increased, given that the variability of any trait typically scales with its mean magnitude. Therefore, it is possible that comparison of different species with *modest* differences in mean lifespan will uncover evolutionary S-M correlations, which may occur at least as frequently as between populations of the same species. Alternatively, one could rescale (e.g. by mean or median lifespan) the mortality trajectories of species with greater lifespan differences, prior to Gompertz parameter estimation, which I also predict may uncover evolutionary S-M correlations.

Thus far I have argued that my reinterpretation of  $\beta$  can resolve the S-M paradoxes relating to parametric antagonism and evolutionary theory. However, my reinterpretation of  $\alpha$  is additionally helpful. I have shown that in my nematode cohorts,  $\alpha$  is a measure of healthspan duration (particularly in shorter-lived population members), which may reasonably be equated with biological ageing rate (section 3.5). This reassignment of ageing rate measurability from  $\beta$  to  $\alpha$  not only resolves the paradoxes, but offers a parsimonious alternative understanding in which changes in  $\alpha$  (i.e. age of mortality onset) are consistent with the expected change in biological ageing rate, without having to also accommodate biological interpretations of  $\beta$ . Instead,  $\beta$  reflects only inter-individual variation, which has no necessary bearing on biological ageing rate and longevity. Similarly, there is no longer any challenge to evolutionary theory because with the reassignment of ageing rate measurability from  $\beta$  to  $\alpha$ , the S-M correlation no longer makes any prediction about the level of ageing-independent mortality. This proposed resolution of the two S-M paradoxes is summarised in Figure 4.2.

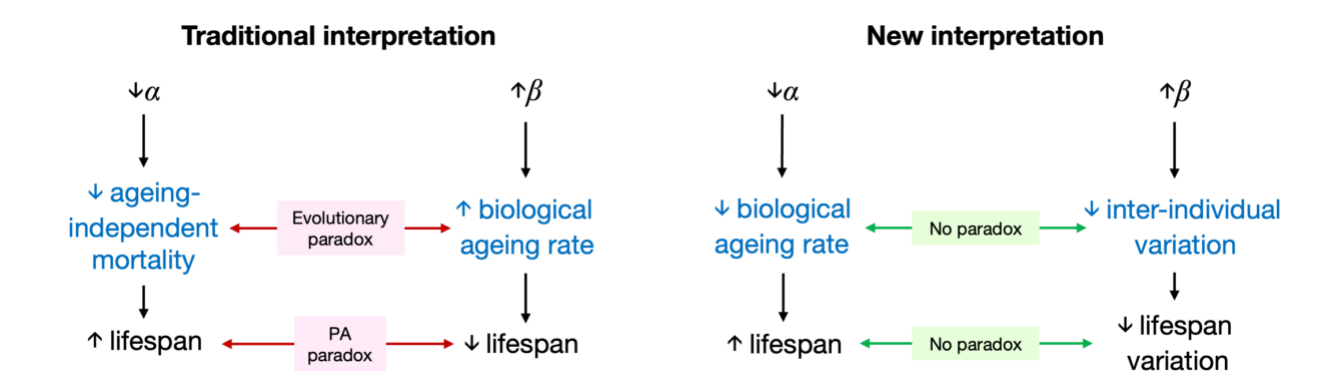


Figure 4.2. Reinterpretation of the Gompertz parameters resolves two S-M paradoxes. Summary schematic of two paradoxes that arise from traditional interpretations of the Gompertz parameters (left), and their resolution by the new biological view of the parameters (right, from conclusions of Chapter 3), using the example of an S-M treatment that decreases  $\alpha$  and increases  $\beta$ . PA (parametric antagonism) paradox: simultaneous occurrence of mechanisms with opposite effects on lifespan, resulting from the traditional biological interpretations of the Gompertz parameters. Evolutionary paradox: conflict of the relationship between the two parameters (in evolutionary comparative studies only) with that predicted by classic evolutionary theory. The latter expects ageing-independent mortality and biological ageing rate to be positively related, yet in S-M correlations they are inversely related according to traditional views of the two parameters. With the new view, there are no opposing mechanisms affecting lifespan (there is no conflict between lifespan and lifespan variation, thus resolving the PA paradox) and the evolutionary paradox also disappears because there is no longer any expectation about ageing-independent mortality.

#### 4.2 – *Life-extending interventions in C. elegans produce S-M correlations*

Re-examining the life-extending treatments from the 24-cohorts dataset investigated in Chapter 3, 25/46 (54%) exhibit a S-M correlation, while in the remainder,  $\alpha$  and  $\beta$  co-vary (change in the same direction) (Figure 4.3a–c). These inverse Gompertz parameter changes between any two cohorts are included within our definition of the S-M correlation, and the responsible lifespanaltering treatments we will refer to as "S-M treatments". Of these S-M and co-varying treatments, respectively, 13/25 (52%) and 7/21 (33%) involve statistically significant changes in both parameters. This reveals a mild predominance of S-M correlations within these lifespanextending treatments. Consistent with this, there is a weak inverse relationship between changes in  $\alpha$  and  $\beta$  across all 24 cohorts (Figure 4.3d).

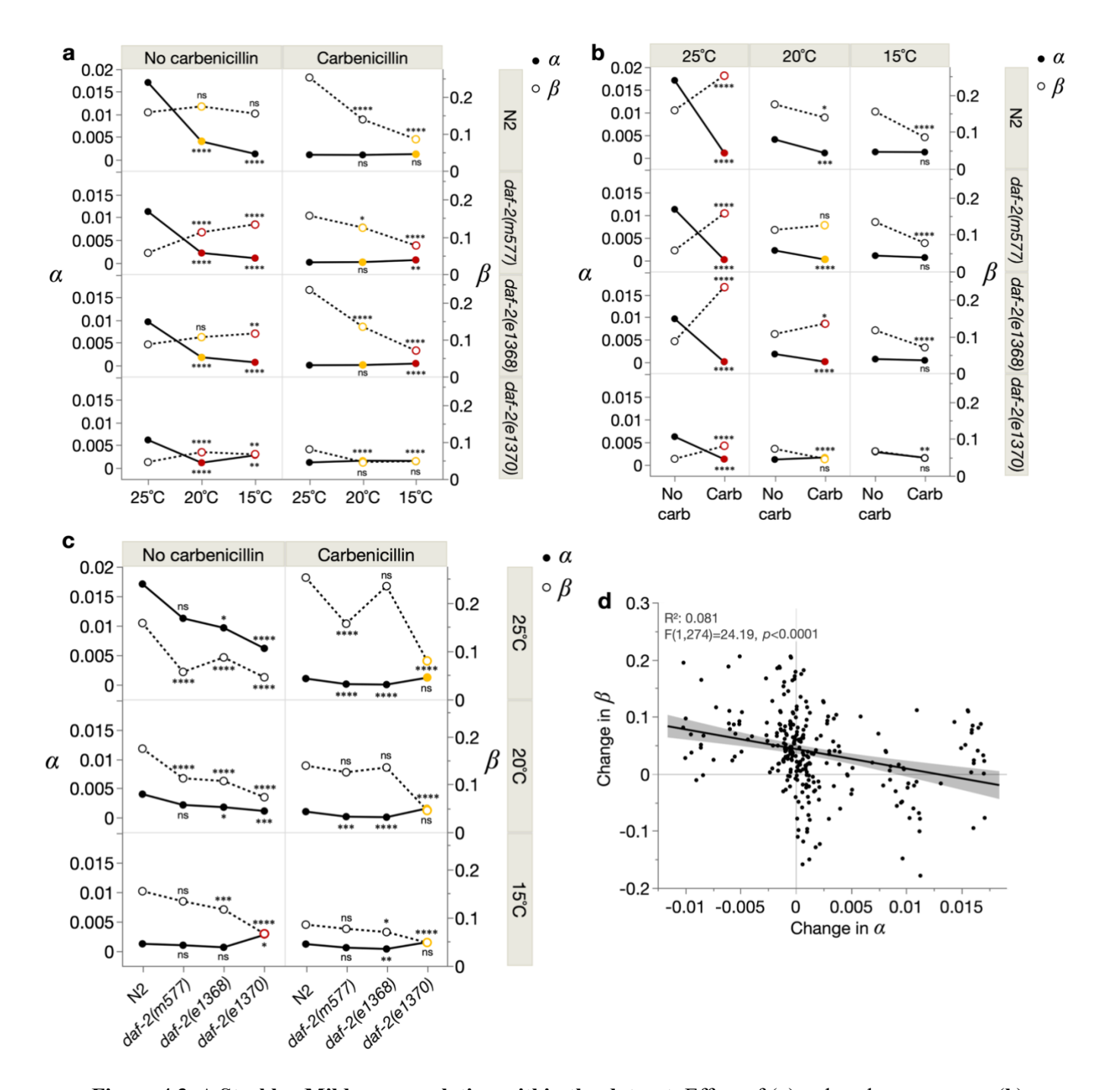


Figure 4.3. A Strehler-Mildvan correlation within the dataset. Effect of (a) reduced temperature, (b) carbenicillin and (c) daf-(rf) on  $\alpha$  and  $\beta$ . Yellow treatments indicate those causing inverse changes in  $\alpha$  and  $\beta$  where none or only one parameter changes statistically significantly, while red treatments indicate those causing inverse changes in  $\alpha$  and  $\beta$  where both parameters change statistically significantly (assessed by likelihood ratio tests); ns p > 0.05, \* $p \le 0.05$ , \*\* $p \le 0.01$ , \*\*\*\*  $p \le 0.001$ , \*\*\*\*  $p \le 0.001$ . Where datapoints overlap, the statistical significance notation for  $\alpha$  and  $\beta$  is labelled below and above the datapoints, respectively. Pool of Trials 3–6. (d) Least-squares linear regression of the changes in  $\beta$  between all possible pairs of the 24 cohorts, over the corresponding change in  $\alpha$  for those pairs. The relationship was assessed by an F-test, with the 95% confidence region shaded. Pool of Trials 1-6.

Inverse changes in  $\alpha$  and  $\beta$  (i.e. the S-M correlation) entail transformations such as the commonly-encountered rectangularisation (or its opposite: de-rectangularisation) (Figure 4.4a) and less common intersection (crossing over) (Figure 4.4b) of survival curves. Effects on survival

curves of my 13 S-M treatments (Figure 4.3a–c, red treatments) largely agree with these idealised transformations, exhibiting mainly rectangularisation (Figure 4.5), including two instances of minor intersection near the curve tail (Figure 4.5a, top left). In these treatments, life-extension involves reduction in  $\alpha$  and increase in  $\beta$  (Figure 4.3a–c), which respectively shifts the survival curve shoulder rightward and steepens the curve (Figure 4.4a).

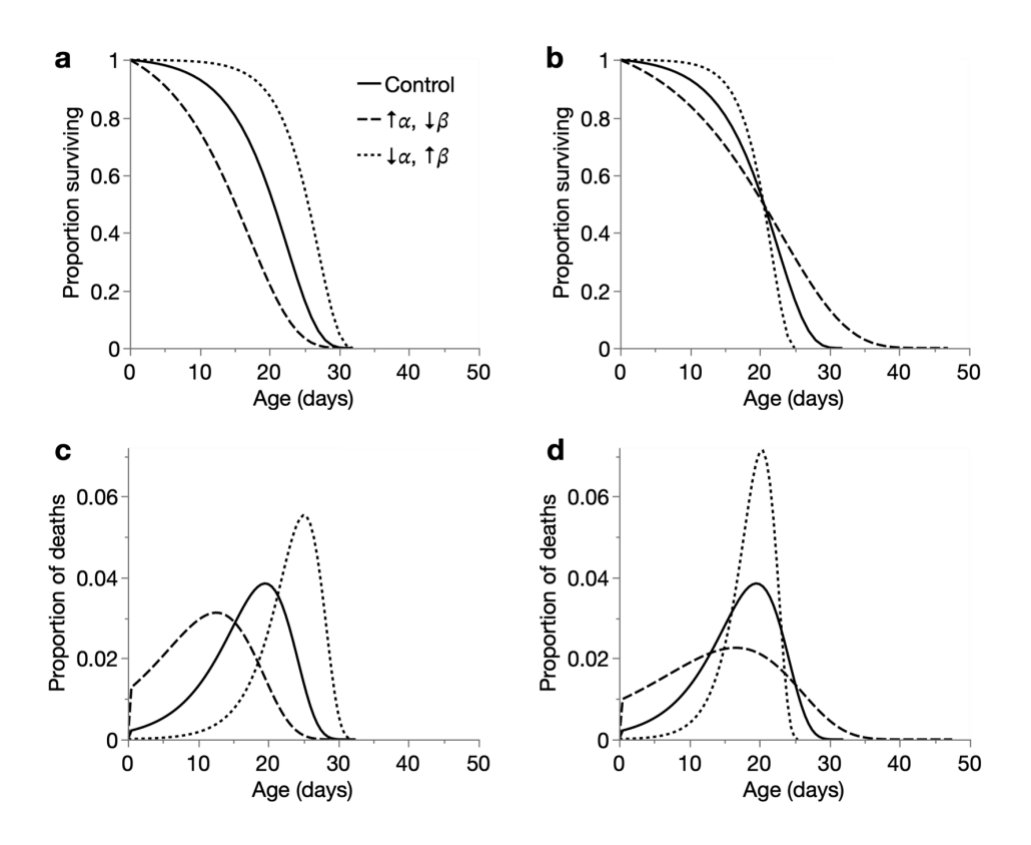


Figure 4.4. Common effects of the Strehler-Mildvan correlation on survival and mortality frequency. (a–b) Two forms of survival curve transformation characteristic of the S-M correlation: (a) rectangularisation and de-rectangularisation, and (b) intersection of survival curves. In these examples, the Gompertz parameters have been set so that maximum (a) and median (b) lifespans are approximately equivalent, but these values can vary. The parameters are: (a) Control:  $\alpha$ =0.002,  $\beta$ =0.2;  $\uparrow \alpha \downarrow \beta$ :  $\alpha$ =0.012,  $\beta$ =0.14;  $\downarrow \alpha \uparrow \beta$ :  $\alpha$ =0.0001,  $\beta$ =0.29, and (b) Control:  $\alpha$ =0.002,  $\beta$ =0.2;  $\uparrow \alpha \downarrow \beta$ :  $\alpha$ =0.012,  $\beta$ =0.08;  $\downarrow \alpha \uparrow \beta$ :  $\alpha$ =0.0001,  $\beta$ =0.37. (c–d) Respectively, effects of Gompertz parameter changes in a and b on mortality frequency over time. Survival proportions in a–b were calculated using 1 day age intervals, and mortality proportions in c–d using 0.5 day age intervals.

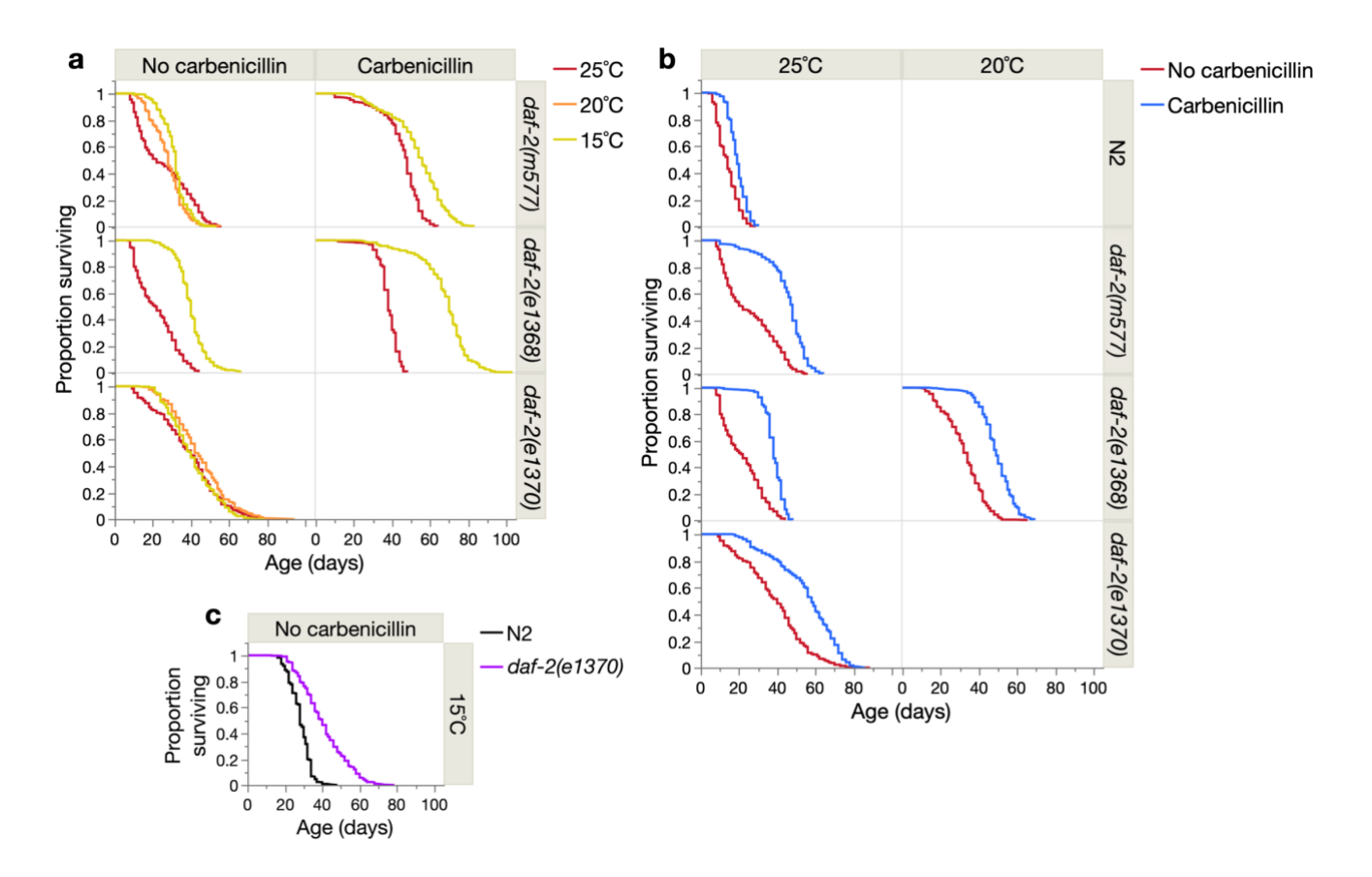


Figure 4.5. Survival curves of treatments in which the Gompertz parameters changed inversely. Effect of (a) reduced temperature, (b) carbenicillin and (c) daf-2(rf) on lifespan for those treatments identified in Figure 4.3a–c where both  $\alpha$  and  $\beta$  varied statistically significantly, in opposite directions. As discussed in the main text (below), three treatments did not rectangularise the survival curve, where instead  $\alpha$  is increased and  $\beta$  decreased (opposite to the rectangularising treatments): 15°C in daf-2(m577) and daf-2(e1368) on carbenicillin (a, right panels), and daf-2(e1370) at 15°C off carbenicillin (c). Pool of Trials 1–6. Log-rank p-values of depicted comparisons are presented in Table 3.1.

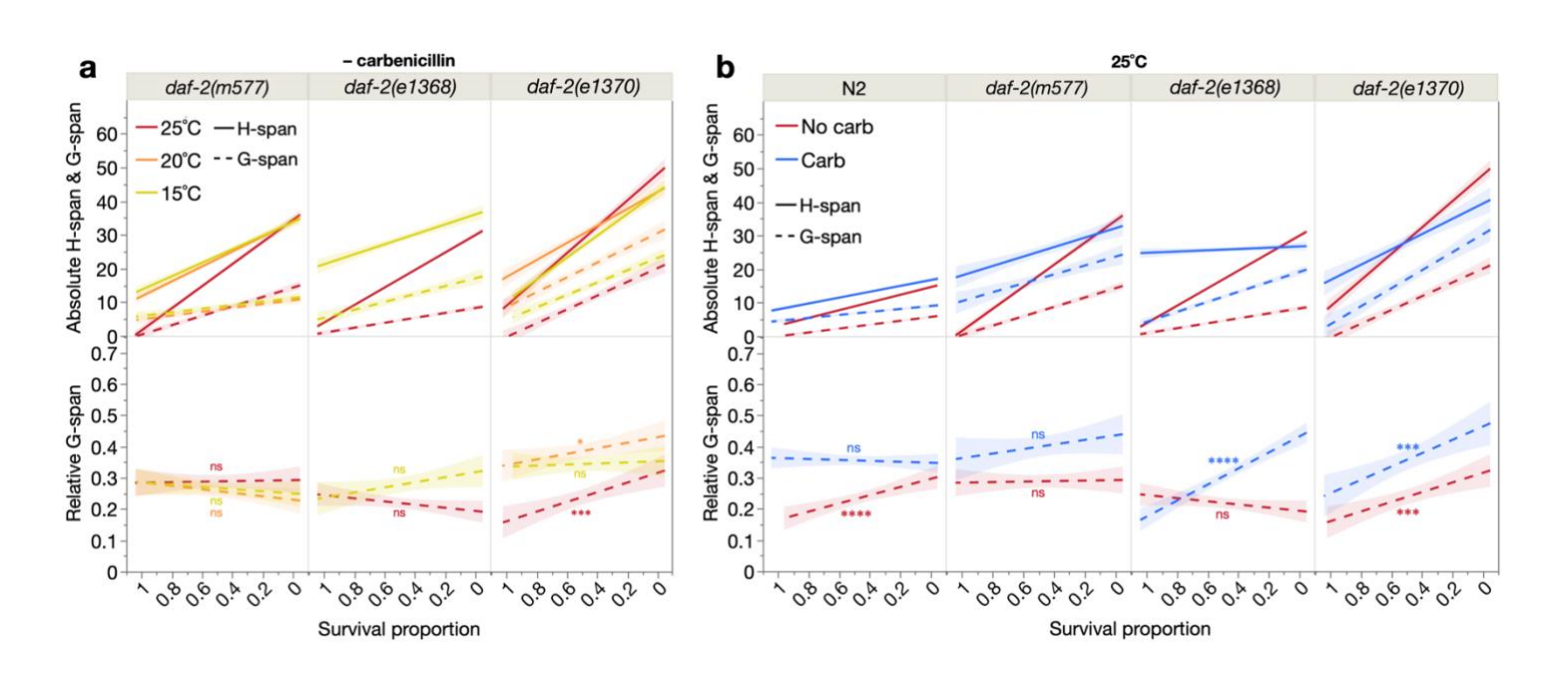
A small number (3/13) of treatments did not exhibit these transformations (Figure 4.5a right, and c), instead showing more minor extensions in the survival curve shoulder and more marked extension of the curve tail. These changes are opposite to those in the rectangularising S-M treatments; here, it is instead  $\alpha$  that is increased and  $\beta$  that is decreased (Figure 4.3a, c).

In the next sections, I will empirically characterise the biological basis of these two types of S-M correlation, starting with the rectangularising cases. I will show that my resolution of the S-M paradoxes in the previous section, derived from my re-interpretation of the Gompertz parameters in Chapter 3, is indeed empirically supported in these S-M treatments.

# 4.3 – Rectangularising S-M correlations reflect decelerated ageing and inter-individual homogenisation

My proposed understanding of the S-M correlation (in section 4.1), from my re-interpretations of the Gompertz parameters in Chapter 3, offers a potential biological explanation of S-M correlations. In the case of rectangularising S-M correlations, I would predict that the reduction in  $\alpha$  arises from an extension of healthspan in short-lived population members (which ordinarily have shorter healthspans), and the resulting reduction in healthspan variability would reduce overall lifespan variability, thereby increasing  $\beta$ . This would provide a simple explanation for the inverse correlation between  $\alpha$  and  $\beta$  in rectangularising S-M correlations.

To assess this prediction, absolute and relative healthspan (H-span<sup>abs</sup>, H-span<sup>rel</sup>) and gerospan (G-span<sup>abs</sup>, G-span<sup>rel</sup>) can be quantified for all individuals across the cohorts (c.f. section 3.4). Here, in Figure 4.6a–c (upper boxes in each panel), one can see that these S-M treatments (reduced temperature and carbenicillin) increased G-span<sup>abs</sup> relatively equally across all survival proportions, which correspond to parallel right-shifts of the survival curve. Notably, this is in contrast to the extended twilight longevity (ETL) characterised in section 3.4, where G-span<sup>abs</sup> was increased more in longer-lived individuals. The lack of variable G-span<sup>abs</sup> increase here is consistent with the rectangularisation of the survival curve, where its tail is shortened rather than extended (i.e.  $\beta$  is increased rather than decreased).



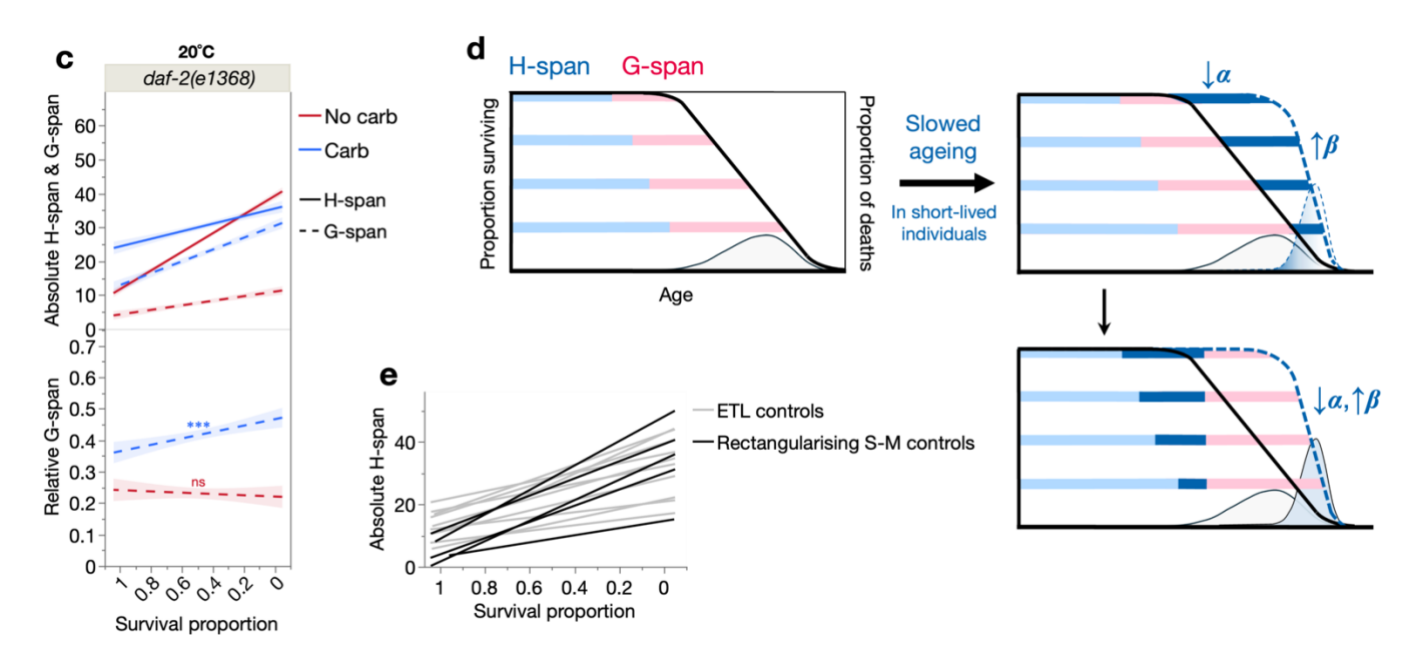


Figure 4.6. Strehler-Mildvan treatments rectangularise survival curves by increasing healthspan in shorter-lived individuals. Effects of (a) low temperature and (b-c) carbenicillin in 10 rectangularising S-M treatments, on absolute healthspan and gerospan (upper boxes) and relative gerospan (lower boxes), plotted over survival proportion (i.e. x-axis left: shorter-lived individuals, x-axis right: longer-lived individuals). All panels show least-squares linear regressions with 95% confidence regions shaded, assessed by F-tests for relative gerospan (lower boxes); ns p > 0.05, \*  $p \le 0.05$ , \*\*  $p \le 0.01$ , \*\*\*  $p \le 0.001$ , \*\*\*\*  $p \le 0.0001$ . (d) Summary schematic of the biological basis of the rectangularising S-M treatments. H-span expansion in shorter-lived population members both delays mortality onset (i.e.  $\alpha$  reduction) and steepens the survival curve (i.e.  $\beta$  reduction). Because H-span is shorter in short-lived population members (especially in cohorts undergoing rectangularisation, see e), the greater H-span expansion in these individuals reduces inter-individual variation in H-span. Bottom panel: overall effect with H-span and Gspan arranged in order. In all panels, probability distributions of death times are overlaid (right y-axis, thin data lines), showing that rectangularisation concentrates mortality at late ages without increasing maximum lifespan. The areas under these distributions are shaded to reflect inter-individual variation in H-span/G-span: rectangularisation involves an inter-individually variable H-span expansion (blue gradient), but which ultimately homogenises the population (solid blue). (e) Least-squares linear regression of absolute H-span over survival proportion for control cohorts of ETL treatments (those indicated in Figure 3.11) versus that of control cohorts of rectangularising S-M treatments (those in panels a-c). For visual clarity, 95% confidence regions are not shown, but can be seen in Figure 3.7 (for ETL treatments) and panels a-c (for rectangularising S-M treatments). The 10 ETL control cohorts are: N2 at 20°C, 15°C, 25°C +carb & 20°C +carb; daf-2(m577) at 15°C & 25°C +carb; daf-2(e1368) at 15°C; daf-2(e1370) at 20°C, 15°C & 25°C +carb. The 5 rectangularising S-M control cohorts are: all genotypes (N2, daf-2(m577), daf-2(e1368), daf-2(e1370)) at 25°C, & daf-2(e1368) at 20°C, all without carb.

In contrast to these G-span<sup>abs</sup> changes, H-span<sup>abs</sup> increased primarily in shorter-lived individuals in 9/10 treatments, with the one exception of 15°C in *daf-2(e1370)* (Figure 4.6a–c, upper boxes). H-span<sup>abs</sup> was even modestly decreased in the longest-lived individuals in several of these treatments, particularly in carbenicillin treatment. These changes in H-span<sup>abs</sup> are therefore responsible for rectangularisation of the survival curve and the S-M correlation, by preferentially extending lifespan in shorter-lived individuals (Figure 4.6d). This concentrates

mortality into later ages (but with little increase in maximum lifespan), resulting in reduction of  $\alpha$  and increase in  $\beta$ . In some cases,  $\beta$  was further increased through the shortening of H-span<sup>abs</sup> (and therefore lifespan) in longer-lived individuals. Importantly, the magnitude of increase in short-lived individuals was also generally greater for H-span<sup>abs</sup> than G-span<sup>abs</sup>. Together, these results show that amongst these treatments, the S-M correlation arises from change in healthspan (rather than gerospan), which alone is sufficient to explain opposite changes in the Gompertz parameters (Figure 4.6d).

These findings validate my prediction that in these S-M treatments  $\alpha$  reduction arises from greater healthspan extension in shorter-lived population members, and that this steepens the survival curve, thus increasing  $\beta$ . Importantly, this occurs because H-span is ordinarily (in the control cohorts) shorter in shorter-lived individuals, such that greater H-span increases in these individuals bring their lengths closer to that in longer-lived individuals (Figure 4.6d). Intriguingly, this variation in H-span (between short and long-lived population members) is generally greater in the control cohorts of these rectangularising S-M treatments than those of the ETL treatments characterised in Chapter 3 (section 3.4) (Figure 4.6e). This suggests that there are fundamental biological differences between these control cohorts, which predispose them to respond to life-extending interventions via either gerospan expansion in longer-lived individuals (i.e. ETL) or healthspan expansion in shorter-lived individuals (as in rectangularising S-M treatments). Indeed, these cohorts consistently responded with either ETL or rectangularising S-M changes, and never both, across all the treatments (see Figure 4.6e caption).

The increases in  $\beta$  suggest that these rectangularising treatments homogenise the population, which may be assessed in three ways with the available data: by evaluating interindividual heterogeneity in locomotory G-span, end-of-life pathology, and early-life bacterial contact. Beginning with locomotory G-span, homogenisation of individuals may be expected to reduce inter-individual variation in G-span<sup>rel</sup>. However, in only 3/10 treatments (20°C and 15°C in daf-2(e1370), and carbenicillin in N2 at 25°C) was G-span<sup>rel</sup> variation reduced (Figure 4.6a–c, lower boxes); it was even increased in three treatments (carbenicillin in daf-2(e1368) and daf-2(e1370) at 25°C, and carbenicillin in daf-2(e1368) at 20°C). Against expectation, this appears to suggest that these increases in  $\beta$  do not reflect a simple homogenisation of individuals.

However, measuring variation another way, as that in H-span<sup>abs</sup> and G-span<sup>abs</sup>, does support this homogenisation hypothesis. The 10 S-M treatments all reduced heterogeneity in H-span<sup>abs</sup>, specifically by increasing H-span<sup>abs</sup> in shorter-lived individuals and mildly decreasing it in longer-lived individuals (Figure 4.6a–c, upper boxes). Meanwhile, G-span<sup>abs</sup> increased by an approximately equal number of days in all individuals, such that its inter-individual variation was largely unchanged. In this view, the overall effect of these S-M treatments is to homogenise the

population by reducing inter-individual variation in H-span<sup>abs</sup> duration (Figure 4.6d). Importantly, H-span<sup>abs</sup> and G-span<sup>abs</sup> are likely to be more biologically relevant metrics of variation than G-span<sup>rel</sup>, as they indicate the rate of ageing, whereas the latter indicates only the ratio between them; this dependency of G-span<sup>rel</sup> on both H-span<sup>abs</sup> and G-span<sup>abs</sup> also makes it more sensitive to noise, and thus a less reliable measure.

Homogenisation of the population can also be interrogated using the end-of-life pathology data. Regarding the lower temperature S-M treatments, Figures 3.15 and 3.16c (pp. 71, 74) show that the treatments increase the prevalence of the longest-lived subpopulation, which in most cases is that of pIC deaths (p with intestinal colonisation by bacteria). This has the effect of redistributing earlier P and/or pnIC deaths to later ages, as pIC deaths, which rectangularises the survival curve in line with differential heterogeneity explanations of the S-M correlation (Vaupel and Yashin, 1985, Yashin et al., 2001, Hawkes et al., 2012) (Figure 4.4a, c, p. 92). This redistribution of deaths involves the "conversion" of shorter-lived subpopulations into pathologically distinct longer-lived subpopulations, thus homogenising the population in favour of the latter. A simple analogy for this phenomenon is the reduction of early-life human mortality from communicable diseases over much of the last two centuries, which homogenised human populations for ageing-related mortality (Riley, 2001).

Whether the antibiotic S-M treatments also homogenise individuals is more difficult to evaluate, given that carbenicillin entirely eliminates these bacterial pathologies (Figure 3.14b, p. 70). However, one possible view is that carbenicillin similarly "converts" both shorter-lived, bacterially-colonised subpopulations (P and pIC, but especially P) into a single, infection-free longer-lived one (pnIC) (Figure 3.14a, 3.15), thus rectangularising the survival curve. But if this is true, then why do the other (non-S-M) carbenicillin treatments decrease  $\beta$  (Figure 4.3b, p. 91), which would suggest heterogenisation of the population? One possible explanation is that in those specific treatment backgrounds (i.e. temperature and/or genotype), elimination of bacterial pathologies unmasks effects on mortality of other, unidentified, inter-individually-variable pathologies.

Finally, I will assess the homogenisation prediction using the early-adulthood bacterial contact data. In 7/10 of the S-M treatments, variance in early-adulthood bacterial contact was decreased, in 5 of which the decrease was statistically significant (Figure 4.7). Thus, overall, these bacterial contact data support the result that in these rectangularising S-M treatments, the increase in  $\beta$  reflects a homogenisation of individual biology, even in behavioural phenotypes prior to ageing.

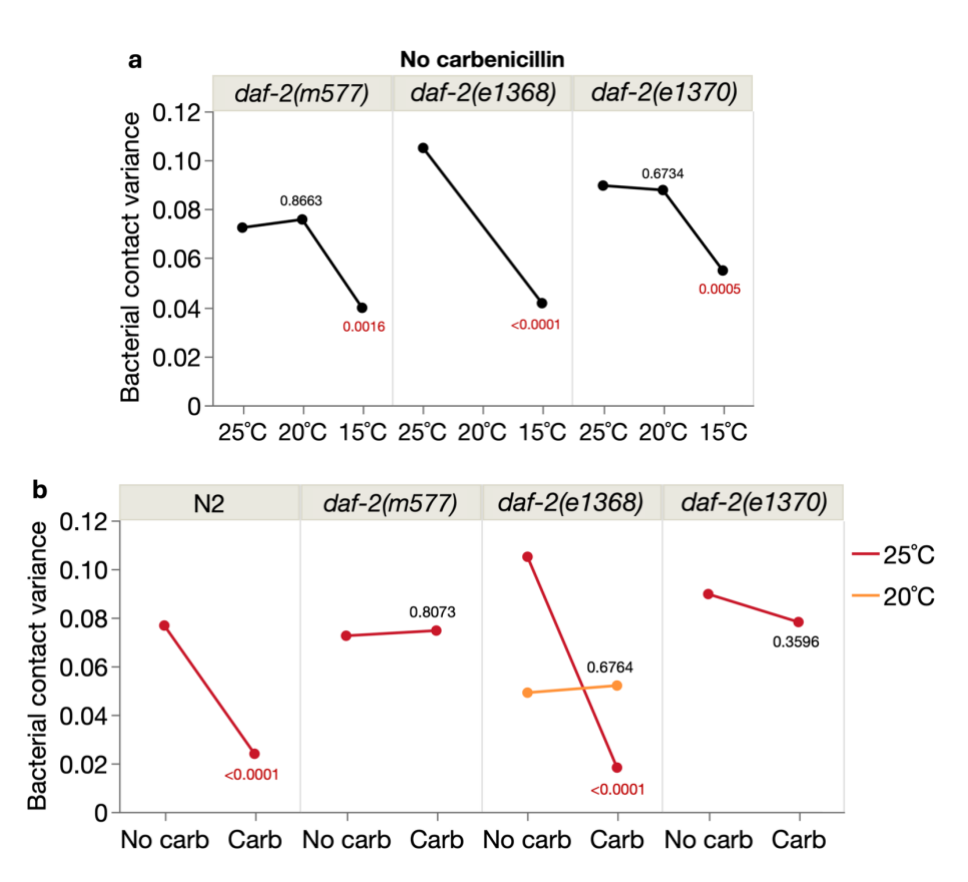


**Figure 4.7. Strehler-Mildvan treatments reduce inter-individual variation in early-adulthood bacterial contact.** Effects of (a) low temperature and (b) carbenicillin (10 rectangularising S-M treatments identified in Figure 4.3a–c and 4.5) on variance in individual bacterial contact (proportion of locomotory healthspan observed on bacterial lawn). Data from pool of Trials 4–6. Differences between variances were assessed by a Levene test for unequal variances; *p*-values overlaid next to treatment datapoints.

In summary, I have demonstrated that S-M correlations that rectangularise the survival curve decrease  $\alpha$  and increase  $\beta$  via an expansion of healthspan (i.e. deceleration of ageing) in shorter-lived population members. This increases healthspan in individuals in which it would otherwise be shortest, thereby reducing overall healthspan and lifespan variability, which increases  $\beta$  (Figure 4.6d). Rectangularisation thus also reflects a reduction in inter-individual variation in several ageing and pre-ageing traits. This biological explanation of rectangularising S-M treatments agrees closely with the new biological understanding of the Gompertz parameters characterised in Chapter 3, whose explanatory power was also demonstrated (in section 4.1) in resolving the S-M paradoxes that emerge from traditional views of  $\alpha$  and  $\beta$ .

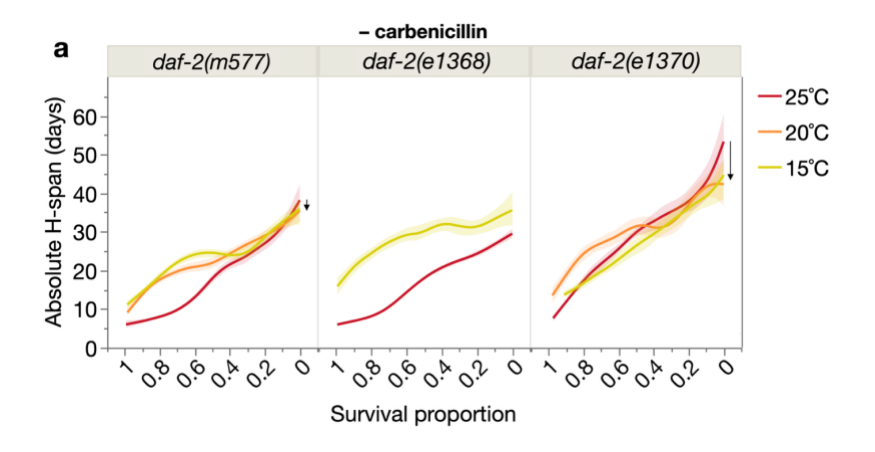
#### 4.4 – Testing the antagonistic pleiotropy explanation of rectangularising S-M correlations

In the last section, I provided evidence for a differential heterogeneity (DH) explanation of the S-M correlation, where associated survival curve rectangularisation/de-rectangularisation

reflects the degree of inter-individual heterogeneity in several ageing and pre-ageing traits. This view suggests that reducing this heterogeneity involves the preferential postponement of early mortality, thereby compressing mortality into later ages. In this section, I will assess the alternative, antagonistic pleiotropy (AP) explanation of the S-M correlation, where survival curve rectangularisation/de-rectangularisation arises from antagonistically pleiotropic traits with opposite effects on early and late life mortality, as introduced in section 4.1.

According to this view, the Gompertz parameters vary inversely because of this trade-off between early and late mortality (Yashin et al., 2001). For instance, in rectangularisation, reduced early mortality (decreased  $\alpha$ ) results from increased levels of some trait that is beneficial in early life, which consequently increases late mortality (increased  $\beta$ ) due to that trait being deleterious in later life, and vice versa in de-rectangularisation. Importantly, allowing reasonable flexibility in definitions, DH and AP are not necessarily mutually exclusive mechanisms underlying the S-M correlation and may co-occur. For instance, AP can be considered the biological mechanism from which the demographic DH phenomenon emerges.

I will evaluate the AP hypothesis by first searching for antagonistic patterns in ageing-related measures, between short and long-lived individuals, in the 10 rectangularising S-M treatments. Starting with locomotory health; I showed earlier that locomotory H-span is extended predominantly in shorter-lived individuals, and even mildly shortened in the longest-lived individuals of some treatments (Figure 4.6a–c). To better assess this potential antagonism, I replotted these data with a non-linear smoother (instead of a linear fit), to more accurately visualise and assess whether H-span is decreased in these longest-lived individuals (Figure 4.8). In these new plots, the mild shortening of H-span in the longest-lived persisted, showing that they are not artefacts of linear regression. However, this shortening was very weak, therefore providing only tentative support for the possibility that rectangularisation results from AP affecting locomotory H-span.



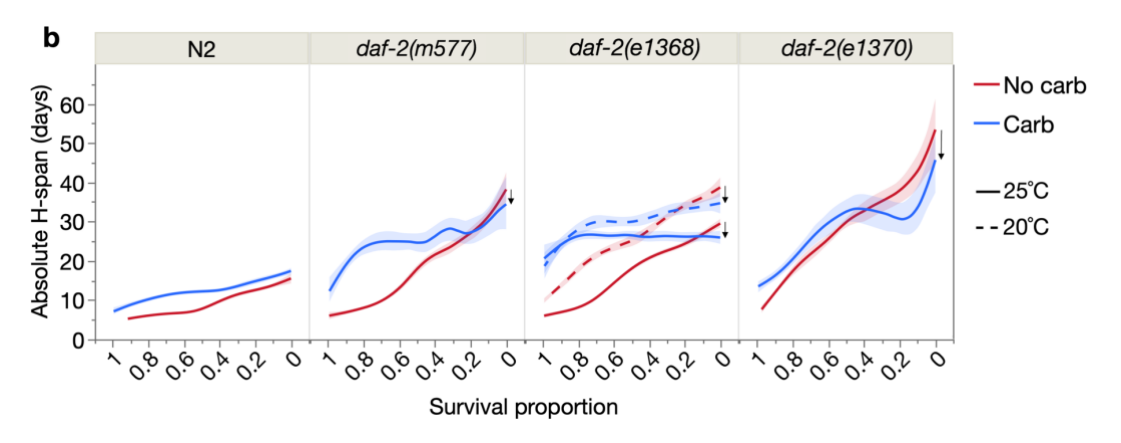


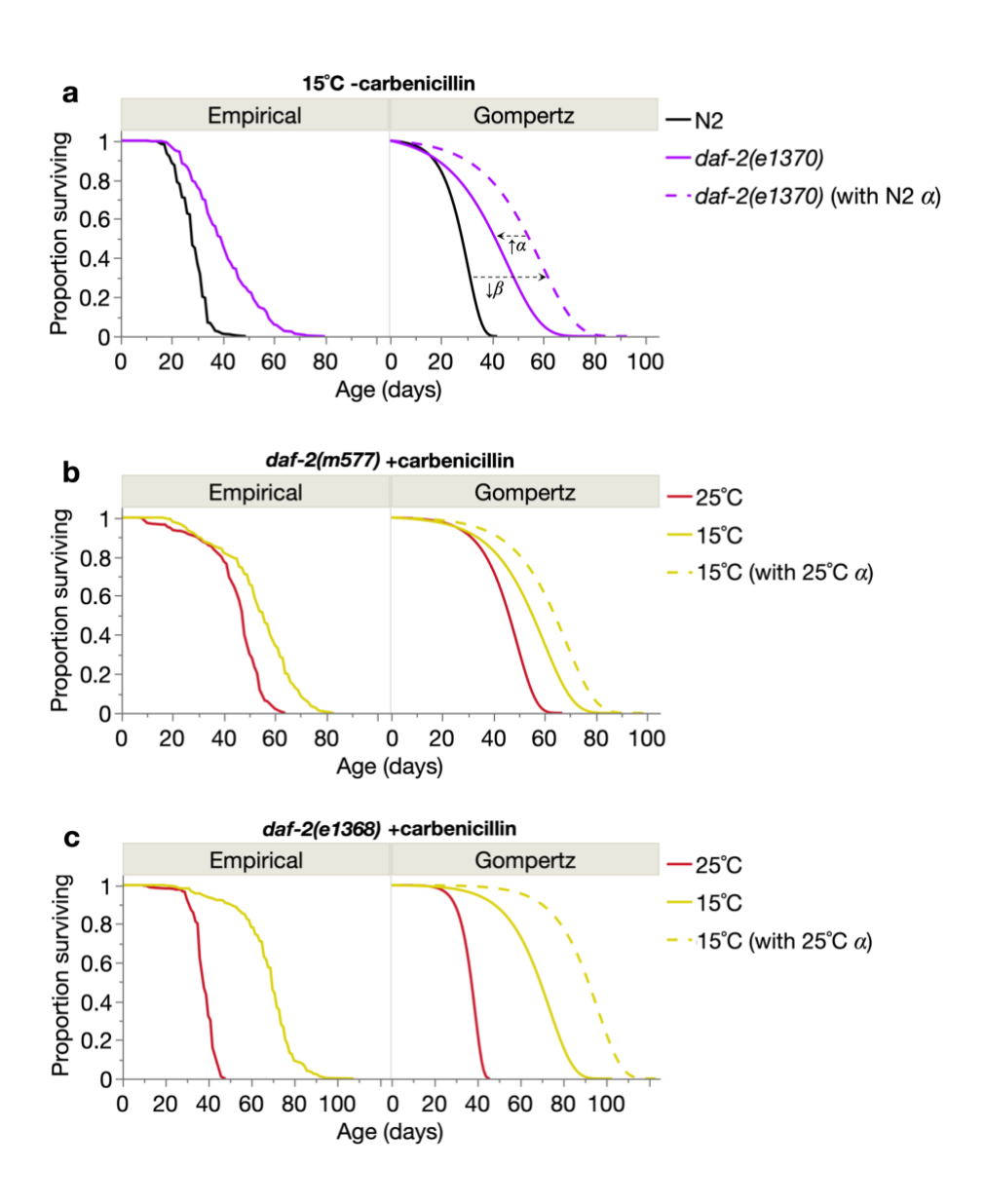
Figure 4.8. Strehler-Mildvan treatments mildly shorten locomotory H-span in the longest-lived. Effects of (a) low temperature and (b) carbenicillin (10 rectangularising S-M treatments identified in Figures 4.3a—c and 4.5) on absolute locomotory healthspan. Instead of a linear regression fit as in Figure 4.6, here a non-linear smoother is employed (spline method, lambda=0.05), with 95% confidence regions shaded. Reductions of H-span in longer-lived population members are indicated with arrows.

Next, I will assess end-of-life pathology in these S-M treatments for signs of AP. In most lower temperature treatments (daf-2(m577)) and daf-2(e1368) backgrounds), pharyngeal infection (P) prevalence (in shorter-lived individuals) was modestly decreased, while intestinal colonisation (pIC) (in longer-lived individuals) was markedly increased (Figures 3.15 and 3.16c, pp. 71, 74). This suggests the presence of a temperature-regulated trade-off between susceptibility to bacterial pathogenicity in different tissues. In daf-2(e1370), reducing temperature to 20°C caused P and pIC prevalence to also vary inversely, but in the opposite direction (i.e. more P and less pIC). Further reducing temperature to 15°C increased both P and pIC prevalence. Thus, the daf-2(e1370) background complicates the relationship between the two end-of-life pathologies. However, in most backgrounds the relationship is inverse, indicating a potential AP mechanism. For the carbenicillin S-M treatments, these unfortunately cannot be assessed here, given that all infection-related pathologies were eliminated (Figure 3.14b, p. 70).

In summary, I have attempted to search for an AP explanation of the S-M correlation in my 10 rectangularising S-M treatments. Inverse changes between early and later-dying individuals in locomotory healthspan and bacterial pathology (pharyngeal infection and intestinal colonisation) are modestly consistent with such an AP mechanism. However, overall, I find clearer evidence (described in the last section) for a differential heterogeneity explanation of these rectangularising S-M correlations, although it need not be mutually exclusive with AP. Specifically, I show that rectangularisation slows biological ageing in shorter-lived population members, thereby homogenising individuals and concentrating deaths at later ages (summarised in Figure 4.6d).

In section 4.2, I presented the 13 S-M treatments from my nematode cohorts, of which the majority (10/13) were rectangularising S-M treatments (Figure 4.5, p. 93). The remaining 3 treatments exhibited the opposite pattern, where  $\alpha$  was increased and  $\beta$  decreased, and lifespan was extended more in longer-lived individuals (Figure 4.3a, c, 4.5, pp. 91, 93). In this final section of Chapter 4, I will examine this type of S-M correlation.

One might expect the increase in  $\alpha$  in these treatments to shift the survival curve shoulder leftward (i.e. hasten mortality onset), yet the opposite was true. To investigate this, I compared the empirical and fitted Gompertz survival curves for these three treatments, examining the separate component effects of increasing  $\alpha$  and decreasing  $\beta$  (Figure 4.9a–c).



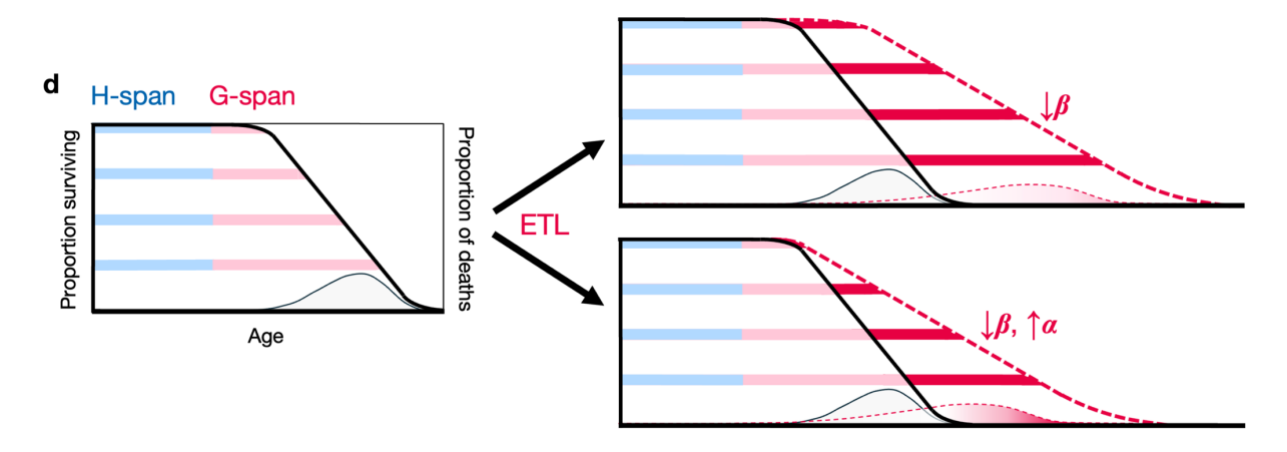


Figure 4.9. Strehler-Mildvan treatments that triangularise the survival curve. Empirical versus idealised Gompertz survival curves for three S-M treatments identified in Figure 4.3a-c and 4.5 that increase  $\alpha$  and decrease  $\beta$ : (a) daf-2(e1370) mutation at 15°C without carbenicillin, (b) reducing temperature to 15°C in daf-2(m577) on carbenicillin, and (c) reducing temperature to 15°C in daf-2(e1368) on carbenicillin. The dashed lines show simulated Gompertz survival curves that retain the control  $\alpha$ value, while  $\beta$  is reduced to the value of the treatment cohort. This illustrates how the inverse parameter changes combine to produce an overall survival curve that fits the data; for example, the individual contributions of each parameter are shown with arrows in a. Data from pool of Trials 1-6. (d) Both  $\beta$ reduction (top) and S-M triangularisation (bottom) arise from extended twilight longevity (ETL). Both arise from inter-individually variable G-span expansion (greater in longer-lived individuals), as characterised in section 3.4; however, this increase is more inter-individually variable in triangularisation. Probability distributions of death times corresponding to the survival curves are overlaid (right y-axis, thin data lines), showing that both ETL scenarios stretch this distribution, but which is also shifted leftward by the  $\alpha$  increase in triangularisation. The area under these probability distributions is shaded to reflect inter-individual variation in G-span; triangularisation involves a more variable G-span expansion (i.e. more extreme ETL) than in  $\beta$  reduction alone, depicted as greater contrast in gradient shading. Importantly, in S-M triangularisation,  $\alpha$  increase and  $\beta$  reduction both (together) reflect the ETL event.

This revealed that reduction of  $\beta$  alone (Figure 4.9a–c, dashed curves) greatly overestimates lifespan, especially in shorter-lived population members. Therefore, the  $\alpha$  increase effectively shifts the curve leftward, allowing the empirical curve to be correctly modelled (see arrows in panel a). Importantly, the small magnitude of  $\alpha$  increase and co-occurrence with mild postponement of mortality onset from  $\beta$  reduction explains why overall mortality onset is not earlier in these treatments (despite  $\alpha$  being increased). Further increasing the magnitude of  $\alpha$  increase would bring mortality onset earlier, leading first to intersecting survival curves (Figure 4.4b, p. 92) and then to de-rectangularisation at very high  $\alpha$  values (Figure 4.4a).

A salient feature of this type of S-M correlation (Figure 4.9a–c) is that it involves a highly inter-individually variable increase in lifespan. This occurs because the  $\alpha$  increase effectively truncates the lifespan extension gained from  $\beta$  reduction, by an approximately *equal amount* in all population members (see arrows in panel a). However, because  $\beta$  reduction extends lifespan more in longer- than shorter-lived population members, the truncation of this extension will be

disproportionately greater in shorter-lived members. Consequently, the overall gain in lifespan in these treatments will be more inter-individually variable than that resulting from  $\beta$  reduction alone. Accordingly, this type of S-M correlation increases lifespan variation more than in  $\beta$  reduction alone.

To my knowledge, there is no established terminology to describe this type of S-M correlation. I will refer to it as a "triangularising" S-M correlation (c.f. rectangularisation), given that it causes a lowered survival curve slope and extended tail, resembling the elongated right corner of a triangle. While  $\beta$  reduction alone also results in survival curve triangularisation (to a lesser degree), I will use this term specifically to refer to the S-M scenario, unless specified otherwise.

Interestingly, 2/3 of these triangularising S-M treatments are ETL treatments that I already characterised in section 3.4, and in all 3,  $\beta$  reduction primarily reflects greater G-span (than H-span) extension in longer-lived individuals (Figure 3.7a, d, p. 55). Triangularising S-M correlations hence result from an ETL event with greater inter-individual G-span variability than in  $\beta$  reduction alone (see Figure 4.9d for a summary schematic).

Thus, this type of S-M correlation is consistent with my reinterpretation of Gompertzian mortality in Chapter 3, where extension of the survival curve tail arises from inter-individually variable gerospan expansion. My reinterpretation also predicts that the increase in  $\alpha$  should reflect a shortening of healthspan in shorter-lived population members. A very weak trend suggestive of this was observed in these three triangularising S-M treatments (Figure 3.7a, d, p. 55; 15°C treatment in daf-2(m577) and daf-2(e1368) on carbenicillin, and daf-2(e1370) treatment at 15°C without carbenicillin).

One reason for this could be the small magnitude of  $\alpha$  increase in these treatments (Figure 4.3a, c, p. 91), for instance in comparison to far greater magnitudes of  $\alpha$  reduction in the rectangularising S-M treatments (Figure 4.3a–b). However, the reduction in lifespan by  $\alpha$  increase in these triangularising treatments (Figure 4.9a–c) is still clearly greater than this minor reduction in healthspan (Figure 3.7a, d, p. 55). Triangularising S-M correlations are thus rare (3/46 treatments) exceptions to the inverse relationship between  $\alpha$  and healthspan demonstrated in section 3.5. Instead, both parameters together reflect a strong ETL event consisting of a highly inter-individually variable expansion of gerospan (Figure 4.9d).

In summary, I have demonstrated the biological basis of rectangularising and triangularising S-M correlations across my nematode cohorts. Both types of S-M correlation involve an inter-individually variable change, of healthspan in shorter-lived population members in rectangularisation/de-rectangularisation, and gerospan in longer-lived population members in triangularisation/de-triangularisation (i.e. ETL). However, these changes have contrasting effects

on population homogeneity: rectangularisation ultimately decreases inter-individual variation (or increases it in de-rectangularisation), whereas triangularisation increases it (or decreases it in detriangularisation). Notably, these biological explanations of the S-M correlations agree closely with my reinterpretation of the Gompertz parameters in Chapter 3, and can additionally resolve paradoxes of the S-M correlation (section 4.1), demonstrating their ability to make sense of diverse survival and mortality patterns.

# 5.1 – Roles of daf-16 in Gompertzian biogerodemography

Reduction of insulin/IGF-1 signalling (IIS) was one of the first interventions found to increase C. elegans lifespan (Friedman and Johnson, 1988, Kenyon et al., 1993), and has remained amongst those causing the greatest magnitudes of life-extension, and its effects on lifespan are conserved across species (Barbieri et al., 2003, van Heemst et al., 2005). In Chapter 3, I characterised the biological basis of demographic mortality patterns in response to three classes of longevity intervention: reduced ambient temperature, antibiotic treatment and genetic reduction of IIS. This revealed that on the whole, across treatments (both in IIS reduction and independent of IIS level), the  $\alpha$  and  $\beta$  parameters of the Gompertz model reflect healthspan length and inter-individual variability in ageing, respectively. In this chapter, I further develop and apply this biogerodemographic method to understand the relationship between IIS and ageing and lifespan in C. elegans. Accordingly, the approaches taken will similarly focus on explaining the biological basis of demographic patterns, to refocus discovery on individual biology.

To start, I extended the 24-cohorts dataset to include several cohorts of the FOXO transcription factor null mutant daf-16(mgDf50). DAF-16 is inhibited by DAF-2, and therefore hyperactive in daf-2 mutants; notably, daf-16(0) suppresses daf-2 mutant longevity. Thus, the effects of daf-16(0) are similar to an increase in IIS, and indeed the mutant is short-lived under standard culture conditions (Patel et al., 2008). This added 6 additional cohorts: daf-16 at 25°C, 20°C, and 15°C, with and without carbenicillin. We can thus ask: (1) how does the increased IIS-like effects of daf-16(0) mutation affect biogerodemography (Gompertz parameters and individual ageing), and (2) are reduced temperature and carbenicillin treatment effects on biogerodemography daf-16-dependent?

As expected, *daf-16* lifespan was shortened relative to N2, and this was true in most (5/6) treatment conditions (Figure 5.1a, Table 5.1). The one exception was at 20°C without carbenicillin, which disagrees with previous reports (Saul et al., 2008, Zhao et al., 2021), possibly due to variability in *E. coli* pathogenicity. These *daf-16* cohorts expand my observed continuum of IIS effects on lifespan, where reduced IIS by *daf-2(rf)* extends lifespan and unconstrained IIS due to *daf-16(0)* shortens lifespan (Figure 5.1a). Meanwhile, both lowered ambient temperature and carbenicillin robustly increased lifespan in *daf-16* animals (Figure 5.1b–c, Table 5.1), as observed in all the other genotypes (Figure 3.3a–b, Table 3.1, pp. 49, 46),

implying that these longevity interventions are largely *daf-16*-independent. This is consistent with an earlier report of *daf-16*-independence in the regulation of lifespan by thermosensory neurons (Lee and Kenyon, 2009).

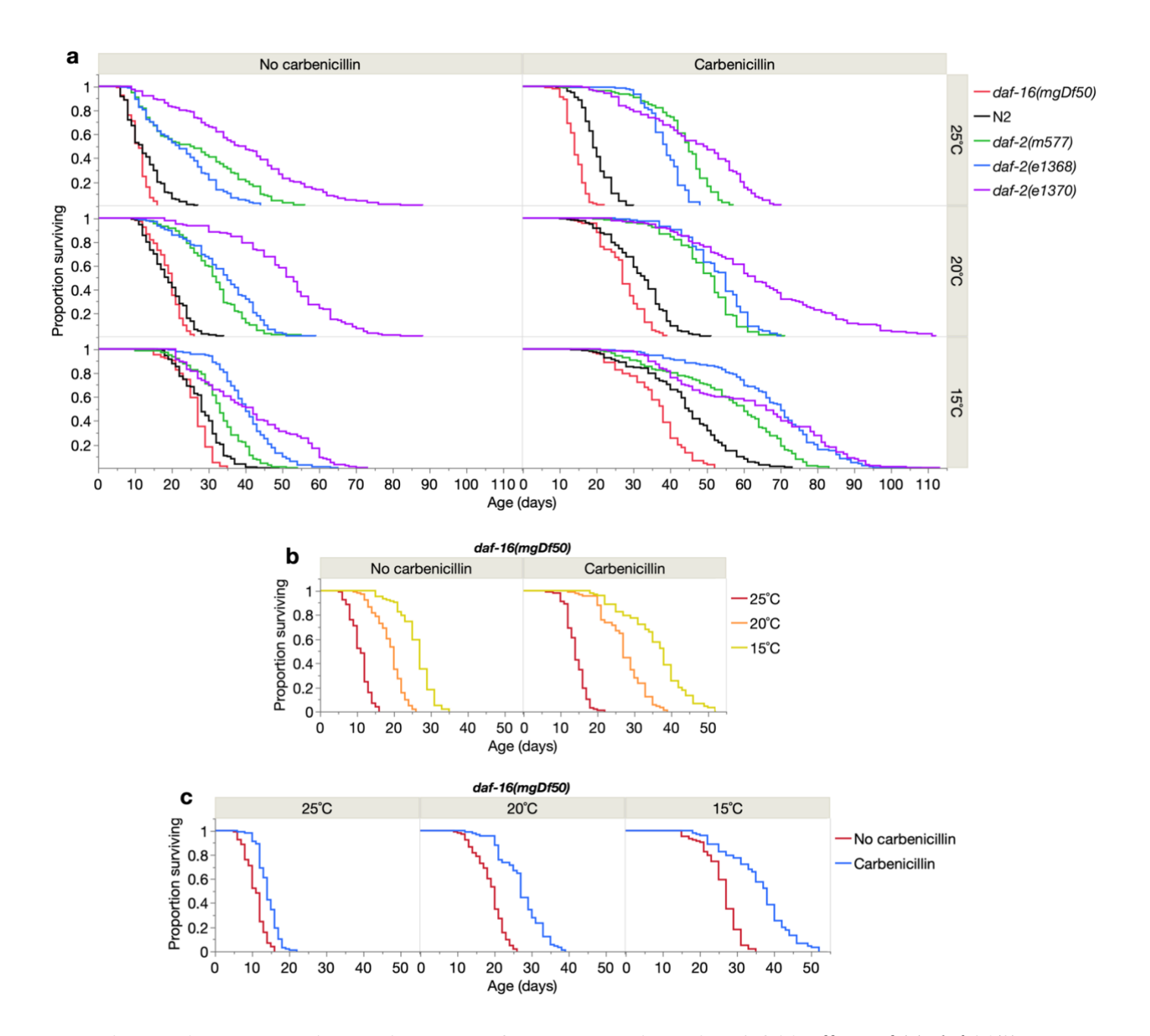


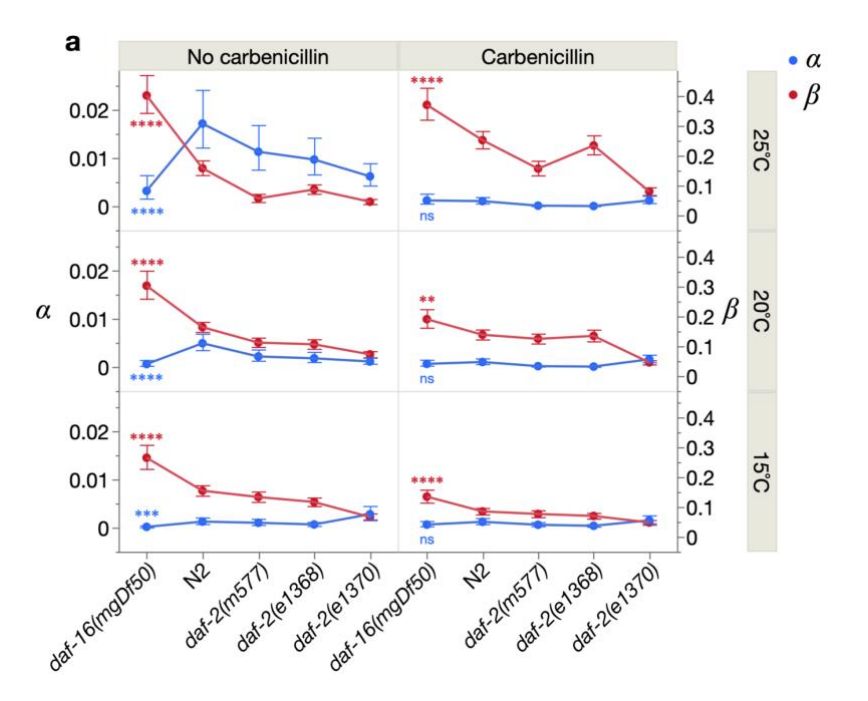
**Figure 5.1. Kaplan-Meier survival curves for treatments involving** *daf-16.* Effects of (a) *daf-16(0)* and *daf-2(rf)*, (b) reducing ambient temperature, and (c) carbenicillin treatment. N2: wild-type. Genotypes in the legend of a are ordered by decreasing IIS level (precisely, increasing DAF-16 activation). Pool of 3 trials for *daf-16* cohorts and 4 trials (Trials 3–6 in Table 3.1) for all *daf-2* and N2 cohorts, except N2 at 20°C without carbenicillin (6 trials). Log-rank *p*-values of relevant comparisons and their summary statistics are presented in Table 5.1 below.

			Effect of reducin	ng temperature	Effect of carbenicillin		Effect of daf-16(0)	
Cohort	No. dead/ censors	Mean lifespan (days since L4)	% change vs. 25°C	p vs. 25°C (Log-Rank)	% change vs. no carb.	p vs. no carb. (Log-Rank)	% change vs. N2	p vs. N2 (Log-Rank)
N2 25°C	[C] 169/8	12.6		(LUG-Nalik)	no carb.	(LUG-Nailk)	V5. IV2	(LUG-Kalik)
	[3] 70/1 [4] 33/2	11.3 13.7						
	[5] 31/4	11.6 14.9						
	[6] 35/1 [7]	14.9						
N2 20°C	[8] [C] 246/12	19.0						
112 20 C	[3] 67/2 [4] 33/3	19.9 20.6						
	[5] 33/3	18.1						
	[6] 36/0 [7] 44/2	17.4 19.8						
N2 15°C	[8] 33/4 [C] 159/10	16.8 <b>28.2</b>						
142 13 0	[3] 62/8	27.4						
	[4] 33/3 [5] 30/5	33.5 25.2						
	[6] 34/2 [7]	27.3						
N2 25°C carb	[8] [C] 173/4	19.8						
N2 25°C carb.	[3] 70/2	18.2						
	[4] 34/1 [5] 35/1	20.8 24.0						
	[6] 34/2 [7]	17.6						
Na 20°C carda	[8]							
N2 20°C carb.	[C] 173/5 [3] 70/1	<b>31.8</b> 29.0						
	[4] 33/3 [5] 35/1	32.2 32.4						
	[6] 35/1 [7]	36.4						
	[8]							
N2 15°C carb.	[C] 161/9 [3] 62/1	<b>44.3</b> 38.2						
	[4] 32/4 [5] 34/2	50.2 47.0						
	[6] 33/3 [7]	47.3						
	[8]							
daf-16(mgDf50) 25°C	[C] 102/5 [3]	10.8					-14.0	<0.0001
	[4] [5]							
	[6] 36/0 [7] 33/1	10.3 11.1					-30.7	<0.0001
	[8] 33/4	11.0						
daf-16(mgDf50) 20°C	[C] 103/4 [3]	18.8	74.5	<0.0001			-0.6	0.0650
	[4] [5]							
	[6] 36/0	18.1 20.2		<0.0001 <0.0001			3.5 2.3	0.6922 0.8207
	[7] 35/0 [8] 32/4	18.2		<0.0001			8.1	0.5354
daf-16(mgDf50) 15°C	[C] 100/6 [3]	26.1	141.8	<0.0001			-7.5	<0.0001
	[4] [5]							
	[6] 35/1 [7] 33/1	24.8 25.7		<0.0001 <0.0001			-9.1	0.0234
	[8] 32/4	27.9	153.0	<0.0001				
daf-16(mgDf50) 25°C carb.	b. <b>[C] 99/8</b> [3]	14.2			31.5	<0.0001	-28.4	<0.0001
	[4] [5]							
	[6] 36/0	13.0			25.8	<0.0001 <0.0001	-26.2	<0.0001
	[7] 32/4 [8] 31/4	14.0 15.7			26.5 42.5	<0.0001		
daf-16(mgDf50) 20°C carb.	b. <b>[C] 90/8</b> [3]	27.3	92.2	<0.0001	44.8	<0.0001	-14.2	<0.0001
	[4] [5]							
	[6] 35/1	26.3		<0.0001		<0.0001	-27.8	<0.0001
	[7] 25/4 [8] 30/3	28.3 27.5		<0.0001 <0.0001		<0.0001 <0.0001		
daf-16(mgDf50) 15°C carb.	b. <b>[C] 94/11</b> [3]	36.0	153.9	<0.0001	38.0	<0.0001	-18.8	<0.0001
	[4]							
	[5] [6] 35/1	37.1		<0.0001			-21.7	<0.0001
	[7] 34/2 [8] 25/8	35.6 35.1	154.1 123.7	<0.0001 <0.0001	38.5 26.0	<0.0001 <0.0001		

Table 5.1. Lifespan data for treatments involving daf-16(0). N2: wild-type, [C]: combined (pooled) data from all displayed trials, [n]: trial number, carb.: carbenicillin. Blank cells in the last two columns for Trials 7 and 8: comparisons that were not made, due to control and test cohort experiments being conducted at different times. Trial 8 was performed together with Zibo Gong.

Consistent with a continuum of DAF-16 effects (where increased DAF-16 function by daf-2(rf) decreases  $\beta$ ), daf-16(0) increased  $\beta$  relative to N2, at all temperatures and with and without carbenicillin (Figure 5.2a). Meanwhile,  $\alpha$  was decreased by daf-16 on proliferating bacteria but unchanged on carbenicillin-treated bacteria. Notably, there was a triangularising Strehler-Mildvan correlation between N2 and daf-16 on proliferating bacteria, where life-extension (from daf-16 to N2) involved a simultaneous increase in  $\alpha$  and decrease in  $\beta$ . In section 4.5, I showed that triangularising S-M correlations emerge when lifespan increases in a highly inter-individually variable manner (more so than in  $\beta$  reduction alone), with greater increases in longer-lived population members (Figure 4.9d, p. 101). Indeed, the survival curves of N2 and daf-16 have closely overlapping shoulders and diverge only at later ages, and even with earlier N2 mortality onset in one case (at 20°C, producing intersecting curves) (Figure 5.1a, left boxes).

Meanwhile, lower temperature decreased  $\alpha$  only on proliferating E. coli, but decreased  $\beta$  in all cases (but most strongly on non-proliferative bacteria) (Figure 5.2b), in line with temperature effects in N2 and daf-2(rf) mutants (Figure 4.3a, p. 91). Similarly, as in the other genotypes (Figure 4.3b), carbenicillin decreased  $\alpha$  at higher temperatures (25°C), but  $\beta$  at lower temperatures (20°C and 15°C) (Figure 5.2c). Thus, effects of daf-16 and a daf-16 background on the Gompertz parameters are highly consistent with my findings in the earlier chapters.



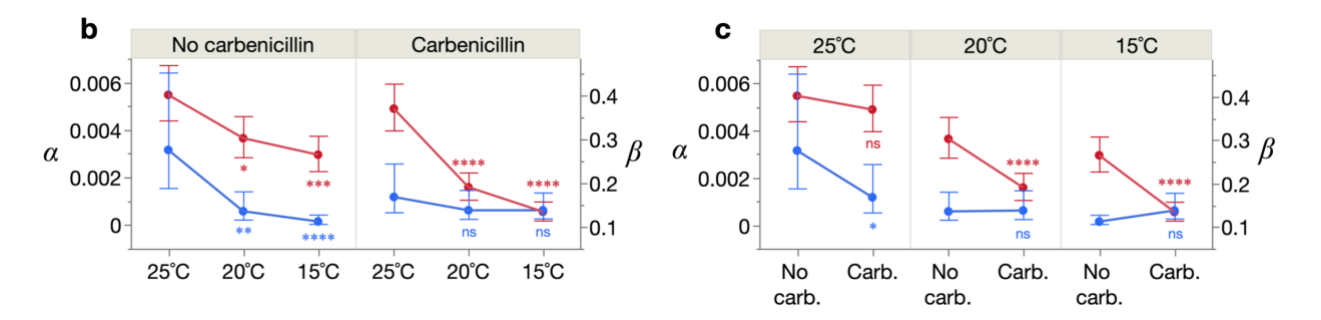


Figure 5.2. Effects of daf-16(0) and daf-16(0) background on the Gompertz parameters. Effects of (a) daf-16(mgDf50) and daf-2(rf), and (b) reduced temperature and (c) carbenicillin in daf-16(mgDf50) populations, on  $\alpha$  and  $\beta$ . Error bars: 95% confidence intervals. In a, the statistical significance symbols describe the comparison of daf-16(mgDf50) with N2 (wild-type); statistical significance symbols are not included for comparisons of N2 with daf-2(rf) mutants, which can be found in Figure 4.3c (p. 91). Gompertz parameters from the pool of Trials 3–6 for all cohorts except N2 at 20°C without carbenicillin (Trials 3–8) and all daf-16 cohorts (Trials 6–8); see Table 5.1.

Do these Gompertz parameter changes also arise from the healthspan and gerospan dynamics demonstrated in Chapters 3 and 4? That is, does  $\alpha$  reduction reflect healthspan expansion, and  $\beta$  reduction inter-individually variable gerospan expansion (i.e. ETL)? To evaluate this, I again examined how absolute healthspan and gerospan change in response to these lifespan-altering treatments, for all individuals across the population, ordered by survival proportion (i.e. in order of increasing lifespan).

A prediction, based on the findings of Chapter 3, would be that the increased  $\beta$  of daf-16 arises predominantly from compression of gerospan (G-span), specifically with greater compression in longer-lived individuals (i.e. ETL in the reverse, life-shortening direction). Unexpectedly, however, it was healthspan (H-span) that was compressed in this manner (Figure 5.3a, upper boxes). At all temperatures in the absence of carbenicillin, and  $25^{\circ}$ C on carbenicillin, daf-16 G-span was virtually identical to that of N2. The H-span compression thus increased relative G-span (G-span<sup>rel</sup>) of daf-16 animals, particularly in longer-lived individuals (Figure 5.3a, lower boxes). Importantly, this effect on G-span<sup>rel</sup> does *not* reflect ETL because it involves a variable change in H-span rather than G-span, and in the life-shortening direction. At  $20^{\circ}$ C and  $15^{\circ}$ C on carbenicillin, daf-16 G-span was compressed more in longer-lived individuals; however, this compression co-occurred with a proportional compression of H-span (also primarily in longer-lived individuals), resulting in an unaltered G-span<sup>rel</sup> across the population (Figure 5.3a). Thus,  $\beta$  (and  $\alpha$ ) differences between N2 and daf-16 appear to arise more from changes in H-span than G-span, presenting an exception to the G-span-driven (i.e. ETL-mediated)  $\beta$  changes described in Chapter 3.

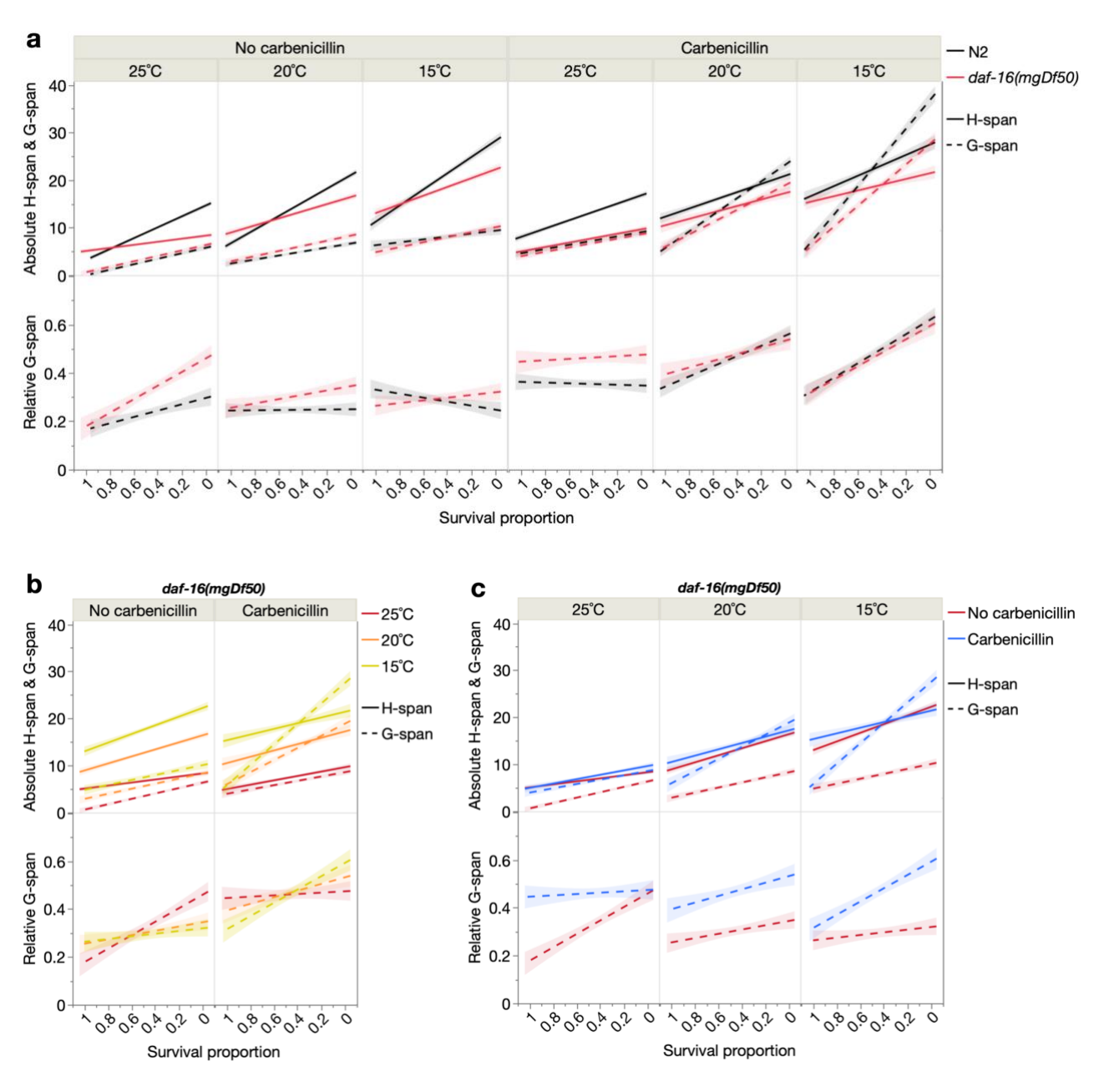


Figure 5.3. Effects of daf-16(0) and daf-16(0) background on locomotory healthspan and gerospan. Effects of (a) daf-16(mgDf50), and (b) reduced temperature and (c) carbenicillin in daf-16(mgDf50) animals, on absolute healthspan and gerospan (upper panels) and relative gerospan (lower panels), plotted over survival proportion (i.e. x-axis left: shorter-lived individuals, x-axis right: longer-lived individuals). All panels show least-squares linear regressions with 95% confidence regions shaded. Data from pool of Trials 3–6 for all cohorts except for N2 at 20°C without carbenicillin (Trials 3–8) and all daf-16 cohorts (Trials 6–8); see Table 5.1.

Why might  $\beta$  changes by daf-2(rf) arise from G-span changes and by daf-16(0) from H-span changes, when both modulate effects of IIS downstream of daf-16? A possibility is that daf-2, being upstream of daf-16, might have additional, daf-16-independent effects upon H-span and G-span. More tentatively, daf-16 may also regulate distinct ageing processes and pathologies at different ages, such that  $\beta$  reduction between the shorter-lived daf-16(mgDf50) and N2 may differ fundamentally to  $\beta$  reduction between N2 and the longer-lived daf-2 mutants.

This would be consistent with the "onion model" of ageing, which posits that effects on latelife mortality of some pathologies can mask those of others (Gems, 2022). Interestingly, in line with this hypothesis, daf-16 mutation caused coupled compression of H-span and G-span (versus N2) under the two longest-lived culture conditions (20°C and 15°C, on carbenicillin) (Figure 5.3a). This marks a potential transition to greater contribution of G-span to  $\beta$  at these later ages. Indeed, ETL (greater variable expansion of G-span than of H-span) was more common in the longest-lived daf-2(rf) mutant (Figure 3.7d–f, p. 55).

Notably, however, amongst the three longevity intervention classes explored in Chapter 3 (reduced temperature, antibiotics and daf-2(rf)), daf-2(rf) overall still exhibited fewer instances of ETL, with reductions in  $\beta$  also arising from H-span (alongside G-span) expansions in longer-lived individuals (Figure 3.7d–f). (Although most daf-2(rf) treatments still exhibited ETL.) Thus, IIS-related interventions may be unique in modulating  $\beta$  through more coupled changes in healthspan and gerospan.

I similarly examined the determinants of  $\alpha$  and  $\beta$  in daf-16(0) populations given reduced temperature. On proliferating bacteria, reducing temperature to 20°C and 15°C increased H-span with a mild bias in longer-lived individuals, while G-span increased more weakly and equally in all individuals (leading to a parallel upward shift of the G-span regression line) (Figure 5.3b). Therefore, here H-span expansion is again primarily responsible for reducing both  $\alpha$  and  $\beta$ . In contrast, on carbenicillin, reducing temperature increased H-span equally in all individuals, while G-span increased markedly more in longer-lived individuals, therefore extending the survival curve tail; here, reduction of  $\beta$  results from ETL as expected.

Finally, carbenicillin had little effect on H-span at all three temperatures, while increasing G-span in a temperature-dependent manner (Figure 5.3c). At 20°C and 15°C, G-span increased strongly in longer-lived individuals, as observed in N2 and daf-2 (Figure 3.7b–c, p. 55), corroborating my earlier demonstration that carbenicillin decreases  $\beta$  through ETL. At 25°C, G-span increased equally in all individuals, as also observed in N2 and daf-2 (Figure 4.6b, p. 94). However, this differed in not being coupled to an extension of H-span in shorter-lived individuals, with the implication that here,  $\alpha$  reduction arises from expansion of G-span rather than H-span.

In summary, effects of daf-16(0) and daf-2(rf) on biogerodemography differ, despite both involving daf-16, in that  $\beta$  is more a function of healthspan variation in the former and more of gerospan variation in the latter; the reason for this difference remains uncertain. By contrast, the biogerodemography of temperature and antibiotic treatments was largely daf-16-independent, and mostly concurred with my findings in N2 and daf-2(rf) backgrounds:  $\alpha$ : healthspan length;  $\beta$ : gerospan variation.

To try to understand the overall pattern beyond these specific treatments, I examined the relationship between the Gompertz parameters and H-span/G-span measures for all possible pairwise comparisons between the 12 relevant cohorts (N2 and daf-16, at three temperatures,  $\pm$  carbenicillin). As expected, changes in  $\alpha$  were better predicted by changes in H-span than G-span (Figure 5.4a), and notably, consistent with my findings in Chapter 3, changes in  $\beta$  were better predicted by changes in G-span variation than H-span variation (Figure 5.4b). However, this fit of  $\beta$  against G-span variation was only moderately superior (R<sup>2</sup>=0.68, vs 0.60 against H-span variation), and the regression slope was steeper for H-span than G-span, suggesting that H-span has greater effects on  $\beta$  per unit change in lifespan standard deviation. This shows that across these cohorts, overall, it is indeed variation in both H-span and G-span that contribute to  $\beta$ .

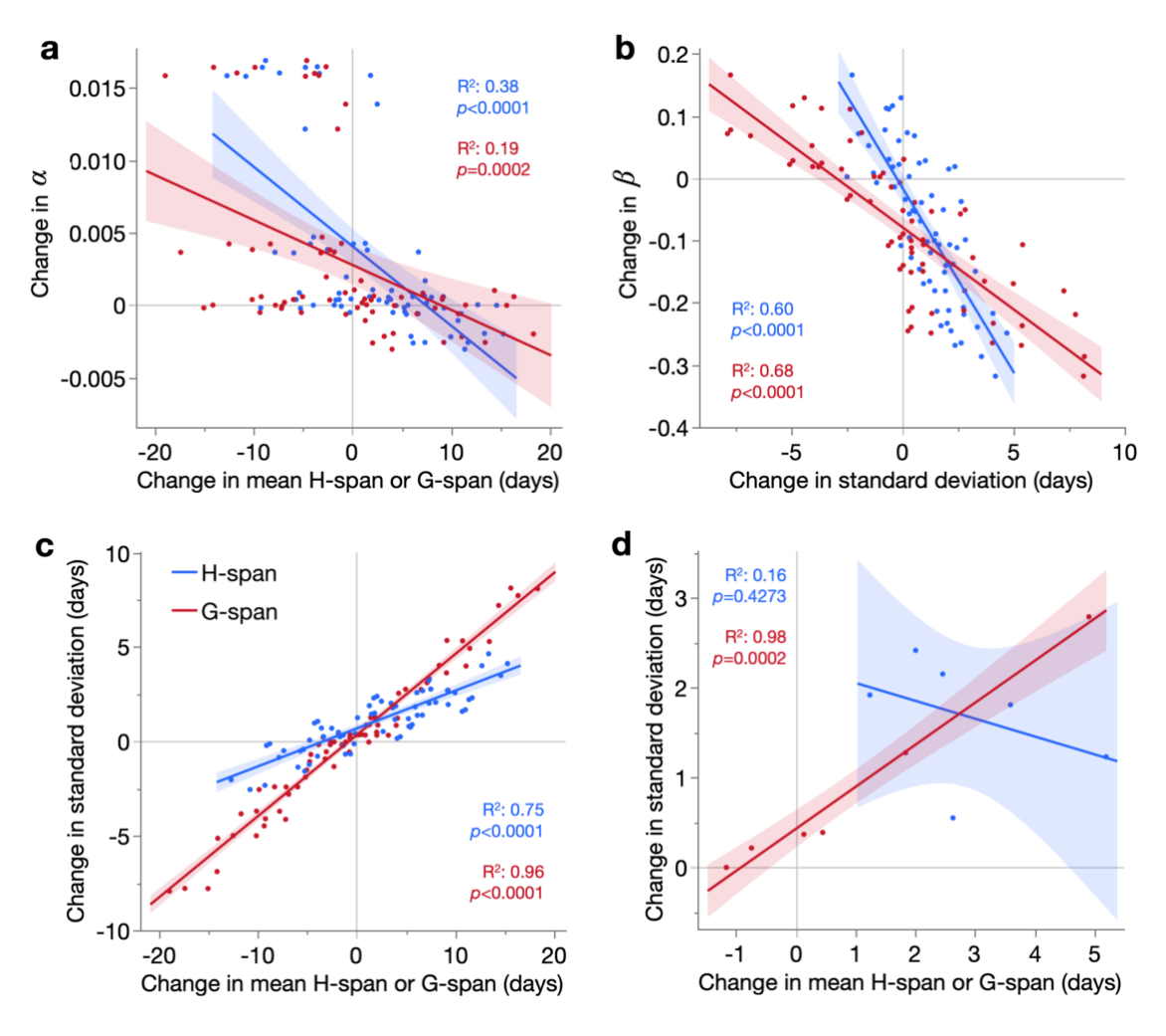


Figure 5.4. daf-16(0) and daf-16(0) background control  $\alpha$  through healthspan, and  $\beta$  through healthspan and gerospan variation. (a) Effect of changes in mean H-span and G-span on changes in  $\alpha$ . (b) Effect of changes in standard deviation of H-span and G-span on changes in  $\beta$ . (c-d) Effect of changes in mean H-span and G-span on respective changes in standard deviation of H-span and G-span, for (c) all pairwise treatments (see next) or (d) only the 6 daf-16 treatments (versus N2, at 3 temperatures and  $\pm$  antibiotic). In  $\mathbf{a}$ - $\mathbf{c}$ , the relationship is assessed as a linear regression of changes between all

possible pairwise comparisons (n=66) of the 12 cohorts (N2 and daf-16, each at 3 temperatures and  $\pm$  antibiotic). 95% confidence regions are shaded and regression F-test p-values labelled.

To better dissect their relative contribution, I examined the respective relationships between "span-length" and variation, for H-span and G-span (Figure 5.4c). Remarkably, changes in mean G-span correlated very strongly (and with a steeper slope) with changes in G-span variation ( $R^2$ =0.96), compared to a weaker (but still strong) correlation between changes in mean H-span and H-span variation ( $R^2$ =0.75). This shows that across these cohorts, life-extension results primarily from increases in G-span variation, supporting the  $\beta$  as gerospan variation (ETL) hypothesis.

Yet the data in Figure 5.3a imply that between the daf-16 and N2 cohorts, increases in H-span (rather than G-span) variation are responsible for reductions in  $\beta$ , in an apparent exception to the rule. One interpretation is that these daf-16 treatments are unique cases where H-span is indeed a stronger mediator of  $\beta$ . To verify this, I reassessed these daf-16 treatments using the more quantitative approach of examining the respective relationships between 'spanlength' and variation, for H-span and G-span, for only these 6 treatments (effect of daf-16 against N2, at three temperatures,  $\pm$  carbenicillin) (Figure 5.4d). Surprisingly, even across only these 6 treatments, changes in G-span variation remained an excellent predictor of changes in mean G-span (R<sup>2</sup>=0.98), in contrast to H-span, which did not exhibit a significant relationship between its mean and variation. Thus, within many of these daf-16 treatments (4/6: all three temperatures without carbenicillin and 25°C with carbenicillin; Figure 5.3) H-span is the primary determinant of  $\beta$ , but between all 6 daf-16 treatments, G-span is in fact the more consistent determinant.

In summary, these daf-16 and daf-16 background treatments provide further evidence of  $\alpha$  as corresponding to healthspan duration and for the most part,  $\beta$  as gerospan variation. Regarding the latter, a complex picture has emerged: daf-16(0) differs from other interventions examined (lower temperature, antibiotic and daf-2(rf)) in that  $\beta$  reflects mainly healthspan rather than gerospan variation. This shows that  $\beta$  reduction need not always result from G-span expansion alone. Importantly, however, at the same time, gerospan variation also does contribute to  $\beta$  across these daf-16(0) treatments, and in fact with a stronger (more consistent) relationship. Thus, healthspan variation can determine  $\beta$  within treatments, but across treatments, gerospan variation remains the greater determinant. Therefore, variable G-span expansion does contribute (in part) to  $\beta$  in these daf-16(0) treatments.

The above hints at an intriguing, potential property of the fundamental relationship between H-span and G-span, which is that while they can change independently of each other in magnitude, their internal, relative variability remains fixed across populations, with G-span being more variable than H-span. This could indicate the presence of an intrinsic property of populations (presumably, some biological mechanism) that ensures a tight scaling between gerospan length and its inter-individual variation, which is maintained across different interventions.

## 5.2 – Effects of age-specific IIS reduction on Gompertzian biogerodemography

Thus far, I have investigated the biological basis of the Gompertz parameters using different interventions (temperature reduction, antibiotics and IIS modulation). Another strategy is to apply one intervention in different ways, to obtain a more in-depth view of biogerodemographic dynamics for that particular intervention, and general principles governing the Gompertz parameters. In the remainder of this chapter, I will attempt to use this approach to investigate insulin/IGF-1 signalling (IIS) in greater detail.

A useful approach for this aim is DAF-2 auxin-inducible degradation (DAF-2 AID), which allows age-specific reduction of IIS (Venz et al., 2021, Roy et al., 2022, Zhang et al., 2022, Molière et al., 2024). In brief, exposure to auxin of *C. elegans* of the strain RAF2181 (expressing degron-tagged DAF-2) induces proteasomal degradation of DAF-2 protein, thus reducing IIS. By administering auxin from different ages, one can explore age-specific effects of IIS on ageing and lifespan. In addition, by tracking animals individually, one can observe inter-individual variation in these age-patterns, thus permitting biogerodemographic analyses of the type developed in this thesis. In this section, I will use this approach to examine how the chronological age-pattern of inter-individual variation in biological age can influence the Gompertz parameters that result from age-specific commencement of IIS reduction. Before beginning this investigation (on p. 123), I will first introduce and contextualise the data, which will then be examined in the rest of the chapter.

To begin with, I compared effects on lifespan of DAF-2 AID and genetic IIS reduction. Administration of auxin (in RAF2181 animals) from L4 stage increased lifespan even more than the strong *daf-2(rf)* alleles, *daf-2(e1368)* and *daf-2(e1370)*, compared to the DMSO-treated RAF2181 control (auxin is administered dissolved in DMSO) (Figure 5.5a, Table 5.2, p. 118). This is in line with previous reports (Venz et al., 2021, Zhang et al., 2022) and the presumably weaker reduction of IIS in these reduction-of-function *daf-2* mutants (Gems et al., 1998).

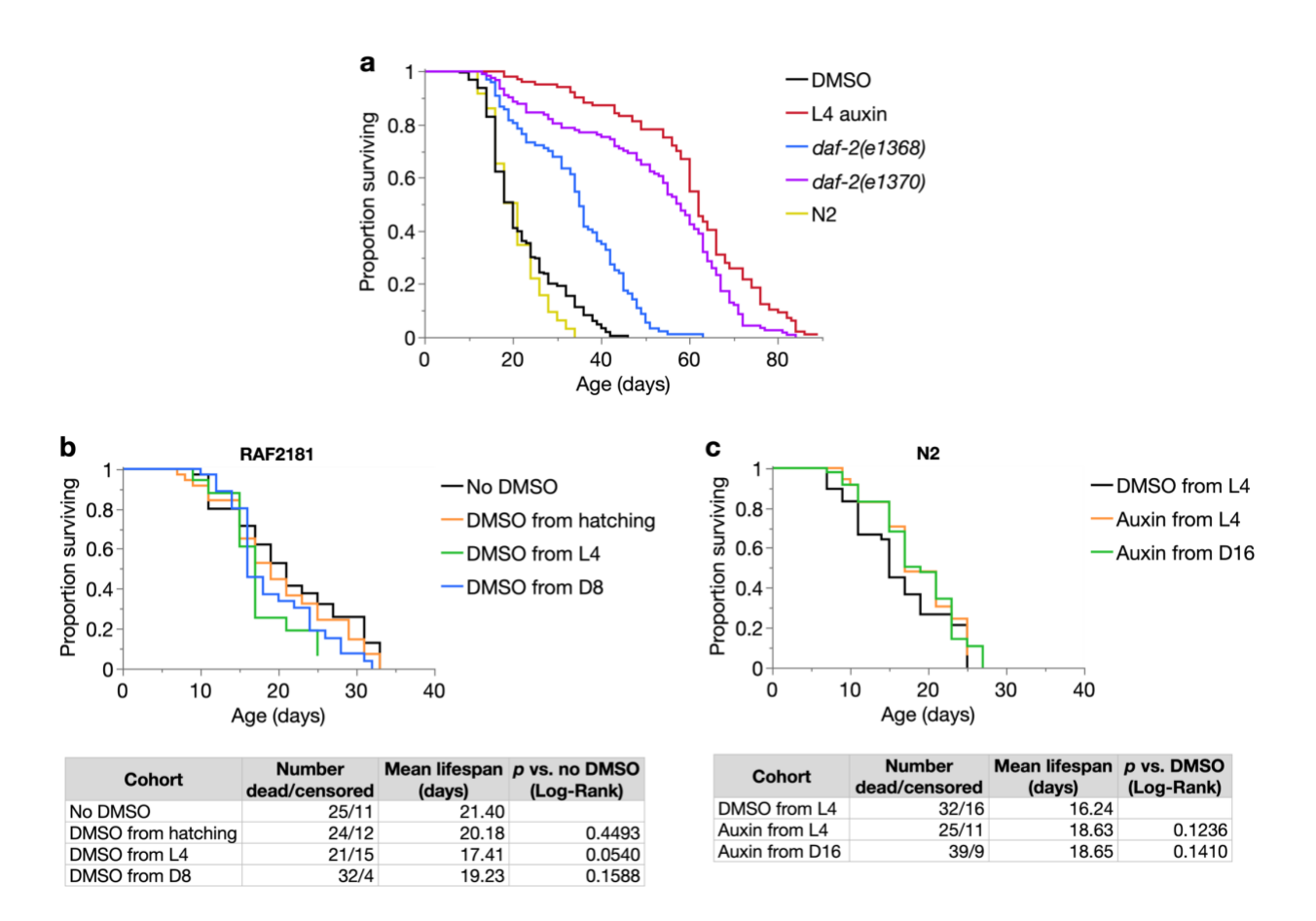
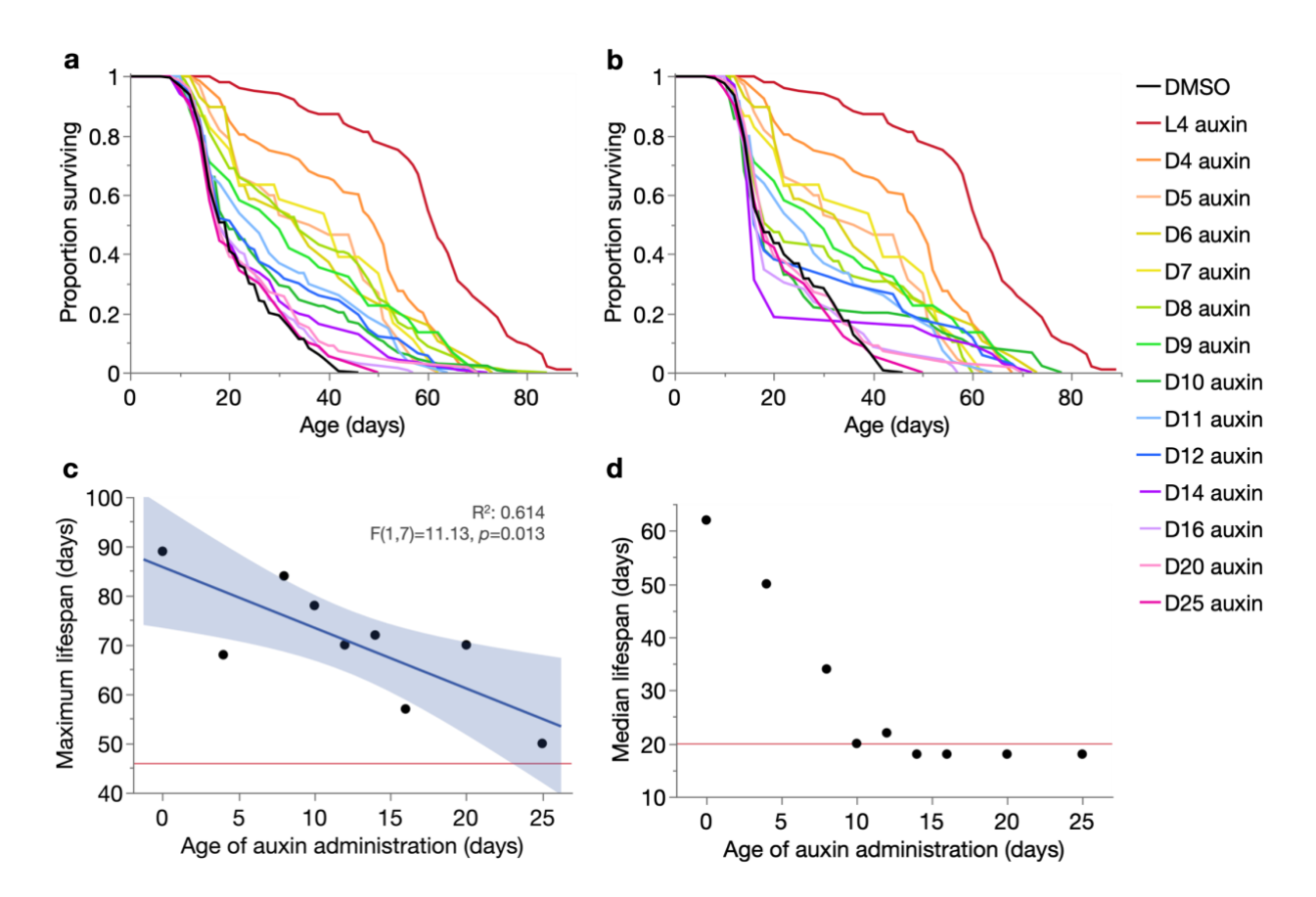


Figure 5.5. Auxin-inducible degradation of DAF-2 extends lifespan. (a) Kaplan-Meier survival curves of RAF2181 treated from L4 with 0.25% DMSO or 1mM auxin dissolved in DMSO (final concentrations in plate), and *daf-2(rf)* mutants and N2 without DMSO or auxin. These data are from the pool of Trials 1–6 (see Table 5.2); the DMSO cohort includes one trial performed with Reva Biju, one trial by Kuei Ching Hsiung, and one trial between Kuei Ching Hsiung and Xiaoya Wei. (b) Kaplan-Meier survival curves of RAF2181 animals without DMSO or with DMSO starting from different ages (continuing until death). (c) Kaplan-Meier survival curves of N2 animals treated with DMSO or 1mM auxin dissolved in DMSO, starting from different ages (continuing until death). The data in b and c were collected with Reva Biju; further trials to increase sample size would be helpful, although any statistically significant emergent effects of DMSO, or auxin on N2 lifespan, would likely be minor in magnitude compared to DAF-2 AID effects on RAF2181 lifespan.

Lifespans of the DMSO-treated RAF2181 control and N2 (without DMSO) did not differ (log-rank p=0.219), although a longer survival curve tail was observed in the former. Importantly, DMSO and auxin themselves were not observed to have notable effects on lifespan, whether administered early or late in adulthood, although a small, statistically non-significant life-extending effect of auxin was observed (Figure 5.5b–c), in line with other reports (Loose and Ghazi, 2021, Venz et al., 2021). This confirms that DAF-2 AID is a suitable system for investigating age-specific effects of IIS on ageing and lifespan.

I next assessed the effect of initiating DAF-2 AID from different ages. Unsurprisingly, auxin administration starting from later than L4 yielded progressively smaller increases in mean lifespan (Figure 5.6a, Table 5.2), consistent with previous reports (Venz et al., 2021). These

increases were no longer statistically significant (log-rank p>0.05) when auxin was started from day 16 or later (Table 5.2). Extension of maximum lifespan was also reduced in magnitude with later auxin commencement (Figure 5.6c). Nonetheless, these results recapitulated the earlier, remarkable observation (Venz et al., 2021) that auxin treatment even very late in life, when many individuals have already died, can markedly extend lifespan (see e.g. D20 auxin, Figure 5.6a, b).



**Figure 5.6.** Effect of age-specific DAF-2 AID on lifespan. Kaplan-Meier survival curves for (a) the pool of all trials (Trials 1–6) and (b) the pool of those trials in which locomotory ageing was scored (Trials 1–4) by the ABC system (see Methods). Note that most cohorts have fewer total trials than 6 or 4 ("Trials 1–6" and "Trials 1–4" refer to trial names rather than numbers; see Table 5.2 for details). (c–d) Effect of age of commencement of auxin administration on (c) maximum and (d) median lifespan (from pool of Trials 1–6), for cohorts with at least 60 individuals. The horizontal red lines (y-axis=46 in c and 20 in d) denote the maximum and median lifespans of the DMSO control, respectively.

These lifespan data are presented in Figure 5.6 in two ways, as the pool of all available trials (Figure 5.6a) or pool of only those trials in which locomotory healthspan and gerospan were scored (Figure 5.6b) (see Table 5.2 for trial details). There is a close correspondence between the two pools for most cohorts, especially in the overall change in survival curve shape with the age of auxin commencement. The latter pool (only trials scoring locomotory health) will be used in subsequent analyses where information about individual ageing is required.

Where direct comparison to individual ageing is not required, the former pooling arrangement (all available trials) with greater sample sizes will be used.

I preface the following analyses with the caveat that some cohorts are comprised of single trials and/or low (pooled) sample sizes (see Table 5.2). However, these data nonetheless appear highly consistent amongst themselves, with a clear continuum of effects on them by age of DAF-2 AID commencement (e.g. Figure 5.6, and as I will demonstrate for other traits); further trials seem unlikely to change these overall patterns. Additionally, these analyses focus on effects of DAF-2 AID timing between multiple rather than specific cohorts; my wide coverage of cohorts at many, closely-timed treatment starting ages therefore helps to reveal overall patterns amidst cohort-specific noise. Thus, those with smaller sample sizes/trial numbers were included out of opportunity rather than necessity, given that those data were available and readily consistent with each other.

					Lifes	span		α	<i>I</i>	3
Cohort	No. dead/ censors	Mean lifespan (days since L4)	а	β	% change vs. DMSO	p vs. DMSO (Log-Rank)	% change vs. DMSO	p vs. DMSO (LRT)	% change vs. DMSO	p vs. DMSO (LRT)
RAF2181 + DMSO	[1-6] 247/11 [1-4] 162/11	23.0	0.010 0.010	0.091 0.082						
	[1] 65/0 [2] 36/0	23.6 22.3								
	[3] 36/0	21.4 23.9								
	[4] 25/11 [5] 20/0	21.3								
RAF2181 + L4 auxin	[6] 65/0 <b>[1-6] 97/22</b>	19.9 <b>60.5</b>	0.0005	0.075	174.8	<0.0001	<del>-</del> 95.2	6.87E-18	-17.3	0.0687
NAFZ161 + L4 duxiii	[1-4] 97/22	60.5	0.0005	0.075	162.7	<0.0001				0.4504
	[1] 47/0	60.0			153.8	<0.0001				
	[2] 24/12	63.6			185.4	<0.0001				
	[3] 26/10 [4]	58.8			175.1	<0.0001				
	[5]									
	[6]									
RAF2181 + D4 auxin	[1-6] 120/16		0.002	0.071	102.6	<0.0001	-81.2	1.27E-08	-21.5	0.0237
	[1-4] 120/16		0.002	0.071	93.7	<0.0001		1.06E <b>-</b> 07	-13.3	0.2478
	[1] 64/0	43.1			82.5	<0.0001 <0.0001				
	[2] 32/4 [3]	47.6			113.6	<0.0001				
	[4] 24/12	43.8			83.5	<0.0001				
	[5]									
	[6]									
RAF2181 + D5 auxin	[1-6] 28/8	36.6	0.004 0.004	0.063 0.063	66.3	<0.0001 <0.0001				0.0555 0.1999
	[1-4] 28/8 [1]	36.6	0.004	0.063	59.0	<0.0001	-56.6	0.0826	-23.2	0.1999
	[2]									
	[3]									
	[4] 28/8	36.6			53.3	0.0013				
	[5] [6]									
RAF2181 + D6 auxin	[1-6] 22/14	37.3	0.007	0.044	69.3	<0.0001	-28.7	0.4332	-51.0	0.0001
TWI 2101 · Bo daxiii	[1-4] 22/14	37.3	0.007	0.044	61.9	<0.0001				0.0030
	[1]									
	[2]									
	[3] [4] 22/14	37.3			56.1	0.007				
	[4] 22/14 [5]	37.3			56.1	0.007				
	[6]									
RAF2181 + D7 auxin	[1-6] 22/14	37.7	0.005	0.057	71.1	<0.0001	-50.8	0.1439	-37.0	0.0218
	[1-4] 22/14	37.7	0.005	0.057	63.6	<0.0001	<del>-</del> 51.8	0.1424	-30.5	0.0963
	[1]									
	[2] [3]									
	[4] 22/14	37.7			57.8	0.0037				
	[5]									
	[6]									
RAF2181 + D8 auxin	[1-6] 161/12 [1-4] 60/12	36.5 30.3	0.008 0.013	0.043 0.036	65.9					5.11E-11 1.04E-05
	[1]	30.3	0.013	0.036	31.8	<0.0001	33.0	0.3515	-56.3	1.04E-05
	[2] 34/2	29.8			33.9	0.007				
	[3]									
	[4] 26/10	31.0			29.8					
	[5] 43/0 [6] 58/0	44.9 37.1			111.4 86.8	<0.0001 <0.0001				
	[1-6] 29/7	34.2	0.012	0.033	55.5			0.6693	-63.9	1.10E-06
NAF2101 + D9 duxiii	[1-4] 29/7	34.2	0.012	0.033	48.7	<0.0001				0.0001
	[1]									
	[2]									
	[3] [4] 29/7	34.2			43.4	0.0721				
	[4] 29/7 [5]	34.2			40.4	0.0721				
	[6]									
RAF2181 + D10 auxin	[1-6] 145/10		0.018	0.032	24.5					
	[1-4]60/10	26.9	0.025	0.018	17.1	0.1441	148.7	0.0009	-78.1	4.84E-12
	[1] [2] 34/0	25.6			15.1	0.3881				
	[3]	23.0			10.1	0.5001				
	[4] 26/10	26.7			11.9	0.8406				
	[5] 19/0	31.7			49.1					
	[6] 66/0	27.4			37.9	<0.0001	<u> </u>			11

RAF2181 + D11 auxin	[1-6]30/6	30.2	0.011	0.044	37.1	<0.0001	15.2	0.7175	-51.5	0.0002
	[1-4]30/6	30.2	0.011	0.044	31.1	0.0008	12.9	0.7643	-46.4	0.0034
	[1]									
	[2]									
	[3]									
	[4] 30/6	30.2			26.4	0.217				
	[5]									
D. F. C.	[6]		0.045	0.000			55.0	0.0540		
RAF2181 + D12 auxin	[1-6] 123/2	28.5	0.015	0.036	29.6	<0.0001	55.0	0.0513	-60.5	2.03E-12
	[1-4] 34/2	29.3	0.017	0.026	27.4	0.0017	74.7	0.1326	<del>-</del> 67.7	9.69E <b>-</b> 07
	[1] [2] 34/2	20.2			21.0	0.0179				
	[3]	29.3			31.6	0.0179				
	[4]									
	[5] 20/0	38.7			82.1	<0.0001				
	[6] 69/0	25.2			26.6	0.0035				
RAF2181 + D14 auxin	[1-6] 116/4	25.2	0.019	0.036	14.7	0.004	92.3	0.0029	-60.3	3.56E-12
TAI 2101 · D14 duxiii	[1-4]32/4	24.1	0.027	0.018	4.9	0.295	172.5	0.0023	-78.3	5.65E-09
	[1]	24.1	0.027	0.010	4.5	0.233	172.5	0.0040	-70.5	J.03L-03
	[2] 32/4	24.1			8.3	0.2909				
	[3]	2			0.0	0.2000				
	[4]									
	[5] 16/0	34.9			64.1	<0.0001				
	[6] 68/0	23.4			17.9	0.0097				
RAF2181 + D16 auxin	[1-6] 130/2	23.0	0.015	0.059	4.5	0.2645	53.1	0.0548	-34.7	0.0002
	[1-4] 46/2	22.9	0.019	0.043	-0.4	0.6012	95.7	0.0396	-47.7	0.0008
	[1]									
	[2] 46/2	22.9			2.9	0.6111				
	[3]									
	[4]									
	[5] 23/0	22.5			6.0	0.2385				
	[6] 61/0	23.2			16.8	0.0049				
RAF2181 + D20 auxin	[1-6] 67/5	24.8	0.019	0.038	12.5	0.055	95.7	0.0087	-58.3	1.59E <b>-</b> 09
	[1-4] 67/5	24.8	0.019	0.038	7.6	0.2332	91.8	0.0178	-54.0	4.62E-06
	[1]									
	[2] 67/5	24.8			11.2	0.3187				
	[3]									
	[4]									
	[5]									
DATO404 - DOEi-	[6]	20.5	0.010	0.070	0.4	0.4470	00.0	0.0045	00.4	0.0400
RAF2181 + D25 auxin	[1-6] 90/5	22.5	0.013	0.070	2.1	0.4172	32.2	0.2845	-23.1	0.0406
	[1-4] 90/5	22.5	0.013	0.070	-2.4	0.9712	29.5	0.3571	-15.1	0.2604
	[1] [2] 90/5	22.5			0.8	0.9122				
	[3]	22.5			0.0	0.9122				
	[4]									
	[5]									
	[6]									
daf-2(e1368)	[1-6]93/20	34.3	0.003	0.087	55.8	<0.0001	-71.1	4.38E-05	-4.0	0.7168
	[1-4]93/20	34.3	0.003	0.087	48.9	<0.0001	-71.7	0.0001	6.1	0.6381
	[1]43/0	32.7			38.3	<0.0001				
	[2] 24/12	33.8			51.9	0.0005				
	[3] 26/8	37.5			75.5	<0.0001				
	[4]									
	[5]									
	[6]									
daf-2(e1370)	[1-6] 117/7	52.0	0.001	0.066	136.1	<0.0001	-86.8	4.02E-11	-27.3	0.0027
	[1-4] 117/7	52.0	0.001	0.066	125.8	<0.0001	-87.0	6.90E <b>-</b> 10	-19.7	0.0755
	[1] 54/0	49.7			110.2	<0.0001				
	[2] 33/1	48.8			119.0	<0.0001				
	[3] 30/6	58.8			174.9	<0.0001				
	[4]			1						
	[5]			1						
	[6]									
N2	[1-6] 33/3	20.6	0.010	0.093	-6.6	0.2189	7.5	0.8094	2.5	0.8588
	[1-4] 33/3	20.6	0.010	0.093	-10.7	0.0728	5.3	0.8711	13.2	0.4171
	[1]			1						
	[2]			1						
	[3] 33/3	20.6		1	-3.9	0.4619				
	[4]			1						
	[5]			1						
	[6]		J	J	1					

**Table 5.2. Lifespan and Gompertz parameters of all cohorts.** N2: wild-type, + Dn auxin: auxin given from day n of adulthood (n days since L4) until death, [1-6]: pool of Trials 1–6, [1-4]: pool of Trials 1–4 in which locomotory function (ABC system) was scored, [n]: trial number. Trial 4 was performed together with Reva Biju, Trial 5 by Kuei Ching Hsiung and Xiaoya Wei, and Trial 6 by Kuei Ching Hsiung. Note that most cohorts have fewer total trials than 6 or 4 ("Trials 1-6" and "Trials 1-4" refer to trial names rather than numbers). LRT: likelihood ratio test, used to assess statistical significance of differences between Gompertz parameters. Gompertz parameters and associated LRTs were performed for pooled data rather than individual trials, given larger sample sizes of the former.

For later auxin treatment cohorts, a proportion of the population will have already died before treatment. Thus, including these untreated individuals in the survival analysis is likely to underestimate DAF-2 AID effects on lifespan extension. Indeed, excluding pre-auxin treatment deaths from the analysis almost doubled the magnitude of later auxin treatments, increasing mean lifespan by 8.3%, 23.7% and 3.6% (auxin from day 16, 20, and 25; p=0.059, 0.002, 0.217, respectively) (Table 5.3), compared to 4.5%, 12.5% and 2.1% (p=0.265, 0.055, 0.417, respectively) when pre-treatment deaths were included (Table 5.2).

A further consideration is that individuals alive at the time of auxin treatment will differ in biological age and thus, potentially, in their responses to DAF-2 AID. Consequently, without longitudinal data on individual ageing, one cannot assess how much of a given effect on lifespan is attributable to true age-specific responses to IIS reduction, and how much to population heterogeneity in this response due to differences in biological age. Such confounding effects of heterogeneity are especially clear on median lifespan, which is increased only by auxin administration from before day 10 (Figure 5.6d), despite clear increases in mean and maximum lifespan in later treatments (Figure 5.6c, Table 5.2). Therefore, the distribution of interindividual variation in biological age at the time of DAF-2 AID commencement is a key determinant of resultant population survival.

	DMSO-treat	ed (control)	Auxin	-treated			
Transfer out day	No. dead/	Mean lifespan	No. dead/	Mean lifespan	% change vs.	p vs. DMSO	
Treatment day	censors	(days since L4)	censors	(days since L4)	DMSO	(Log-Rank)	
0 (L4)	[1-6] 247/11		[1-6] 97/22	60.5	174.8	<0.0001	
	[1-4] 162/11		[1-4] 97/22	60.5	162.7	<0.0001	
	[1] 65/0		[1] 47/0	60.0	153.8	<0.0001	
	[2] 36/0		[2] 24/12	63.6	185.4	< 0.0001	
	[3] 36/0		[3] 26/10	58.8	175.1	<0.0001	
	[4] 25/11	23.9					
	[5] 20/0	21.3					
	[6] 65/0	19.9					
4	[1-6] 247/11		[1-6] 120/16	44.6	102.6	<0.0001	
	[1-4] 162/11	23.0	[1-4] 120/16	44.6	93.7	<0.0001	
	[1] 65/0	23.6	[1] 64/0	43.1	82.5	<0.0001	
	[2] 36/0	22.3	[2] 32/4	47.6	113.6	<0.0001	
	[3] 36/0	21.4	[3]				
	[4] 25/11	23.9	[4] 24/12	43.8	83.5	<0.0001	
	[5] 20/0	21.3	[5]				
	[6] 65/0	19.9	[6]				
5	[1-6] 247/11	22.0	[1-6] 28/8	36.6	66.3	<0.0001	
	[1-4] 162/11	23.0	[1-4] 28/8	36.6	59.0	<0.0001	
	[1] 65/0	23.6	[1]				
	[2] 36/0	22.3	[2]				
	[3] 36/0	21.4					
	[4] 25/11		[4] 28/8	36.6	53.3	0.0013	
	[5] 20/0	21.3					
	[6] 65/0	19.9					
6	[1-6] 247/11		[1-6] 22/14	37.3	69.3	<0.0001	
	[1-4] 162/11		[1-4] 22/14	37.3	61.9	<0.0001	
	[1] 65/0	23.6					
	[2] 36/0	22.3					
	[3] 36/0	21.4					
	[4] 25/11		[4] 22/14	37.3	56.1	0.007	
	[5] 20/0	21.3		37.0	55.12	5.557	
	[6] 65/0	19.9					
7	[1-6] 247/11		[1-6] 22/14	37.7	71.1	<0.0001	
	[1-4] 162/11		[1-4] 22/14	37.7	63.6	<0.0001	
	[1] 65/0	23.6					
	[2] 36/0	22.3					
	[3] 36/0	21.4					
	[4] 25/11		[4] 22/14	37.7	57.8	0.0037	
	[5] 20/0	21.3					
	[6] 65/0	19.9					
8	[1-6] 246/11		[1-6] 161/12	36.5	65.4	<0.0001	
	[1-4] 161/11		[1-4]60/12	30.3	31.3	<0.0001	
	[1] 64/0	23.9			52.0		
	[2] 36/0		[2] 34/2	29.8	33.9	0.007	
	[3] 36/0	21.4			33.0	2.207	
	[4] 25/11		[4] 26/10	31.0	29.8	0.2345	
	[5] 20/0		[5] 43/0	44.9	111.4	< 0.0001	
	[6] 65/0		[6] 58/0	37.1	86.8	<0.0001	
9	[1-6]246/11		[1-6] 29/7	34.2	55.1	<0.0001	
-	[1-4] 161/11		[1-4] 29/7	34.2	48.1	<0.0001	
	[1] 64/0	23.9		34.2	70.1	-0.0001	
	[2] 36/0	22.3					
	[3] 36/0	21.4					
	[4] 25/11		[4] 29/7	34.2	43.4	0.0721	
	[5] 20/0	21.3		34.2	45.4	0.0721	
	[6] 65/0	19.9					
	[0] 03/0	19.9	ردا				

10	[1-6] 239/11	22.4	[1-6] 141/10	27.9	24.4	<0.0001
	[1-4] 158/11	23.3	[1-4]60/10	26.9	15.5	0.2007
	[1] 63/0	24.1				
	[2] 34/0		[2] 34/0	25.6	11.5	0.5465
	[3] 36/0	21.4				
	[4] 25/11		[4] 26/10	26.7	11.9	0.8406
	[5] 20/0		[5] 19/0	31.7	49.1	0.0043
	[6] 61/0		[6] 62/0	28.5	39.0	< 0.0001
11	[1-6] 239/11		[1-6] 30/6	30.2	34.7	0.0001
	[1-4] 158/11		[1-4] 30/6	30.2	29.3	0.0011
	[1] 63/0	24.1				
	[2] 34/0	23.0				
	[3] 36/0	21.4				
	[4] 25/11		[4] 30/6	30.2	26.4	0.217
	[5] 20/0	21.3		30.2	20.4	0.217
	[6] 61/0	20.5				
12	[1-6] 231/11		[1-6] 115/0	29.7	30.7	<0.0001
1-2	[1-4] 151/11		[1-4] 33/0	29.8	25.2	0.0025
	[1] 61/0	24.5		25.5	20.2	0.0020
	[2] 32/0		[2] 33/0	29.8	25.9	0.0421
	[3] 34/0	21.9		25.0	23.3	0.0421
	[4] 24/11	24.2				
	[5] 20/0		[5] 20/0	38.7	82.1	<0.0001
	[6] 60/0			26.8	29.5	
14			[6] 62/0 [ <b>1-6] 91/0</b>	28.7	20.0	0.001 <b>0.0002</b>
14	[1-6] 203/10 [1-4] 126/10		[1-4] 24/0	28.7 27.6	7.7	
		25.6 25.6		27.6	/./	0.1447
	[1] 55/0		[2] 24/0	27.6	6.4	0.3259
	[2] 26/0	24.0		27.6	6.4	0.3239
	[3] 27/0	26.3				
	[4] 18/10			24.0	64.4	<0.0001
	[5] 20/0 [6] 57/0		[5] 16/0	34.9 27.2	64.1 29.5	<0.0001 <0.0001
16			[6] 51/0	28.7		
10	[1-6] 150/6		[1-6] 79/0	30.6	8.3 3.2	0.0594 0.2372
	[1-4] 86/6		[1-4] 24/0	30.6	3.2	0.2372
	[1] 41/0	28.9		20.0	7.0	0.8429
	[2] 15/0		[2] 24/0	30.6	-7.9	0.8429
	[3] 17/0	28.7				
	[4] 13/6	28.6		07.0	00.0	0.0040
	[5] 17/0		[5] 14/0	27.3	23.0	0.0043
	[6] 47/0		[6] 41/0	28.0	27.0	<0.0001
20	[1-6] 97/5		[1-6] 25/2	37.6	23.7	0.0022
	[1-4] 66/5		[1-4] 25/2	37.6	15.1	0.05
	[1] 33/0	31.4				
	[2] 13/0		[2] 25/2	37.6	6.3	0.775
	[3] 10/0	36.0				
	[4] 10/5	30.5				
	[5] 10/0	23.9				
	[6] 21/0	26.0				
25	[1-6] 69/3		[1-6]31/0	34.5	3.6	0.217
	[1-4] 55/3		[1-4] 31/0	34.5	-0.2	0.6349
	[1] 28/0	32.9				
	[2] 11/0		[2] 31/0	34.5	-8.9	0.4062
	[3] 10/0	36.0				
	[4] 6/3	33.4				
	[5] 3/0	27.0				
I	[6] 11/0	28.4	[6]			

**Table 5.3. Lifespan statistics for post-auxin treatment deaths only.** [1-6]: pool of Trials 1–6, [1-4]: pool of Trials 1–4 in which locomotory function (ABC system) was scored, [n]: trial number. Trial 4 was performed together with Reva Biju, Trial 5 by Kuei Ching Hsiung and Xiaoya Wei, and Trial 6 by Kuei Ching Hsiung. Individuals that died or became censored on or before treatment day (with auxin or DMSO) were excluded from these analyses, such that sample sizes decrease down the table (as treatment day gets later). This affects treatments from day 8 (statistics for the earlier treatments are the same as those in Table 5.2).

It is very likely that the distribution of inter-individual variation in biological age changes with chronological age. One might expect an increase in variation as individuals begin and progress through the ageing process, before it decreases again at more advanced ages as the population dwindles to a small residuum of similarly decrepit individuals. Such age changes offer a means to further explore the biological basis of mortality patterns, such as those captured by the Gompertz model. In Chapter 3, I showed that the  $\alpha$  parameter reflects the approximate age of mortality onset (i.e. ageing of the shortest-lived individuals), whereas the  $\beta$  parameter reflects the degree of inter-individual variation in not only lifespan but the life course preceding it. Here, I will use the different age-specific DAF-2 AID cohorts to further test these ideas.

Specifically, my working model is that early commencement of DAF-2 AID will affect a relatively homogeneous population (prior to the individually-variable ageing process), leading to homogeneous individual responses, thereby reducing  $\alpha$  but not  $\beta$  (i.e. extending lifespan without much change in its variation). In contrast, later commencement of DAF-2 AID will affect a progressively more heterogeneous (ageing) population, leading to more heterogeneous individual responses, thereby decreasing  $\beta$ . Then, very late commencement of DAF-2 AID will affect a population that has become once again more homogeneous (as explained earlier), leading to smaller reductions in  $\beta$ . In terms of  $\alpha$ , the increased variability of responses in later auxin cohorts should entail weaker life-extension in shorter-lived individuals, which presumably age faster and/or earlier. Consequently, the magnitude of  $\alpha$  reduction should be reduced (or  $\alpha$  even increased, in the case of triangularising S-M treatments) in later DAF-2 AID cohorts. This proposed model of effects of individual variation on demography is depicted in Figure 5.8a (right box, p. 125) as survival curves. Next, I will show how the model is in fact fully supported by the data.

As predicted,  $\alpha$  was strongly decreased by early auxin treatment from L4, whereas  $\beta$  was unchanged (Figure 5.7). The lack of change in  $\beta$  here is striking, given various earlier observations that mutation of daf-2 (and also age-1) reduce  $\beta$  (e.g. Johnson, 1990, Samuelson et al., 2007, Hughes and Hekimi, 2016, and in this thesis see Figure 3.5), which is also evident from the differences in curve shape in Figure 5.5a (p. 115). The different demography of these L4 DAF-2 AID populations may reflect greater reduction of IIS, the adult-limited effects, or both. Whatever the reason, DAF-2 AID from L4 potentially provides a less confounded view of the biogerodemography of IIS effects than that provided by IIS pathway mutants. Indeed, a striking implication of the  $\alpha$  reduction here, according to my findings in Chapters 3–4, is that IIS reduction slows the biological rate of ageing (revealed by this less confounded mode of IIS reduction). I will discuss these ideas in greater detail in section 5.4.

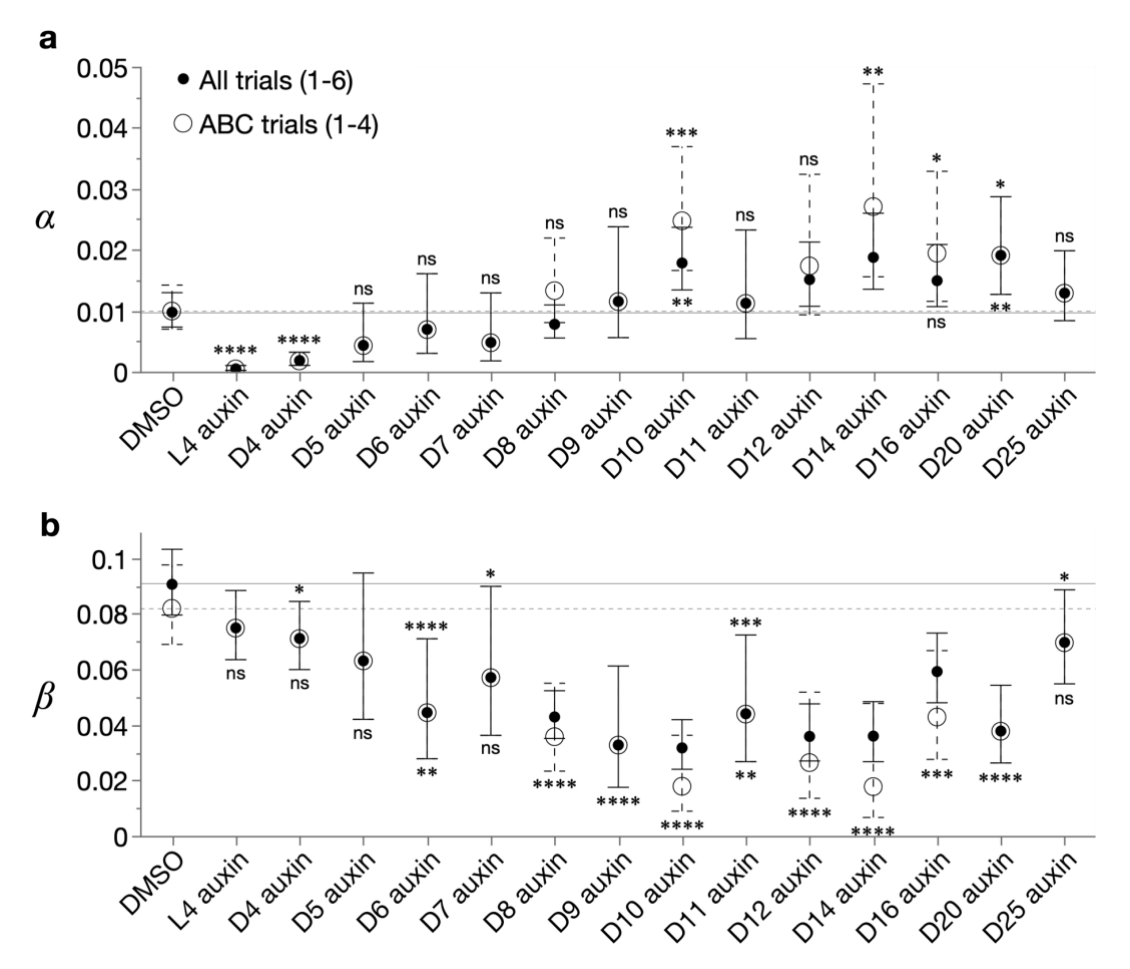


Figure 5.7. Effect of age-specific DAF-2 AID commencement on the Gompertz parameters. Effect of auxin administration from different ages (in RAF2181 animals) on (a)  $\alpha$  and (b)  $\beta$ , for the pools of all trials (Trials 1–6; solid circles and error bars) or only trials in which locomotory ageing was scored using the ABC system (see Methods) (Trials 1–4; open circles and dashed error bars). Statistical significance of parameter differences (via likelihood ratio tests) between cohorts (versus DMSO) is indicated below and above the error bars (95% confidence intervals), respectively, for solid and open circles in **a**, and vice versa in **b**. Where *p*-values of the solid and open circles fall within the same significance range, only one symbol is given for that cohort, either above or below the error bars.

Also as predicted, later treatments progressively decreased  $\beta$  and the magnitude of reduction in  $\alpha$ . Interestingly, the latter trajectory (of  $\alpha$ ) continued in treatments later than ~day 8, even changing into an increase in  $\alpha$  above DMSO control values (Figure 5.7a). Finally, and again as predicted, auxin treatment starting from very old ages (days 16 to 25) produced smaller reductions in  $\beta$  (Figure 5.7b). Thus, these results support all three predictions about the causal role of inter-individual variation in determining Gompertzian mortality patterns. Importantly, overall effects of DAF-2 AID commencement age on the Gompertz parameters were unaltered by the trial pooling system (all trials or only those scoring locomotory ageing) (Figure 5.7).

These Gompertz parameter changes are readily visible in the survival curves (Figure 5.6a–b, p. 116). Early, L4 auxin treatment shifted the survival curve to the right (i.e.  $\alpha$  reduction only), while later treatments achieved progressively smaller reductions in early mortality but were better at postponing late mortality; this steepened the survival curve at earlier ages while extending the survival curve tail (i.e. increased  $\alpha$  and decreased  $\beta$ , relative to earlier auxin cohorts). Meanwhile, very late auxin treatments (e.g. days 16 to 25) yielded weaker extensions of the survival curve tail (i.e. increased  $\beta$ , relative to mid-late auxin cohorts). These survival curve changes are summarised in Figure 5.8a (left box), which shows fewer cohorts for visual clarity (auxin treatment from every 4 days, excluding day 20 treatment). Importantly, these overall changes are well-captured by the Gompertz parameter changes (Figure 5.8a, right box).

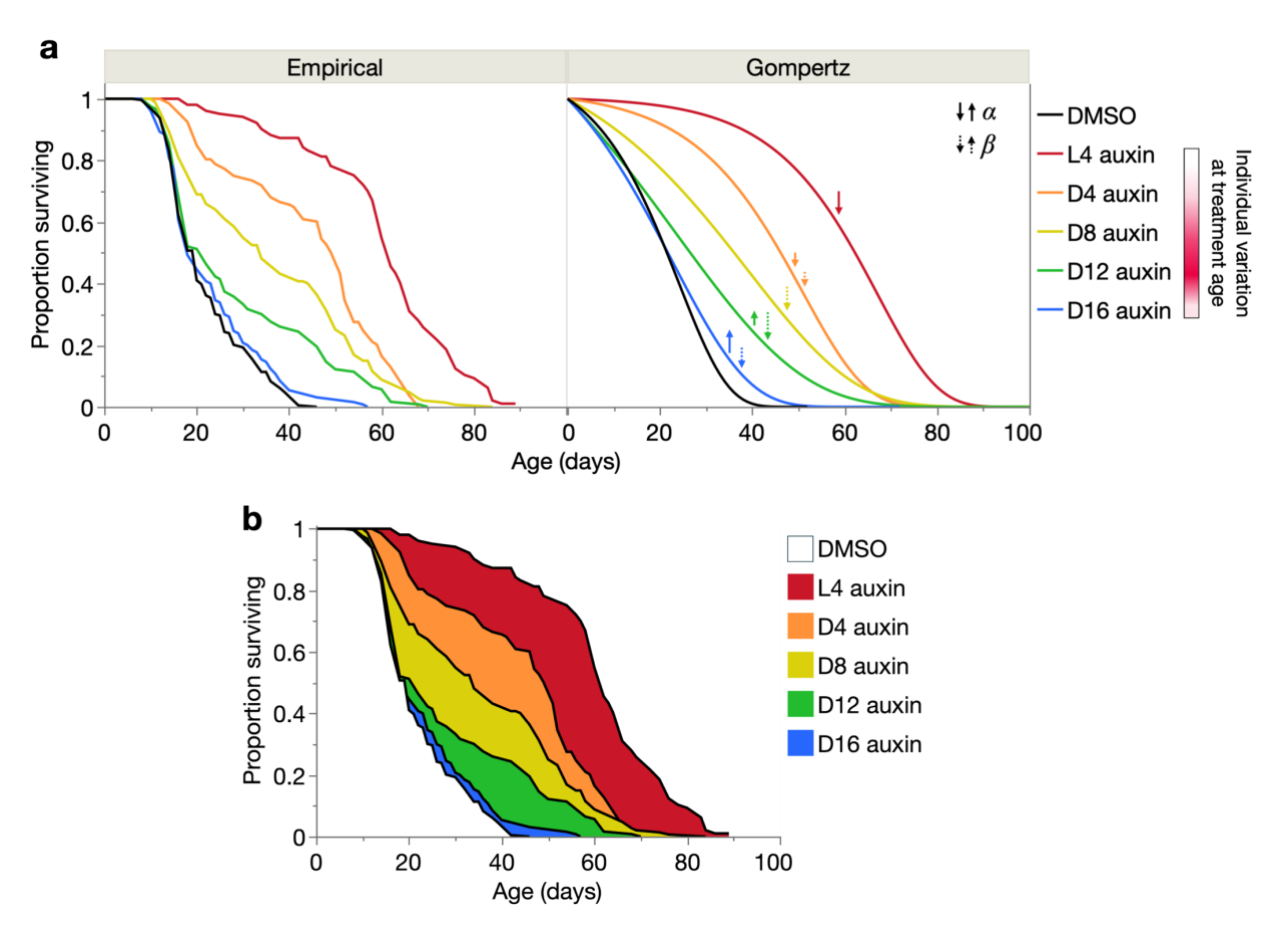


Figure 5.8. Age-specific IIS reduction produces a Strehler-Mildvan correlation. (a) Kaplan-Meier survival curves (left panel) and idealised Gompertzian survival curves (right panel; modelled using Trials 1–6 Gompertz parameter estimates from Figure 5.7) for select auxin treatment cohorts (from every 4 days, excluding D20 auxin). Effects on the Gompertz parameters (increases/decreases) compared to the DMSO control are indicated by solid and dashed arrows for  $\alpha$  and  $\beta$ , respectively; the arrow lengths indicate the relative magnitudes of change (not to exact scale). The red gradient indicates the hypothetical (but confirmed in section 5.3, p. 126) age pattern of the level of inter-individual variation within the population (darker red = more variation), as explained in the main text (p. 123). (b) Kaplan-Meier survival curves from a (left panel) with coloured regions between them, to illustrate how DAF-2 AID increases lifespan via two S-M changes: rectangularisation and triangularisation.

Intriguingly, the Gompertz parameters changed inversely: later DAF-2 AID increased  $\alpha$  while decreasing  $\beta$ , and vice versa at very late ages (after ~day 14) (Figure 5.7). This reveals a Strehler-Mildvan (S-M) correlation in the age-specific effects of IIS reduction on mortality rates. In Chapter 4, I explained the survival curve changes that can occur in S-M correlations, including rectangularisation/de-rectangularisation (Figure 4.4a, p. 92), as well as triangularisation/de-triangularisation (Figure 4.9, p. 101). Here, in DAF-2 AID, one can see both types of S-M correlation. Later auxin administration progressively redistributed deaths to earlier ages (with little change in maximum lifespan), or in other words, shortened lifespan more in shorter-lived population members (Figure 5.8a). This resulted in de-rectangularisation of the survival curve, involving an increase in  $\alpha$  (increased early mortality) and reduction in  $\beta$  (increased lifespan variation).

Meanwhile, still comparing cohorts in the life-shortening direction, auxin administration from even later ages (after  $\sim$ day 14) mildly reversed this pattern (now decreasing  $\alpha$  and increasing  $\beta$ ). This switched to a triangularising S-M correlation, where here, lifespan was shortened more in *longer* rather than shorter-lived individuals, thereby shortening the survival curve tail (i.e. de-triangularisation). This can be seen as similar survival curve shoulders between the DMSO control and later auxin cohorts, with divergence of the curves only after  $\sim$ 30% or more of the population has died (Figure 5.6a–b, p. 116).

The effects of these two types of S-M correlation upon the survival curve are alternatively represented in Figure 5.8b, showing that life-extension occurs exclusively in longer-lived individuals in the latest auxin treatments, but progressively includes shorter-lived individuals in earlier treatments, such that the earliest (L4) treatment extends lifespan equally in all individuals.

Interestingly, these plots (Figure 5.8) resemble recent historical changes in human populations, where survival curves have typically rectangularised (c.f. from day 12 auxin to day 4 auxin) over the last two centuries, and in more recent decades shifted in an approximately parallel manner towards the right (c.f. from day 4 auxin to L4 auxin). This likeness between human and nematode demography emphasises that regardless of organism and biological mechanism, general principles of Gompertzian biogerodemography are applicable across ageing populations, and may be investigated through similar approaches.

In the last section, I showed that reduction of IIS by DAF-2 AID starting at different ages alters the Gompertz parameters in a manner predicted by population heterogeneity (Figure 5.7). That is, that IIS reduction in a young, pre-senescent (more homogeneous) population should produce similar longevity responses in all individuals, and indeed only  $\alpha$  was decreased (increasing lifespan at all survival proportions). Meanwhile, later IIS reduction in ageing (increasingly heterogeneous) populations should produce increasingly variable longevity responses across individuals and, supporting this,  $\alpha$  reductions were suppressed and  $\beta$  was progressively reduced instead (increasing lifespan more in longer-lived population members).

As described, this age-specific effect of IIS on  $\alpha$  and  $\beta$  produced an S-M correlation (Figure 5.8). In section 4.1, I discussed how S-M correlations can arise from population heterogeneity or antagonistic pleiotropy within individuals, and in sections 4.3 and 4.4, showed that there is more evidence for the former in my *C. elegans* data. This differential heterogeneity hypothesis posits that biological (or environmental) differences between individuals or subpopulations can result in different effects of longevity interventions upon them, for instance, extending lifespan more in shorter-lived individuals (survival curve rectangularisation) (Vaupel and Yashin, 1985, Yashin et al., 2001, Hawkes et al., 2012), or longer-lived individuals (survival curve triangularisation) (see section 4.5, Figure 4.9, p. 101).

Intriguingly, this also applies to my DAF-2 AID cohorts: mid-to-early auxin treatment progressively rectangularised the survival curve (decreasing  $\alpha$  and increasing  $\beta$ ), while very late treatment triangularised it (increasing  $\alpha$  and decreasing  $\beta$ ) relative to the DMSO control (Figures 5.7, 5.8). The emergence of these S-M correlations in these age-specific DAF-2 AID cohorts therefore provides additional support to my proposed role of inter-individual variation in shaping Gompertzian mortality.

In this section, I will directly test these ideas by examining the biological variation within these cohorts at the age at which treatment was commenced. To enable this, locomotory health was scored every 2–3 days throughout the full lifespan of these DAF-2 AID cohorts and the DMSO control. Locomotion was scored using the ABC system, as also employed for the 24-cohorts dataset in Chapters 3 and 4 and *daf-16* dataset in section 5.1. To reiterate, nematodes were assigned to one of three movement classes depending on their response to a controlled physical stimulus from a platinum wire: A class (sinusoidal locomotion), B class (non-sinusoidal locomotion), and C class (moving but non-locomotory). The days of life spent in each class yields measures of A-span, B-span, and C-span, which together sum up to lifespan.

However, in contrast to the 24-cohorts and *daf-16* datasets where A-span was designated as healthspan and the sum of B-span and C-span as gerospan, here each class was kept separate to provide a higher resolution of inter-individual variation in locomotory health.

As predicted, in earlier adulthood (up to day 9), the DMSO control population was highly homogeneous with all individuals in the healthiest, A class (Figure 5.9a last panel, 5.9b). After day 9, the population became increasingly heterogeneous as individuals began to enter B and C classes (and also die). This variation emerged first at earlier survival proportions, consistent with faster and/or earlier ageing in these shorter-lived individuals. A similar cross-sectional age-pattern of heterogeneity increase was present in the auxin-treated cohorts, for their specific ages of auxin administration (Figure 5.9a), showing that prior to auxin commencement, all cohorts are reliable replicates of the untreated (DMSO only) control.

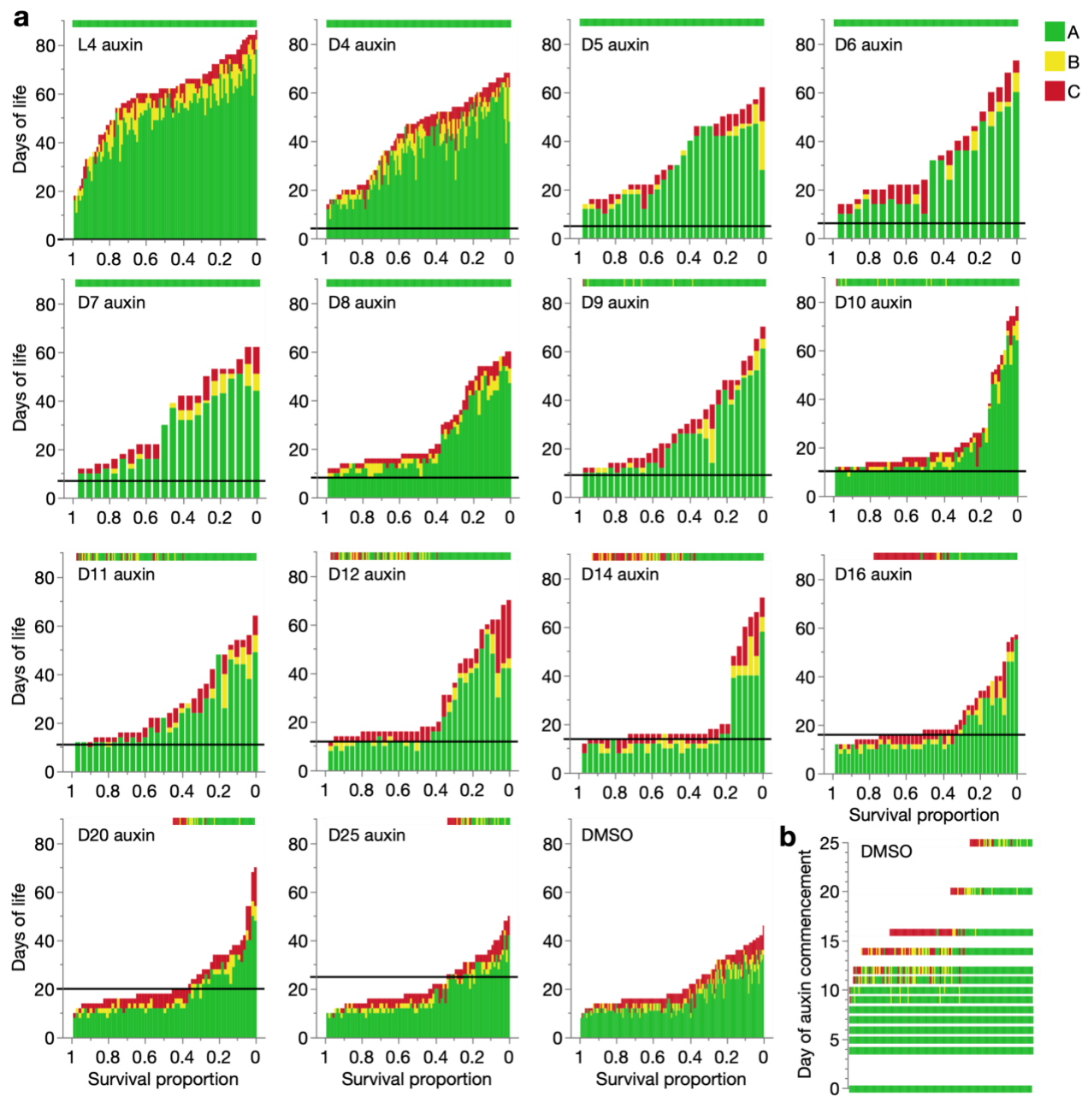


Figure 5.9. Event history charts showing inter-individual variation in locomotory health at DAF-2 AID commencement. (a) Vertically stacked days of life spent by each individual in A, B and C locomotory classes, ordered along the x-axis by decreasing survival proportion (increasing lifespan). Each vertical bar represents one individual. The horizontal black lines indicate the day of auxin commencement. A cross-sectional slice of the DMSO control event history chart corresponding to the day of auxin commencement is displayed above each auxin-treated cohort for comparison. (b) Cross-sectional slices of the DMSO control event history chart, for each day that auxin was commenced. These data (in a and b) are from the pool of Trials 1–4, and censored individuals were excluded.

Interestingly, these data reveal a greater contribution of A-span (healthspan) expansion to the DAF-2 AID lifespan increases, than of changes in B and C-span (gerospan); I will explore this more quantitatively in the next section, but this is consistent with the suggested view that full, adult-specific loss of DAF-2 simply slows biological ageing. In summary, the observed age-increase in inter-individual variation in locomotory health is consistent with its hypothesised role in determining the Gompertz parameters (Figure 5.8a, right, p. 125).

How does this variation in health at auxin commencement determine survival curve shape? As predicted in the previous section, Figure 5.9a shows that the magnitude of lifespan extension by DAF-2 AID is greater at lower survival proportions (longer-lived individuals), such that ordinarily shorter-lived individuals benefit less; this is most pronounced with later auxin treatment. Thus, the age-related emergence of inter-individual variation, in the form of biologically older individuals at higher survival proportions (shorter-lived individuals), results in an accordingly variable response to DAF-2 AID, where lifespan is increased more at lower survival proportions (extending the survival curve tail and decreasing  $\beta$ ). Indeed, the inevitable nonresponsiveness of already deceased individuals (at higher survival proportions) to very late auxin administration (from day 14 and later) is an extreme case of how variation in treatment condition can lead to variation in response.

If shorter-lived individuals (at higher survival proportions) respond more weakly to DAF-2 AID due to being biologically older at treatment commencement, then lifespan extension should be greater when treating A class than B class individuals, and similarly B class than C class individuals. This proved to be the case at all treatment ages, although differences between B and C class survival were less pronounced than between A and B classes (Figure 5.10a), affirming that B and C classes likely represent more terminal, irreversible stages in the ageing process. Indeed, mean survival of animals treated when in B or C class never exceeded 6.7 days (B class for day 8 auxin), whereas animals treated when in A class survived from 12.1 to 59.9 days (day 25 and L4 auxin, respectively).

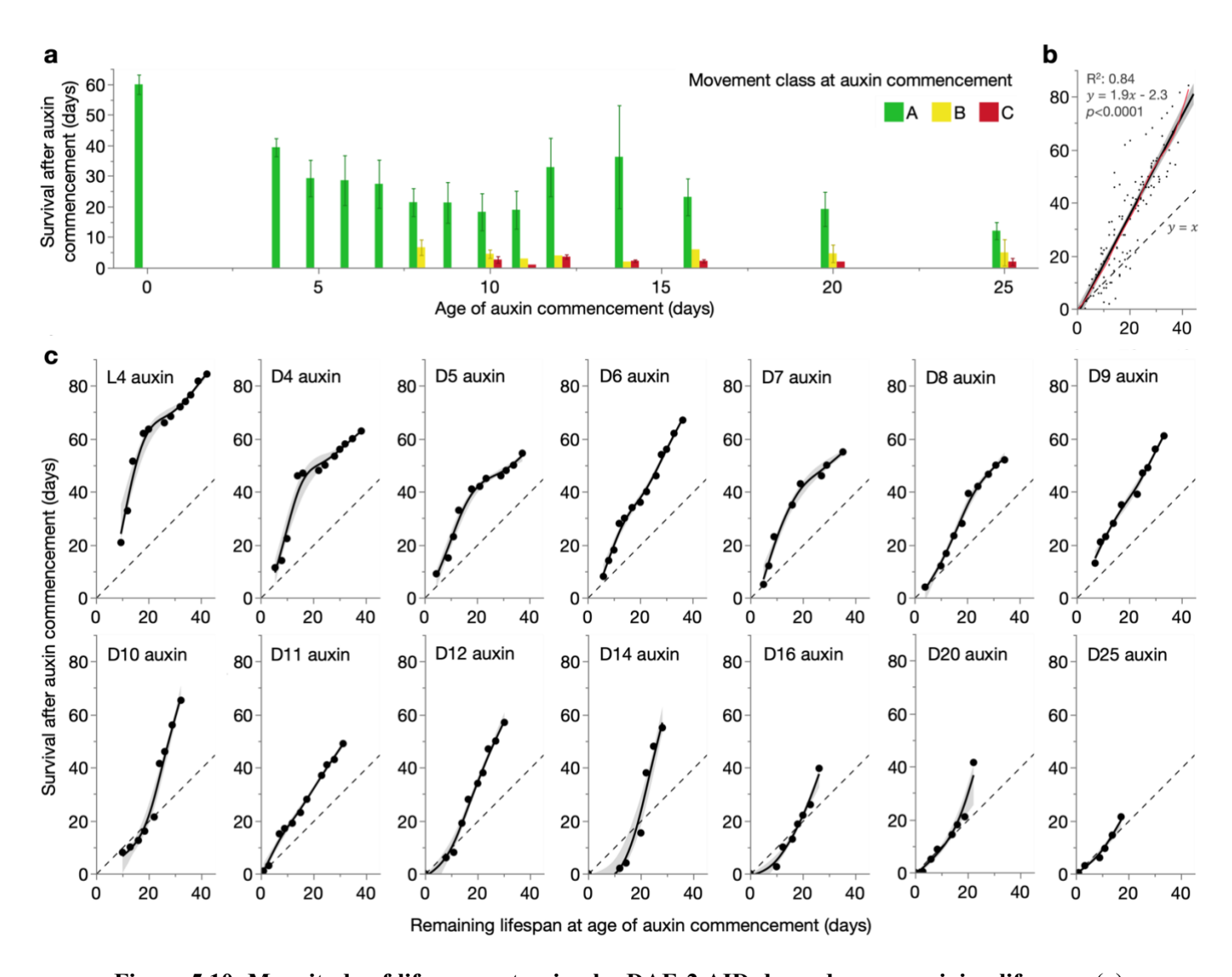


Figure 5.10. Magnitude of lifespan extension by DAF-2 AID depends on remaining lifespan. (a) Effect of locomotory class (A, B or C) on mean days survived after auxin commencement, for each age of auxin commencement. 95% confidence intervals shown. (b-c) Effect of remaining lifespan at the age of auxin commencement (in the DMSO control) on days survived after auxin commencement (in the auxin-treated cohorts), for all auxin-treated cohorts combined (b) or separate (c). To plot this relationship, these two quantities were related to one another by survival proportion, which was categorised into 0.05-unit bins. Remaining control lifespan and post-auxin survival of individuals falling within these bins were averaged to yield one value per bin, and these were plotted as above (depicted datapoints) and their relationship summarised with a non-linear smoother (spline method with lambda of 0.05, showing 95% confidence regions). The dashed lines represent a 1:1 relationship between the axis variables, which would be expected if DAF-2 AID has no effect on lifespan, and the red curve in b is a smoother obtained by the same method as in c (spline method, lambda=0.05). These data (a-c) are from the pool of Trials 1–4, and censored individuals were excluded from the analyses.

Notably, post-treatment lifespan decreased with later auxin commencement even when all population members were in the healthiest A class (Figure 5.10a). This was also visible in Figure 5.9a, where auxin treatment from L4 up to  $\sim$ day 8 affected only A class individuals, yet lifespan-extension already began to decrease in magnitude across these treatments. Similarly,  $\beta$ 

already began to decrease in the early auxin treatments (relative to the earliest: L4 auxin) when all individuals were still in A class (Figure 5.7, p. 124, and 5.9b).

What might this mean in biological terms? One likely explanation for these observations is that A class is sufficiently broad as to capture not only pre-senescent individuals but also those undergoing early stages of ageing that are too mild to fall into B class (including non-pathological changes that become pathological later in life). Certainly, ageing-related physiological changes must occur and progress to a certain severity before their functional manifestation as locomotory debilities (i.e. B and C class behaviour) become visible. Therefore, life-extension by IIS reduction may be closer associated to the younger biological age of A class animals (particularly in the earlier stages of A-span), than the A class state itself.

To more formally investigate the dependency of DAF-2 AID efficacy on individual age of treatment, I examined the relationship between control and auxin-treated animals of survival following auxin commencement, across all auxin-treated cohorts (Figure 5.10b). Here, a perfect 1:1 relationship (dashed line, y = x) would indicate no difference between control and treatment cohorts, that is, that their survival curves are identical. A relationship with slope greater than 1 would indicate a positive effect of remaining lifespan upon DAF-2 AID longevity. Post-treatment survival increased linearly with remaining control lifespan, and as hypothesised, with a slope greater than 1 (Figure 5.10b). This shows that reducing IIS increases lifespan more when administered earlier in individuals' lives. Specifically, post-treatment survival increased with a slope of 1.9, meaning that on average across the cohorts, DAF-2 AID approximately doubles the remaining lifespan of any treated individual.

Considering age-specific treatments separately, one observes in each a similar near-linear relationship between remaining control lifespan and post-treatment survival, with a gradient higher than 1 (Figure 5.10c). Notably, this relationship exists also with auxin treatments before ~day 8, when all population members were still in A class, thus demonstrating that even during this most youthful stage of adulthood (A-span), earlier DAF-2 AID is more effective. This supports the view that responsivity to IIS reduction of lifespan declines from early adulthood, before clear deterioration of locomotory coordination.

Notably, in the earlier auxin treatments (from L4 to  $\sim$ day 5), a bimodality was observed in the relationship, with an initially greater slope that then lowered to become approximately parallel with the standard curve (y = x) when remaining lifespan reached  $\sim$ day 20. One possibility is that the first steeper stage corresponds to effects of reducing IIS in individuals experiencing pharyngeal infection, which typically die between days 10 and 20 under standard conditions in wild-type animals (Zhao et al., 2017). These individuals, which age faster and die earlier than individuals without pharyngeal infection, likely benefit more from earlier DAF-2

AID, explaining the steeper relationship between remaining lifespan at treatment and subsequent survival. In contrast, the second flatter stage, whose slope of ~1 indicates no benefit of earlier treatment, likely reflects a diminution of treatment efficacy in longer-lived individuals when started already sufficiently early in life.

Careful comparison of the age-specific treatment plots of Figure 5.10c reveals an important difference between them, despite all having a greater slope than 1. For a given remaining lifespan at auxin commencement, the corresponding post-treatment survival differs greatly. For instance, for a remaining lifespan of 20 days, post-treatment survival ranges from ~60 days in L4 treatment to only ~20–25 days in day 25 treatment. This means that not all individuals with the same number of days of remaining life respond the same to DAF-2 AID; those treated at earlier ages (i.e. shorter-lived individuals) live longer. The implication here is two-fold: that (1) these individuals are treated at a biologically younger point in life and thus attain a greater extension of lifespan, and (2) longer-lived individuals age slower rather than later; their ageing process does not begin at a later age, but simply progresses more slowly.

To further test these interpretations, I assessed the relationship between post-treatment survival and survival proportion (i.e. lifespan), for a given remaining lifespan, across the treatment cohorts. The expectation here is that post-treatment survival should be shorter for individuals dying at lower survival proportions (i.e. longer-lived individuals), despite sharing the same remaining lifespan at auxin commencement. This proved to be true of all remaining lifespans examined (except 0–3 days, as expected of this terminal stage of life), and statistically significantly for remaining lifespans of between 9 and 21 days (Figure 5.11a). Notably, this relationship occurred even for a remaining lifespan of as long as 36–39 days, showing that the age-decline in responsivity of lifespan to IIS reduction (as part of the ageing process) begins in early adulthood and proceeds at different rates between individuals.

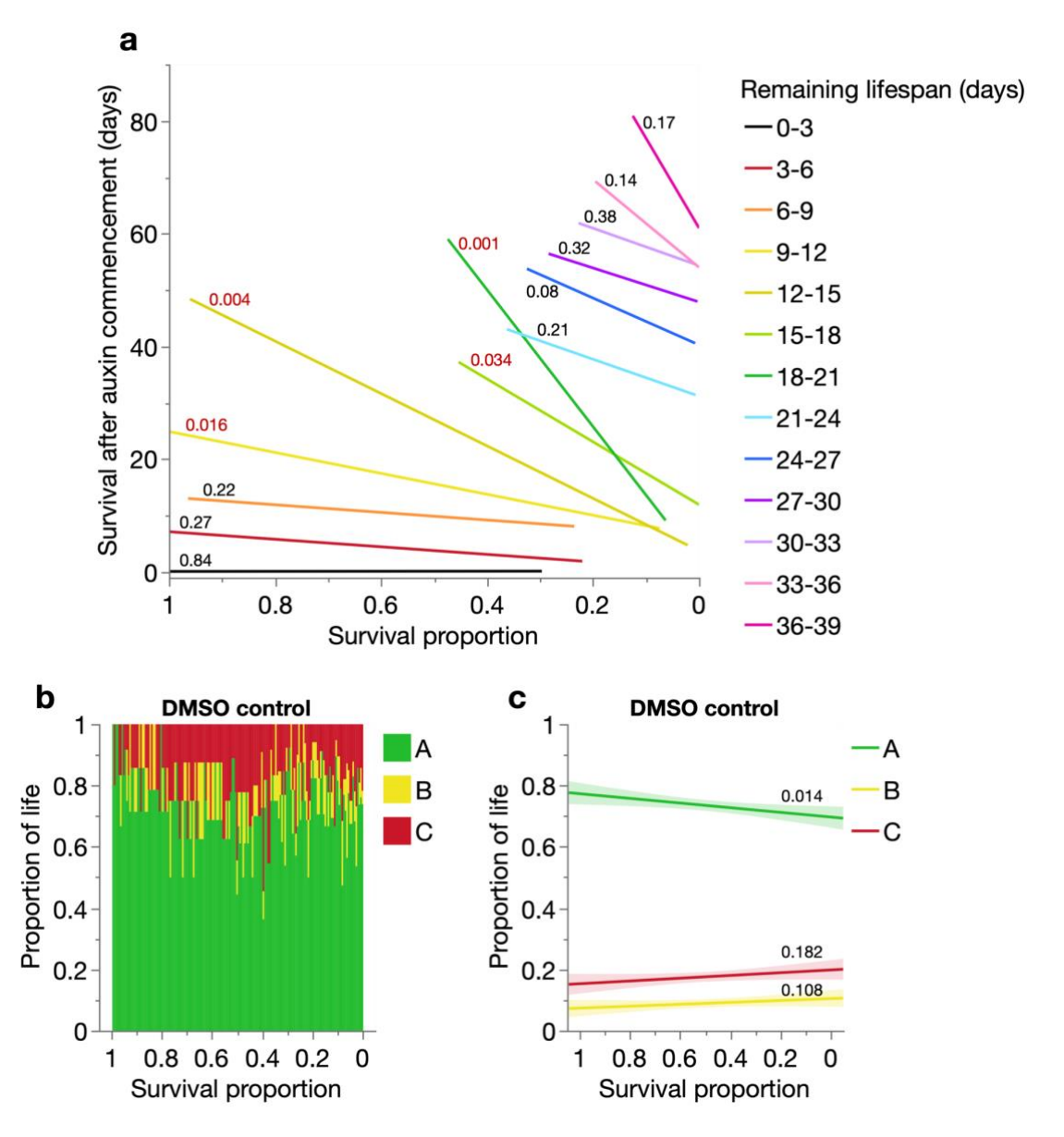


Figure 5.11. DAF-2 AID increases lifespan more in biologically younger individuals. (a) Linear regressions of mean days survived after commencement of DAF-2 AID over mean survival proportion (left: shorter-lived; right: longer-lived), for specific intervals (3-day bins) of mean remaining lifespan (of the DMSO control). The data values for the y-axis and overlay variable (remaining lifespan bins) were taken/derived from those producing Figure 5.10b–c, in the caption of which details of their calculation are provided. For each remaining lifespan bin (i.e. each colour), the y-axis and x-axis values are from auxin-treated individuals that have the same survival proportion bin (see Figure 5.10b–c) as the DMSO control individuals. For visual clarity, confidence regions of the regression fit are not shown; instead, regression F-test *p*-values are labelled (in red and to 3 decimals places for those <0.05). Note that the regression lines do not always cover the full x-axis (survival proportion), because this value depends on the remaining lifespan bin (e.g. remaining lifespan of 36–39 days includes only the longest-lived individuals, which hence have lower survival proportion values). (b–c) Relationship between survival proportion and the proportion of life spent in A, B and C locomotory classes for DMSO-treated control individuals, displayed as a life-history chart in b and linear regression in c. Regression F-test *p*-values are labelled in c for each locomotory class, and 95% confidence regions shaded.

These findings are consistent with the earlier entry of shorter-lived individuals into the senescent B and C locomotory classes (Figure 5.9, p. 128). Furthermore, the proportion of life

spent in each locomotory class in DMSO control animals was relatively constant across survival proportions (Figure 5.11b–c), suggesting an approximate stretching out of the ageing process in longer-lived individuals. Relative A-span (proportion of life in A class) was even observed to be mildly reduced in longer-lived individuals, opposite in expectation to the alternative scenario where ageing begins later (rather than more slowly), which should increase relative A-span.

Therefore, the inter-individual variation in ageing rate characterised here, explains the variation in lifespan responses to IIS reduction, and how this response variability itself varies with the age of IIS reduction. This is a further demonstration of the ability of individual-focused strategies to make sense of demographic mortality phenomena, by revealing the central but often-neglected role of inter-individual variation in the ageing process.

The importance of this biogerodemographic approach may be illustrated in the reevaluation of a previous study using the same DAF-2 AID system, which argued that extension
of lifespan by DAF-2 AID from advanced ages (days 20–25) demonstrates that DAF-2
degradation can extend lifespan even in geriatric animals close to death (Venz et al., 2021).
However, my present analyses show that even at these late ages, most remaining individuals
are still in the healthiest (A) locomotory class (Figure 5.9, p. 128), due to the slower rate of
ageing in these longer-lived individuals. These individuals are therefore relatively youthful at
the time of auxin treatment, in which case it is relatively unsurprising that the treatment can
increase lifespan. The earlier report therefore confounds biological with demographic ageing,
and does not actually show that late-life IIS reduction can improve longevity. On the contrary,
my data argue that reducing IIS during true decrepitude (B-span and C-span) has no effect on
increasing lifespan, which I will demonstrate in section 5.6.

## 5.4-Effects of healthspan and gerospan on $\alpha$ and $\beta$ given age-specific IIS reduction

In the previous section, I explained how inter-individual variation in ageing rate can lead to accordingly variable longevity responses to IIS reduction. This biogerodemographic analysis aimed to define the relationship between individual (biological) ageing and demographic mortality and survival trajectories. In this section, I re-utilise the locomotory ageing data from these cohorts to investigate how changes in locomotory health may explain changes in the Gompertz parameters, as similarly performed for the 24-cohorts (Chapters 3–4) and *daf-16* (section 5.1) datasets. As a first clue, it was seen in the previous section than gains in lifespan from DAF-2 AID result predominantly from healthspan (A-span) expansion (Figure 5.9, p.

128). This is somewhat surprising since  $\beta$  was reduced by DAF-2 AID from most ages (Figure 5.7, p. 124), and I showed in section 3.4 and again in section 5.1 that  $\beta$  reductions result (primarily or in part) from expansion of gerospan (B-span + C-span) rather than healthspan.

To investigate this, I assessed the effect of DAF-2 AID on the number of days spent in healthspan (absolute H-span) and gerospan (absolute G-span) of all individuals in each age-specific auxin commencement cohort (Figure 5.12). Strikingly, and as suspected, G-span was largely unaffected by auxin administration from almost all ages, except for small increases in early treatments from L4 and D4 and in the very longest-lived individuals in treatments from days 12 and 14. In contrast, H-span was strongly increased in all cases, thereby accounting almost in full for lifespan extension by DAF-2 AID, and by corollary, the associated changes in survival curve shape (Figure 5.6a–b, p. 116).

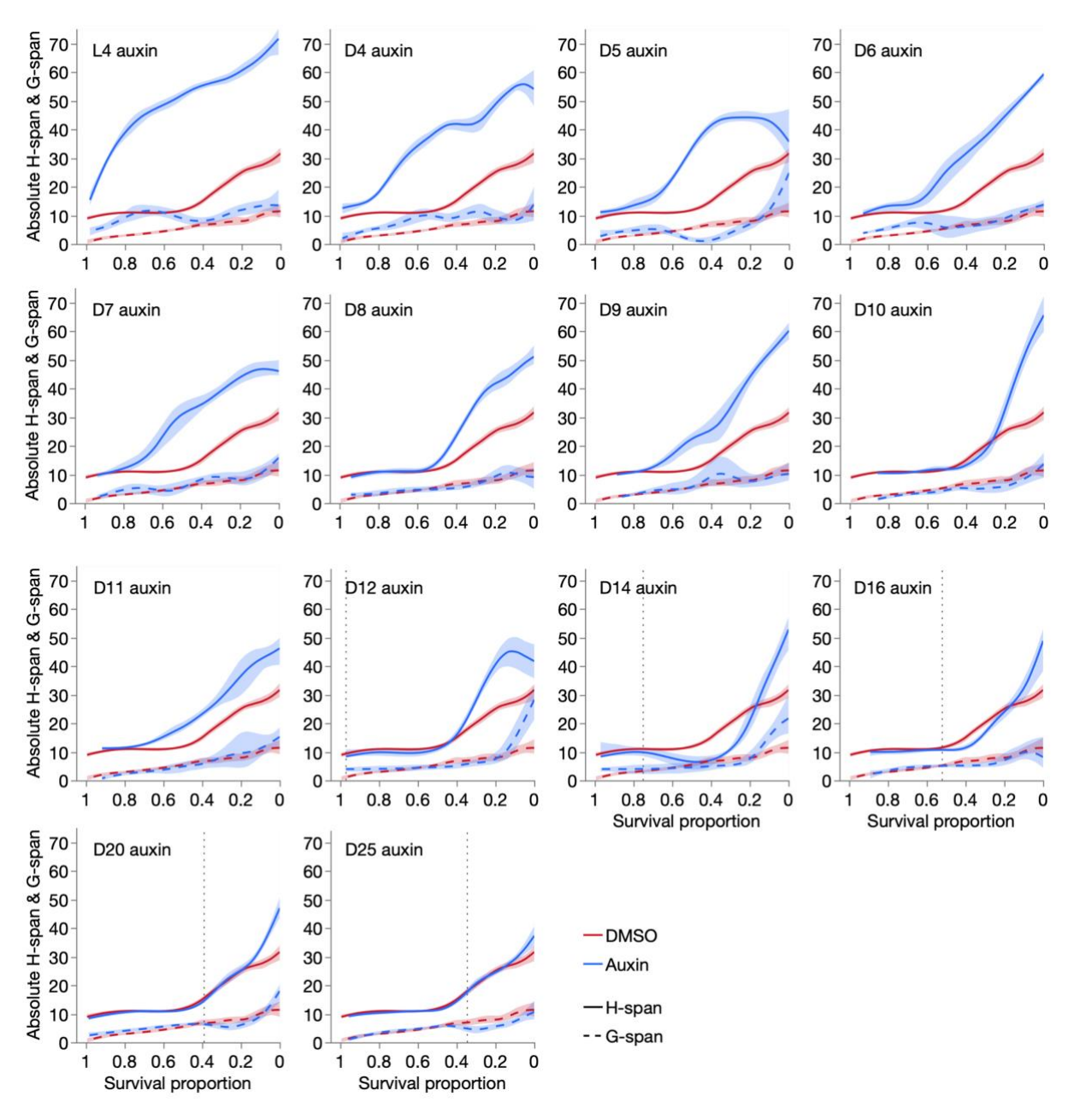


**Figure 5.12. DAF-2 AID increases lifespan by extending healthspan.** Effect of age-specific DAF-2 AID on absolute (days spent in) H-span and G-span, compared to a DMSO-treated control, across individuals of each population as ordered by survival proportion (left: shorter-lived; right: longer-lived). The relationships are presented as smoothers (spline method, lambda=0.05, with 95% confidence regions shaded), and dotted lines in the later auxin treatments show the timing of auxin commencement.

As expected of increases in absolute H-span against a constant absolute G-span, the proportion of life spent by individuals in G-span (relative G-span) was decreased in treatments from all ages (Figure 5.13). Unsurprisingly, these decreases were restricted to longer-lived individuals when auxin administration was commenced later.

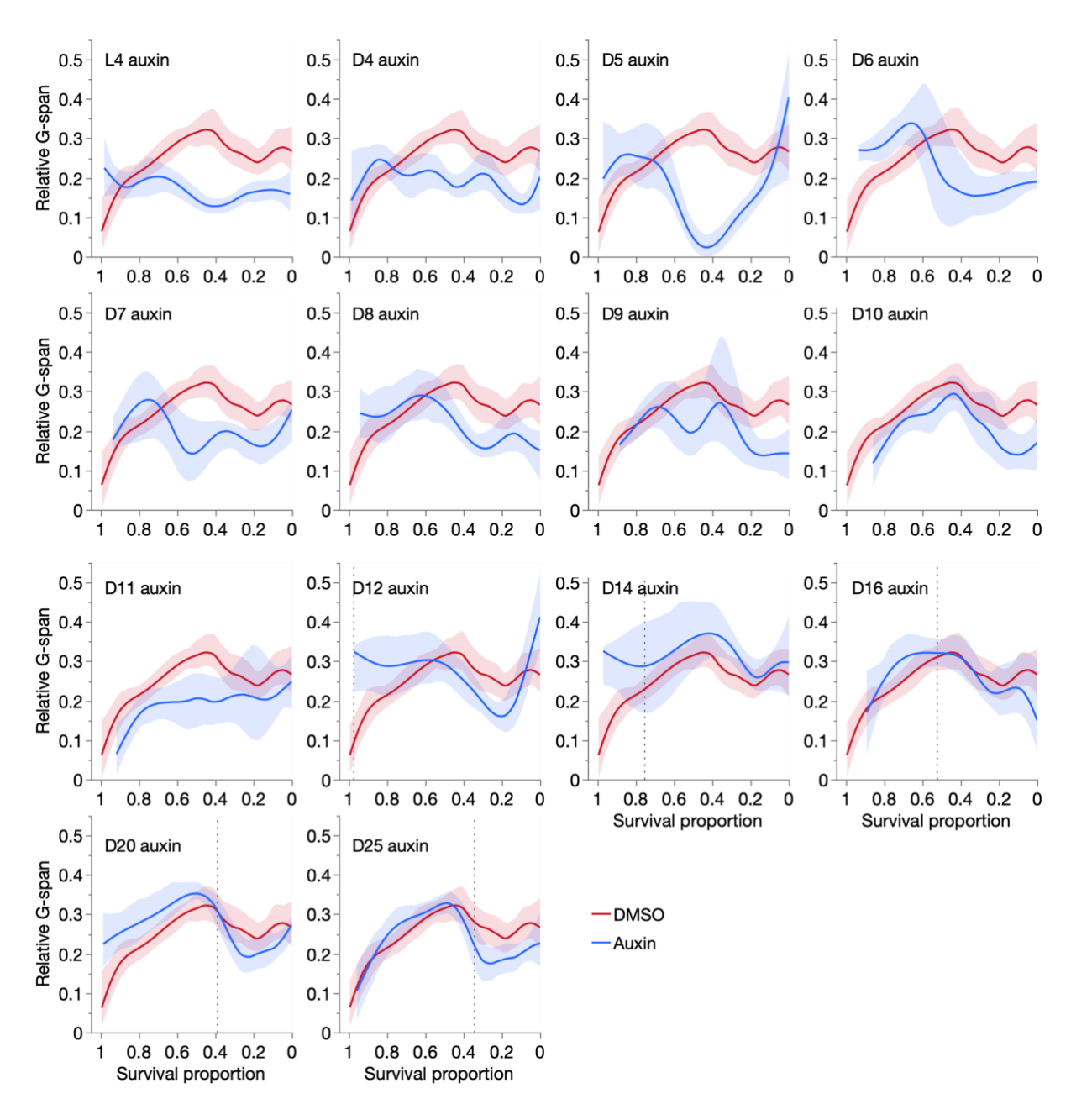


**Figure 5.13. DAF-2 AID decreases relative gerospan.** Effect of age-specific DAF-2 AID on relative (proportion of life spent in) G-span, compared to a DMSO-treated control, across individuals of each population as ordered by survival proportion (left: shorter-lived; right: longer-lived). The relationships

are presented as smoothers (spline method, lambda=0.05, with 95% confidence regions shaded), and dotted lines in the later auxin treatments show the timing of auxin commencement.

These findings challenge my earlier conclusions about the relationship between locomotory ageing and the Gompertz parameters. In Chapters 3–4 and section 5.1, from data on effects of antibiotics, lower temperature, daf-2(rf) and daf-16(0), I showed that  $\alpha$  reductions reflect H-span expansion, and that  $\beta$  reductions reflect increased G-span variation (and H-span variation in daf-16(0)). Here, with IIS reduction by DAF-2 AID, almost all changes in lifespan are attributable to changes in H-span; thus, here both Gompertz parameters mainly reflect changes relating to H-span.

However, as I demonstrated in section 5.1, an additional assessment of overall patterns across all cohorts (rather than between specific cohorts only) can yield a more accurate picture of the underlying relationships. Therefore, assessing  $\alpha$  first in this manner, H-span length was indeed a better overall predictor of  $\alpha$  than G-span length (R<sup>2</sup>=0.41, vs 0.11 for G-span) (Figure 5.14a). In contrast, against my earlier findings (but in agreement with visual inspection of Figure 5.12), inter-individual variation in H-span (rather than in G-span) was a better overall predictor of  $\beta$  (Figure 5.14b).

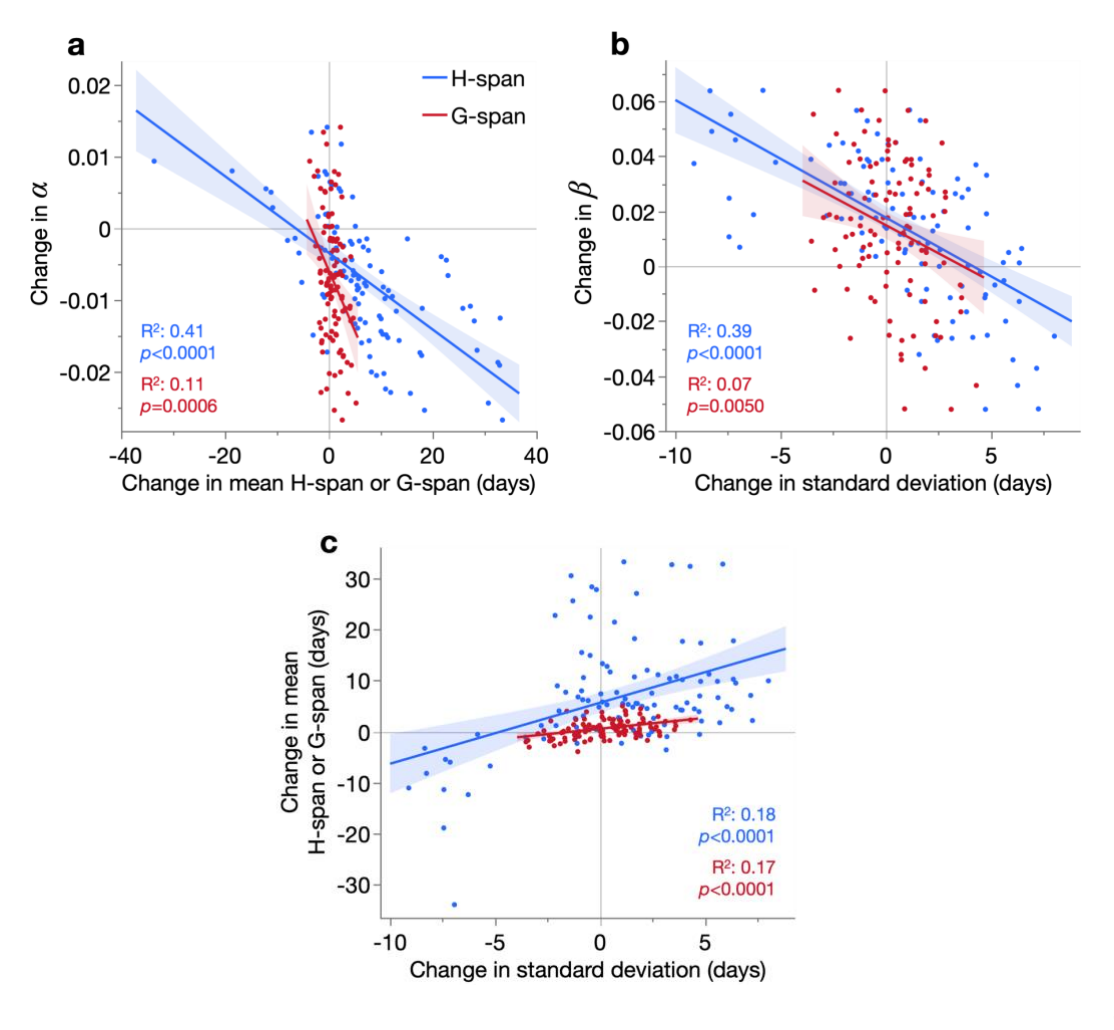


Figure 5.14. DAF-2 AID alters  $\alpha$  through healthspan, and  $\beta$  through healthspan and gerospan variation. (a) Effect of changes in mean H-span and G-span on changes in  $\alpha$ . (b) Effect of changes in standard deviation of H-span and G-span on changes in  $\beta$ . (c) Effect of changes in standard deviation of H-span and G-span on respective changes in mean H-span and G-span. In all plots, the relationship is assessed as a linear regression of changes between all possible pairwise comparisons (n=105) of the 15 cohorts (DMSO control and 14 auxin-treated cohorts). 95% confidence regions are shaded and regression F-test p-values labelled.

Thus, as in the daf-16(0) treatments (section 5.1), DAF-2 AID affects  $\beta$  through greater absolute changes in H-span variation than G-span variation. However, as demonstrated for the daf-16(0) treatments, G-span variation can simultaneously be an important determinant of  $\beta$  across cohorts, through a stronger scaling of G-span length and variation. Consistent with this, changes in mean G-span correlated with greater changes in G-span variation, than changes in mean H-span with H-span variation (Figure 5.14c, visible as a lower G-span slope, and note near-identical R<sup>2</sup> values). This again suggests that while H-span and G-span can change independently of each other in magnitude, their relative variability appears to be largely fixed (with G-span more variable than H-span). Therefore, as in the daf-16(0) treatments, both healthspan and gerospan contribute to determining  $\beta$  in DAF-2 AID. Note, however, that in the following section (5.5) I will present evidence that this contribution of H-span could potentially reflect an underestimation of the full G-span contribution.

But based on the present information, why might the relative magnitude of change in H-span and G-span differ for different modes of IIS reduction (DAF-2 AID mainly extends H-span, *daf-2* mutation mainly extends G-span)? Although both reduce IIS, they still differ as interventions. For instance, *daf-2(rf)* strains typically have missense mutations of the *daf-2* gene, leading to expression of DAF-2 protein with reduced function (Patel et al., 2008); in contrast, DAF-2 AID post-translationally reduces the level of functional DAF-2 protein to a low level (Venz et al., 2021). DAF-2 AID also appears to cause a stronger reduction in IIS, as auxin administration from before the dauer decision window during the L1 to L2 developmental stages induces formation of developmentally arrested dauer larvae, while the *daf-2(rf)* mutations used in this thesis do not (at this temperature of 20°C), despite reducing IIS all throughout development.

Consistent with a stronger reduction of IIS by DAF-2 AID, auxin from L4 increased lifespan more than the stronger daf-2(rf) alleles examined (daf-2(e1368) and daf-2(e1370)) (Figure 5.5a, p. 115). Finally, DAF-2 AID was commenced at the earliest from the final larval stage (L4), whereas in daf-2(rf) IIS is reduced throughout development. A possibility therefore is that stronger and/or adult-restricted IIS reduction affects H-span, whereas weaker and/or developmental reduction affects G-span.

A notable possibility, briefly introduced in section 5.2, is that this stronger, adult-restricted IIS reduction is a "purer" mode of reducing IIS (than IIS pathway mutants, e.g. *daf-2(rf)*), by increasing the effect size and removing confounding developmental effects of IIS reduction. In particular, stronger IIS reduction may also reduce heterogeneity that could otherwise result from inter-individually variable penetrance of hypomorphic IIS mutations. If correct, this would argue that IIS reduction does slow biological ageing rate, extending lifespan *and* healthspan, and even compresses morbidity (since gerospan is not extended). This may explain the reason for ongoing disagreements about how IIS reduction affects healthspan in nematodes (Hahm et al., 2015, Podshivalova et al., 2017, Statzer et al., 2022).

In summary, IIS-related interventions (DAF-2 AID, daf-16(0) and to a small extent daf-2(rf)) have a complex biogerodemography, where in specific treatments H-span variation is the main determinant of  $\beta$ , while G-span variation has a stronger relationship with  $\beta$  across all cohorts. Thus, that  $\alpha$  reduction reflects healthspan expansion while  $\beta$  reduction reflects increased gerospan variation (in full or part) are relatively consistent phenomena across these different lifespan-modulating interventions. In the next section, I will show that these findings may even be more consistent than this, due to possible overestimation of the contribution of H-span variation to determining  $\beta$  in DAF-2 AID.

## 5.5 – Characterisation of an intermediate stage of locomotory ageing in DAF-2 AID longevity

While performing these DAF-2 AID experiments, I noticed that auxin-treated individuals often exhibited little immediate response to the physical stimulus of the platinum wire, yet when given sufficient time, displayed standard A class locomotion (and were therefore scored as such). Similar reduced motility has been reported with DAF-2 AID (Roy et al., 2022) and in class 2 *daf-2(rf)* mutants (Gems et al., 1998, Hahm et al., 2015), and interpreted as a recapitulation of dauer immotility. However, another possibility is that the atypical A class animals described above (in these DAF-2 AID data), which I will call A', are in an early stage of senescence in comparison to canonical A animals, hence their reduced responsiveness to stimuli.

To better characterise the A' state, in selected cohorts in Trial 3, A' individuals were scored, and recorded as a subset of A class animals. As observed, a higher proportion of animals treated with auxin from L4 exhibited A' locomotion (18/26 or 69%) than DMSO-treated control animals (9/36 or 25%) (chi-squared p=0.0005). Indeed, auxin-treated animals had a higher mean relative A'-span (proportion of life in A') than DMSO-treated controls (Figure 5.15a).

Notably, *daf-2(e1370)* also had an increased relative A'-span, whereas *daf-2(e1368)* and N2 did not, consistent with known dauer-like immotility in the former only (Gems et al., 1998).

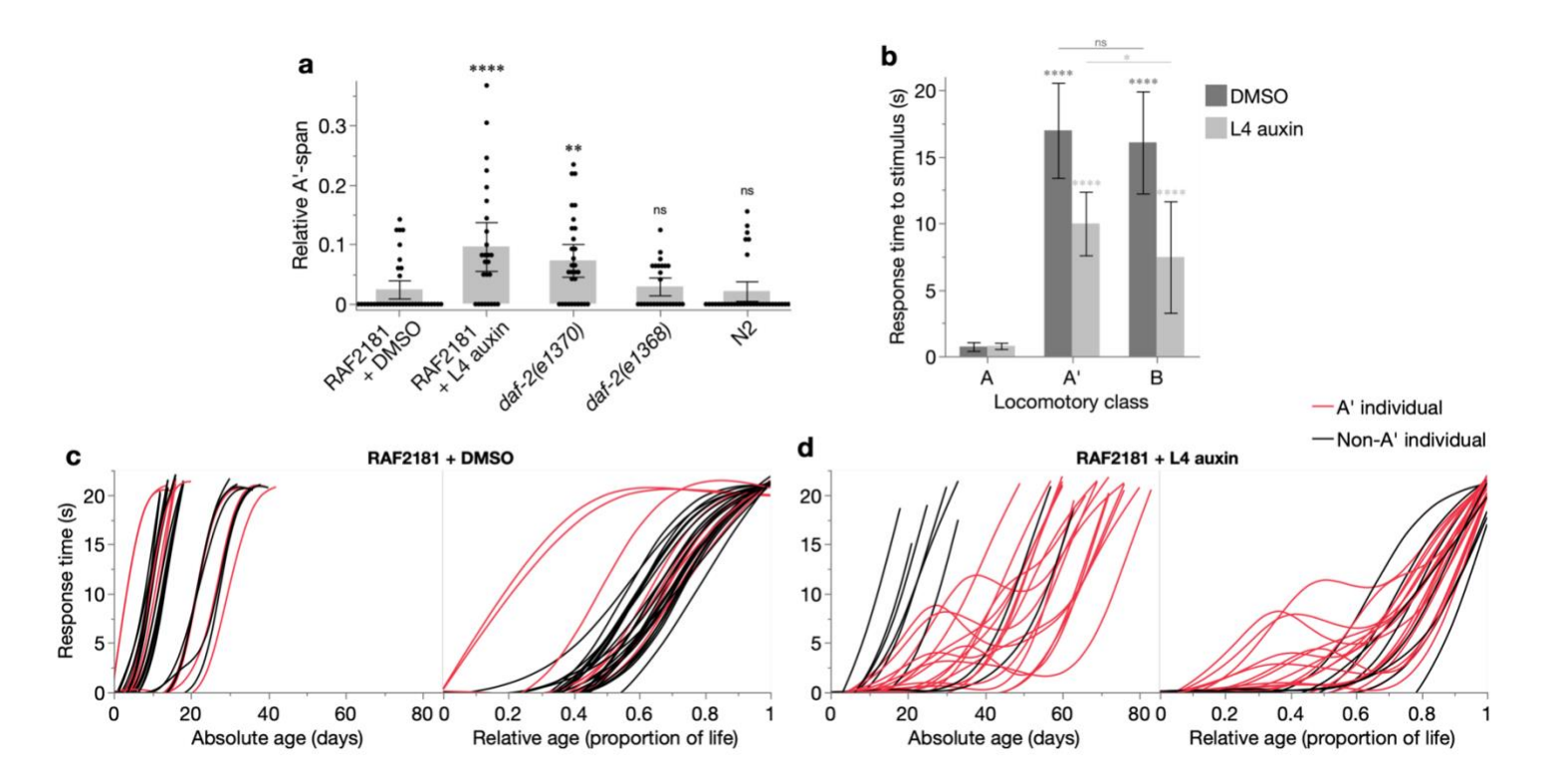


Figure 5.15. A locomotory subclass (A') with delayed but intact locomotion occurs in DAF-2 AID. (a) Mean relative A'-span (proportion of life spent in A') of different cohorts. (b) Mean time taken to begin locomoting away from the gentle touch of a platinum wire on the tail, for A, A', and B class animals, averaged from measurements taken throughout life. In a and b, 95% confidence intervals are shown, and statistical comparisons (two-tailed Student's t-tests) are made with the first condition, except where indicated otherwise; ns p > 0.05, \* $p \le 0.05$ , \*\* $p \le 0.01$ , \*\*\*\*  $p \le 0.001$ , \*\*\*\*  $p \le 0.0001$ . (c-d) Trajectories of age-changes in response time (same measure/dataset as in b) of individual animals, plotted over absolute age or relative age (absolute age as a proportion of that individual's lifespan). Trajectories were fit with a smoother (spline method, lambda=0.05). A' individuals (red) were defined as any individual that has spent at least 1 day in A'. All data in this full figure are from Trial 3, in which A' was scored (see Table 5.2).

To further characterise the A' state, I measured the time taken by animals to locomote away from a gentle touch with a platinum wire, at regular intervals until death. As expected, mean response time of A' animals was longer than that of canonical A animals, and interestingly, comparable to that of B class animals (Figure 5.15b). The latter suggests (tentatively) that A' locomotion may be a senescent rather than behavioural phenotype, given that B animals have both delayed and uncoordinated locomotion. In other words, A' may be a stage of transition between A and B animals that is extended by DAF-2 AID.

Examination of individual age trajectories of response time aids visualisation of these findings: auxin administration increased the proportion of individuals exhibiting A' locomotion, and these individuals had a higher response time (i.e. less responsive) for approximately the

first half of life (as measured by relative age) (Figure 5.15c–d). Notably, in DAF-2 AID, A' was observed primarily in longer-lived individuals (Figure 5.15d, left). Plotting over relative age revealed that these longer-lived individuals had a faster rate of decline in responsivity in early-mid adulthood, which plateaued and then accelerating again, at which point the shorter-lived, non-A' individuals caught up (Figure 5.15d, right). If A' locomotion is a senescent phenotype, this would imply that these individuals spend a larger portion of mid-life in an intermediate senescent state.

Another way to assess whether A' is a state of true senescence, is to examine the timing of its incidence over the life course. Notably, A' locomotion was observed to be clustered in later adulthood (after day 16), towards the end of A-span (Figure 5.16a). In comparison, behavioural effects of IIS reduction can be observed as early as day 1 of adulthood (Gems et al., 1998, Roy et al., 2022). This suggests that A' is an intermediate stage in true locomotory senescence between the A and B classes.

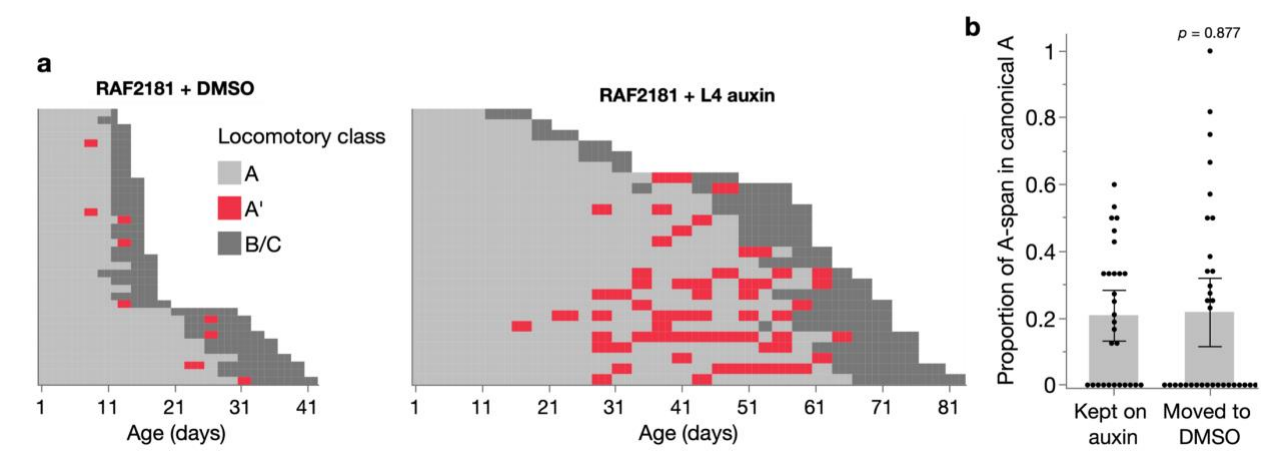


**Figure 5.16.** A' represents an intermediate stage in locomotory senescence. (a) Event history charts of the locomotory class of each individual throughout life. Each row represents one individual. These data are from Trial 3, in which A' was scored (see Table 5.2). (b) Mean proportion of post-transfer day A-span that was in only canonical A-span (rather than A'-span), for animals kept on auxin or taken off it (moved to just DMSO). Animals were treated with auxin from D12 and transfer day was when they were first observed to exhibit A' locomotion. Two-tailed Student's t-test; ns p > 0.05, \* $p \le 0.05$ , \*\* $p \le 0.001$ , \*\*\*\*  $p \le 0.001$ , \*\*\*\*  $p \le 0.0001$ . Pool of two trials, one performed with Melisa Kelaj.

Gems et al. (1998) also observed that the reduced motility phenotype of *daf-2(e1370)* cultured at 25.5°C is readily reversible, returning to wild-type motility within 2 days of shifting the animals to 15°C. I therefore asked whether the A' state is similarly reversible. RAF2181 animals were treated with auxin from D12, and at first observation (checked every 1–2 days) of A' locomotion were washed in buffer solution and transferred to either auxin or DMSO plates; subsequent locomotory class was scored every 1–2 days until death. The mean proportion of post-transfer A-span occupied by canonical A locomotion (i.e. a measure of reversal rate from

A' to A) was not significantly different between animals kept on auxin or transferred to DMSO (Figure 5.16b). Similarly, the proportion of animals that reverted to canonical A class was not significantly different between animals kept on auxin (18/33) or transferred to DMSO (15/36) (chi-squared p=0.285). Together, these results suggest that A' locomotion represents a true stage of ageing between the A and B life stages of locomotory health.

This may warrant a redefinition of H-span and G-span. Specifically, H-span could be redefined as the canonical A-span alone, and G-span as the sum of three stages: A'-span, B-span and C-span. With these definitions, I reassessed the effects of DAF-2 AID on H-span and G-span. As expected, with the A'-adjusted definitions, auxin treatment from L4 caused a smaller increase in H-span and greater increase in G-span, compared to that obtained using the canonical definitions (Figure 5.17a).

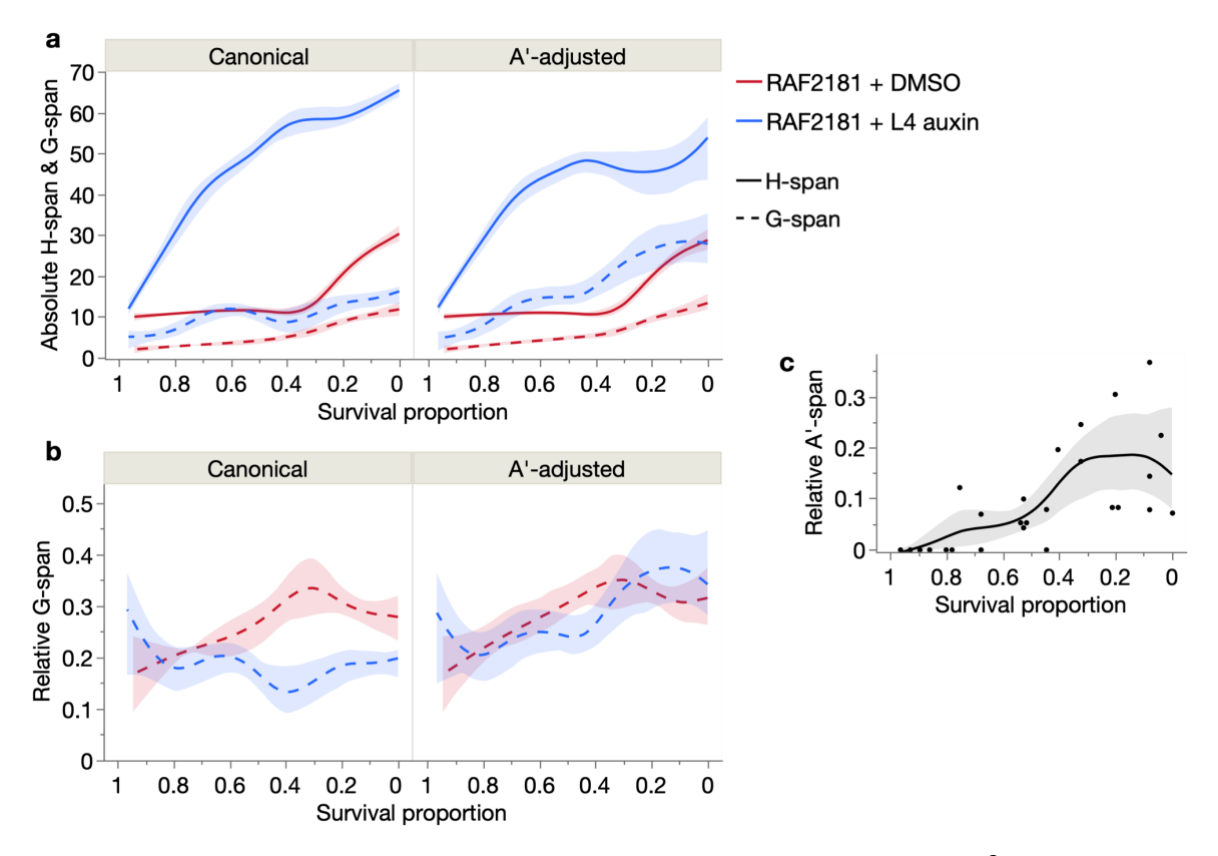


Figure 5.17. Inclusion of A'-span in G-span increases G-span determinacy of  $\beta$  in IIS reduction. (a–b) Effect of L4 auxin treatment on absolute H-span and G-span (a) and relative G-span (b), using either the canonical definitions (H-span = A-span, G-span = B+C-span) or A'-adjusted definitions (H-span = canonical A-span, G-span = A'+B+C-span). Relationships are fit with a smoother (spline method, lambda=0.05) with 95% confidence regions. (c) Relationship between relative A'-span (proportion of life in A'-span) and survival proportion (x-axis left: shorter-lived individuals, x-axis right: longer-lived individuals), also fit with a spline smoother with 95% confidence regions shaded. All data in this full figure are from Trial 3, in which A' was scored (see Table 5.2).

Notably, this redistribution of H-span to G-span occurred primarily in longer-lived individuals (i.e. at lower survival proportions). The effect is that in this analysis auxin treatment increased G-span primarily in longer-lived individuals, while H-span became extended more equally across the population. Consequently, the reduction in relative G-span in longer-lived individuals by auxin treatment was abolished with the A'-adjusted definition (Figure 5.17b); indeed, the proportion of life spent in A' was greater in longer-lived individuals (Figure 5.17c). Importantly, these new results are more consistent with the relationships observed in Chapter 3 between survival curve shape (i.e. Gompertz parameters) and H-span and G-span. That is, where the  $\alpha$  parameter reflects inter-individually homogeneous changes in H-span, whereas  $\beta$  reflects inter-individually variable changes in G-span (with greater magnitude of change in longer-lived individuals).

Taken together, these results suggest that IIS reduction by DAF-2 AID produces an extended intermediate stage in the ageing process, characterised by a delayed but largely intact locomotory aversion response to physical stimuli. This stage (A'-span) may be appropriately included within the present definition of locomotory gerospan, which includes any readily visible abnormalities in locomotion. In doing so, the meaning of the Gompertz parameters in terms of H-span and G-span becomes even closer to that demonstrated so far: that  $\alpha$  reduction reflects healthspan expansion and that  $\beta$  reduction reflects variable gerospan expansion.

A notable possibility is that the greater contribution of H-span than G-span variation to  $\beta$  in the DAF-2 AID treatments (sections 5.1 and 5.4) could arise from the inter-individually variable A'-span. Specifically, the stronger relationship between  $\beta$  and H-span variation in these treatments could simply reflect the omission of A'-span from G-span – thus underestimating the full G-span contribution to  $\beta$ . If included, G-span could become the greater determinant of  $\beta$  reductions, as observed in most other treatments (lower temperature, antibiotic and daf-2(rf)). In this thesis, A' and canonical A locomotion were only distinguished for the cohorts in this section, including only L4 commencement of DAF-2 AID. Further characterisation of the A'-span in the other DAF-2 AID cohorts (and potentially even daf-16(0)) may thus help explain their biogerodemography.

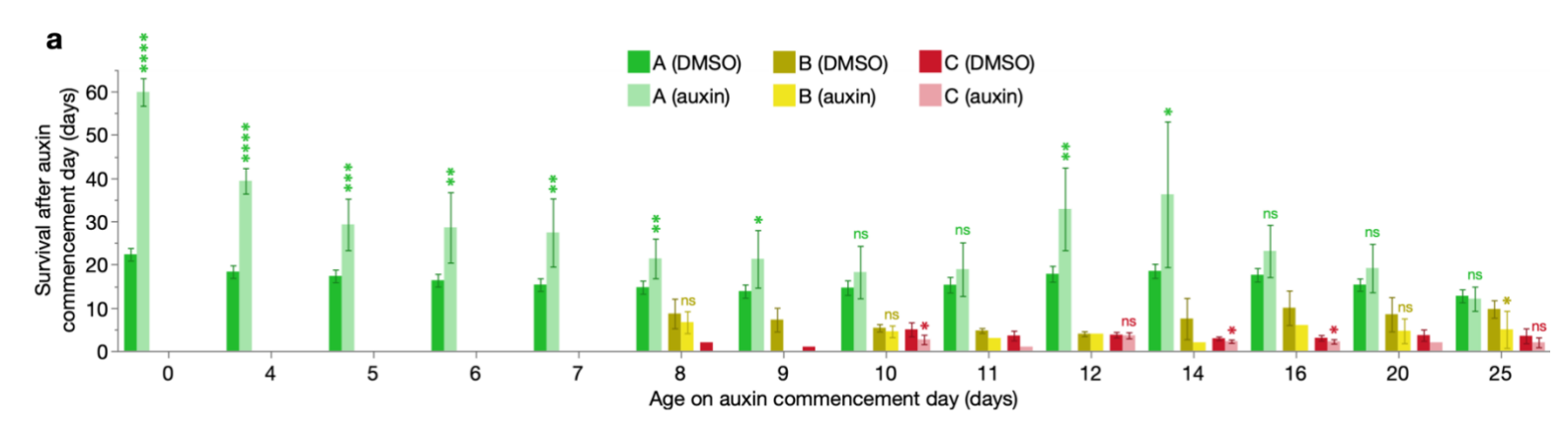
In the previous section, I discussed the idea (p. 139) that stronger, adult-restricted IIS reduction by L4 DAF-2 AID may better reveal the ability of IIS reduction to slow ageing, compared to hypomorphic IIS pathway mutants. How do the findings of this section, about the A'-span, affect this hypothesis? Here, I have shown that including the A'-span within G-span transfers a portion of H-span to G-span in longer-lived population members (Figure 5.17a). However, this only mildly reduces the H-span expansion resulting from L4 DAF-2 AID. Notably, using the A'-adjusted definitions of H-span and G-span reveals a conservation of

relative G-span between the DMSO control and L4 DAF-2 AID cohort, which indicates a simple stretching of the overall life course, consistent with a slowed biological ageing rate. These results, and those of the preceding sections, thus support the idea that IIS reduction in early adulthood causes a strong and inter-individually homogeneous reduction in biological ageing rate.

## 5.6 – Late-life elevation of IIS enhances longevity

In section 5.3, I investigated the effects of inter-individual variation in biological age on consequent variation in responses to DAF-2 AID. I showed that earlier commencement (in biological age) of DAF-2 AID resulted in greater individual lifespan increases, explaining the changes in survival curve shape. To better characterise this effect of biological age on responsiveness to DAF-2 AID, I here compared the post-treatment survival of animals that began auxin treatment during their A, B or C-span stages of life (Figure 5.18a).

As expected, auxin commencement in youthful, A class animals extended their lifespan, by a magnitude that decreased with later age of commencement. This is consistent with the age-dependent efficacy of DAF-2 AID even during A-span, as shown in section 5.3. A possibility is that the reduced efficacy in older A animals results in part from their being in the early-senescent A' class; unfortunately, A' data was not collected in these cohorts starting auxin from later than L4. Importantly, auxin commencement in biologically older B and C class animals did not extend lifespan, showing that reduction of IIS from older biological ages is ineffective as a longevity intervention. As discussed in section 5.3 (p. 134), this argues against an earlier report that commencing DAF-2 AID in geriatric animals can extend lifespan (Venz et al., 2021), and by extension, the claim that some aspects of senescence are reversed (Molière et al., 2024).



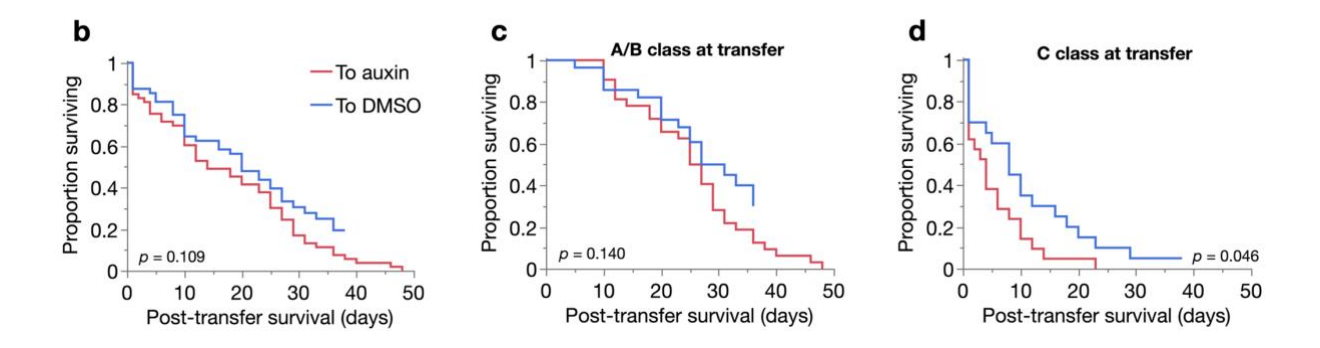


**Figure 5.18. Late-life cessation of DAF-2 AID extends lifespan.** (a) Effect of auxin treatment on mean days survived after auxin commencement for different locomotory classes (A, B or C), for each age of auxin commencement. 95% confidence intervals shown, and statistical comparisons between DMSO and auxin cohorts made by two-tailed Student's t-tests; ns p > 0.05, \*  $p \le 0.05$ , \*\*  $p \le 0.01$ , \*\*\*\*  $p \le 0.001$ . Data from the pool of Trials 1–4, and censored individuals were excluded from the analyses. (**b**–**d**) Kaplan-Meier survival curves of RAF2181 animals started on auxin from day 12 and transferred to either auxin (red) or DMSO (blue) on day 25; for all individuals (**b**; To auxin: n=60[0], To DMSO: n=59[11]), or only those in A or B class on day 25 (**c**; To auxin: n=35[0], To DMSO: n=32[10]), or only those in C class on day 25 (**d**; To auxin: n=25[0], To DMSO: n=27[1]). n[n]: total[censored]. Survival curves were statistically compared with log-rank tests. Data from 1 trial.

Surprisingly, remaining lifespan of animals treated with auxin during B-span and, particularly C-span, was often decreased relative to the DMSO control (Figure 5.18a). This suggests that reducing IIS at advanced biological ages may not only be ineffective at extending lifespan, but even shorten it.

To directly test this unexpected finding, I treated animals with auxin from day 12, and on day 25 transferred half to another auxin plate, and the remaining half to a DMSO-only plate. Both groups were picked into a large drop of buffer solution and left to swim for 10 minutes before transferring to the auxin or DMSO plate, to minimise auxin carry-over. In line with the hypothesis, the animals removed from auxin lived longer, although this increase was not statistically significant (Figure 5.18b). However, right-censoring of the longest-lived individuals removed from auxin may have truncated the full magnitude of lifespan extension. Separating these individuals by their movement class on the day of transfer (to auxin or DMSO) revealed longer survival in those transferred to DMSO, for both motile (A or B class) and immotile C class stages of life, reaching statistical significance in the latter (Figure 5.18c–d).

To overcome the impracticality and sample size limitations of a day 25 intervention (when few individuals remain alive), I again commenced auxin from day 12, but transferred individuals to either auxin or DMSO when they each entered the start of C-span. In this way, all individuals from the starting population will contribute to the final sample size (reducing starting population size), and the biological age of individuals at transfer can be controlled across the population. Additionally, one can study variation in responses to the intervention

across the population (e.g. do individuals reaching C-span later respond better or worse to removal from auxin?). This revealed a clear increase in post-treatment survival of animals removed from auxin (Figure 5.19a). Commencing auxin from L4 rather than day 12 yielded the same result: animals transferred at C-span onset to DMSO lived longer than those remaining on auxin (Figure 5.19b), suggesting that IIS effects on lifespan during C-span may be independent of earlier-life conditions. Notably, the magnitude of post-transfer survival increase was non-significantly different between auxin commenced from day 12 or L4 ( $\pm$ 45.0% vs  $\pm$ 47.6%, Cox proportional hazards likelihood-ratio test  $\pm$ 0.709), showing that the longevity effects of earlier life IIS reduction and later-life IIS increase are additive.

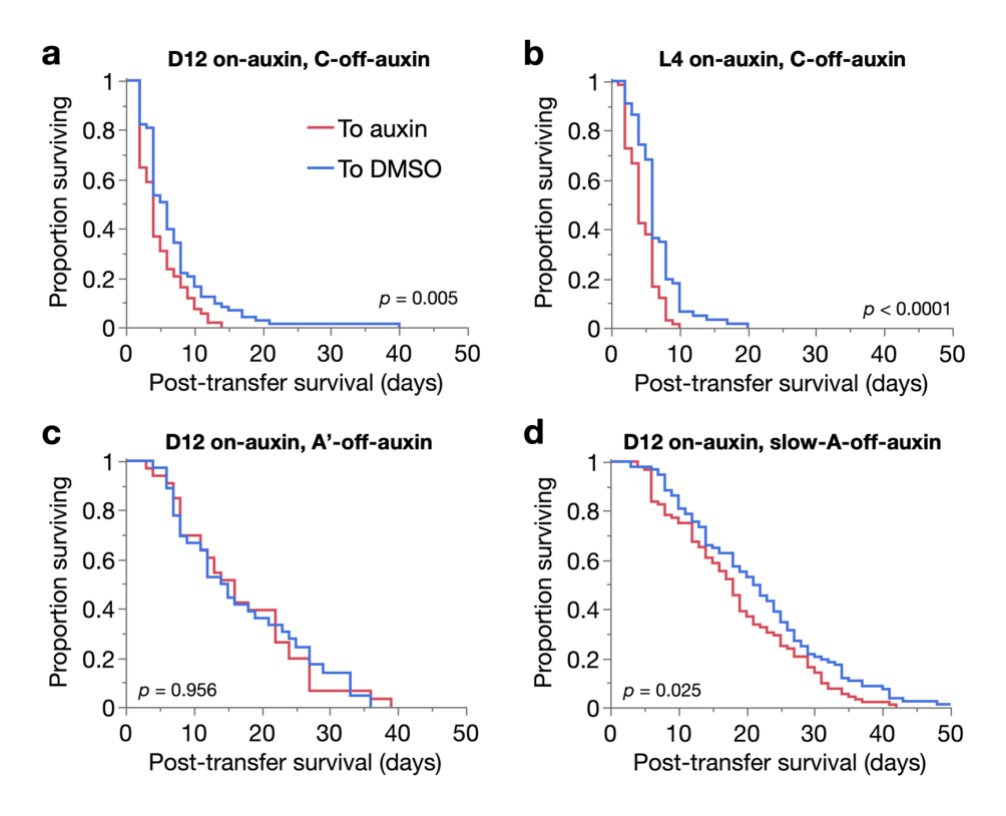


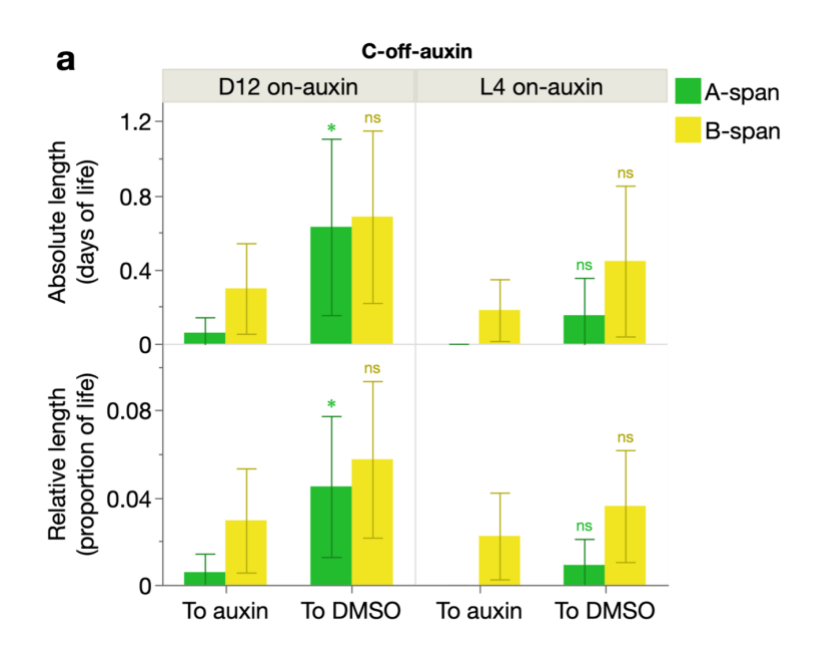
**Figure 5.19. Cessation of DAF-2 AID after A'-onset extends lifespan.** (**a**–**d**) Kaplan-Meier survival curves of RAF2181 animals started on auxin from day 12 (**a**, **c**, **d**) or L4 (**b**) and transferred to auxin (red) or DMSO (blue) at the onset of C class locomotion (**a**–**b**), A' locomotion (**c**) or slow-A locomotion (**d**). Survival curves were compared by log-rank tests and all data are from the pool of two trials: **a** (To auxin: n=68[1], To DMSO: n=73[0]); **b** (To auxin: n=66[0], To DMSO: n=66[1]); **c** (To auxin: n=33[1], To DMSO: n=36[3]); **d** (To auxin: n=92[0], To DMSO: n=94[2]). n[n]: total[censored]. One trial in **a** was performed with Reva Biju and one trial in **c** was performed with Melisa Kelaj.

I next wondered how early in the ageing process DAF-2 AID cessation can increase lifespan. To explore this, animals treated with auxin from day 12 were transferred to auxin or DMSO at A' onset, defined in the previous section as an intermediary senescent state of delayed locomotory responsiveness, in between the A and B-spans. Notably, here transfer to DMSO did not extend post-transfer survival (Figure 5.19c).

To try to better pinpoint the threshold age of IIS effects, I also transferred animals (treated with auxin from day 12) to auxin or DMSO at the onset of "slow-A" locomotion, which is slow but prompt sinusoidal locomotion (see Methods for a detailed description), a stage through which all individuals pass in their senescent transition from A to B class. These slow-A animals transferred to DMSO did have extended post-transfer survival (Figure 5.19d), but of a smaller magnitude (+19.1%) than from transfer of biologically older C animals (+45.0–47.6%) (Figures 5.19a–b).

Together these findings suggest that the transition from beneficial to deleterious effects of DAF-2 AID occurs in the late stages of A-span, around the age of the A' and slow-A-spans (Figure 5.22a, p. 150). Useful further tests to verify this would be to transfer animals off auxin at the onset of B-span, and during late A-span (but prior to A' and slow-A onset).

I next assessed whether the extended post-transfer survival of animals removed from auxin is accompanied by an extended healthspan. To a small extent, C animals left on auxin were observed to revert to A and B classes, probably reflecting those on the cusp of transition to C-span (Figure 5.20a). Notably however, regardless of auxin commencement age (L4 or day 12), animals removed from auxin at C-span onset had a consistently (although mostly non-significantly) greater mean post-transfer A-span and B-span (Figure 5.20a). This was true for both the number of days (upper panels) and proportion of life (lower panels) spent in A-span and B-span. This effectively demonstrates a mild rejuvenation to healthier A and B classes of C class individuals, or at least those on the cusp of entering C-span.



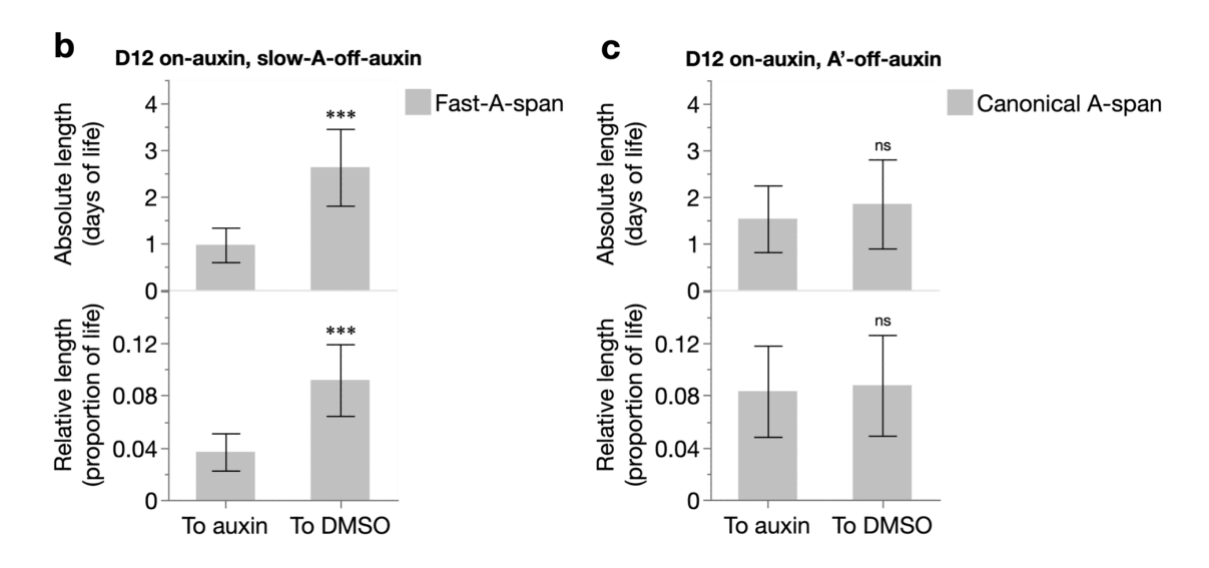


**Figure 5.20. Cessation of DAF-2 AID rejuvenates locomotory health.** Effect of transferring RAF2181 animals off auxin (to DMSO) from the onset of C class locomotion (a), slow-A locomotion (b), or A' locomotion (c), on absolute and relative durations of A-span and B-span (a), fast-A-span (b), and canonical A-span (c). Statistical comparisons between auxin and DMSO cohorts were made by two-tailed Student's t-tests; ns p > 0.05, \* $p \le 0.05$ , \*\* $p \le 0.01$ , \*\*\*\*  $p \le 0.001$ , \*\*\*\*  $p \le 0.0001$ . All data are from the pool of two trials (see Figure 5.19 caption for sample sizes), and censored individuals were excluded from the analyses. One trial in a (for D12 on-auxin) was performed with Reva Biju and one trial in c was performed with Melisa Kelaj.

Similarly, animals transferred to DMSO at slow-A onset (which lived longer) showed a strong increase in both absolute and relative "fast-A"-span (i.e. not slow-A) post transfer (Figure 5.20b), revealing a reversal of locomotory speed decline. Finally, consistent with the lack of lifespan increase in animals transferred off auxin at A' onset, no clear change in reversal to canonical A class was observed (Figure 5.20c). These results suggest that restoration of IIS at advanced biological ages may extend lifespan in part through a rejuvenating mechanism.

As a final probe into the late-life effects of IIS on ageing, I directly transferred animals onto auxin (or DMSO) for the first time at individual C-span or slow-A onset. The expectation here is that lifespan should be shortened in those transferred to auxin, if IIS reduction at these advanced biological ages is harmful. Consistent with this, post-transfer survival was reduced by approximately 10% (C-span onset: -8.1%, slow-A onset: -11.6%), although these decreases were not statistically significant (Figure 5.21a–b). A possibility is that in these decrepit animals, the efficiency of DAF-2 AID is reduced, leading to weak IIS reduction and thus also weak reduction of lifespan. Alternatively, IIS reduction in earlier life may be a prerequisite for continued reduction in later life to become life-limiting. Hence, the weak reduction of lifespan may have been because IIS was not reduced in earlier life.

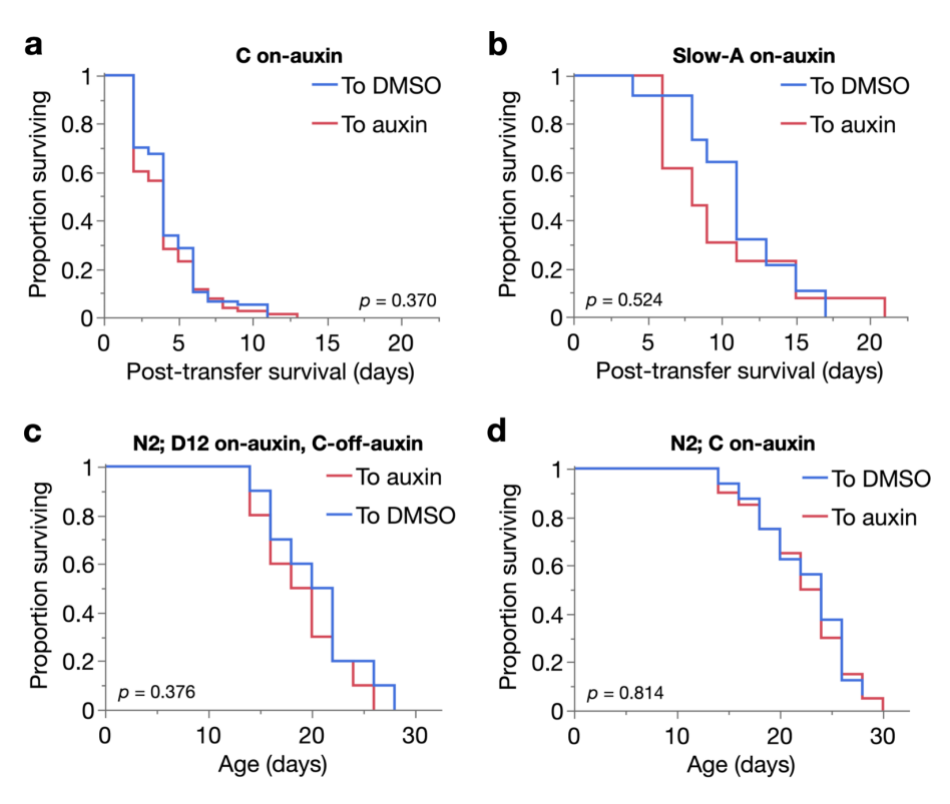


Figure 5.21. Late-life DAF-2 AID is weakly life-limiting and is not an artefact of auxin-only effects. (a–b) Kaplan-Meier survival curves of RAF2181 animals started on auxin or DMSO from the onset of C class locomotion (a) or slow-A locomotion (b). (c–d) Kaplan-Meier survival curves of N2 animals started on auxin from day 12 and transferred to auxin or DMSO at the onset of C class locomotion (c), or started on auxin for the first time from the onset of C class locomotion (d). Survival curves were compared by log-rank tests; and are from the pool of one (b–d) or two (a) trials: a (To DMSO: n=77[0], To auxin: n=78[0]); b (To DMSO: n=12[2], To auxin: n=13[0]); c (To auxin: n=10[0], To DMSO: n=10[0]); d (To DMSO: n=16[1], To auxin: n=20[0]). n[n]: total[censored]. b was performed by Chiminh Nguyen and c–d by Aihan Zhang.

To confirm that these late-life IIS effects are not an artefact of auxin-alone effects, N2 (rather than RAF2181) animals were started on auxin from day 12 and then transferred to auxin or DMSO at C-span onset, and additionally, N2 animals were transferred to DMSO or auxin for the first time at C-span onset. In neither case was lifespan altered by the removal or introduction of auxin itself (Figure 5.21c–d), consistent with my earlier finding that auxin does not significantly affect N2 lifespan when administered from L4 or day 16 (Figure 5.5c, p. 115). In addition, although auxin itself has been reported to mildly extend lifespan (Loose and Ghazi, 2021, Venz et al., 2021), here auxin exposure correlated with lifespan in the opposite direction (i.e. lifespan of auxin-treated cohorts was slightly shorter).

To summarise, I have shown that restoration of wild-type IIS at advanced biological ages further increases the longevity of animals with reduced IIS earlier in life, accompanied by a modest rejuvenation of locomotory health (Figure 5.22a). This implies that wild-type IIS promotes longevity in senescent animals, i.e. that at some point during ageing (here, shown to

be around slow-A-span), IIS switches from pro-senescence to a pro-longevity in action. What remains unclear is whether lifespan and health could be further increased by increasing IIS above wild-type levels in these aged animals. A critical future experiment would be to quantify IIS level in response to these age-specific effects of transferring to or off auxin, for instance through detection of DAF-2 protein levels as performed in younger animals (Venz et al., 2021). Additionally, it would be fascinating to study the mechanisms involved, e.g. by comparing the transcriptomes of C class worms with or without transfer away from auxin.

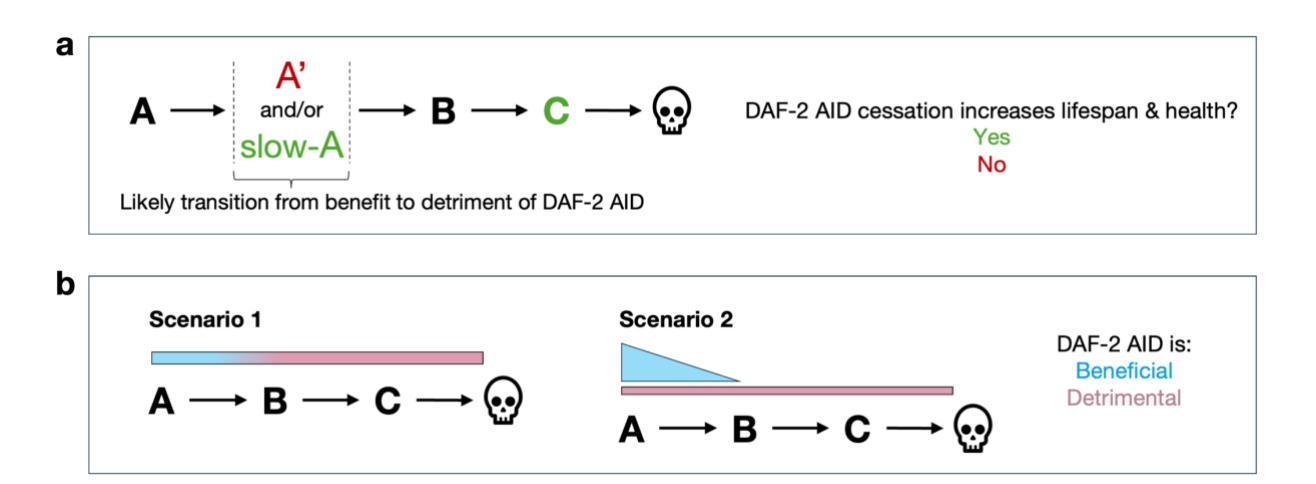


Figure 5.22. Models of the effects of DAF-2 AID on health over the nematode life course. (a) Summary of the sequence of locomotory health stages in ageing *C. elegans*, and effects of stopping DAF-2 AID at either A'-span onset (no effect on lifespan & health) or slow-A-span or C-span onset (both increase lifespan & health). This suggests the transition from beneficial to detrimental effects of reducing IIS is in late A-span, before B-span. Note the uncertainty of the life course ordering of A'-span and slow-A-span, but which both are intermediary stages between A-span and B-span. (b) Two scenarios explaining why late-life DAF-2 AID cessation might increase lifespan and health. Scenario 1: DAF-2 AID simply switches in mid-late life from being beneficial to detrimental. Scenario 2: there are two separate, parallel effects (e.g. on different pathologies) of DAF-2 AID, one strongly beneficial but which decreases in magnitude with age, and the other constantly and weakly detrimental. When the magnitude of benefit becomes less than the magnitude of detriment, the detrimental effects are unmasked and become life and health-limiting.

Possible scenarios for why late-life cessation of DAF-2 AID improves health and survival include: (1) reducing IIS is beneficial in earlier life but detrimental in later life, or (2) reducing IIS is simultaneously (more) beneficial and (less) detrimental (possibly affecting different age-related pathologies), but the magnitude of benefit decreases during ageing, thereby unmasking the detrimental effects in later life (Figure 5.22b). A scenario mentioned earlier, that (beneficial) IIS reduction in earlier life is necessary for later life reduction to become harmful, would be one example of scenario 1 above. Another example, could be that severe IIS deficiency (resulting from DAF-2 AID) is simply a major physiological disruption to less-resilient, decrepit animals, thus becoming harmful in later life. Interestingly, this would

imply that decrepit individuals are rapidly killed off by IIS reduction (once they enter gerospan), which could contribute to the very short (mostly unchanged) gerospans given DAF-2 AID treatments (e.g. Figure 5.12, p. 135). Restoring wild-type IIS may thus also restore wild-type gerospan (in addition to modest rejuvenating increases in healthspan, Figure 5.20).

To conclude, it is notable that all the scenarios above are consistent with antagonistic pleiotropy theory, where a single trait may both ameliorate and exacerbate the ageing process, either at same or different times in life. Most importantly, the findings of this chapter were made possible through a focus on individual ageing trajectories. This demonstrates the utility and biological relevance of individual-focused methods for understanding ageing in populations, as the central aim of biogerodemography.

## **Chapter 6** – Impacts and perspectives

# 6.1 – A biogerodemographic approach to understanding ageing

In this thesis, I have used a "biogerodemographic" approach to understand the phenomenon of ageing. This employs the simultaneous assessment of biological (individual-level) and demographic (population-level) information about ageing, allowing one to be understood in terms of the other. For instance, I have used this approach to investigate the biological basis of the parameters of the Gompertz mortality model, which can capture demographic patterns of mortality in diverse human and animal populations. The biogerodemographic methodologies presented in this thesis should provide a useful template for studying the complex and understudied relationship between biological and demographic ageing (Vaupel and Yashin, 1985, Wilmoth and Horiuchi, 1999, Finkelstein, 2012).

An important strength of the present approach is its emphasis on non-parametric methods. By measuring biological ageing in all individuals of a population, it becomes possible to directly and "causally" explain changes in the Kaplan-Meier survival curve in terms of changes in individual ageing. In other words, because measurements of biological and demographic ageing are taken from the exact same individuals, changes in one measure must translate to changes in the other. This is most easily observed in my regressions of absolute healthspan and gerospan over survival proportion (e.g. Figure 3.7, p. 55), where changes in either must result in equivalent changes in lifespan, since healthspan and gerospan sum up to lifespan. And because these regression plots and survival curves share a common axis that orders individuals by survival proportion, it becomes possible to pinpoint in which individuals these changes occur. This approach thus depends on very few prior assumptions.

Several further advantages stem from the above. Firstly, the approach does not require population survival/mortality to adhere to parametric mortality models. Although I related my findings, obtained by this approach, to the Gompertz model, this was not necessary for my primary aims. Simultaneous population-wide assessment of the ageing process and lifespan (e.g. in the linear regressions described above) alone already fulfils the aim of relating biological and demographic ageing. For instance, I found that parallel rightward shifts of the survival curve typically arise from approximately equal increases of healthspan in all population members, while greater extensions of the survival curve tail typically arise from greater gerospan increases in longer-lived population members. Coincidentally, these survival curve changes correspond closely with those arising from changes in the Gompertz parameters ( $\alpha$  and  $\beta$ , respectively), allowing me to relate them to one another. Therefore, this non-

parametric approach can make sense of mortality patterns in diverse populations, including those with unusual mortality patterns that do not correspond readily to available parametric models.

This flexibility also means that the approach can be used to probe the biological basis of other mortality model parameters. Indeed, the mortality in my cohorts may be readily fit to other models besides Gompertz, such as the Gompertz-Makeham, Weibull, or logistic models, with little loss or even improvement in goodness-of-fit (particularly for models with more parameters).

Another advantage is that the analysis is informative regardless of the definition of healthspan and gerospan (e.g. decline in locomotory capacity versus cardiovascular function), including whether they are discrete (as in this thesis) or continuous measures. By repeating the analysis with different mechanistic definitions of healthspan and gerospan, it also becomes possible to understand how different biological traits/processes vary between individuals during ageing, and how their combined variation explains the demographic survival and mortality patterns. Thus, the analysis is also possible between populations of any condition and species, given that all experience ageing, and therefore all have healthspans and gerospans. Of course, however, these analyses would require the availability of health data, ideally of a longitudinal nature, for each individual within the control and treatment populations.

In this thesis, I defined healthspan and gerospan based on locomotory capacity decline (see Methods), which captures well-characterised stages of nematode ageing (Hosono et al., 1980, Herndon et al., 2002) and is a physiologically integrative measure of overall health relevant across species. How might altering the definition of healthspan and gerospan affect their relationship with measures of demographic ageing, including the Gompertz parameters? I showed that locomotory gerospan was a consistently more inter-individually variable stage of life than locomotory healthspan, across 45 different cohorts (from the 24-cohorts, daf-16(0) and DAF-2 AID experiments). This is consistent with the conventional wisdom that ageing is highly variable between individuals, likely due to the late-life natural selection shadow, a key determinant of the evolution of ageing (Medawar, 1952, Williams, 1957) that predicts greater optimisation (thus, standardisation) of early than later-life traits. Given this, one prediction is that most definitions of healthspan and gerospan will reveal greater variability in the latter, including for non-health-impairing traits, such as loss of hair pigmentation. Therefore, it may be that  $\beta$  is generally a better measure of that more variable final stage of life (gerospan), whereas  $\alpha$  better captures the more stereotypical, earlier stages of life (healthspan).

Another consideration is that given the gradual nature of ageing, any delineation of healthspan and gerospan is inevitably somewhat arbitrary (Zhang et al., 2016, Newell Stamper

et al., 2018). Thus, it is likely that I have even underestimated the contribution of gerospan variation to  $\beta$ , given that gerospan as I defined it excluded earlier ages with subtler senescent changes.

## 6.2 – *An empirical reinterpretation of the Gompertz parameters*

Using my biogerodemographic approach, I set out to test long-standing biological interpretations of the Gompertz parameters. These traditional views are that the scale parameter  $\alpha$  reflects ageing-independent mortality, while the rate parameter  $\beta$  reflects the biological rate of ageing. As I show in section 2.3 (p. 31), these views are widely used to draw biological conclusions about populations, including the effects of lifespan interventions. However, these interpretations of the Gompertz parameters have not been empirically validated and have also been contested on theoretical grounds (Driver, 2001, Yashin et al., 2002b, Driver, 2003, Masoro, 2006, Rozing and Westendorp, 2008, Koopman et al., 2011, Hughes and Hekimi, 2016).

Across 45 different cohorts (from the 24-cohorts, daf-16(0) and DAF-2 AID experiments), I found a consistent pattern in that  $\alpha$  was a stronger predictor of healthspan duration than  $\beta$ , suggesting that  $\alpha$  is in fact a robust measure of biological ageing rate, rather than of ageing-independent mortality. In contrast,  $\beta$  was more consistently a measure of the degree of inter-individual variation (in several traits, but most notably in gerospan duration) rather than of biological ageing rate within individuals. These results not only argue against the traditional interpretations of the parameters but invert them. Additionally, both parameters reflected (in different ways) the presence of subpopulations with distinct pathologies (section 3.6), despite all individuals having identical genomes and environmental exposures.

Notably, this reinterpretation of the Gompertz parameters was supported across a diverse range of biogerodemographic changes. Over the course of this thesis, I characterised the biological basis of different combinations of changes in the Gompertz parameters. Here, I collect and present together these different biogerodemographic changes, which provide biological explanations for all the ways in which lifespan can be increased according to the Gompertz model (Figure 6.1).

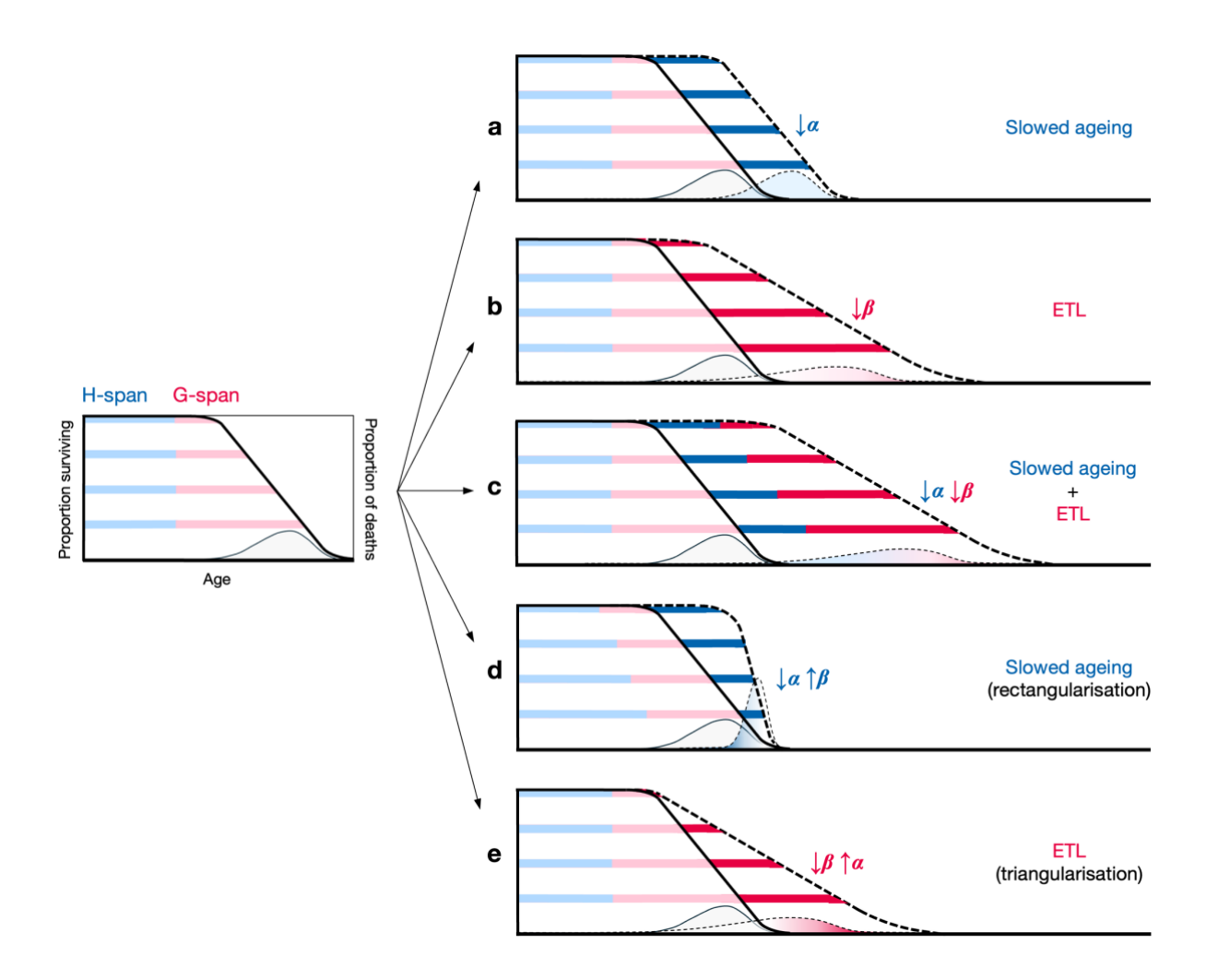


Figure 6.1. Biological basis of different life-extending Gompertzian biogerodemographic changes. Compilation of all the biogerodemographic changes characterised in this thesis, which captures all the ways in which Gompertz parameter changes can extend lifespan. For detailed explanations, see the same component figures in their respective earlier sections. In brief, increases in lifespan arise from increases in healthspan (H-span, darker blue) or gerospan (G-span, darker red), which respectively reflect slowed biological ageing and extended twilight longevity (ETL). Increases in H-span are depicted on the far right to show its effect on the survival curve, but in reality occur before G-span. The shading within the death frequency distributions indicates the type of change (increase in H-span or G-span) and the interindividual variation of this change across the population (solid or gradient).

I found that rightward shifts of the survival curve ( $\alpha$  reduction) result from equivalent increases in healthspan (H-span) in all population members, thus reflecting slowed biological ageing (Figure 6.1a). Meanwhile, stretching of the survival curve ( $\beta$  reduction) results in most cases from gerospan (G-span) increases (in some cases H-span increases, e.g. in daf-16(0) and possibly DAF-2 AID), which occur mainly in longer-lived population members (Figure 6.1b). This causes an expansion of relative morbidity (proportion of life in G-span), particularly in longer-lived individuals. I termed this phenomenon "extended twilight longevity" (ETL), after the extended relative "twilight" used to describe greater relative gerospans of longer-lived individuals within (rather than between) populations (Zhang et al., 2016). Notably, these H-

span and G-span changes were observed to combine additively in treatments that stretched *and* shifted the survival curve (reductions in both  $\alpha$  and  $\beta$ ) (Figure 6.1c).

I also showed that rectangularisation of the survival curve, involving a type of Strehler-Mildvan correlation (simultaneous  $\alpha$  reduction and  $\beta$  increase), results from increases in H-span in shorter-lived population members, reflecting slowed ageing in these individuals (Figure 6.1d). Finally, the opposite form of life-extending S-M correlation (triangularisation, entailing  $\alpha$  increase and  $\beta$  reduction) results from G-span increase in longer-lived population members, as another case of ETL (Figure 6.1e). These 5 biogerodemographic transformations of the survival curve capture all the different ways in which lifespan is extended in my nematode treatment cohorts.

Most notably, across these biogerodemographic changes, a consistent pattern exists in how H-span and G-span change. H-span increases either equally in all population members or primarily in shorter-lived ones. In contrast, G-span always increases more in longer-lived population members. Thus, H-span determines the age of population mortality onset (position of the survival curve shoulder, i.e.  $\alpha$ ), while G-span determines the length of the curve tail (i.e.  $\beta$ ). Importantly however,  $\beta$  reflects more than just variation in G-span. More precisely, it reflects the *degree* of inter-individual variation, of any trait: here, an increase in G-span variation when  $\beta$  decreases (Figure 6.1b–c, e), and decrease in H-span variation when  $\beta$  increases (in rectangularisation, Figure 6.1d). I also showed this relation between  $\beta$  and inter-individual variation for other traits, including end-of-life pathologies and bacterial contact behaviour in early-adulthood. I will discuss in section 6.4 and 6.5 potential biological and evolutionary reasons for this striking, stereotypical H-span and G-span behaviour (changing in shorter- and longer-lived population members, respectively).

This reinterpretation of the Gompertz parameters demonstrates the critical distinction between biological and demographic ageing (Vaupel and Yashin, 1985, Wilmoth and Horiuchi, 1999, Finkelstein, 2012). My data show that biological ageing is more complex than that predicted by traditional views of Gompertzian ageing. For instance, despite having identical genomes and environments, I find within my populations subpopulations exhibiting distinct trajectories of late-life disease, whose prevalence and lifespan are consistently reproduced across trials. Thus, even if one acknowledges that demographic ageing is an *indirect* metric of biological ageing, it is rarely safe in practice to assume equivalence between them. Therefore, direct quantification of biological ageing should always be performed where possible.

My reinterpretation of the Gompertz parameters also offers perspectives on unresolved concepts in gerodemography. In particular, is a new view of the Strehler-Mildvan (S-M) correlation, which describes an inverse relationship between  $\alpha$  and  $\beta$  that is often observed across human and animal populations (Strehler and Mildvan, 1960). My biological explanation of rectangularising S-M correlations (Figure 6.1d) provides empirical support for differential heterogeneity explanations of the S-M correlation, which to date have remained largely theoretical hypotheses (Vaupel and Yashin, 1985, Yashin et al., 2001, Hawkes et al., 2012). My finding here is highly reminiscent of survival in human populations, which has rectangularised over the last two centuries due to improved prevention of earlier life mortality (Riley, 2001), a pattern which has been predicted to both homogenise individuals and facilitate the compression of morbidity (Fries, 1980). Interestingly, a recent report (Yang et al., 2025) showed that interventions in model organisms that increase the relative steepness of survival curves can indeed compress morbidity, in line with my findings; I will discuss this study further in the next section.

I also describe a second type of life-extending (triangularising) S-M correlation, arising from a highly variable ETL event (Figure 6.1e). To my knowledge, the effects of this type of S-M correlation on the survival curve have not been described before, so to aim communication of this concept, I have called it a "triangularising" S-M correlation (c.f. rectangularising S-M correlations), given its effect upon the survival curve.

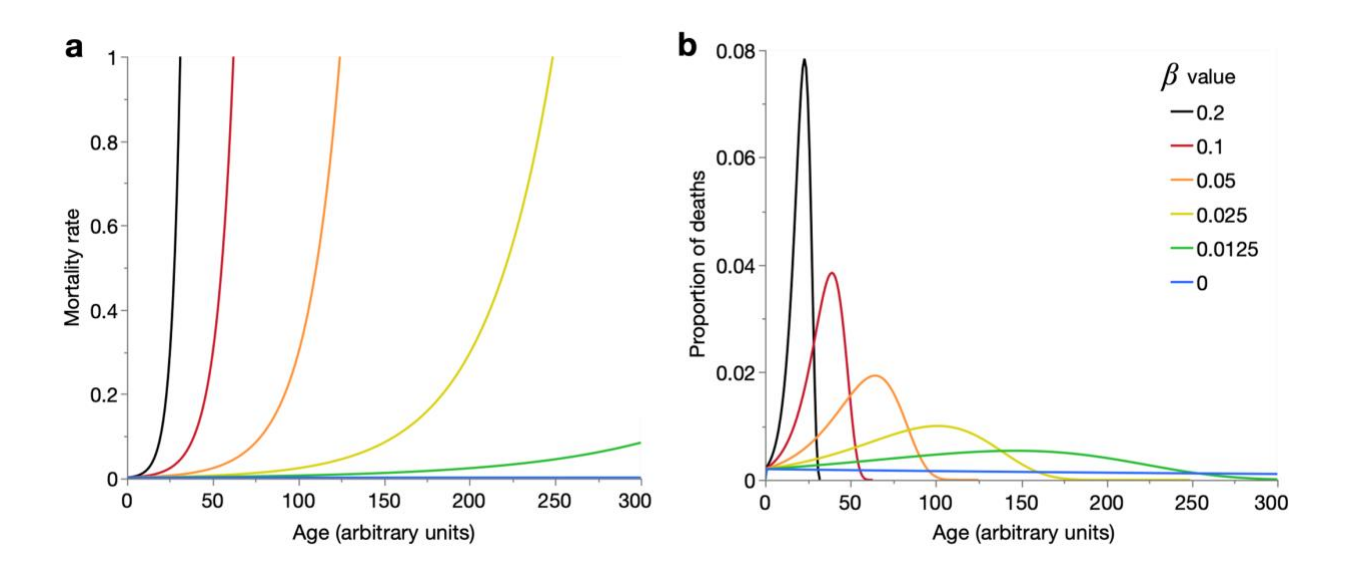
Interestingly, my new views of the Gompertz parameters also resolve two paradoxes arising from attempts to understand the S-M correlation using the traditional views (section 4.1, p. 84): (1) the simultaneous "parametric antagonism" of ageing-related ( $\beta$ ) and ageing-independent ( $\alpha$ ) effects on lifespan, and (2) the evolutionary paradox relating to the expected relationship between extrinsic mortality ( $\alpha$ ) and ageing rate ( $\beta$ ). My reinterpretation of  $\alpha$  and  $\beta$  therefore offers an empirical biological explanation of the S-M correlation that is also parsimoniously consistent with existing data and theory.

My findings also offer a perspective on the late-life mortality deceleration observed in many model organism and possibly human populations (Vaupel et al., 1998, Gavrilova and Gavrilov, 2014). No clear consensus yet exists about the cause of this mortality deceleration, although explanations typically argue either for the occurrence of real deceleration of biological ageing rate, or the presence of intra-population heterogeneity in frailty (which increases the proportion of robust individuals at later ages). This late-life mortality deceleration causes an extension of the survival curve tail, not unlike (but differently to) that resulting from  $\beta$ 

reduction. A possibility therefore is that this preferential increase of lifespan in longer-lived population members also results from ETL, that is, an expansion of gerospan in these individuals. Indeed, the logistic model of mortality which includes a third, deceleration parameter (Kannisto, 1994, Pletcher, 1999; Eq. 1.3, p. 17) fits many of my cohorts as well or even better than the Gompertz model (data not shown).

If late-life mortality deceleration reflects ETL, this would provide support for the population heterogeneity explanation, as the extended survival curve tail would reflect increased *variation* in gerospan length, rather than deceleration of biological ageing rate within individuals. Interestingly, however, this gerospan expansion suggests that the "robustness" of these longer-lived individuals applies to lifespan rather than healthspan, given that the latter is not also extended. I will discuss the complex relationships between healthspan, gerospan and lifespan in greater detail in section 6.5.

Finally, my reinterpretation of the Gompertz parameters has intriguing implications for Gompertzian mortality itself. A possibility is that the uncoupling of demographic and biological ageing that I have demonstrated also extends to the *exponentiality* of Gompertzian mortality. Importantly, the Gompertz rate parameter  $\beta$  controls not only the rate of exponential increase in mortality rate, but existence of the exponential itself. When  $\beta$  is reduced to zero, the exponential mortality rate function collapses to a horizontal line, denoting constant mortality over time (Figure 6.2a). As I found that  $\beta$  reflects the degree of inter-individual heterogeneity in ageing rather than biological ageing rate itself, the exponential mortality trajectory, which is determined by  $\beta$ , may thus also reflect inter-individual variation in ageing rather than the ageing process itself.



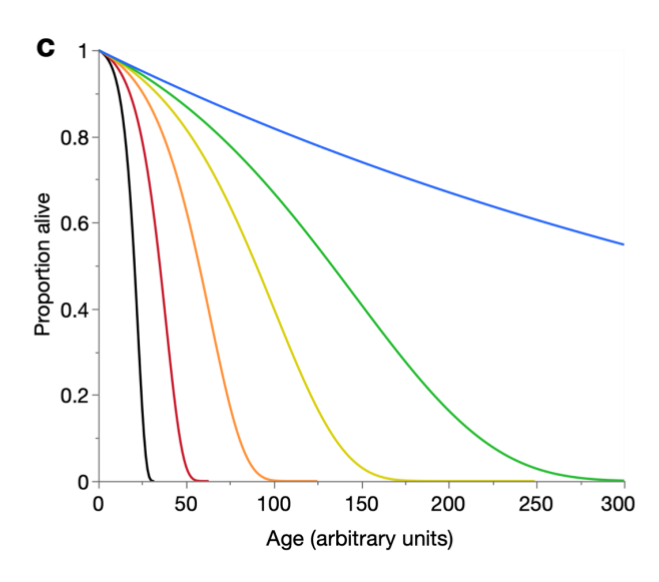


Figure 6.2.  $\beta$  controls the rate and existence of exponential mortality. Simulated effects of progressive reduction of the Gompertz rate parameter  $\beta$  on (a) mortality rate, (b) frequency distribution of deaths, and (c) survival proportion. The x-axes are truncated at 300 (arbitrary units). In all cohorts,  $\alpha$ =0.002.

Supporting this idea, I showed earlier in this thesis that the probability distribution of deaths in a theoretical population with Gompertzian mortality is unimodal (single-peaked), with a moderate right skew (longer left tail) (Figure 2.1d, p. 25); importantly, reduction of  $\beta$  stretches out this distribution, increasing lifespan variation. Further reducing  $\beta$  to zero causes this unimodality (i.e. peak) to disappear entirely (Figure 6.2b), just as the exponentiality of mortality rate disappears when  $\beta$  reaches zero (Figure 6.2a). This illustrates how the exponential trajectory emerges simply where there is a tendency for individuals to die around a certain age, and not necessarily due to any particular nature of mechanism leading up to death. Indeed, a generalised normal distribution has been reported to better fit certain human mortality frequency distributions than a Gompertzian distribution (Clark et al., 2013). This is therefore another instance of the distinction between demographic (the unimodal distribution of deaths) and biological ageing (the cause of death). Thus, in the same way that  $\beta$  does not reflect biological ageing rate, the exponentiality of Gompertzian mortality may not reflect the ageing process.

This may be understood through theoretical and real examples. It is conceivable that exponential mortality rates can arise in a population of young (or even non-ageing) individuals, if extrinsic mortality kills them with a frequency distribution similar to that observed in ageing individuals. Indeed, exponential increases are frequently observed in breakdown rates of machines and rates of change in other non-biological phenomena, showing (in an albeit simplistic, *a priori* way) that the exponential itself need not be related to ageing. Similarly, it is not uncommon that populations comprised of ageing individuals do not exhibit exponential

mortality increases. For instance, constant mortality rates have been observed in populations of biologically ageing organisms, such as of the long-lived *C. elegans* mutants daf-2(e1368) and age-1 (Vaupel et al., 1998, Chen et al., 2007), fission yeast (Spivey et al., 2017) and captive chimpanzees (Hill et al., 2001). The constant mortality in these cases could reflect specific environmental or methodological conditions (unrelated to ageing) that greatly increase lifespan variation. Evidence is also emerging of biological ageing processes in naked mole rats (Horvath et al., 2021, Kerepesi et al., 2022, Fatima et al., 2022), which exhibit approximately constant mortality rates and thus lack demographic ageing (Ruby et al., 2018, Ruby et al., 2024). Survival curves of such populations with constant mortality ( $\beta$ =0) have a form resembling an extremely elongated tail, as expected of reductions in  $\beta$  (Figure 6.2c).

Therefore, it is possible that in many populations, the exponentiality of Gompertzian mortality more accurately reflects the amount of inter-individual variation in ageing, rather than any specific mechanism of the ageing process itself. If correct, this simple "explanation" of Gompertzian mortality could help explain its great pervasiveness across species and environments, given that variability in the ageing process is a universal feature of all populations, regardless of their specific ageing mechanisms. It would also argue against interpreting any increase in mortality rates as the presence of ageing without empirical support, and similarly, against the designation of organisms as "non-ageing" based solely upon having non-Gompertzian mortality (Martínez, 1998, Ruby et al., 2018).

# 6.4 – Understanding the Gompertz parameters in higher organisms

An overarching aim of the investigations of this thesis is to understand general properties of the biology of demographic ageing, especially ones that may be relevant to human populations. So, to what extent are my nematode-derived interpretations of Gompertzian mortality likely to be applicable to higher animals?

The frequent occurrence of Gompertzian ageing throughout the animal kingdom (Finch et al., 1990, Jones et al., 2014) and the universality of healthspan and gerospan (irrespective of specific mechanisms) at least suggests this possibility. The ways in which the Gompertz parameters change are also conserved across species. For instance, any extension of lifespan must entail a reduction in at least one parameter (Figure 6.1, p. 155). Specific combinations of parameter changes are also conserved, such as the S-M correlation that is frequently observed in human and model organism populations (Strehler and Mildvan, 1960, Shen et al., 2017).

However, organism-specific patterns in parameter changes have also been reported. For example, it has been suggested that most life extension in *C. elegans* appears to result from reduction of  $\beta$ , whereas life extension in rodents and humans arises more from reductions in  $\alpha$  (Finch, 1990, Yen et al., 2008, Hughes and Hekimi, 2016), although this view about rodent demography is contentious (de Magalhães et al., 2005, Simons et al., 2013). Consistent with this, out of all the nematode treatments examined in this thesis (24-cohorts, daf-16(0) and DAF-2 AID experiments), 29/73 (40%) significantly decreased  $\alpha$ , compared to 51/73 (70%) that significantly decreased  $\beta$ . If my findings about the biological meaning of the Gompertz parameters are correct across species, it would imply that the biological basis of life-extension is fundamentally different between such species. Specifically, that life-extension in nematodes primarily reflects gerospan expansion, but in mammals, more so healthspan expansion.

Intriguingly, a recent study supports my findings across several species (Yang et al., 2025). The authors describe a mathematical model of the ageing process that predicts a compression of relative gerospan by life-extending treatments that increase the relative steepness of the survival curve, and negligible to mild expansion of relative gerospan by treatments that maintain relative steepness. Translating these survival curve effects into approximate Gompertz terms reveals a close concordance between our two findings: rightward shifts and rectangularisation of the survival curve (i.e. involving  $\alpha$  reduction) involve healthspan expansion, while horizontal stretching of the survival curve (i.e. involving  $\beta$ reduction) involves mild gerospan expansion. Importantly, the authors supported their theoretical predictions with mined population-average health and mortality data from nematodes, fruit flies and mice, where interventions that increased relative steepness indeed compressed relative morbidity. These data thus provide independent support for my findings, and extend their potential relevance to other species. My investigations further extend these findings through individual-level analyses of the relationship between healthspan, gerospan and lifespan, which is required to explain (rather than correlate) survival curve shape in terms of the inter-individual distribution of biological ageing profiles.

Another intriguing possibility is that this biological basis of the Gompertz parameters may also apply *between* species. Like interventions that extend lifespan in *C. elegans*, the evolution of longer-lived species from shorter-lived ones often involves coupled reductions in both  $\alpha$  and  $\beta$ , where mortality is both postponed and spread out over greater lengths of time. For instance,  $\alpha$  at puberty decreases from 0.03 in laboratory mice to 0.0002 in humans, and subsequent mortality rate doubling time (an inverse measure of  $\beta$ ) respectively increases from 0.27 to 8 years (Finch et al., 1990). This raises the question of whether evolution of greater longevity might also reduce  $\alpha$  by extending healthspan and reduce  $\beta$  by ETL (Figure 6.3). In

other words, the reduction of  $\beta$  in longer-lived mammals might only indirectly reflect reduced biological ageing rate, which is instead directly reflected in the reduction of  $\alpha$ .

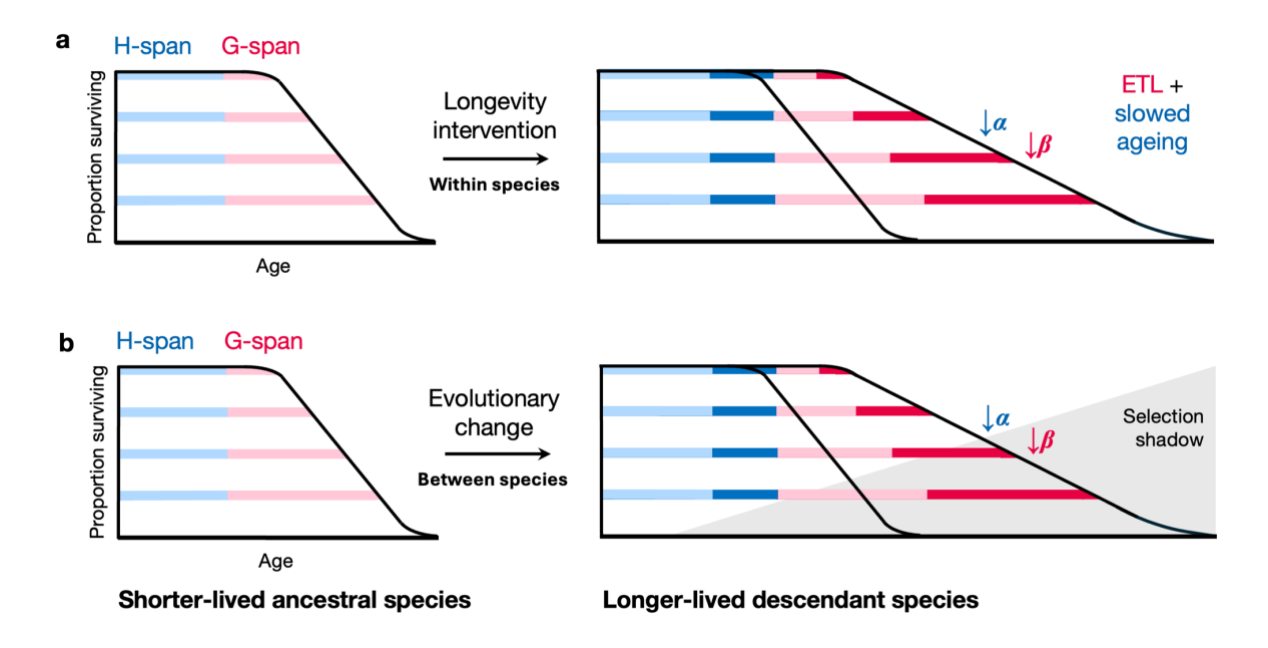


Figure 6.3. Potential role for healthspan extension and ETL in the evolution of longevity. Schematic of the biological basis of the Gompertz parameters within and hypothetically, between, species. (a) Reduction of  $\alpha$  by healthspan (H-span) extension and reduction of  $\beta$  by extended twilight longevity (ETL). As I show in *C. elegans*, the increased variance in lifespan that reduces  $\beta$  arises from interindividually variable expansion of gerospan (G-span), as part of the phenotypic variability that emerges and progressively increases during ageing. This simplified representation shows no inter-individual variation or change in H-span. (b) Reduction in  $\alpha$  and  $\beta$  during evolution of increased longevity (hypothetical scheme). Here again, reduced  $\beta$  reflects increased lifespan variance due to interindividually variable expansion of G-span, arising from the selection shadow (reduced force of selection) in later life on the evolved genome. This evolutionary ETL is coupled to a less variable expansion of H-span, corresponding to slowed ageing, that reduces  $\alpha$ .

This coupled evolution of healthspan and gerospan expansion, and therefore  $\alpha$  and  $\beta$ , could emerge from biological constraints present between mechanisms of development and ageing (Gems and Kern, 2024) that exhibit evolutionary conservation. This would be consistent with the proportional scaling between life stages across mammalian species, such as that between ontogenetic span and adult lifespan (~1:4) (Charnov, 1993). Additionally, the greater variability of gerospan than healthspan could arise from the late-life natural selection shadow, a key determinant of the evolution of ageing (Medawar, 1952, Williams, 1957) that predicts greater optimisation (thus, standardisation) of early than later-life traits (Figure 6.3b).

Finally, as I explained in section 6.1, the non-parametric approach by which my results were obtained suggests that they are likely to be relevant to species with non-Gompertzian mortality patterns. At their most fundamental level, my findings show that gerospan is an inherently more variable stage of life than healthspan, and that increases in healthspan and

gerospan occur preferentially in shorter and longer-lived population members, respectively (Figure 6.1, p. 155). Therefore, the effects of healthspan and gerospan on demography are not specific to Gompertzian populations, and likely to be applicable to a wider range of changes in mortality and survival.

## 6.5 – A complex relationship between ageing and lifespan

Throughout this thesis, I have examined the relationships between healthspan, gerospan and lifespan across many differently longevous nematode populations. These relationships have emerged to be more complex than assumed by traditional mortality model parameters, yet exhibit several surprisingly straightforward patterns, despite a range of possible survival curve changes. Most strikingly, H-span tends to change in shorter-lived or all population members (though sometimes in longer-lived ones, e.g. with *daf-16(0)* and DAF-2 AID), while G-span tends to change in longer-lived ones (Figure 6.1, p. 155). If these patterns also occur beyond these particular nematode cohorts (including in other species), an important implication would be that one could, with reasonable accuracy, predict the biological basis (in the broad terms of H-span and G-span) of a change in the survival curve. Conversely, but more tentatively, one could in principle predict the effects of life-extending interventions on the survival curve by measuring the health of treatment animals shortly after control animals begin dying (without having to complete the full treatment lifespan).

Why might H-span and G-span change in shorter-lived/all and longer-lived population members, respectively? Across all the nematode cohorts examined in this thesis, G-span was a consistently more variable stage of life than H-span (Figures 3.10, 5.4c, 5.14c, pp. 60, 112, 137). Specifically, increases in mean G-span were coupled to faster increases in G-span variation, than in mean H-span to H-span variation. In the last section, I suggested that this invariance of H-span and variability of G-span may reflect greater evolutionary selection and standardisation of earlier life traits (H-span). Thus, if H-span is inter-individually invariant, then naturally it would increase relatively equally in all population members. Similarly, because G-span is more variable, it would exhibit a wider range of magnitudes of increase across the population; naturally, the smaller increases would belong to shorter-lived individuals and larger increases to longer-lived individuals. Thus, G-span tends to increase more in longer-lived population members.

However, this does not explain why H-span can also increase more in shorter-lived population members, which occurs in rectangularising S-M treatments (Figure 6.1d, p. 155).

Here, a possibility is that in populations that undergo rectangularisation, H-span is to an extent truncated in shorter-lived individuals. Indeed, I showed that H-span of these populations was more inter-individually variable than in populations that underwent ETL in response to life-extending treatment (Figure 4.6e, p. 94). Therefore, in populations with more variable H-span, interventions may more readily rescue this "hypo-H-span" of shorter-lived population members (restoring it to H-span lengths of longer-lived members), than further extend maximum H-span. This is my current working model of the biological basis of rectangularising S-M treatments (Figure 6.1d). Thus, H-span would be increased more in shorter-lived population members.

What do these increases in H-span and G-span mean biologically? Throughout this thesis, I have interpreted H-span increases to reflect a slowing of biological ageing rate, given that more time elapses before animals reach G-span onset. Another possibility is that animals begin ageing later, but at the same subsequent rate, although in the case of DAF-2 AID treatments, I provided evidence of the former scenario (ageing slower rather than later) (see sections 5.3 and 5.5, pp. 132, 143). However, in either scenario (which could also co-occur), functional healthspan is extended, reflecting a desirable improvement in the ageing process.

Interestingly, by the same logic, one could potentially interpret G-span expansion (e.g. in ETL) as a reduction in biological ageing rate during these later ages (given more time to reach death). Note however, that this does not imply that  $\beta$  reflects biological ageing rate (as traditionally viewed);  $\beta$  remains a measure of the inter-individual *variation* in G-span, and is only an indirect measure of the G-span itself. However, in more precise terms, it could be correct to say that reduction of  $\beta$  reflects slowed biological ageing rate specifically during G-span and primarily in longer-lived population members (for a visual aid, see Figure 6.1b, p. 155). And, that increases in  $\beta$  (in rectangularisation) reflect slowed biological ageing rate during H-span and mainly in shorter-lived population members (see Figure 6.1d). Notice that this complex relationship between  $\beta$  and biological ageing rate is far from that assumed in the much simpler traditional understanding of the relationship (that  $\beta$  is a positive metric of ageing rate in all population members).

The above discussions highlight a curious feature of the ageing process in these treatment cohorts, which is that H-span or G-span can increase alone without constrained increases in the other. Consequently, this leads to the surprising interpretation that ageing rate is slowed only during earlier adulthood (if only H-span increases, e.g. in  $\alpha$  reduction or rectangularising S-M) or only later in life (if only G-span increases, e.g. in  $\beta$  reduction or triangularising S-M). Two possible scenarios (amongst others) that could explain this uncoupling of H-span and G-span are:

- 1. There is a single biological process determining both H-span and lifespan, which indeed slows down only during H-span (in H-span expansion) or only during G-span (in G-span expansion) (Figure 6.4a).
- 2. There are separate biological processes determining H-span and lifespan, with relatively constant rates throughout life: both slow down in H-span expansion, while only that determining lifespan slows down in G-span expansion (Figure 6.4b).

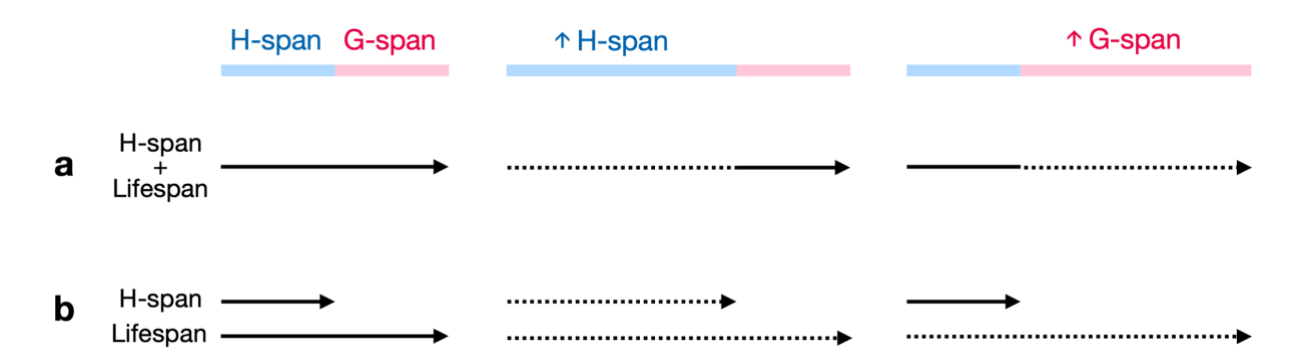


**Figure 6.4. Two biological models of the decoupling of H-span and G-span.** Two hypothetical biological explanations of increases in healthspan (H-span) alone or gerospan (G-span) alone. For simplicity, these explanations are depicted for a single hypothetical individual, but they apply the same to changes in multiple individuals (i.e. a population). (a) H-span and lifespan are determined by a single biological process, which slows down (dashed line) during H-span in H-span expansion, or during G-span in G-span expansion. (b) H-span and lifespan are determined by different biological processes, which both slow throughout life in H-span expansion, but only the lifespan-determining process in G-span expansion.

Which of these two scenarios is more relevant in my cohorts would be important to determine. In support of the second model, an earlier study suggested that the increased G-span of daf-2(rf) mutants arises from enhanced resistance against life-limiting  $E.\ coli$  infection, but not other aspects of ageing (Podshivalova et al., 2017). This model would also be consistent with the multifactorial nature of ageing, where multiple parallel and/or interacting processes may determine some or all ageing-related outcomes, including death (Gems, 2015). Importantly, if this second model is correct, this would imply that H-span and G-span as defined here (based on locomotory health) are specifically measures of *functional* H-span and G-span (i.e. quality of life), rather than those describing an organism's ability to remain alive during ageing. To distinguish between these cases, one could subject animals upon individual entry to G-span to a strong stressor; if this G-span were a state of *life*-limiting (rather than H-span-limiting) frailty, individual post-stress survival should be relatively invariant.

To conclude this final section, I will return to a central recurring theme of this thesis: the role of inter-individual variation in determining ageing and lifespan. I have shown that

individuals vary in ageing rate and trajectory, and that the distribution of this variation can directly explain the shape of survival curves. Thus, identifying the origin of this variation is essential to understanding ageing in populations, and effects of interventions upon them. I demonstrated in section 3.7 (p. 80) that lifespan variation (and  $\beta$ ) can be predicted by bacterial contact behaviour in early adulthood (during H-span), suggesting that the origin of such variation may be relatively early in life. Indeed, several early-life predictors of individual mortality (within populations) have been identified in *C. elegans*: ROS levels in L2 larvae (Bazopoulou et al., 2019), nucleolus size in day 1 adults (Tiku et al., 2017), lipid droplet number in day 1 and 6 adults (Papsdorf et al., 2023), mitochondrial superoxide generation frequency in day 3 adults (Shen et al., 2014), and intestinal *E. coli* content in day 3 adults (Baeriswyl et al., 2010), amongst others (Pincus and Slack, 2010).

The origin of lifespan variation can thus emerge as early as during development (or earlier in the event of variation in oocyte composition). Notably, these are isogenic individuals cultured under tightly controlled environmental conditions, arguing against a wholly random origin of this lifespan variation. Thus, a thorough understanding of the biogerodemography of a population requires comprehension of the origin of inter-individual variation.

Identification of early-life lifespan predictors (i.e. biomarkers) could also provide an invaluable research tool. In this thesis, I assume that survival proportions between control and treatments cohorts are directly comparable. For instance, in ETL, I make the interpretation that G-span is increased in longer-lived population members (Figure 6.5, upper outcome). However, this is of course an assumption, given that the control and treatment cohorts are comprised of different individuals. For example, it could be (though perhaps unlikely) that G-span is in fact increased most in individuals that would have been the shortest-lived control population members (Figure 6.5, lower outcome). If one could predict prior to treatment the approximate lifespan of individuals using the aforementioned biomarkers, it would become possible to directly "track" individuals between control and treatments cohorts.

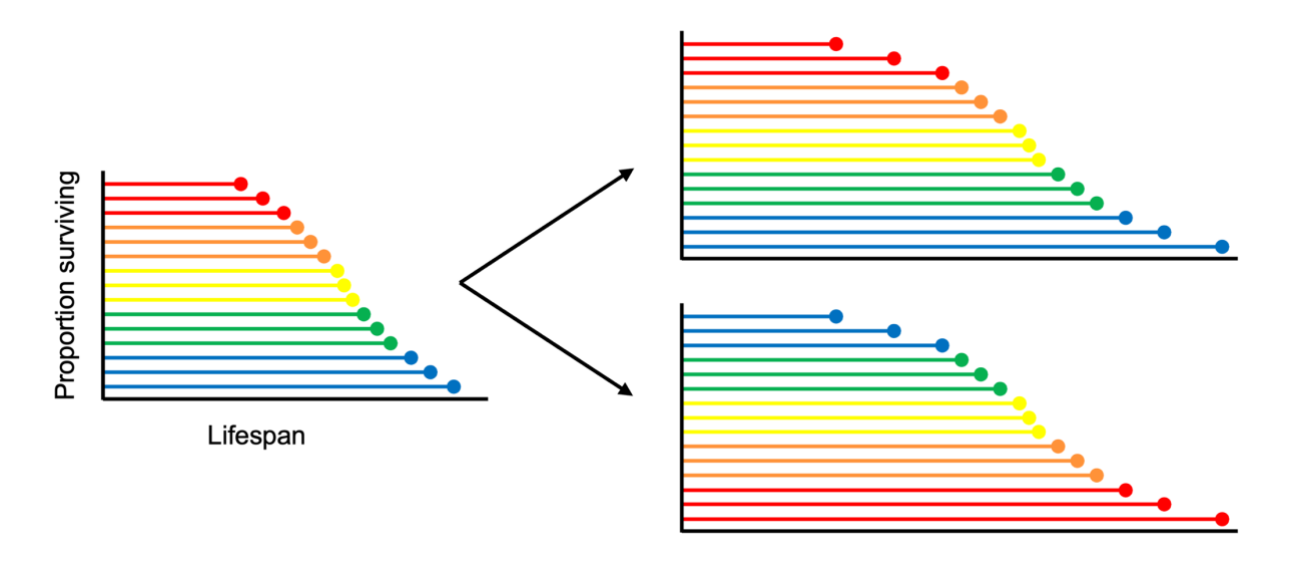


**Figure 6.5.** Hypothetical effects of a life-extending intervention on different population members. Different individuals/subpopulations are represented as different colours. On the right, the upper outcome entails a preservation of the population death order, where individuals that would have died first in the control still die first in the treatment cohort. In contrast, the lower outcome entails a hypothetical reversal of the death order (as a simple example), where individuals that would have died earlier in the control now live the longest, in response to the treatment.

In summary, the inherent variation within populations provides an important and powerful means to understand the biology of ageing. Because the ageing process differs between all individuals (particularly in reproducible, non-random ways), its study by definition concerns its variable presentations between and within populations. An understanding of the variability of ageing is critical for research on interventions affecting the ageing process, particularly in the management of ageing in (highly variable) human populations. Furthermore, the existing lifespan variation within populations may offer readily attainable clues about the mechanisms determining lifespan, which could also be relevant between populations. Thus, any effective biological theory of ageing should also be a *biogerodemographic* theory of ageing, with the ability to explain differences in ageing not only between, but within populations.

#### **Conclusions**

In this thesis, I have developed a "biogerodemographic" approach to understanding the biology of ageing in Caenorhabditis elegans. This entailed the simultaneous measurement of biological ageing (of all population members) and demographic ageing (of the population), enabling a direct investigation of the complex relationship between them. I used this approach to determine, across 73 life-extending treatments, the biological basis of the two parameters of the Gompertz model of mortality, which has been widely employed to describe exponential mortality trajectories in human and animal populations. Notably, I found an inversion within my data of the traditional (but untested) biological interpretations of these parameters: the scale parameter  $\alpha$  reflected the rate of biological ageing (as the duration of healthspan) rather than ageing-independent mortality, while the rate parameter  $\beta$  reflected the amount of interindividual variation in the ageing process (particularly of gerospan duration), rather than the rate of biological ageing (Chapter 3). These new, empirical interpretations of  $\alpha$  and  $\beta$  could also make sense of the enigmatic, inverse Strehler-Mildvan correlation between the Gompertz parameters (Chapter 4), as well as the broader biogerodemography of the insulin/IGF-1 signalling pathway (Chapter 5). Importantly, beyond the Gompertz parameters, my findings show that gerospan is a more inter-individually variable stage of life than healthspan, and is increased in longer-lived population members by life-extending interventions. In contrast, healthspan tends to increase equally in all, or selectively in shorter-lived, population members. Thus, these two life stages have distinct and consistent effects upon demographic mortality and survival, maintained across different lifespan-extending conditions. Whether these relationships between biological and demographic ageing are evolutionarily conserved, and relevant to human populations, is of great interest. The methodologies and concepts developed in this thesis provide a starting point for making these next discoveries.

#### Methods

#### General methods

#### Strains and stock maintenance

C. elegans were maintained using standard protocols (Brenner, 1974), on 60 mm nematode growth media (NGM)-filled Petri plates seeded with an E. coli OP50 bacterial food source 2 days prior to use, and without the addition of 5-fluoro-2-deoxyuridine (FUDR), which is sometimes used to block progeny production. E. coli OP50 cultures were prepared by inoculating 100 mL of OP50 culture media with several colonies from an OP50 streak plate, and growing for 16 hours at 37°C in a shaking incubator. OP50 cultures were stored at 4°C and replaced every 3–4 months if not used up. 10 mL (6 cm diameter) plates were seeded with approximately 80 μL of OP50 culture, and each 2 mL well of 24-well tissue culture plates with approximately 5 μL of OP50 culture. Bacteria was seeded in the middle of the plate/well, swirled carefully to increase lawn diameter, but not spread over the full media surface. Nematode strains used included N2 (N2 hermaphrodite stock), GA1959 daf-2(m577) III, GA1960 daf-2(e1368) III, GA1928 daf-2(e1370) III, GA1952 daf-16(mgDf50) I, and RAF2181 ieSi57 [eft-3p::TIR1::mRuby::unc-54 3'UTR + Cbr-unc-119(+)] II; daf-2(bch40 [degron::3xFLAG::STOP::SL2::SV40::degron::wrmScarlet::egl-13 NLS]) III.

All strains were thawed from Gems laboratory frozen stocks, and maintained at 20°C with an uninterrupted supply of live *E. coli* for several generations before using animals in experiments. For longer term maintenance between experimental trials, stocks were kept at 15°C. Fresh stocks were thawed approximately every 5–10 months to prevent the accumulation of spontaneous mutations. Leading up to experiments, stocks were maintained by either picking several animals and/or eggs to fresh plates with a sterilised platinum wire, or by transferring a chunk of agar containing animals with a sterilised scalpel to a fresh plate.

All maintenance and experimentation were performed under monoxenic (with *E. coli* OP50 only) conditions. Stocks were cleared of bacterial and fungal contamination by picking several gravid adults into a drop of bleach solution (1:2:1 of M9 buffer, sodium hypochlorite [15% available chlorine], and 5 M sodium hydroxide) on a clean plate, and transferring newly-hatched larvae to a new plate the following day. Mild fungal contamination and newly-discovered bacterial contamination were also cleared by either transferring animals several times between clean plates, or by careful killing of contamination with the round tip of a hot glass pipette. Preventative measures against agar mite contamination were taken by encircling

the outside of stock and experimental containers with a strip of double-sided tape; this sticky barrier prevents mites from entering and exiting each container.

## Age synchronisation of experimental individuals

In all experiments, age-synchronised populations were obtained either by an egg lay (allowing 10–20 gravid adults to lay eggs for 2–3 hours, followed by immediate removal of the adults and picking of L4s ~2.5 days later), or by picking L4s directly from plates with animals of different life stages.

#### *Microscopy*

Stock maintenance and scoring of survival, locomotory health and necropsy pathologies were performed using a standard dissecting microscope (Leica MZ8 stereomicroscope, 50x magnification). Higher magnification images of corpses were captured using a Hamamatsu digital camera C13440 ORCA-Flash4.0 V3 and Zen software (see section-specific methods).

## Lifespan experiments

Age-synchronised L4 animals were placed on 60 mm NGM Petri plates (25–40 animals/plate depending on the experiment) and thereafter transferred to fresh plates every two days to separate them from their progeny. After the reproductive period, animals were transferred to fresh plates (60 mm Petri plates or 24-well tissue culture plates, depending on the experiment) weekly, or before desiccation of the media or depletion of the bacterial food source. In longer lifespan experiments, plates were also wrapped with gas-permeable Parafilm to slow media desiccation and reduce airborne contamination.

Survival was scored every 1–3 days depending on the experiment, by scoring for movement. Animals that did not move spontaneously were gently touched with a cooled, flame-sterilised platinum wire on the head and/or tail; animals that did not move in response were scored as dead. To ensure that non-responding individuals were dead, the platinum wire was applied again with slightly greater pressure, by placing the flattened end on the tail and/or head and sliding it towards the closer end of the worm with a measured downward force. This method I found to reveal movement of terminally ill animals that otherwise do not respond to lighter touches of the wire. Animals that could not be found, were accidently killed during handling, died due to desiccation on the Petri plate wall, had ruptured through the vulva, died due to internal hatching of larvae, or were contaminated by non-*E. coli* bacteria or fungi were recorded as censored. All lifespan data values represent days survived since L4 rather than since hatching (~2.5 days prior to L4).

#### Quantification of locomotory health and ageing

Locomotory health class was scored by classifying individuals into one of three classes, adapted from earlier systems (Hosono et al., 1980, Herndon et al., 2002): A – sinusoidal locomotion; B – non-sinusoidal locomotion; C – no locomotion. To accurately determine locomotory class, animals were first gently touched on the tail with a platinum wire worm pick for up to 20 seconds to induce an escape response that reveals true movement capacity, and where necessary, additionally on the head as a final check. Animals had to travel at least one body length's distance for sinusoidal (S-shaped) locomotion to be confirmed; any irregularities to S-shaped locomotion or failure to travel at least one body length's distance within the 20 seconds resulted in classification as B class. C class individuals were scored if animals could not travel at all and exhibited only stationary movements, usually of the head and/or tail. Very old C class animals were distinguished from dead animals by application of a greater wire force, as described in "Lifespan experiments" above.

A class animals were split into three subclasses in some experiments (sections 5.5, 5.6): (1) A' animals, which begins sinusoidal locomotion only after 5 seconds of a single touch of the tail with the platinum wire, (2) slow-A animals, which begin sinusoidal locomotion within 5 seconds of the touch but travel very slowly in comparison to more youthful A class animals, and (3) fast-A animals, which are those remaining animals which begin sinusoidal locomotion within 5 seconds of the touch and travel faster than slow-A animals.

#### Definition of healthspan and gerospan

In this thesis, locomotory capacity is used as a marker of the ageing process and its rate of progression in *C. elegans*, being a physiologically integrative measure of overall health (Hosono et al., 1980, Herndon et al., 2002). In the analysis of most experiments (unless specified otherwise), the duration of life spent in A class was defined as healthspan and the summed duration of life spent in B and C classes as gerospan. In most cohorts, B-span was very short and had little effect when included within gerospan. Additionally, B and C classes were summed to improve data tractability, and to provide a definition of G-span that captures both early and late-stage functional declines. I distinguished between absolute and relative healthspan and gerospan, to describe the days or proportion of life, respectively, spent in these states.

#### Necropsy scoring of ageing-related bacterial pathologies

Necropsy to define patterns of *E. coli*-associated pathology was performed by examining fresh corpses under a Leica MZ8 stereomicroscope (50x magnification). Scoring of swollen,

bacterially-infected pharynxes (P), and uninfected, atrophied pharynxes (p) was performed as previously described (Zhao et al., 2017). Intestinal colonisation (IC) by *E. coli* was scored where severe bacterial accumulation was observed in the anterior and/or posterior intestine. Such colonisation presented as extreme lumenal distension by proliferating bacteria and/or colonisation of the intestine beyond the lumenal barrier, with concomitant intestinal tissue degeneration and atrophy. These changes are highly suggestive of pathogenic invasion by infective bacteria.

Consistent across pharyngeal and intestinal tissues, sites of bacterial colonisation exhibit a yellowish-brown colour (as that of the *E. coli* lawn and colocalising with RFP-labelled *E. coli*), translucent and uniform texture (loss of healthy tissue structures that otherwise appear dark, granular and opaque), and swollen/distended morphology (extensive proliferation of live *E. coli*). Images of representative examples of the three corpse subpopulations (P [swollen, infected pharynx], pIC [uninfected pharynx but intestine colonised by *E. coli*] and pnIC [uninfected pharynx and no intestinal colonisation by *E. coli*]) are presented in Figure 3.14a (p. 70).

## Statistics and software

All statistical tests were performed in JMP Pro (SAS Institute, Inc.), except for Gompertz parameter estimation by maximum likelihood estimation, and assessment of statistical differences between the Gompertz parameters by likelihood ratio tests, which were performed in WinModest (Pletcher, 1999), provided by Scott Pletcher. All differences between cohort survival were assessed by the log-rank test, except where specified otherwise. Censored individuals were included as right censors in all Kaplan-Meier and WinModest analyses, and indirectly in analyses involving mortality pseudofrequencies (see section-specific methods). Censors were excluded from all other analyses, including most of those involving locomotory ageing and necropsy pathologies, except where specified otherwise. Further, specific statistical tests and relevant methodological details are described in the respective figure/table captions. Notation of statistical significance in all figures is as follows: p > 0.05, \*  $p \le 0.05$ , \*\*  $p \le 0.01$ , \*\*\*\*  $p \le 0.001$ , \*\*\*\*  $p \le 0.0001$ . Necropsy image capture, processing and editing was performed using Zen software and ImageJ. Preparatory data cleaning and analyses were performed in Microsoft Excel, and figures were prepared in JMP Pro (SAS Institute, Inc.) and Microsoft PowerPoint.

Literature survey on interpretations of the Gompertz parameters (Table 2.1 in section 2.3)

A systematic and careful reading of the model organism literature surrounding the Gompertz model of mortality was undertaken. Only studies published since 2000 were included in this survey, and only those using the Gompertz model (or Gompertz family models, e.g. Gompertz Makeham and two-stage Gompertz) to describe their mortality data. Both primary studies and meta-analytical studies were included. These studies were found by searching for key terms in the PubMed database and manual screening of returned hits, as well as through the reference lists of relevant studies. Preprints that have not yet undergone peer-review were not included.

# 24-cohorts experiment (Chapters 3 and 4)

This set of 24 cohorts was subjected simultaneously to survival, locomotory ageing, and necropsy assessments. All strains were raised at 20°C and transferred at L4 to their treatment temperature (15°C, 20°C, or 25°C), at which they remained for the rest of their lives. Carbenicillin cohorts were similarly transferred at L4 onto carbenicillin plates. These plates were prepared by topically adding 80 µL of 500 mM carbenicillin (Fisher Scientific Ltd, catalogue no. 12737149) (dissolved in MilliQ water, and stored long-term at -25°C and up to 7 days at 4°C) around the lawn, one day before adding animals. Carbenicillin-treated plates were stored at room temperature for no more than 7 days; storage at 4°C immediately after carbenicillin addition appeared to reduce the efficacy of this antibiotic treatment, with differences in bacterial appearance and consistency.

In 2/6 trials (Trials 1–2), animals were cultured throughout life in 60 mm Petri plates (containing 10 mL of NGM) seeded with approximately 80 μL of *E. coli*. At L4 stage, 30–40 animals were placed on each plate, with three plates per condition. Animals were transferred every two days during the reproductive period, and approximately every seven days thereafter. Scoring of survival was performed every two days.

In the remaining 4 trials (Trials 3–6), prior to the end of egg laying, nematodes were handled as above for Trials 1–2, but with two plates containing 25 animals each, per condition. Following the end of egg laying, animals were transferred to individual wells of 24-well tissue culture plates, containing 2 mL of nematode growth media (NGM) and seeded with 3.5 μL of *E. coli* OP50, and where relevant, treated with 16 μL of 500 mM carbenicillin (all concentrations scaled in proportion to media volume). Animals were transferred to fresh plates monthly, and media desiccation was prevented by wrapping of plates with Parafilm. Survival was scored every 2–3 days, alongside scoring of locomotory class and necropsy pathologies.

*Imaging of necropsy pathologies (section 3.6)* 

Microscopy slides were prepared by placing individual nematode corpses in a small drop of M9 buffer on 2% agar pads, under glass coverslips. Brightfield images were captured using an ApoTome.2 Zeiss microscope with a Hamamatsu digital camera C13440 ORCA-Flash4.0 V3 and Zen software, at 100x total magnification, with 125 ms exposure time and 1.1 V illumination intensity. The presence of colonised *E. coli* OP50-RFP in the pharynx and intestine was assayed using the mRF12 channel (excitation: 577–604 nm; emission: 612 nm) at the same magnification, with 750 ms exposure time and 75% LED intensity. Brightness and contrast were adjusted equally across the entire image, and where applicable applied equally to controls. Brightfield and RFP epifluorescence necropsy images were overlaid in ImageJ and backgrounds removed with Adobe Express (online tool). The maximum intensity threshold of RFP channel images was adjusted in ImageJ from 255 to 70 for all images.

*E. coli* OP50 expressing red fluorescent protein (OP50-RFP, transformed by Marina Ezcurra with plasmid pRZT3, provided by J.F. Rawls) was streaked onto LB media petri plates containing 25 μg ml<sup>-1</sup> tetracycline, from which colonies were used to inoculate 100 mL of OP50 culture media containing 25 μg ml<sup>-1</sup> tetracycline. These cultures were grown overnight for 16 hours at 37°C in a shaking incubator. When using this culture to seed plates, OP50-RFP was not resuspended in fresh culture media (done previously by Zhao et al. (2017) to pre-empt possible tetracycline effects on the bacteria), due to concerns that removal of tetracycline might enable loss of the pRZT3 plasmid over successive divisions. No effects on this approach on apparent bacterial pathogenicity were observed. Nematodes were transferred from L4 stage onto OP50-RFP plates.

## Subpopulation mortality deconvolution analyses (section 3.6)

Age-specific survival proportions for full (not deconvolved into subpopulations) populations were obtained by conventional Kaplan-Meier analysis (including censors), from which age-specific mortality "pseudofrequencies" (which sum to 1) were calculated. For each age, these pseudofrequencies were partitioned into subpopulation pseudofrequencies, weighted by the proportion of total mortality at that age belonging to each subpopulation (P, pIC, pnIC). Standard survival and mortality analyses of subpopulations were then performed utilising these pseudofrequencies (in place of conventional mortality frequency), to enable unbiased inclusion of censor data in subpopulation analyses. Survival analyses in Figure 3.15 (p. 71) and 3.16a–b (p. 74) were performed in this manner.

Contributions of subpopulation changes to the Gompertz parameters in Figure 3.17 (p. 76) were similarly performed on simulated (mortality pseudofrequency-derived) survival data. Simulated survival data was generated for each component change (in subpopulation prevalence or lifespan), by accordingly combining simulated control and treatment subpopulations. Specifically, changes in subpopulation prevalence were simulated by combining treatment cohort subpopulation prevalence with control subpopulation lifespans (based on principles of parsimony in Figure 3.16c–d; i.e. the scenario requiring the fewest changes between subpopulation prevalence), and changes in lifespan were simulated by combining treatment cohort subpopulation lifespan with control subpopulation prevalence, for each subpopulation at a time.

The sum of these component changes closely predicted the true change between control and treatment cohorts (Figure 3.19a, p. 79). Contributions of component changes to  $\alpha$  and  $\beta$  were then estimated as the change in, respectively, lifespan of the 10% shortest-lived individuals and lifespan variance, which strongly predicted  $\alpha$  and  $\beta$  across these 12 non-antibiotic cohorts (Figure 3.19b–c) and whose component sum of these changes predicted their true change between control and treatment cohorts (Figure 3.19d–e).

### *Bacterial contact scoring (section 3.7)*

Bacterial contact was scored every 1–2 days, for nematodes kept individually in 24-well tissue culture plates, as part of the 24-cohorts experiment. Animals were scored as in contact with bacteria if they were observed inside the lawn at first sighting; each animal was checked only once during each scoring session. Importantly, plates were handled carefully to avoid sudden movements or knocks that could startle animals and therefore affect their location within their wells. Interestingly, animals were often observed to be stationary at the edge of the lawn, resting with their heads outside of the lawn; these animals were scored as *not* in contact with the bacteria. Accordingly, animals resting with their heads inside the lawn but tail outside were scored as *in* contact with the bacteria. Where nematode tracks led to growth of *E. coli* outside of the central lawn, nematode interaction with these colonies were treated the same as for the central lawn. If the media surface approached complete coverage by *E. coli*, animals were transferred to fresh wells to allow detection of bacterial avoidance.

For analysis, bacterial contact was quantified as the proportion of locomotory healthspan (A-span) spent in contact with the bacteria, with scoring as described above. Because scoring commenced in most cases after the reproductive period (when animals were moved to 24-well plates), A-span was here modified by subtracting the number of days during which bacterial contact was not scored.

# Age-specific DAF-2 AID (sections 5.2–5.5)

All age-specific DAF-2 AID (auxin-inducible degradation) cohorts (RAF2181 animals) were cultured on DMSO plates from L4 until their age of auxin commencement, when they were then transferred to auxin plates. DMSO plates were prepared one day before use, by topically adding 5 µL of 100% DMSO to the side of the bacterial lawn of each 2 mL NGM-filled well of 24-well tissue culture plates. Similarly, 24-well auxin plates were prepared by topically adding 5 µL of 400 mM auxin (indole-3-acetic acid, Sigma #I3750; dissolved in DMSO and stored long-term at -25°C or 4°C for up to 1 week) to each well, one day prior to use. Auxin crystals may initially precipitate on the media surface, but redissolve by the next day.

# Late-life cessation of DAF-2 AID (section 5.6)

Prior to auxin commencement, animals were cultured on standard NGM plates (without DMSO). All experiments in this section were performed in 24-well tissue culture plates, except for the first experiment (Figure 5.18b–d, p. 144), which was performed on 10 mL NGM plates (containing 25  $\mu$ L of 100% DMSO or 25  $\mu$ L of 400 mM auxin).

#### References

- Aalen OO (1995). Phase type distributions in survival analysis. *Scandinavian Journal of Statistics*, 22(4), 447-463.
- Anisimov V, Labunets I, Popovich I, Tyndyk M, Yurova M & Golubev A (2019). In mice transgenic for IGF1 under keratin-14 promoter, lifespan is decreased and the rates of aging and thymus involution are accelerated. *Aging*, 11(7), 2098-2110.
- Anisimov V, Semenchenko A & Yashin A (2003). Insulin and longevity: Antidiabetic biguanides as geroprotectors. *Biogerontology*, 4(5), 297-307.
- Atlan H (1968). Strehler's theory of mortality and the second principle of thermodynamics. *Journal of Gerontology*, 23(2), 196-200.
- Austad SN & Hoffman JM (2018). Is antagonistic pleiotropy ubiquitous in aging biology? *Evolution, Medicine, and Public Health*, 2018(1), 287-294.
- Ayyadevara S, Dandapat A, Singh S, Benes H, Zimniak L, Shmookler R, Rj & Zimniak P (2005). Lifespan extension in hypomorphic *daf-2* mutants of *Caenorhabditis elegans* is partially mediated by glutathione transferase CeGSTP2-2. *Aging Cell*, 4(6), 299-307.
- Back P, Braeckman BP & Matthijssens F (2012). ROS in aging *Caenorhabditis elegans*: Damage or signaling? *Oxidative Medicine and Cellular Longevity*, 2012, 608478.
- Baeriswyl S, Diard M, Mosser T, Leroy M, Manière X, Taddei F & Matic I (2010). Modulation of aging profiles in isogenic populations of *Caenorhabditis elegans* by bacteria causing different extrinsic mortality rates. *Biogerontology*, 11(1), 53-65.
- Bansal A, Zhu LJ, Yen K & Tissenbaum HA (2015). Uncoupling lifespan and healthspan in *Caenorhabditis elegans* longevity mutants. *PNAS*, 112(3), E277-E286.
- Barbieri M, Bonafè M, Franceschi C & Paolisso G (2003). Insulin/IGF-I-signaling pathway: An evolutionarily conserved mechanism of longevity from yeast to humans. *American Journal of Physiology. Endocrinology and Metabolism*, 285(5), E1064-E1071.
- Bazopoulou D, Knoefler D, Zheng Y, Ulrich K, Oleson BJ, Xie L, Kim M, Kaufmann A, Lee Y-T, Dou Y, Chen Y, Quan S & Jakob U (2019). Developmental ROS individualizes organismal stress resistance and lifespan. *Nature*, 576(7786), 301-305.
- Bergeron-Boucher M-P, Ebeling M & Canudas-Romo V (2015). Decomposing changes in life expectancy: Compression versus shifting mortality. *Demographic Research*, 33(14), 391-424.
- Bjorksten J (1968). The crosslinkage theory of aging. *Journal of the American Geriatrics Society*, 16(4), 408-427.

- Blagosklonny M (2006). Aging and immortality: Quasi-programmed senescence and its pharmacologic inhibition. *Cell Cycle*, 5(18), 2087-2102.
- Blagosklonny MV (2010). Why the disposable soma theory cannot explain why women live longer and why we age. *Aging (Albany NY)*, 2(12), 884-887.
- Bongaarts J (2005). Long-range trends in adult mortality: Models and projection methods. *Demography*, 42(1), 23-49.
- Brenner S (1974). The genetics of Caenorhabditis elegans. Genetics, 77(1), 71-94.
- Briga M, Koetsier E, Boonekamp J, Jimeno B & Verhulst S (2017). Food availability affects adult survival trajectories depending on early developmental conditions. *Proceedings: Biological Sciences*, 284(1846), 20162287.
- Bronikowski A, Alberts S, Altmann J, Packer C, Carey K & Tatar M (2002). The aging baboon: Comparative demography in a non-human primate. *Proceedings of the National Academy of Sciences of the United States of America*, 99(14), 9591-9595.
- Brooks A, Lithgow GJ & Johnson TE (1994). Mortality rates in a genetically heterogeneous population of *Caenorhabditis elegans*. *Science*, 263(5147), 668-671.
- Bross T, Rogina B & Helfand S (2005). Behavioral, physical, and demographic changes in *Drosophila* populations through dietary restriction. *Aging Cell*, 4(6), 309-317.
- Burger O & Missov T (2016). Evolutionary theory of ageing and the problem of correlated Gompertz parameters. *Journal of Theoretical Biology*, 408, 34-41.
- Carnes B & Olshansky S (1997). A biologically motivated partitioning of mortality. *Experimental Gerontology*, 32(6), 615-631.
- Charlesworth B (1994). Evolution in age-structured populations, Cambridge University Press.
- Charlesworth B (2001). Patterns of age-specific means and genetic variances of mortality rates predicted by the mutation-accumulation theory of ageing. *Journal of Theoretical Biology*, 210(1), 47-65.
- Charnov EL (1993). *Life history invariants: Some explorations of symmetry in evolutionary ecology*, Oxford University Press.
- Chaves L, Hernandez M, Revilla T, Rodríguez D & Rabinovich J (2004). Mortality profiles of *rhodnius prolixus* (Heteroptera: Reduviidae), vector of Chagas disease. *Acta Tropica*, 92(2), 119-125.
- Chen J, Senturk D, Wang J, Müller H, Carey J, Caswell H & Caswell-Chen E (2007). A demographic analysis of the fitness cost of extended longevity in *Caenorhabditis elegans*. *The Journals of Gerontology*. *Series A, Biological Sciences and Medical Sciences*, 62(2), 126-135.

- Chereji E, Gatz M, Pedersen NL & Prescott CA (2013). Reexamining the association between fertility and longevity: Testing the disposable soma theory in a modern human sample of twins. *The Journals of Gerontology: Series A*, 68(5), 499-509.
- Christensen K, Doblhammer G, Rau R & Vaupel J (2009). Ageing populations: The challenges ahead. *Lancet*, 374(9696), 1196-1208.
- Christiansen-Jucht C, Parham P, Saddler A, Koella J & Basáñez M (2014). Temperature during larval development and adult maintenance influences the survival of *Anopheles gambiae* s.s. *Parasites & Vectors*, 7, 489.
- Churgin M, Jung S, Yu C, Chen X, Raizen D & Fang-Yen C (2017). Longitudinal imaging of *Caenorhabditis elegans* in a microfabricated device reveals variation in behavioral decline during aging. *eLife*, 6, e26652.
- Clancy D, Gems D, Harshman L, Oldham S, Stocker H, Hafen E, Leevers S & Partridge L (2001). Extension of life-span by loss of CHICO, a *Drosophila* insulin receptor substrate protein. *Science*, 292(5514), 104-106.
- Clark J, Kaczmarczyk M, Mongiało Z, Ignaczak P, Czajkowski A, Klęsk P & Ciechanowicz A (2013). Skew-*t* fits to mortality data--can a Gaussian-related distribution replace the Gompertz-Makeham as the basis for mortality studies? *The Journals of Gerontology. Series A, Biological Sciences and Medical Sciences*, 68(8), 903-913.
- Conti B, Sanchez-Alavez M, Winsky-Sommerer R, Morale M, Lucero J, Brownell S, Fabre V, Huitron-Resendiz S, Henriksen S, Zorrilla E, De Lecea L & Bartfai T (2006). Transgenic mice with a reduced core body temperature have an increased life span. *Science*, 314(5800), 825-828.
- Cuanalo-Contreras K, Schulz J, Mukherjee A, Park K, Armijo E & Soto C (2023). Extensive accumulation of misfolded protein aggregates during natural aging and senescence. *Frontiers in Aging Neuroscience*, 14, 1090109.
- Davies S, Bundy J & Leroi A (2015). Metabolic youth in middle age: Predicting aging in *Caenorhabditis elegans* using metabolomics. *Journal of Proteome Research*, 14(11), 4603-4609.
- De Magalhães J & Church G (2005). Genomes optimize reproduction: Aging as a consequence of the developmental program. *Physiology (Bethesda)*, 20, 252-259.
- De Magalhães JP, Cabral JAS & Magalhães D (2005). The influence of genes on the aging process of mice: A statistical assessment of the genetics of aging. *Genetics*, 169(1), 265-274.
- Di Francesco A, Deighan AG, Litichevskiy L, Chen Z, Luciano A, Robinson L, Garland G, Donato H, Vincent M, Schott W, Wright KM, Raj A, Prateek GV, Mullis M, Hill WG, Zeidel ML, Peters LL, Harding F, Botstein D, Korstanje R, Thaiss CA, Freund A &

- Churchill GA (2024). Dietary restriction impacts health and lifespan of genetically diverse mice. *Nature*, 634(8034), 684-692.
- Dilman V (1994). Development, aging and disease: A new rationale for an intervention strategy, Harwood Academic Publishers.
- Driver C (2001). The Gompertz function does not measure ageing. *Biogerontology*, 2(1), 61-65.
- Driver C (2003). A further comment on why the Gompertz plot does not measure aging. *Biogerontology*, 4(5), 325-327.
- Eakin T, Shouman R, Qi Y, Liu G & Witten M (1995). Estimating parametric survival model parameters in gerontological aging studies: Methodological problems and insights. *The Journals of Gerontology. Series A, Biological Sciences and Medical Sciences*, 50(3), B166-B176.
- Eder M, Martin O, Oswal N, Sedlackova L, Moutinho C, Del Carmen-Fabregat A, Menendez Bravo S, Sebé-Pedrós A, Heyn H & Stroustrup N (2024). Systematic mapping of organism-scale gene-regulatory networks in aging using population asynchrony. *Cell*, 187(15), 3919-3935.e19.
- Ellis HM & Horvitz HR (1986). Genetic control of programmed cell death in the nematode *C. elegans. Cell*, 44(6), 817-829.
- Ezcurra M, Benedetto A, Sornda T, Gilliat A, Au C, Zhang Q, Van Schelt S, Petrache A, Wang H, De La Guardia Y, Bar-Nun S, Tyler E, Wakelam M & Gems D (2018). *C. elegans* eats its own intestine to make yolk leading to multiple senescent pathologies. *Current Biology*, 28(16), 2544-2556.
- Fatima I, Chen G, Botchkareva N, Sharov A, Thornton D, Wilkinson H, Hardman M, Grutzkau A, Joao Pedro DM, Seluanov A, Smith E, Gorbunova V, Mardaryev A, Faulkes C & Botchkarev V (2022). Skin aging in long-lived naked mole-rats is accompanied by increased expression of longevity-associated and tumor suppressor genes. *The Journal of Investigative Dermatology*, 142(11), 2853-2863.e4.
- Finch C, Pike M & Witten M (1990). Slow mortality rate accelerations during aging in some animals approximate that of humans. *Science*, 249(4971), 902-905.
- Finch CE (1990). *Longevity, senescence, and the genome,* Chicago, University of Chicago Press.
- Finch CE (2009). Evolution of the human lifespan and diseases of aging: Roles of infection, inflammation, and nutrition. *Proceedings of the National Academy of Sciences of the United States of America*, 107(Suppl 1), 1718-1724.
- Finkelstein M (2012). Discussing the Strehler-Mildvan model of mortality. *Demographic Research*, 26, 191-206.

- Fire A, Xu S, Montgomery MK, Kostas SA, Driver SE & Mello CC (1998). Potent and specific genetic interference by double-stranded RNA in *Caenorhabditis elegans*. *Nature*, 391(6669), 806-811.
- Fisher RA (1930). The genetical theory of natural selection, Clarendon Press.
- Flurkey K, Papaconstantinou J, Miller R & Harrison D (2001). Lifespan extension and delayed immune and collagen aging in mutant mice with defects in growth hormone production. *Proceedings of the National Academy of Sciences of the United States of America*, 98(12), 6736-6741.
- Fok W, Chen Y, Bokov A, Zhang Y, Salmon A, Diaz V, Javors M, Wood W, Zhang Y, Becker K, Pérez V & Richardson A (2014). Mice fed rapamycin have an increase in lifespan associated with major changes in the liver transcriptome. *PLoS One*, 9(1), e83988.
- Fonseca D, Brancato C, Prior A, Shelton P & Sheehy M (2005). Death rates reflect accumulating brain damage in arthropods. *Proceedings: Biological Sciences*, 272(1575), 1941-1947.
- Franceschi C, Bonafè M, Valensin S, Olivieri F, De Luca M, Ottaviani E & De Benedictis G (2000). Inflamm-aging. An evolutionary perspective on immunosenescence. *Annals of the New York Academy of Sciences*, 908, 244-254.
- Friedman D & Johnson T (1988). A mutation in the *age-1* gene in *Caenorhabditis elegans* lengthens life and reduces hermaphrodite fertility. *Genetics*, 118(1), 75-86.
- Fries JF (1980). Aging, natural death, and the compression of morbidity. *The New England Journal of Medicine*, 303(3), 130–135.
- Gaillard J-M, Viallefont A, Loison A & Festa-Bianchet M (2004). Assessing senescence patterns in populations of large mammals. *Animal Biodiversity and Conservation*, 27(1), 47-58.
- Gamelon M & Froy H (2023). Biodemography: Unifying concepts from biology, demography, and mathematics. *Trends in Ecology & Evolution*, 35(6), 475-476.
- Garigan D, Hsu A, Fraser A, Kamath R, Ahringer J & Kenyon C (2002). Genetic analysis of tissue aging in *Caenorhabditis elegans*: A role for heat-shock factor and bacterial proliferation. *Genetics*, 161(3), 1101-1112.
- Garsin D, Villanueva J, Begun J, Kim D, Sifri C, Calderwood S, Ruvkun G & Ausubel F (2003). Long-lived *C. elegans daf-2* mutants are resistant to bacterial pathogens. *Science*, 300(5627), 1921.
- Gavrilov L & Gavrilova N (1991). *The biology of life span: A quantitative approach*, New York, Harwood Academic Publishers.

- Gavrilov L & Gavrilova N (2022). Trends in human species-specific lifespan and actuarial aging rate. *Biochemistry (Moscow)*, 87(12), 1622-1633.
- Gavrilov LA & Gavrilova NS (2001). The reliability theory of aging and longevity. *Journal of Theoretical Biology*, 213(4), 527-545.
- Gavrilova NS & Gavrilov LA (2014). Biodemography of old-age mortality in humans and rodents. *The Journals of Gerontology: Series A*, 70(1), 1-9.
- Gems D (2015). The aging-disease false dichotomy: Understanding senescence as pathology. *Frontiers in Genetics*, 6, 212.
- Gems D (2022). The hyperfunction theory: An emerging paradigm for the biology of aging. *Ageing Research Reviews*, 74, 101557.
- Gems D (2025). How aging causes osteoarthritis: An evolutionary physiology perspective. *Osteoarthritis and Cartilage*, 33(8), 921-932.
- Gems D & De Magalhães JP (2021). The hoverfly and the wasp: A critique of the hallmarks of aging as a paradigm. *Ageing Research Reviews*, 70, 101407.
- Gems D & Kern C (2024). Biological constraint, evolutionary spandrels and antagonistic pleiotropy. *Ageing Research Reviews*, 101, 102527.
- Gems D & Riddle D (2000). Genetic, behavioral and environmental determinants of male longevity in *Caenorhabditis elegans*. *Genetics*, 154(4), 1597-1610.
- Gems D, Sutton A, Sundermeyer M, Albert P, King K, Edgley M, Larsen P & Riddle D (1998). Two pleiotropic classes of *daf-2* mutation affect larval arrest, adult behavior, reproduction and longevity in *Caenorhabditis elegans*. *Genetics*, 150(1), 129-155.
- Giaimo S & Di Fagagna F (2012). Is cellular senescence an example of antagonistic pleiotropy? *Aging Cell*, 11(3), 378-383.
- Gladyshev VN (2014). The free radical theory of aging is dead. Long live the damage theory! *Antioxidants & Redox Signaling*, 20(4), 727-731.
- Gompertz B (1825). On the nature of the function expressive of the law of human mortality, and on a new mode of determining the value of life contingencies. *Philosophical Transactions of the Royal Society of London*, 115, 513-583.
- Govindaraju D, Atzmon G & Barzilai N (2015). Genetics, lifestyle and longevity: Lessons from centenarians. *Applied & Translational Genomics*, 4(4), 23-32.
- Hahm J, Kim S, Diloreto R, Shi C, Lee S, Murphy C & Nam H (2015). *C. elegans* maximum velocity correlates with healthspan and is maintained in worms with an insulin receptor mutation. *Nature Communications*, 6, 8919.
- Haldane J (1941). New paths in genetics, London, Allen and Unwin.

- Hamilton W (1966). The moulding of senescence by natural selection. *Journal of Theoretical Biology*, 12(1), 12-45.
- Hansen M & Kennedy B (2016). Does longer lifespan mean longer healthspan? *Trends in Cell Biology*, 26(8), 565-568.
- Harley CB, Futcher AB & Greider CW (1990). Telomeres shorten during ageing of human fibroblasts. *Nature*, 345(6274), 458-460.
- Harman D (1956). Aging: A theory based on free radical and radiation chemistry. *Journal of Gerontology*, 11(3), 298-300.
- Harman D (1972). The biologic clock: The mitochondria? *Journal of the American Geriatrics Society*, 20(4), 145-147.
- Harper J, Leathers C & Austad S (2006). Does caloric restriction extend life in wild mice? *Aging Cell*, 5(6), 441-449.
- Harper S (2018). Demography: A very short introduction, Oxford University Press.
- Hawkes K, Smith K & Blevins J (2012). Human actuarial aging increases faster when background death rates are lower: A consequence of differential heterogeneity? *Evolution*, 66(1), 103-114.
- Hawkes K, Smith K & Robson S (2009). Mortality and fertility rates in humans and chimpanzees: How within-species variation complicates cross-species comparisons. *American Journal of Human Biology*, 21(4), 578-586.
- Hayflick L (1965). The limited in vitro lifetime of human diploid cell strains. *Experimental Cell Research*, 37, 614-636.
- Hayflick L (2007). Biological aging is no longer an unsolved problem. *Annals of the New York Academy of Sciences*, 1100, 1-13.
- Hayflick L & Moorhead P (1961). The serial cultivation of human diploid cell strains. *Experimental Cell Research*, 25, 585-621.
- Hedgecock EM, Sulston JE & Thomson JN (1983). Mutations affecting programmed cell deaths in the nematode *Caenorhabditis elegans*. *Science*, 220(4603), 1277-1279.
- Herndon LA, Schmeissner PJ, Dudaronek JM, Brown PA, Listner KM, Sakano Y, Paupard MC, Hall DH & Driscoll M (2002). Stochastic and genetic factors influence tissue-specific decline in ageing *C. elegans. Nature*, 419(6909), 808-814.
- Hill K, Boesch C, Goodall J, Pusey A, Williams J & Wrangham R (2001). Mortality rates among wild chimpanzees. *Journal of Human Evolution*, 40(5), 437-450.
- Honda Y & Honda S (2002). Life span extensions associated with upregulation of gene expression of antioxidant enzymes in *Caenorhabditis elegans*; studies of mutation in

- the *age-1*, PI3 kinase homologue and short-term exposure to hyperoxia. *Journal of the American Aging Association*, 25(1), 21-28.
- Horvath S, Haghani A, Macoretta N, Ablaeva J, Zoller JA, Li CZ, Zhang J, Takasugi M, Zhao Y, Rydkina E, Zhang Z, Emmrich S, Raj K, Seluanov A, Faulkes CG & Gorbunova V (2021). DNA methylation clocks tick in naked mole rats but queens age more slowly than nonbreeders. *Nature Aging*, 2(1), 46-59.
- Hosono R, Sato Y, Aizawa S & Mitsui Y (1980). Age-dependent changes in mobility and separation of the nematode *Caenorhabditis elegans*. *Experimental Gerontology*, 15(4), 285-289.
- Howes R (2006). The free radical fantasy: A panoply of paradoxes. *Annals of the New York Academy of Sciences*, 1067, 22-26.
- Huang C, Xiong C & Kornfeld K (2004). Measurements of age-related changes of physiological processes that predict lifespan of *Caenorhabditis elegans*. *Proceedings of the National Academy of Sciences of the United States of America*, 101(21), 8084-8089.
- Hughes B & Hekimi S (2011). A mild impairment of mitochondrial electron transport has sexspecific effects on lifespan and aging in mice. *PLoS One*, 6(10), e26116.
- Hughes BG & Hekimi S (2016). Different mechanisms of longevity in long-lived mouse and *Caenorhabditis elegans* mutants revealed by statistical analysis of mortality rates. *Genetics*, 204(3), 905-920.
- Hughes K, Alipaz J, Drnevich J & Reynolds R (2002). A test of evolutionary theories of aging. *Proceedings of the National Academy of Sciences of the United States of America*, 99(22), 14286-14291.
- Ismail K, Nussbaum L, Sebastiani P, Andersen S, Perls T, Barzilai N & Milman S (2016). Compression of morbidity is observed across cohorts with exceptional longevity. *Journal of the American Geriatrics Society*, 64(8), 1583-1591.
- Johnson T (1987). Aging can be genetically dissected into component processes using long-lived lines of *Caenorhabditis elegans*. *Proceedings of the National Academy of Sciences of the United States of America*, 84(11), 3777-3781.
- Johnson T, Wu D, Tedesco P, Dames S & Vaupel J (2001). Age-specific demographic profiles of longevity mutants in *Caenorhabditis elegans* show segmental effects. *The Journals of Gerontology. Series A, Biological Sciences and Medical Sciences*, 56(8), B331-B339.
- Johnson TE (1990). Increased life-span of *age-1* mutants in *Caenorhabditis elegans* and lower Gompertz rate of aging. *Science*, 249(4971), 908-912.

- Jones HB (1956). A special consideration of the aging process, disease, and life expectancy. *Advances in Biological and Medical Physics*, 4, 281-337.
- Jones OR, Scheuerlein A, Salguero-Gómez R, Camarda CG, Schaible R, Casper BB, Dahlgren JP, Ehrlén J, García MB, Menges ES, Quintana-Ascencio PF, Caswell H, Baudisch A & Vaupel JW (2014). Diversity of ageing across the tree of life. *Nature*, 505(7482), 169-173.
- Kannisto V (1994). Development of oldest-old mortality, 1950–1990: Evidence from 28 developed countries, Odense University Press.
- Karin O, Agrawal A, Porat Z, Krizhanovsky V & Alon U (2019). Senescent cell turnover slows with age providing an explanation for the Gompertz law. *Nature Communications*, 10(1), 5495.
- Keil G, Cummings E & De Magalhães J (2015). Being cool: How body temperature influences ageing and longevity. *Biogerontology*, 16(4), 383-397.
- Kennedy B, Berger S, Brunet A, Campisi J, Cuervo A, Epel E, Franceschi C, Lithgow G, Morimoto R, Pessin J, Rando T, Richardson A, Schadt E, Wyss-Coray T & Sierra F (2014). Geroscience: Linking aging to chronic disease. *Cell*, 159(4), 709-713.
- Kenyon C (2011). The first long-lived mutants: Discovery of the insulin/IGF-1 pathway for ageing. *Philosophical transactions of the Royal Society of London. Series B, Biological sciences*, 366(1561), 9-16.
- Kenyon C, Chang J, Gensch E, Rudner A & Tabtiang R (1993). A *C. elegans* mutant that lives twice as long as wild type. *Nature*, 366(6454), 461-464.
- Kerepesi C, Meer MV, Ablaeva J, Amoroso VG, Lee S-G, Zhang B, Gerashchenko MV, Trapp A, Yim SH, Lu AT, Levine ME, Seluanov A, Horvath S, Park TJ, Gorbunova V & Gladyshev VN (2022). Epigenetic aging of the demographically non-aging naked mole-rat. *Nature Communications*, 13(1), 1-10.
- Kirkwood T & Cremer T (1982). Cytogerontology since 1881: A reappraisal of August Weismann and a review of modern progress. *Human Genetics*, 60(2), 101-121.
- Kirkwood T, Feder M, Finch C, Franceschi C, Globerson A, Klingenberg C, Lamarco K, Omholt S & Westendorp R (2005). What accounts for the wide variation in life span of genetically identical organisms reared in a constant environment? *Mechanisms of Ageing and Development*, 126(3), 439-443.
- Kirkwood TBL (1977). Evolution of ageing. *Nature*, 270(5635), 301-304.
- Kirkwood TBL (2015). Deciphering death: A commentary on Gompertz (1825) 'on the nature of the function expressive of the law of human mortality, and on a new mode of determining the value of life contingencies'. *Philosophical Transactions of the Royal Society of London. Series B, Biological Sciences*, 370(1666), 20140379.

- Klass M (1977). Aging in the nematode *Caenorhabditis elegans*: Major biological and environmental factors influencing life span. *Mechanisms of Ageing and Development*, 6(6), 413-429.
- Klass M (1983). A method for the isolation of longevity mutants in the nematode *Caenorhabditis elegans* and initial results. *Mechanisms of Ageing and Development*, 22(3-4), 279-286.
- Koopman J, Rozing M, Kramer A, De Jager D, Ansell D, De Meester J, Prütz K, Finne P, Heaf J, Palsson R, Kramar R, Jager K, Dekker F & Westendorp R (2011). Senescence rates in patients with end-stage renal disease: A critical appraisal of the Gompertz model. *Aging Cell*, 10(2), 233-238.
- Koopman J, Wensink M, Rozing M, Van Bodegom D & Westendorp R (2015). Intrinsic and extrinsic mortality reunited. *Experimental Gerontology*, 67, 48-53.
- Kowald A & Kirkwood T (2021). Senolytics and the compression of late-life mortality. *Experimental Gerontology*, 155, 111588.
- Kraus C, Pavard S & Promislow D (2013). The size-life span trade-off decomposed: Why large dogs die young. *The American Naturalist*, 181(4), 492-505.
- Krementsova A, Roshina N, Tsybul'ko E, Rybina O, Symonenko A & Pasyukova E (2012). Reproducible effects of the mitochondria-targeted plastoquinone derivative SkQ1 on *Drosophila melanogaster* lifespan under different experimental scenarios. *Biogerontology*, 13(6), 595-607.
- Lapointe J, Stepanyan Z, Bigras E & Hekimi S (2009). Reversal of the mitochondrial phenotype and slow development of oxidative biomarkers of aging in long-lived *Mclk1*<sup>+/-</sup> mice. *The Journal of Biological Chemistry*, 284(30), 20364-20374.
- Larson S, Colchero F, Jones O, Williams L & Fernandez-Duque E (2016). Age and sexspecific mortality of wild and captive populations of a monogamous pair-bonded primate (*Aotus azarae*). *American Journal of Primatology*, 78(3), 315-325.
- Lazarević J, Dorđević M, Stojković B & Tucić N (2013). Resistance to prooxidant agent paraquat in the short- and long-lived lines of the seed beetle (*Acanthoscelides obtectus*). *Biogerontology*, 14(2), 141-152.
- Lee K, Simpson S, Clissold F, Brooks R, Ballard J, Taylor P, Soran N & Raubenheimer D (2008). Lifespan and reproduction in *Drosophila*: New insights from nutritional geometry. *Proceedings of the National Academy of Sciences of the United States of America*, 105(7), 2498-2503.
- Lee S & Kenyon C (2009). Regulation of the longevity response to temperature by thermosensory neurons in *Caenorhabditis elegans*. *Current Biology*, 19(9), 715-722.

- Lenaerts I, Van Eygen S & Van Fleteren J (2007). Adult-limited dietary restriction slows Gompertzian aging in *Caenorhabditis elegans*. *Annals of the New York Academy of Sciences*, 1100, 442-448.
- Lestienne R (1988). On the thermodynamical and biological interpretation of the Gompertzian mortality rate distribution. *Mechanisms of Ageing and Development*, 42(3), 197-214.
- Li T & Anderson J (2015). The Strehler-Mildvan correlation from the perspective of a two-process vitality model. *Population Studies (Cambridge)*, 69(1), 91-104.
- Loose J & Ghazi A (2021). Auxin treatment increases lifespan in *Caenorhabditis elegans*. *Biology Open*, 10(5), bio058703.
- López-Otín C, Blasco M, Partridge L, Serrano M & Kroemer G (2013). The hallmarks of aging. *Cell*, 153(6), 1194-1217.
- López-Otín C, Blasco M, Partridge L, Serrano M & Kroemer G (2023). Hallmarks of aging: An expanding universe. *Cell*, 186(2), 243-278.
- Magwere T, Chapman T & Partridge L (2004). Sex differences in the effect of dietary restriction on life span and mortality rates in female and male *Drosophila* melanogaster. The Journals of Gerontology: Series A, 59(1), B3-B9.
- Mair W, Goymer P, Pletcher S & Partridge L (2003). Demography of dietary restriction and death in *Drosophila*. *Science*, 301(5640), 1731-1733.
- Makeham WM (1860). On the law of mortality and the construction of annuity tables. *The Assurance Magazine, and Journal of the Institute of Actuaries*, 8(6), 301-310.
- Maklakov A, Friberg U, Dowling D & Arnqvist G (2006). Within-population variation in cytoplasmic genes affects female life span and aging in *Drosophila melanogaster*. *Evolution*, 60(10), 2081-2086.
- Mannucci P, Mari D, Merati G, Peyvandi F, Tagliabue L, Sacchi E, Taioli E, Sansoni P, Bertolini S & Franceschi C (1997). Gene polymorphisms predicting high plasma levels of coagulation and fibrinolysis proteins. A study in centenarians. *Arteriosclerosis, Thrombosis, and Vascular Biology*, 17(4), 755-759.
- Marden J, Rogina B, Montooth K & Helfand S (2003). Conditional tradeoffs between aging and organismal performance of *Indy* long-lived mutant flies. *Proceedings of the National Academy of Sciences of the United States of America*, 100(6), 3369-3373.
- Martin C, Yuan T, Ghia E, William WW & Douglas CP (1994). Green fluorescent protein as a marker for gene expression. *Science*, 263(5148), 802-805.
- Martínez D (1998). Mortality patterns suggest lack of senescence in hydra. *Experimental Gerontology*, 33(3), 217-225.

- Masoro E (2006). Caloric restriction and aging: Controversial issues. *The Journals of Gerontology. Series A, Biological Sciences and Medical Sciences*, 61(1), 14-19.
- Mccoll G, Killilea D, Hubbard A, Vantipalli M, Melov S & Lithgow G (2008). Pharmacogenetic analysis of lithium-induced delayed aging in *Caenorhabditis elegans*. *The Journal of Biological Chemistry*, 283(1), 350-357.
- Medawar PB (1952). An unsolved problem of biology. London: H.K. Lewis.
- Medawar PB (1946). Old age and natural death. Modern Quarterly, 1, 30-56.
- Medvedev Z (1990). An attempt at a rational classification of theories of ageing. *Biological Reviews of the Cambridge Philosophical Society*, 65(3), 375-398.
- Miller R, Harrison D, Astle C, Baur J, Boyd A, De Cabo R, Fernandez E, Flurkey K, Javors M, Nelson J, Orihuela C, Pletcher S, Sharp Z, Sinclair D, Starnes J, Wilkinson J, Nadon N & Strong R (2011). Rapamycin, but not resveratrol or simvastatin, extends life span of genetically heterogeneous mice. *The Journals of Gerontology. Series A, Biological Sciences and Medical Sciences*, 66(2), 191-201.
- Mitchell S, Simpson M, Coulet L, Gouedard S, Hambly C, Morimoto J, Allison D & Speakman J (2024). Reproduction has immediate effects on female mortality, but no discernible lasting physiological impacts: A test of the disposable soma theory. Proceedings of the National Academy of Sciences of the United States of America, 121(42), e2408682121.
- Molière A, Park J, Goyala A, Vayndorf E, Zhang B, Hsiung K, Jung Y, Kwon S, Statzer C, Meyer D, Nguyen R, Chadwick J, Thompson M, Schumacher B, Lee S, Essmann C, Macarthur M, Kaeberlein M, David D, Gems D & Ewald C (2024). Improved resilience and proteostasis mediate longevity upon DAF-2 degradation in old age. *GeroScience*, 46(5), 5015-5036.
- Monnier V (1989). Toward a maillard reaction theory of aging. *Progress in Clinical and Biological Research*, 304, 1-22.
- Mueller L, Nusbaum T & Rose M (1995). The Gompertz equation as a predictive tool in demography. *Experimental Gerontology*, 30(6), 553-569.
- Mulla S, Ludlam A, Elragig A, Slack C, Balklava Z, Stich M & Cheong A (2023). A biphasic model of lifespan in nematode *Caenorhabditis elegans* worm. *Royal Society Open Science*, 10(2), 220991.
- Myers G & Manton K (1984). Compression of mortality: Myth or reality? *The Gerontologist*, 24(4), 346-353.
- Nakagawa S, Lagisz M, Hector K & Spencer H (2012). Comparative and meta-analytic insights into life extension via dietary restriction. *Aging Cell*, 11(3), 401-409.

- Nakaoka H & Wakamoto Y (2017). Aging, mortality, and the fast growth trade-off of *Schizosaccharomyces pombe*. *PLoS Biology*, 15(6), e2001109.
- Newell Stamper B, Cypser J, Kechris K, Kitzenberg D, Tedesco P & Johnson T (2018). Movement decline across lifespan of *Caenorhabditis elegans* mutants in the insulin/insulin-like signaling pathway. *Aging Cell*, 17(1), e12704.
- Nuland SB (1994). How we die, Vintage Books.
- Olby R (1996). The molecular revolution in biology. 1 ed.: Routledge.
- Olshansky S & Carnes B (1997). Ever since Gompertz. *Demography*, 34(1), 1-15.
- Orgel L (1963). The maintenance of the accuracy of protein synthesis and its relevance to ageing. *Proceedings of the National Academy of Sciences of the United States of America*, 49(4), 517-521.
- Oswal N, Martin O, Stroustrup S, Bruckner M & Stroustrup N (2022). A hierarchical process model links behavioral aging and lifespan in *C. elegans. PLoS Computational Biology*, 18(9), e1010415.
- Palani S, Sellegounder D, Wibisono P & Liu Y (2023). The longevity response to warm temperature is neurally controlled via the regulation of collagen genes. *Aging Cell*, 22(5), e13815.
- Panchenko A, Tyndyk M, Fedoros E, Maydin M, Semenov A, Gubareva E, Golubev A & Anisimov V (2019). Comparative analysis of experimental data about the effects of various polyphenols on lifespan and aging. *Advances in Gerontology*, 32(3), 325-330.
- Papsdorf K, Miklas JW, Hosseini A, Cabruja M, Morrow CS, Savini M, Yu Y, Silva-García CG, Haseley NR, Murphy LM, Yao P, De Launoit E, Dixon SJ, Snyder MP, Wang MC, Mair WB & Brunet A (2023). Lipid droplets and peroxisomes are co-regulated to drive lifespan extension in response to mono-unsaturated fatty acids. *Nature Cell Biology*, 25(5), 672-684.
- Partridge L 1997. Evolutionary biology and age-related mortality. *In:* WACHTER, K. W. & FINCH, C. E. (eds.) *Between Zeus and the salmon: The biodemography of longevity.* Washington (DC): National Academies Press (US).
- Partridge L, Pletcher S & Mair W (2005). Dietary restriction, mortality trajectories, risk and damage. *Mechanisms of Ageing and Development*, 126(1), 35-41.
- Patel D, Garza-Garcia A, Nanji M, Mcelwee J, Ackerman D, Driscoll P & Gems D (2008). Clustering of genetically defined allele classes in the *Caenorhabditis elegans* DAF-2 Insulin/IGF-1 receptor. *Genetics*, 178(2), 931-946.
- Pearl R (1928). The rate of living, New York, Knopf.

- Pietrzak B, Dawidowicz P, Prędki P & Dańko M (2015). How perceived predation risk shapes patterns of aging in water fleas. *Experimental Gerontology*, 69, 1-8.
- Pincus Z & Slack F (2010). Developmental biomarkers of aging in *Caenorhabditis elegans*. *Developmental Dynamics*, 239(5), 1306-1314.
- Pletcher S (1999). Model fitting and hypothesis testing for age-specific mortality data. *Journal of Evolutionary Biology*, 12(3), 430-439.
- Pletcher SD, Khazaeli AA & Curtsinger JW (2000). Why do life spans differ? Partitioning mean longevity differences in terms of age-specific mortality parameters. *The Journals of Gerontology: Series A*, 55(8), B381–B389.
- Podshivalova K, Kerr R & Kenyon C (2017). How a mutation that slows aging can also disproportionately extend end-of-life decrepitude. *Cell Reports*, 19(3), 441-450.
- Praticò D (2002). Lipid peroxidation and the aging process. 2002(50), re5.
- Promislow D & Haselkorn T (2002). Age-specific metabolic rates and mortality rates in the genus *Drosophila*. *Aging Cell*, 1(1), 66-74.
- Rangaraju S, Solis G, Thompson R, Gomez-Amaro R, Kurian L, Encalada S, Niculescu A, Salomon D & Petrascheck M (2015). Suppression of transcriptional drift extends *C. elegans* lifespan by postponing the onset of mortality. *eLife*, 4, e08833.
- Reznick DN, Bryant MJ, Roff D, Ghalambor CK & Ghalambor DE (2004). Effect of extrinsic mortality on the evolution of senescence in guppies. *Nature*, 431(7012), 1095-1099.
- Ricklefs R (1998). Evolutionary theories of aging: Confirmation of a fundamental prediction, with implications for the genetic basis and evolution of life span. *The American Naturalist*, 152(1), 24-44.
- Riffe T, Nepomuceno MR & Basellini U 2020. Mortality modeling. *Encyclopedia of gerontology and population aging*. Springer International Publishing.
- Riley JC (2001). Rising life expectancy: A global history, Cambridge University Press.
- Robinson W (2009). Ecological correlations and the behavior of individuals. *International Journal of Epidemiology*, 38(2), 337-341.
- Rodríguez J, Marigorta U, Hughes D, Spataro N, Bosch E & Navarro A (2017). Antagonistic pleiotropy and mutation accumulation influence human senescence and disease. *Nature Ecology & Evolution*, 1(3), 55.
- Roy C, Molin L, Alcolei A, Solyga M, Bonneau B, Vachon C, Bessereau J & Solari F (2022). DAF-2/insulin IGF-1 receptor regulates motility during aging by integrating opposite signaling from muscle and neuronal tissues. *Aging Cell*, 21(8), e13660.

- Rozing M & Westendorp R (2008). Parallel lines: Nothing has changed? *Aging Cell*, 7(6), 924-927.
- Ruan H, Tang X, Chen M, Joiner M, Sun G, Brot N, Weissbach H, Heinemann S, Iverson L, Wu C & Hoshi T (2002). High-quality life extension by the enzyme peptide methionine sulfoxide reductase. *Proceedings of the National Academy of Sciences of the United States of America*, 99(5), 2748-2753.
- Ruby J, Smith M & Buffenstein R (2018). Naked mole-rat mortality rates defy Gompertzian laws by not increasing with age. *eLife*, 7, e31157.
- Ruby J, Smith M & Buffenstein R (2024). Five years later, with double the demographic data, naked mole-rat mortality rates continue to defy Gompertzian laws by not increasing with age. *Geroscience*, 46(5), 5321-5341.
- Sacher G 1977. Life table modifications and life prolongation. *In:* FINCH, C. & L, H. (eds.) *Handbook of the biology of aging.* New York: Van Nostrand Rheinhold.
- Sacher GA & Trucco E (1962). The stochastic theory of mortality. *Annals of the New York Academy of Sciences*, 96, 985-1007.
- Samuelson AV, Carr CE & Ruvkun G (2007). Gene activities that mediate increased life span of *C. elegans* insulin-like signaling mutants. *Genes & Development*, 21(22), 2976–2994.
- Saul N, Pietsch K, Menzel R & Steinberg C (2008). Quercetin-mediated longevity in *Caenorhabditis elegans*: Is DAF-16 involved? *Mechanisms of Ageing and Development*, 129(10), 611-613.
- Schriner S, Linford N, Martin G, Treuting P, Ogburn C, Emond M, Coskun P, Ladiges W, Wolf N, Van Remmen H, Wallace D & Rabinovitch P (2005). Extension of murine life span by overexpression of catalase targeted to mitochondria. *Science*, 308(5730), 1909-1911.
- Schumacher B, Pothof J, Vijg J & Hoeijmakers JHJ (2021). The central role of DNA damage in the ageing process. *Nature*, 592, 695-703.
- Seguchi M (2007). Soul and ageing: The views of Plato and Aristotle on old age. *Journal of Classical Studies*, 55, 63-75.
- Shahrestani P, Quach J, Mueller L & Rose M (2012). Paradoxical physiological transitions from aging to late life in *Drosophila*. *Rejuvenation Research*, 15(1), 49-58.
- Sheeba V, Sharma V, Shubha K, Chandrashekaran M & Joshi A (2000). The effect of different light regimes on adult life span in *Drosophila melanogaster* is partly mediated through reproductive output. *Journal of Biological Rhythms*, 15(5), 380-392.

- Shen E-Z, Song C-Q, Lin Y, Zhang W-H, Su P-F, Liu W-Y, Zhang P, Xu J, Lin N, Zhan C, Wang X, Shyr Y, Cheng H & Dong M-Q (2014). Mitoflash frequency in early adulthood predicts lifespan in *Caenorhabditis elegans*. *Nature*, 508(7494), 128-132.
- Shen J, Ford D, Landis G & Tower J (2009). Identifying sexual differentiation genes that affect *Drosophila* life span. *BMC Geriatrics*, 9, 56.
- Shen J, Landis G & Tower J (2017). Multiple metazoan life-span interventions exhibit a sexspecific Strehler-Mildvan inverse relationship between initial mortality rate and agedependent mortality rate acceleration. *The Journals of Gerontology. Series A, Biological Sciences and Medical Sciences*, 72(1), 44-53.
- Shouman R & Witten M (1995). Survival estimates and sample size: What can we conclude? *The Journals of Gerontology. Series A, Biological Sciences and Medical Sciences*, 50(3), B177-B185.
- Sierra F, Hadley E, Suzman R & Hodes R (2009). Prospects for life span extension. *Annual Review of Medicine*, 60, 457-469.
- Simons MJP, Koch W & Verhulst S (2013). Dietary restriction of rodents decreases aging rate without affecting initial mortality rate -- a meta-analysis. *Aging Cell*, 12(3), 410-414.
- Slack C, Alic N, Foley A, Cabecinha M, Hoddinott M & Partridge L (2015). The Ras-Erk-ETS-signaling pathway is a drug target for longevity. *Cell*, 162(1), 72-83.
- Son H, Altintas O, Kim E, Kwon S & Lee S (2019). Age-dependent changes and biomarkers of aging in *Caenorhabditis elegans*. *Aging Cell*, 18(2), e12853.
- Spencer CC & Promislow DEL (2005). Age-specific changes in epistatic effects on mortality rate in *Drosophila melanogaster*. *Journal of Heredity*, 96(5), 513-521.
- Spivey E, Jones S, Rybarski J, Saifuddin F & Finkelstein I (2017). An aging-independent replicative lifespan in a symmetrically dividing eukaryote. *eLife*, 6, e20340.
- Statzer C, Reichert P, Dual J & Ewald C (2022). Longevity interventions temporally scale healthspan in *Caenorhabditis elegans*. *iScience*, 25(3), 103983.
- Strehler BL & Mildvan AS (1960). General theory of mortality and aging. *Science*, 132(3418), 14-21.
- Strenk S, Strenk L & Koretz J (2005). The mechanism of presbyopia. *Progress in Retinal and Eye Research*, 24(3), 379-393.
- Stroustrup N, Anthony W, Nash Z, Gowda V, Gomez A, López-Moyado I, Apfeld J & Fontana W (2016). The temporal scaling of *Caenorhabditis elegans* ageing. *Nature*, 530(7588), 103-107.
- Stroustrup N, Ulmschneider B, Nash Z, López-Moyado I, Apfeld J & Fontana W (2013). The *Caenorhabditis elegans* lifespan machine. *Nature Methods*, 10(7), 665-670.

- Sutphin GL & Korstanje R 2016. Longevity as a complex genetic trait. *Handbook of the biology of aging.* 8 ed.
- Tarkhov A, Menshikov L & Fedichev P (2017). Strehler-Mildvan correlation is a degenerate manifold of Gompertz fit. *Journal of Theoretical Biology*, 416, 180-189.
- The *C. elegans* Sequencing Consortium (1998). Genome sequence of the nematode *C. elegans*: A platform for investigating biology. *Science*, 282(5396), 2012-2018.
- Tiku V, Jain C, Raz Y, Nakamura S, Heestand B, Liu W, Späth M, Suchiman HED, Müller R-U, Slagboom PE, Partridge L & Antebi A (2017). Small nucleoli are a cellular hallmark of longevity. *Nature Communications*, 8(16083).
- Toïgo C, Gaillard J, Festa-Bianchet M, Largo E, Michallet J & Maillard D (2007). Sex- and age-specific survival of the highly dimorphic alpine ibex: Evidence for a conservative life-history tactic. *The Journal of Animal Ecology*, 76(4), 679-686.
- Tozzini E, Dorn A, Ng'oma E, Polačik M, Blažek R, Reichwald K, Petzold A, Watters B, Reichard M & Cellerino A (2013). Parallel evolution of senescence in annual fishes in response to extrinsic mortality. *BMC Evolutionary Biology*, 13, 77.
- Tu M, Epstein D & Tatar M (2002). The demography of slow aging in male and female *Drosophila* mutant for the insulin-receptor substrate homologue *chico*. *Aging Cell*, 1(1), 75-80.
- Tuljapurkar S & Edwards R (2011). Variance in death and its implications for modeling and forecasting mortality. *Demographic Research*, 24, 497-526.
- Van De Pol M & Verhulst S (2006). Age-dependent traits: A new statistical model to separate within- and between-individual effects. *The American Naturalist*, 167(5), 766-773.
- Van Heemst D, Beekman M, Mooijaart S, Heijmans B, Brandt B, Zwaan B, Slagboom P & Westendorp R (2005). Reduced insulin/IGF-1 signalling and human longevity. *Aging Cell*, 4(2), 79-85.
- Vanfleteren JR, De Vreese A & Braeckman BP (1998). Two-parameter logistic and Weibull equations provide better fits to survival data from isogenic populations of *Caenorhabditis elegans* in axenic culture than does the Gompertz model. *The Journals of Gerontology: Series A*, 53A(6), B393–B403.
- Vaupel J, Carey J, Christensen K, Johnson T, Yashin A, Holm N, Iachine I, Kannisto V, Khazaeli A, Liedo P, Longo V, Zeng Y, Manton K & Curtsinger J (1998). Biodemographic trajectories of longevity. *Science*, 280(5365), 855-860.
- Vaupel J & Yashin A (1985). Heterogeneity's ruses: Some surprising effects of selection on population dynamics. *The American Statistician*, 39(3), 176-185.

- Vaupel JW 1997. Trajectories of mortality at advanced ages. *In:* WACHTER, K. W. & FINCH, C. E. (eds.) *Between Zeus and the salmon: The biodemography of longevity.* Washington (DC): National Academies Press (US).
- Vaupel JW, Manton KG & Stallard E (1979). The impact of heterogeneity in individual frailty on the dynamics of mortality. *Demography*, 16(3), 439-454.
- Venz R, Pekec T, Katic I, Ciosk R & Ewald C (2021). End-of-life targeted degradation of DAF-2 insulin/IGF-1 receptor promotes longevity free from growth-related pathologies. *eLife*, 10, e71335.
- Vijg J & Kennedy BK (2015). The essence of aging. Gerontology, 62(4), 381-385.
- Vitale G, Pellegrino G, Vollery M & Hofland L (2019). Role of IGF-1 system in the modulation of longevity: Controversies and new insights from a centenarians' perspective. *Frontiers in Endocrinology*, 10, 27.
- Walsh M, Whittington D & Walsh M (2014). Does variation in the intensity and duration of predation drive evolutionary changes in senescence? *The Journal of Animal Ecology*, 83(6), 1279-1288.
- Wang H, Zhao Y, Ezcurra M, Benedetto A, Gilliat A, Hellberg J, Ren Z, Galimov E, Athigapanich T, Girstmair J, Telford M, Dolphin C, Zhang Z & Gems D (2018). A parthenogenetic quasi-program causes teratoma-like tumors during aging in wild-type *C. elegans. NPJ Aging and Mechanisms of Disease*, 4(6).
- Weibull W (1951). A statistical distribution function of wide applicability. *Journal of Applied Mechanics*, 18(3), 293-297.
- Weismann A (1882). Über die dauer des lebens. Verlag von Gustav Fisher.
- Weismann A (1892). Über leben und tod. Verlag von Gustav Fisher.
- Williams G (1957). Pleiotropy, natural selection and the evolution of senescence. *Evolution*, 11(4), 398-411.
- Wilmoth J & Horiuchi S (1999). Do the oldest old grow old more slowly? *The Paradoxes of Longevity. Research and Perspectives in Longevity.*: Springer, Berlin, Heidelberg.
- Wu D, Cypser J, Yashin A & Johnson T (2009a). Multiple mild heat-shocks decrease the Gompertz component of mortality in *Caenorhabditis elegans*. *Experimental Gerontology*, 44(9), 607-612.
- Wu D, Cypser JR, Yashin AI & Johnson TE (2008). The U-shaped response of initial mortality in *Caenorhabditis elegans* to mild heat shock: Does it explain recent trends in human mortality? *The Journals of Gerontology: Series A*, 63(7), 660-668.
- Wu D, Rea S, Cypser J & Johnson T (2009b). Mortality shifts in *Caenorhabditis elegans*: Remembrance of conditions past. *Aging Cell*, 8(6), 666-675.

- Xiao R, Zhang B, Dong Y, Gong J, Xu T, Liu J & Xu X (2013). A genetic program promotes *C. elegans* longevity at cold temperatures via a thermosensitive TRP channel. *Cell*, 152(4), 806-817.
- Yang Y, Karin O, Mayo A, Song X, Chen P, Santos A, Lindner A & Alon U (2023). Damage dynamics and the role of chance in the timing of *E. coli* cell death. *Nature Communications*, 14(1), 2209.
- Yang Y, Mayo A, Levy T, Raz N, Shenhar B, Jarosz DF & Alon U (2025). Compression of morbidity by interventions that steepen the survival curve. *Nature Communications*, 16(1), 1-14.
- Yashin A, Begun A, Boiko S, Ukraintseva S & Oeppen J (2002a). New age patterns of survival improvement in Sweden: Do they characterize changes in individual aging? *Mechanisms of Ageing and Development*, 123(6), 637-647.
- Yashin A, Ukraintseva S, Boiko S & Arbeev K (2002b). Individual aging and mortality rate: How are they related? *Social Biology*, 49(3-4), 206-217.
- Yashin A, Ukraintseva S, De Benedictis G, Anisimov V, Butov A, Arbeev K, Jdanov D, Boiko S, Begun A, Bonafe M & Franceschi C (2001). Have the oldest old adults ever been frail in the past? A hypothesis that explains modern trends in survival. *The Journals of Gerontology. Series A, Biological Sciences and Medical Sciences*, 56(10), B432-B442.
- Yashin AI, Iachine IA & Begun AS (2000). Mortality modeling: A review. *Mathematical Population Studies*, 8(4), 305-332.
- Yen K & Mobbs CV (2009). Evidence for only two independent pathways for decreasing senescence in *Caenorhabditis elegans*. *AGE*, 32(1), 39-49.
- Yen K, Steinsaltz D & Mobbs CV (2008). Validated analysis of mortality rates demonstrates distinct genetic mechanisms that influence lifespan. *Experimental Gerontology*, 43(12), 1044-1051.
- Yurova M, Tyndyk M, Popovich I, Golubev A & Anisimov V (2019). Gender-specific effects of neonatal administration of melatonin on lifespan and age-associated pathology in 129/Sv mice. *Advances in Gerontology*, 32(1-2), 66-75.
- Zajitschek F, Brassil C, Bonduriansky R & Brooks R (2009). Sex effects on life span and senescence in the wild when dates of birth and death are unknown. *Ecology*, 90(6), 1698-1707.
- Zane F, Bouzid H, Sosa MS, Brazane M, S B, Molina J, Cansell C, Aprahamian F, Durand S, Ayache J, C A, Todd N, Carré C & Rera M (2023). Smurfness-based two-phase model of ageing helps deconvolve the ageing transcriptional signature. *Aging Cell*, 22(11), e13946.

- Zhang W, Sinha D, Pittman W, Hvatum E, Stroustrup N & Pincus Z (2016). Extended twilight among isogenic *C. elegans* causes a disproportionate scaling between lifespan and health. *Cell Systems*, 3(4), 333-345.
- Zhang Y, Zhang W, Zhang P, Li Q, Sun Y, Wang J, Zhang S, Cai T, Zhan C & Dong M (2022). Intestine-specific removal of DAF-2 nearly doubles lifespan in *Caenorhabditis elegans* with little fitness cost. *Nature Communications*, 13(1), 6339.
- Zhao X, Golic F, Harrison B, Manoj M, Hoffman E, Simon N, Johnson R, Maccoss M, Mcintyre L & Promislow D (2022). The metabolome as a biomarker of aging in *Drosophila melanogaster*. *Aging Cell*, 21(2), e13548.
- Zhao Y, Gilliat AF, Ziehm M, Turmaine M, Wang H, Ezcurra M, Yang C, Phillips G, Mcbay D, Zhang WB, Partridge L, Pincus Z & Gems D (2017). Two forms of death in ageing *Caenorhabditis elegans*. *Nature Communications*, 8, 15458.
- Zhao Y, Zhang B, Marcu I, Athar F, Wang H, Galimov E, Chapman H & Gems D (2021). Mutation of *daf-2* extends lifespan via tissue-specific effectors that suppress distinct life-limiting pathologies. *Aging Cell*, 20(3), e13324.
- Zheng H, Yang Y & Land K (2011). Heterogeneity in the Strehler-Mildvan general theory of mortality and aging. *Demography*, 48(1), 267-290.
- Zuev S, Yashin A, Manton K, Dowd E, Pogojev I & Usmanov R (2000). Vitality index in survival modeling: How physiological aging influences mortality. *The Journals of Gerontology. Series A, Biological Sciences and Medical Sciences*, 55(1), B10-B19.